

**ASSESSMENT OF A CONTINUOUS-FLOW ATMOSPHERIC AIR DIELECTRIC
BARRIER DISCHARGE IN THE DEGRADATION OF TRAMADOL, CEFIXIME,
AND CARBAMAZEPINE IN AQUEOUS SOLUTIONS**

By

SAMUEL OLATUNDE BABALOLA

A thesis submitted in fulfilment of the requirements for the degree
Doctor of Philosophy (Chemical Engineering)

In the
Department of Chemical Engineering
Faculty of Engineering, Built Environmental and Information Technology

UNIVERSITY OF PRETORIA

2023

Abstract

Title: Assessment of a continuous-flow atmospheric air dielectric barrier discharge in the degradation of tramadol, cefixime, and carbamazepine in aqueous solutions.

Author: Samuel Olatunde Babalola

Supervisor: Dr. Samuel A. Iwarere

Co-Supervisor: Prof. Michael O. Daramola

Faculty: Engineering Built Environmental and IT

Department: Chemical Engineering

University: University of Pretoria, South Africa

Degree: Doctor of Philosophy in Chemical Engineering

Active pharmaceutical contaminants which are constantly released into both surface and ground water through wastewater treatment plants (WWTP), run-off from agricultural fields, excretion, and disposal of unused or expired medicines into sewage, have become a global concern because of their effects on the aquatic ecosystem and human health. Several studies have examined the use of non-thermal plasma reactors like the dielectric barrier discharge (DBD) in the degradation of various pharmaceutical compounds with significant degradation and mineralization efficiencies. However, most studies are either conducted in batch mode with small solution volumes or in pure synthetic solutions. Also, the working gases have mostly been pure synthetic oxygen gases, which can increase the associated cost of treatment.

In this study, the performance of a continuous-flow atmospheric air dielectric barrier discharge was assessed specifically for the degradation of tramadol, cefixime, and carbamazepine, which are among the commonly discovered pharmaceuticals in the water cycle. By selecting pharmaceutical contaminants from different drug classifications, this study aimed to show the efficacy of a DBD reactor in degrading a wide range of pharmaceutical residues, irrespective of their physicochemical properties. At alternating current (AC) voltage range of 6 – 8 kV and frequency of 20 kHz, 93% degradation of tramadol was observed in 60 min, >99% degradation of cefixime in 8 min, and 92% degradation of carbamazepine in 40 min. Also, the degradation efficiency of each pollutant was susceptible to the operation conditions of the DBD, including applied voltage, initial concentration of pollutant, pH, conductivity, water matrix, and water

flow rate. The chemical species generated were investigated with a spectrometer while radical scavenging experiments were used to establish their respective roles in the degradation of the pollutants.

Experiments conducted in real wastewater effluent confirmed that the presence of HCO_3^- used as pH buffers played a scavenging role in the degradation of analgesic tramadol in the matrix as the ion reacted with hydroxyl radicals ($\bullet OH$) thereby reducing its oxidizing power. Also, a toxicity test revealed that the plasma-treated tramadol solution was less toxic to *Escherichia coli* as opposed to the untreated solution. A new idea was investigated, which was to understand what happens when a metal ion catalyst (Fe^{2+}) is mixed with $\bullet OH$ radical scavengers. In this case, the reactor was able to still achieve significant degradation of cefixime due to the increased production of H_2O_2 in the aqueous solution.

The reactor's performance was also compared with UV-systems for the degradation of carbamazepine at similar experimental conditions. The degradation results obtained in 40 mins were 6.5%, 17.8%, 89%, 91%, and 98% for UV-only, UV/Fe, UV/ H_2O_2 , UV/Fe/ H_2O_2 , and plasma systems, respectively. The plasma system also had the highest energy efficiency (75.24 kWh/m³) and the least required energy cost of treatment (13 USD/m³) compared to the UV-systems considered.

Thus, an assessment of the laboratory-scale studies has demonstrated the feasibility of the novel continuous-flow atmospheric air dielectric barrier reactor in the degradation of tramadol, cefixime, and carbamazepine pollutants in mono-component solutions. This technology has shown potential for field-scale studies as it can be incorporated into existing wastewater treatment plants to degrade active pharmaceutical residues that escape the various treatment stages. However, considering that pharmaceutical pollutants always exist as mixtures and not as a single component in solution, future studies should consider the efficacy of the reactor in degrading a mixture of the pollutants in different water matrices, including real pharmaceutical waste samples.

Keywords: Dielectric barrier discharge; Pharmaceuticals; Advanced oxidation process; Degradation efficiency; Energy yield; Reactive species.

Declaration

I, Samuel Olatunde Babalola, hereby declare that the thesis which I submit for a Doctor of Philosophy in Chemical Engineering degree at the University of Pretoria is to the best of my knowledge original and that neither the whole work nor any part of it has been previously submitted by me for any degree at this or other institution(s).



Samuel Olatunde Babalola

08-02-2024

Date

Dedication

To God

The One who provided this opportunity who is also my ever-present help

To my beloved parents

Mr Isaac O. Babalola and Mrs Ruth A. Babalola

For their love, reliable support, and encouragement

To my siblings

Hannah Babalola and Joseph Babalola

My biggest cheerleaders

This work would never be possible without you ALL!

Acknowledgements

I would like to express my sincere gratitude to my Supervisors, Dr. Samuel Ayodele Iwarere and Professor Michael Olawale Daramola, for accepting me into the Sustainable Energy and Environment Research Group (SEERG) to do this research and for their guidance, mentorship, and sponsorship. Without your push and consistent motivation, I don't think this work would be realised easily.

I would also like to express my profound gratitude to the entire members of the SEERG, both past and present, specifically Dr. John Unuofin, Dr. Joshua Adeniran, Dr. Gbenga Adesina, Paul Kaweesa, Victor Tshigo, Thabang Mosaka and Joshua Nel. I also wish to express my appreciation to the staff and colleagues at the Water Utilization Division at the University of Pretoria for creating a very warm environment to work whilst always willing to give a helping hand. Special mention to Mrs Alette Devega, Mrs. Elmarie Otto, Hilda Kyomuhimbo, Dorcas Adenuga, Emmanuel Ichipi, Ose, Olayile Ejekwu, Samuel Aina, for always helping out.

My appreciation also goes to Professor Paul Steenkamp at the Council for Scientific and Industrial Research (CSIR) for helping with the LC-MS analysis, and to the undergraduate students who worked with me in the plasma laboratory, Thigan Pillay, Andrea D'Sa, Klu Enyonam, and Calvin. I would not forget to mention my adopted Fathers in South Africa, Professor Olufemi Adetunji at the Industrial Systems Engineering and Pastor Bankole.

Finally, I wish to say a big "thank you" to my friends in Pretoria (Debbie, Gaius, Herve, Joy, Doyin, Dr. Kalu, Dr. Dapo, Tunde Awe, Idowu Kekere) for walking through this journey with me and to my spiritual family at Hatfield Christian Church for their constant prayers.

Table of Contents

| | |
|---|--------------|
| Abstract | ii |
| Declaration | iv |
| Dedication | v |
| Acknowledgements | vi |
| Table of Contents | vii |
| List of Figures | xii |
| List of Tables | xv |
| List of Nomenclatures | xvi |
| Research outputs | xviii |
| Chapter 1: Introduction | 1 |
| 1.1 Background | 2 |
| 1.2 Problem Statement | 5 |
| 1.3 Research questions | 6 |
| 1.4 Aim and Objectives | 7 |
| 1.5 Scope of study | 8 |
| 1.6 Methodology | 8 |
| 1.7 Thesis layout | 9 |
| Chapter 2: Literature review | 11 |
| 2.1 State of pharmaceutical pollution | 12 |
| 2.2 Classification of pharmaceutical residues found in water and wastewater sources | 20 |
| 2.3 Pharmaceuticals considered in this study | 22 |
| 2.4 Challenges affecting the detection of pharmaceutical contaminants. | 23 |
| 2.4.1 Low concentrations | 23 |
| 2.4.2 Chemical properties | 23 |
| 2.5 Detection methods for pharmaceutical residues | 25 |

| | |
|---|----|
| 2.5.1 Liquid Chromatography-Mass Spectrometry (LC-MS) | 25 |
| 2.5.2 Gas Chromatography-Mass Spectrometry (GC-MS) | 26 |
| 2.5.3 High-Performance Liquid Chromatography (HPLC) | 26 |
| 2.5.4 Ultra-Performance Liquid Chromatography (UPLC)..... | 27 |
| 2.6 Conventional wastewater treatment | 28 |
| 2.7 Advanced oxidation processes as a tool for the removal of pharmaceuticals..... | 30 |
| 2.7.1 UV and UV-assisted processes | 31 |
| 2.7.2 Fenton process | 33 |
| 2.7.3 Ozonation and O ₃ -assisted processes | 34 |
| 2.7.4 Photocatalytic processes | 35 |
| 2.7.5 An overview of the plasma process | 37 |
| 2.8 Application of non-thermal plasma in water treatment..... | 38 |
| 2.9 Reactive species in a non-thermal plasma..... | 40 |
| 2.9.1 Reactive oxygen species (ROS)..... | 41 |
| 2.9.2 Reactive nitrogen species (RNS)..... | 43 |
| 2.9.3 Ultraviolet light..... | 43 |
| 2.9.4 Shockwave..... | 44 |
| 2.10 Types of non-thermal discharge | 47 |
| 2.10.1 Corona discharge (CD)..... | 47 |
| 2.10.2 Glow discharge (GD)..... | 49 |
| 2.10.3 Gliding arc discharge (GAD)..... | 50 |
| 2.10.4 Dielectric barrier discharge (DBD)..... | 52 |
| 2.11 Configurations of the dielectric barrier discharge..... | 52 |
| 2.12 Factors affecting the electrical discharges from an NTP during water treatment. | 57 |
| 2.12.1 Input power | 57 |
| 2.12.2 Initial concentration of pollutants | 58 |
| 2.12.3 Composition of feed gas | 59 |

| | |
|--|-----------|
| 2.12.4 Reactor design and discharge gap | 59 |
| 2.12.5 pH of the solution | 60 |
| 2.12.6 Conductivity of the solution..... | 61 |
| 2.13 Plasma combined with catalysts..... | 63 |
| 2.13.1 Metal oxide catalysts..... | 63 |
| 2.13.2 Metal ion catalyst | 65 |
| 2.14 Summary of knowledge gaps | 66 |
| Chapter 3: An investigation on the removal of tramadol analgesic in deionised water and final wastewater effluent using a novel continuous flow dielectric barrier discharge reactor. | 68 |
| 3.1 Introduction | 69 |
| 3.2 Experimental method | 71 |
| 3.2.1 Materials | 71 |
| 3.2.2 Experimental procedure..... | 71 |
| 3.2.3 Analytical measurements..... | 72 |
| 3.3 Results and discussion..... | 75 |
| 3.3.1 Electrical and optical characteristics of the dielectric barrier discharge reactor..... | 75 |
| 3.3.2 Influence of operating conditions on the removal TRA | 77 |
| 3.3.3 Contribution of active species: Generation of O ₃ , H ₂ O ₂ , NO ₃ ⁻ and NO ₂ ⁻ during the DBD discharge..... | 81 |
| 3.3.4 Comparison of the degradation of TRA in deionised water and final wastewater effluent..... | 83 |
| 3.3.5 Toxicity investigation | 89 |
| 3.4 Conclusion..... | 89 |
| Chapter 4: Mechanistic study of cefixime degradation with an atmospheric air dielectric barrier discharge and influence of metal ion catalyst | 91 |
| 4.1 Introduction | 91 |
| 4.2 Experimental section | 94 |
| 4.2.1 Materials and chemicals | 94 |

| | |
|---|------------|
| 4.2.2 Experimental procedure..... | 95 |
| 4.2.3 Analytic methods..... | 96 |
| 4.3 Results and discussion..... | 98 |
| 4.3.1 Impact of solution water flowrate..... | 98 |
| 4.3.2 Impact of applied voltage | 98 |
| 4.3.3 Impact of CFX concentration..... | 99 |
| 4.3.4 Impact of initial pH | 103 |
| 4.3.5 Effect of adding a metal ion catalyst..... | 105 |
| 4.3.6 Contribution of plasma reactive species and their roles | 106 |
| 4.3.7 Investigating the combined effect of radical scavengers and metal ion catalyst ... | 111 |
| 4.3.8 Identification of degradation intermediates and possible degradation pathways... | 113 |
| 4.4 Conclusion..... | 117 |
| Chapter 5: Insights into the degradation of carbamazepine using a continuous-flow non-thermal plasma reactor: mechanism and comparison with UV-based systems | 118 |
| 5.1 Introduction | 119 |
| 5.2 Materials and methods | 122 |
| 5.2.1 Chemicals | 122 |
| 5.2.2 DBD plasma experiments..... | 122 |
| 5.2.3 UV experiments | 123 |
| 5.2.4 Analytical procedure | 124 |
| 5.3 Results and discussions | 125 |
| 5.3.1 Investigation of the reactive species generated in the DBD plasma..... | 125 |
| 5.3.2 Investigation of key operating parameters on CBZ degradation..... | 127 |
| 5.3.3 Investigating the effect of radical scavengers..... | 133 |
| 5.3.4 Effect of different water matrices on CBZ degradation | 137 |
| 5.3.5 Comparison of the removal of CBZ in DBD plasma and a UV-based system | 140 |
| 5.4 Conclusions | 144 |

| | |
|---|------------|
| Chapter 6: General conclusion and Recommendations | 146 |
| 6.1 Significant findings | 147 |
| 6.2 Recommendation for future studies | 148 |
| References..... | 150 |
| Appendices..... | 193 |

List of Figures

| | |
|---|----|
| Figure 1.1: Pathway for pharmaceutical drugs in the environment (Adapted from [10]) | 3 |
| Figure 2.1: Statistics of publications on occurrence of PhACs in the water and wastewater (Scopus database for search “pharmaceuticals AND water AND wastewater,” accessed October 10, 2023 [38])..... | 12 |
| Figure 2.2: Common classifications of pharmaceuticals found in water and wastewater [85]. | 21 |
| Figure 2.3: Classification of advanced oxidation processes [122]. | 31 |
| Figure 2.4: Common plasma configurations [164]. | 37 |
| Figure 2.5: Forms of electrical discharges. (a) discharge in gas phase above liquid (b) direct gas discharge in the liquid (c) hybrid gas-liquid discharge. (Adapted from [163])..... | 39 |
| Figure 2.6: A schematic illustration of a corona discharge. (Adapted from [225])..... | 49 |
| Figure 2.7: A schematic illustration of the glow discharge arrangement. (Adapted from [225]). | 50 |
| Figure 2.8: A schematic illustration of the typical gliding arc discharge. (Adapted from [225]). | 51 |
| Figure 2.9: Planar DBD configurations: (a) volume DBD (1-symmetric, 2-asymmetric, 3-floated dielectric) (b) surface DBD [239]...... | 54 |
| Figure 2.10: Cylindrical DBD configurations (a) ring-ring (b) pin-ring [239]..... | 56 |
| Figure 2.11: Effect of reactor design on the plasma discharge characteristics. (a) electrode distance (b) Surface of electrode (Adapted from [256])..... | 60 |
| Figure 2.12: (a) Spark discharge with conductivity of 14 $\mu\text{S}/\text{cm}$ (b) Streamer discharge with conductivity of 70 $\mu\text{S}/\text{cm}$ (c) Corona discharge with conductivity of 300 $\mu\text{S}/\text{cm}$. (Adapted from [263])..... | 62 |
| Figure 3.1: Experimental arrangement for the tramadol degradation process (a) Schematic illustration of the setup (b) DBD plasma reactor showing purple streamer discharges at the edges of the multi-pin electrode..... | 75 |
| Figure 3.2: Optical emission spectrum of the plasma generated in the dielectric barrier discharge reactor at 20 kHz and 8 kV..... | 76 |
| Figure 3.3: Effect of voltage on 5 mg/L TRA degradation. (a) Degradation efficiency and kinetics. (b) Energy yield..... | 80 |

| | |
|--|-----|
| Figure 3.4: Effect of concentration on TRA degradation at 8 kV. (a) Degradation efficiency and kinetics; (b) Energy yield. | 80 |
| Figure 3.5: Reactive species formed during TRA degradation. (a) O ₃ and H ₂ O ₂ concentration; (b) NO ₃ ⁻ and NO ₂ ⁻ concentration. | 82 |
| Figure 3.6: (a) Degradation of tramadol in deionised water and final wastewater effluent as a function of time; (b) Energy yield comparison; (c) pH and conductivity of the solution matrices as a function of time. | 85 |
| Figure 3.7: Degradation of tramadol in different reaction solutions. | 86 |
| Figure 3.8: Bioassay to study the antibacterial activity of TRA samples against Gram-negative E. coli strain. (a) untreated tramadol solution with three zones of inhibition; (b) plasma-treated tramadol solution showing no inhibition zones; (c) is the control. | 89 |
| Figure 4.1: Effect of water flow rate (a) degradation efficiency; (b) kinetics. | 102 |
| Figure 4.2: Effect of applied voltage (a) degradation efficiency; (b) kinetics. | 102 |
| Figure 4.3: Effect of input concentration (a) degradation efficiency; (b) kinetics. | 103 |
| Figure 4.4: Effect of initial solution pH on CFX degradation (a) rate constant; (b) change in solution pH. | 104 |
| Figure 4.5: Effect of Fe ²⁺ on the degradation of CFX (a) degradation efficiency; (b) kinetics. | 105 |
| Figure 4.6: Contribution of reactive oxygen and nitrogen species during the degradation of CFX (a) O ₃ and H ₂ O ₂ (b) NO ₃ ⁻ and NO ₂ ⁻ | 108 |
| Figure 4.7: Effect of scavengers on CFX degradation in the DBD plasma system (a) degradation efficiency; (b) rate constants. | 108 |
| Figure 4.8: Effect of different additives on the degradation efficiency of CFX (a) TBA and Fe; (b) IPA and Fe; (c) NaHCO ₃ and Fe. | 109 |
| Figure 4.9: Effect of various additives on H ₂ O ₂ concentration (a) TBA and Fe; (b) IPA and Fe; (c) NaHCO ₃ and Fe. | 110 |
| Figure 4.10: The rate constant and energy efficiency under different additives. | 111 |
| Figure 4.11: Proposed degradation pathway for the degradation of CFX using the DBD reactor. | 116 |
| Figure 5.1: Setup for the UV-based experiments. | 124 |
| Figure 5.2: Variation in the concentration of O ₃ and H ₂ O ₂ during CBZ degradation. | 127 |
| Figure 5.3: Effect of CBZ initial concentration on the degradation efficiency. | 128 |
| Figure 5.4: Effect of applied voltage on the degradation of CBZ. (a) degradation efficiency; (b) concentration of H ₂ O ₂ and O ₃ | 130 |

| | |
|---|-----|
| Figure 5.5: Effect of solution conductivity on the degradation efficiency of CBZ. | 131 |
| Figure 5.6: Degradation efficiency at different initial pH values. | 132 |
| Figure 5.7: pH and conductivity trends for the control solution versus treatment time.. | 133 |
| Figure 5.8: Influence of isopropanol on the degradation efficiency of CBZ..... | 134 |
| Figure 5.9: Influence of benzoquinone on the degradation efficiency of CBZ. | 135 |
| Figure 5.10: Influence of uric acid on the degradation efficiency of CBZ..... | 136 |
| Figure 5.11: Influence of sodium pyruvate on the degradation efficiency of CBZ..... | 137 |
| Figure 5.12: Effect of water matrices on (a) degradation efficiency of CBZ; (b) reaction rate for CBZ degradation. | 139 |
| Figure 5.13: comparison of the different AOPs (a) degradation efficiency; (b) kinetics. | 142 |

List of Tables

| | |
|--|-----|
| Table 2.1: Reports on the global occurrence of pharmaceutical residues in the environment. | 16 |
| Table 2.2: Physicochemical characteristics of the pharmaceutical compounds studied..... | 19 |
| Table 2.3: Chemical properties of the common reactive oxygen species in a non-thermal plasma reactor [188,189]..... | 44 |
| Table 2.4: Studies on the application of NTP in the degradation of pharmaceutical residues. | 45 |
| Table 3.1: Ion chromatography analysis of the final wastewater effluent obtained from Daspoort Municipality, South Africa..... | 77 |
| Table 3.2: Degradation of TRA in water with selected AOPs..... | 79 |
| Table 4.1: Comparison between selected AOPs used in the degradation of cefixime. | 101 |
| Table 4.2: Degradation by-products for cefixime with the DBD plasma reactor | 114 |
| Table 5.1: Technical characteristics and operating conditions for the DBD plasma reactor. | 123 |
| Table 5.2: Characteristics of deionised water, tap water and final wastewater effluent..... | 125 |
| Table 5.3: Variation of pH and conductivity during the degradation of CBZ in TW and FW. | 139 |
| Table 5.4: Comparison of the degradation efficiency and kinetics for the different AOP setups used in this study..... | 141 |
| Table 5.5: Comparison of the energy efficiency and associated costs of treatment for the AOPs considered in this work. | 144 |

List of Nomenclatures

| | |
|-----------------|---|
| AOP | Advanced oxidation processes |
| CBZ | Carbamazepine |
| CD | Corona discharge |
| CFX | Cefixime |
| Co | Initial concentration |
| C _t | Concentration at particular time |
| DBD | Dielectric Barrier Discharge |
| DI | Deionised water |
| E ₀ | Reduction potential |
| EC | Emerging contaminants |
| E _{EO} | Electrical energy per order |
| FWWE | Final wastewater effluent |
| GAD | Gliding arc discharge |
| GC-MS | Gas chromatography-mass spectrometry |
| GD | Glow discharge |
| HPLC | High-performance liquid chromatography |
| k | rate constant |
| LC-MS | Liquid chromatography-mass spectrometry |
| MN | Membrane bioreactors |
| NF | Nano-filtration |
| NTP | Non – thermal plasma |
| PIE | Pharmaceuticals in the environment |
| PhAC | Pharmaceutically Active Contaminant |

| | |
|----------|---|
| Q-TOF-MS | Quadruple time-of-flight mass spectrometry |
| RO | Reverse osmosis |
| ROS | Reactive oxygen species |
| RON | Reactive nitrogen species |
| TRA | Tramadol |
| t | Treatment time |
| TW | Tap water |
| UPLC | Ultra-performance liquid chromatography-mass spectrometry |
| USD | United States Dollar |
| UV | Ultraviolet |
| V | Volume |
| WWTP | Wastewater treatment plant |
| mg/L | milligram per litre |
| η | Efficiency |
| Y | Energy yield |

Research outputs

Journal articles

- **Samuel O. Babalola**, Michael O. Daramola, Samuel A. Iwarere (2023), “An investigation on the removal of tramadol analgesic in deionized water and final wastewater effluent using a novel continuous flow dielectric barrier discharge reactor.” Published in Elsevier Journal of Water Process Engineering, doi: 10.1016/j.jwpe.2023.104294.
- **Samuel O. Babalola**, Paul A. Steenkamp, Michael O. Daramola, Samuel A. Iwarere (2023), “Mechanistic study of cefixime degradation with an atmospheric air dielectric barrier discharge and influence of metal ion catalyst.” (Submitted to Separation and Purification Technology).
- **Samuel O. Babalola**, Michael O. Daramola, Samuel A. Iwarere (2023), “Insights into the degradation of carbamazepine using a continuous-flow non-thermal plasma reactor: mechanism and comparison with UV-based systems” (Submitted to Journal of Environmental Sciences).

Conference presentation

- In-person oral presentation at the 49th IEEE International Conference on Plasma Science (ICOPS), Seattle, Washington, United States of America (USA): “Comparison of the Degradation and Kinetics of Tramadol Pharmaceutical in Deionized Water and Tertiary Wastewater Effluent by a Dielectric Barrier Discharge.” Available via: 10.1109/ICOPS45751.2022.9813268.

Other publications during the PhD year

- **Samuel O. Babalola**, Joshua J. Nel, Victor Tshigo, Michael O. Daramola, Samuel A. Iwarere (2022), “An integrated waste-to-energy approach: a resilient energy system design for sustainable communities.” Elsevier Energy Conversion and Management Journal, doi: 10.1016/j.enconman.2022.115551.

- **Samuel O. Babalola**, Michael O. Daramola, Samuel A. Iwarere (2022), “Socio-economic Impacts of Energy Access through Off-Grid Systems in Rural Communities: A Case Study of South-West Nigeria.” *Philosophical Transactions A Royal Society Journal*, doi: 10.1098/rsta.2021.0140.

Award/recognition

- Individual: received the People choice’s award (ZAR 5,000) at the University of Pretoria 3-minutes thesis presentation PhD students’ category 2022.
- Team: second-place award at the 2022 Siemens Gamesa Climate Change competition.
https://www.up.ac.za/news/post_3102590-up-team-wins-second-place-in-international-climate-solutions-competition.

Chapter 1: Introduction

This chapter provides a background to the study documented in this thesis. It introduces the problem at hand, the existence of pharmaceutical pollutants in the environment and the unreliability of conventional wastewater treatment units in removing them. This section also expatiates further on why this problem is worth investigating. Also, the contributions made to addressing the challenge of pharmaceutical pollution are mentioned, and some of their limitations. Thereafter, non-thermal plasma technology adopted in this study was introduced and the gap existing in literatures were mentioned. Consequently, the objectives of this study were highlighted. The chapter also provides the scope of the study, the methodology, and the structure of the thesis.

1.1 Background

The massive population expansion and rapid global industrial development occurring in most parts of the world have led to an increase in the discharge of a variety of harmful substances that affect nature's equilibrium at an alarming rate. Special attention has been given to contaminants of pharmaceutical origin which are found in surface water, groundwater, wastewater, and even in drinking waters. The detection of pharmaceutically active compounds (PhACs) has been possible, thanks to advanced analytical technologies that can quantify them even in their low concentrations. PhACs have also been recognised as one of the emerging contaminants (ECs) in the environment because in most places they are still unregulated or are currently undergoing a standardization process, but without a clear directive or legal framework [1–4]. All of these are being discussed under an area of study tagged as “Pharmaceuticals in the Environment – PIE” [5].

Pharmaceuticals are generally described as synthetic or natural chemicals that are either found in prescribed medicines, over-the-counter and veterinary drugs, and they contain active ingredients that cause pharmacological effects [6]. They are continuously being introduced into the environment because of their ubiquitous use by humans and in veterinary applications. In the environment, PhACs and their metabolites may undergo natural attenuation processes like dilution, adsorption, and degradation [7]. However, this depends on their hydrophobicity, biodegradability, and the temperature of the environment. Also, while some pharmaceutical drugs like antibiotic erythromycin, antiepileptic carbamazepine, antihypertensive valsartan, and so on, are persistent in water and accumulate over time, there are other categories like the anti-inflammatory diclofenac which have short half-life [8]. However, the presence of this type of drugs in water is not mitigated by their rapid degradation, as the constant influx of these substances counterbalances their removal, resulting in a sustained concentration in water [5]. Despite being mostly discovered in very low concentrations (ngL^{-1} or μgL^{-1}), PhACs remain bioactive in the environment and can affect water quality and potentially impact drinking water supplies, aquatic species, and even human health [9].

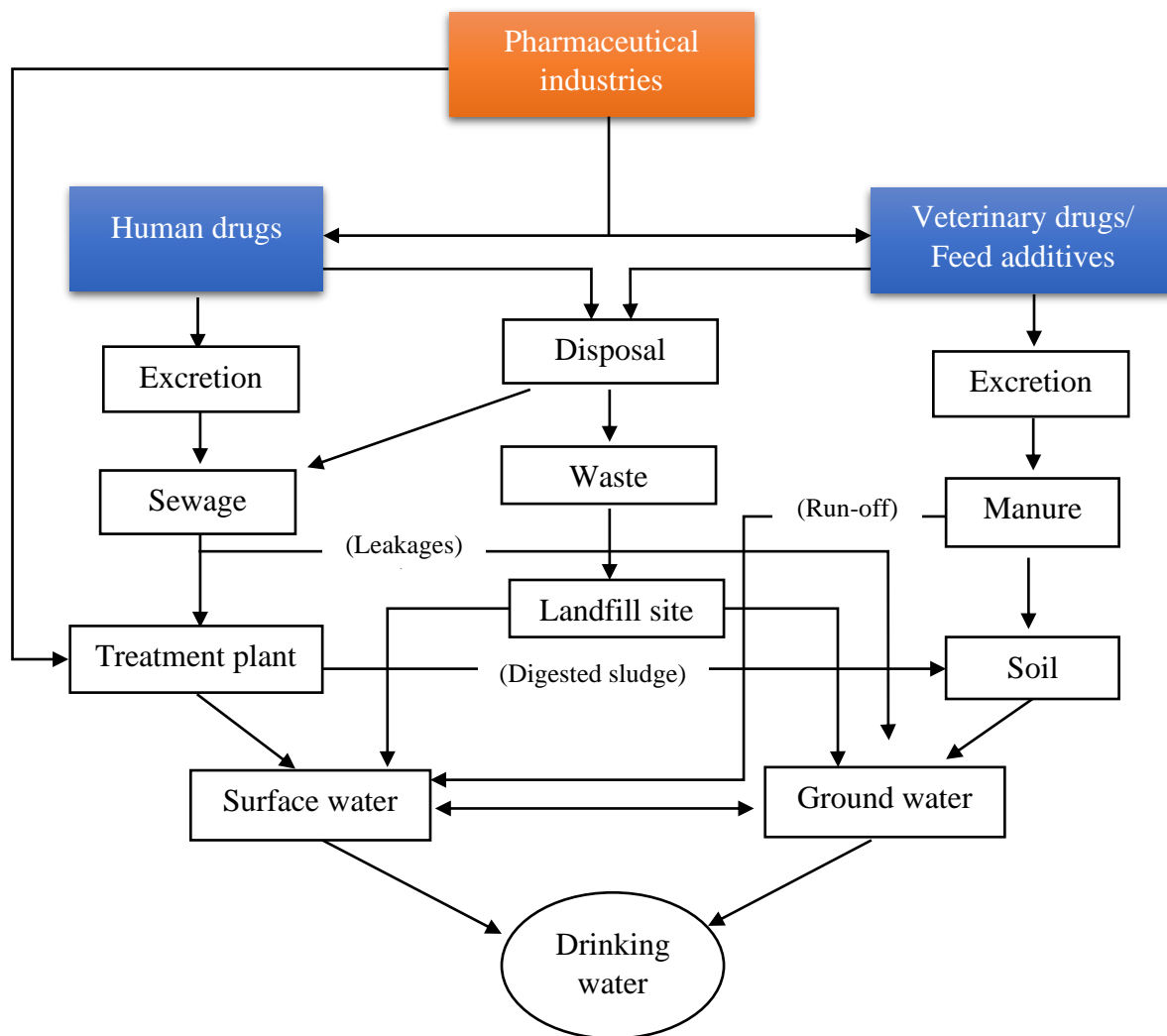


Figure 1.1: Pathway for pharmaceutical drugs in the environment (Adapted from [10])

Figure 1.1 illustrates the routes by which pharmaceuticals get into our environment. These typically include human or animal excreta, careless drug disposal, medical wastes, wastewater effluent, industrial wastes amongst others. Wastewater treatment plants (WWTPs) have been noted to be the major sources of PhACs in the environment [11–13]. They face challenges in effectively removing micro-organic contaminants like PhACs for several reasons. Firstly, the compounds often have complex molecular structures which makes them exhibit unique chemical properties like high stability. Next, the low concentrations in which they are found makes it difficult to be removed by the treatment stages in the WWTP. Some pharmaceutical contaminants like tramadol were even found to have increased in concentration at the effluent points of the WWTP compared to the influent section, due to the transformation of their metabolites to the parent compounds [8]. The United States Geological Survey (USGS)

remarked that conventional wastewater treatment processes were primarily designed to address common pollutants like organic matter, nutrients, and pathogens [14]. Thus, they need to be upgraded to handle micro contaminants which are relatively recent concerns.

To address these challenges, advanced treatment technologies like membrane filtration, activated carbon adsorption, advanced biological processes, and advanced oxidation processes (AOPs) are being explored. Membrane filtration techniques, like reverse osmosis (RO) and nanofiltration (NF), can effectively remove emerging contaminants like pharmaceuticals by rejection through a semi-permeable membrane material [15–17]. Although they offer high removal efficiencies, they can be expensive due to the high-energy requirements for maintaining the adequate pressure needed and frequent membrane maintenance required. Also, the resulting concentrate waste streams may have pollutant concentrations higher than what was treated, which means they will also require further treatment. This challenge is also experienced when using the activated carbon adsorption method, whether granular or powdered form. For this method, the disposal of the spent activated carbon can also pose a significant environmental challenge. Another challenge is the regeneration of the adsorbents for re-use. Advanced biological processes such as membrane bioreactors (MBRs) and sequencing batch reactors (SBRs), rely on microorganisms to biodegrade or transform organic compounds [17–19]. However, they may be susceptible to inhibition and decreased performance in the presence of toxic pharmaceuticals like carbamazepine.

For these reasons, advanced oxidation processes (AOPs) have recently gained attraction. These processes mainly involve the generation of highly potent chemical oxidants (like hydroxyl ion radicals, ozone, etc) for the oxidation of a wide range of contaminants in water, thus disinfecting the water [16,20,21]. However, the high capital cost and energy requirement for most AOPs like those using ozone, and their maintenance must be addressed for their commercial viability to be fully realised. Also, some AOPs like ozonation has a low mineralization degree [22], which might therefore necessitate that they are combined with other technologies for the effective removal of potentially harmful intermediate products. Other methods like Ultraviolet radiation (UV) and photocatalysis face issues like periodic replacement of UV lamps and catalyst recovery for re-use, respectively.

Considering these limitations, this study will explore the application of a dielectric barrier discharge (DBD) plasma, one of the developed forms of non-thermal plasma technology (NTP) for the degradation of pharmaceutical contaminants. An NTP is one of the AOPs that is fast gaining interest in the degradation of persistent micro-organic pollutants in water. The important advantage of this system is its ability to rapidly oxidise contaminants in water into less toxic byproducts and unlike the other AOPs, with less energy. This helps to reduce the overall cost of running the system. In addition, plasma treatment requires no chemical additives. In this study, a DBD plasma reactor was developed for the removal of tramadol, carbamazepine, and cefixime in aqueous solutions. These pharmaceutical contaminants have been popularly reported in final effluent wastewater and even in the water cycle. Also, their toxicity reports have drawn researchers' attention all over the world.

1.2 Problem Statement

The production and consumption of pharmaceutical drugs are expected to increase in the coming decades due to factors like increasing population growth, aging population, disease prevalence and awareness, advances in medical treatment, direct-to-consumer advertisement and changing lifestyles. While a holistic report on their health impacts is still lacking, there are already notable effects of some PhACs on the aquatic ecosystem and human health. At the same time, finding an appropriate method for the effective removal of these contaminants in water can be a challenge. In most cases, pharmaceutical pollutants are found as mixtures, and these compounds exhibit different physicochemical properties. Thus, a one-fit-all removal technology might be difficult. In most cases, the efficacy of a treatment technology is measured by its ability to remove contaminants without leaving harmful intermediates or creating secondary pollution.

Several studies have examined the use of NTP reactors in the degradation of various pharmaceutical compounds and the results have clearly shown that significant degradation and mineralization of these contaminants can be achieved [23–26]. For a particular compound investigated, significant variations in the results amongst open literature have provided evidence for the influence of the plasma reactor design configuration and experimental conditions on the degradation process [27,28]. Inferences from most studies have also shown that the decontamination of water can be enhanced with adequate reactive species generated *in*

situ and transferred into the liquid. This, therefore, necessitates that the plasma reactor is designed in such a way that there would be a large contact area between the plasma generated and the liquid. Also, some studies have reported that pure oxygen was more effective in the production of active oxidizing species than air because in its case, less unwanted by-products and nitrogen compounds were formed [29,30]. However, the selection of an oxygen-rich gas needs to be considered from a cost perspective. The degradation efficiency can also be influenced by the amount of power dissipated in the plasma reactor. High power input will lead to an increase in the concentration of the reactive species, thus enhancing the degradation [31].

One of the major gaps in PhAC degradation with plasma is that the technology has been deployed mostly in batch operations to treat small volumes of solution. There have been questions on the efficacy of the NTP for larger industrial applications, which necessitates the design of continuous-flow plasma reactors. Also, most of the published studies on the degradation of PhACs with NTP reactors have focused on synthetic mono-component solutions of the organic pollutants in high-purity water. Only a few studies like Iervolino *et al.* [31], Liu *et al.* [32], and so on, have reported the effect of water matrices on the targeted compounds. In a complex mixture, cross-interference reactions and the presence of radical scavengers will potentially impact the concentration of the reactive species available for contaminant degradation, thus reducing the efficiency of the process and increasing the energy requirement as compared with pure water. Therefore, there is still a need to have more in-depth research on the degradation of contaminants in real contaminated water to support the evidence of the efficiency of plasma technology. Lastly, while metal ion catalysts have been established as potent boosters of the degradation efficiency of plasma reactors, there is an underexplored area in plasma water treatment and AOPs in general which is the investigation of the technology's performance in the presence metal ion catalysts and radical scavengers.

1.3 Research questions

Considering the statement above, in this study a continuous-flow reactor working with natural atmospheric air was coupled and assessed in the degradation of three commonly reported contaminants in the water cycle (tramadol, cefixime, and carbamazepine). Four research questions were put forward in this study in order to address the gaps in the statement:

1. What is the influence of operating parameters like applied voltage, initial pollutant concentration, solution pH, conductivity, and water flow rate on the degradation efficiency of a continuous-flow atmospheric air DBD for degrading tramadol, cefixime, and carbamazepine?
2. What is/are the specific ion(s) responsible for the differences in the degradation of a pharmaceutical pollutant in deionised water and final wastewater effluent?
3. How does a metal ion catalyst influence the degradation performance of a DBD reactor in the presence of radical scavengers?
4. How does a continuous flow atmospheric air DBD compare with a UV-based system in terms of degradation efficiency, energy efficiency, and energy cost?

1.4 Aim and Objectives

This study aimed to investigate the potential of a continuous-flow dielectric barrier discharge reactor using natural atmospheric air, as a removal technology for persistent pharmaceutical contaminants in water. The three pharmaceutical pollutants mentioned previously (tramadol, cefixime, and carbamazepine) were used to investigate and provide responses to the research questions raised and these are presented as specific objectives of the study. They include:

1. To investigate the effect of operating conditions such as the applied voltage, initial pollutant concentration, solution pH, conductivity, and water flow rate on the degradation of tramadol, cefixime, and carbamazepine.
2. To investigate and compare the removal efficiency and degradation kinetics of an analgesic tramadol in deionised water and final wastewater effluent.
3. To provide a mechanistic study on cefixime antibiotic degradation with an atmospheric air dielectric barrier discharge and examine the influence of metal ion catalyst in the presence of radical scavengers.
4. To provide an insight into the degradation of carbamazepine antiepileptic, examining the influence of radical scavengers, solution matrix, and compare its energy efficiency and its associated energy cost of treatment with a UV-based system.

1.5 Scope of study

The current study assesses the potential of a dielectric barrier discharge reactor, a form of non-thermal plasma technology, in the degradation of persistent pharmaceuticals namely, tramadol analgesic, carbamazepine antiepileptic and cefixime antibiotic to levels below quantification by analytical instruments and possibly human detection. By selecting pharmaceutical contaminants from different drug classifications; opioid, antibiotic, and anti-epileptic, this study aimed to show the efficacy of a DBD reactor irrespective of the physicochemical properties of the pharmaceutical residues it handles. The pollutants were each investigated in a mono-component solution, and not as a mixture. All experiments were performed on a laboratory scale in a continuous flow operation to investigate key aspects of the degradation process, including the influence of different operating conditions of the reactor and in some cases, intermediate products formed. Besides measuring the reactive species generated in the reactor, a detailed investigation of the role of these species was carried out by performing radical scavenger experiments. Also, some experiments were conducted in different water matrices like final wastewater effluent and tap water, to examine the reaction between natural radical scavengers and the available reactive species. Finally, analysis of the degradation products was used to propose a possible degradation pathway for the pollutants.

1.6 Methodology

The methodology employed in achieving the objectives listed in section 1.4 is outlined below:

- a. A detailed literature study to understand the status of pharmaceutical pollution globally and an evaluation of the forms of AOPs used in treating pharmaceutical pollutants with documented performance efficiencies across the common technologies. Then a focus on the studies reported for non-thermal plasma processes to better understand the technical aspects of the process.
- b. Coupling of a continuous flow dielectric barrier discharge reactor to be used for the study with the important balance of systems like the high voltage (HV) alternating power supply locally fabricated to required specifications by Jeanel Technologies Pty, Boksburg, South Africa, and the digital oscilloscope used for power analysis.

- c. Preparation of the mono-component synthetic stock solutions of each contaminant under investigation. Also, wastewater samples were collected at the final discharge point at a municipal water treatment plant in Tshwane, Pretoria, South Africa. The tap water used in the study was collected at the University of Pretoria, South campus kitchen.
- d. Investigation of the degradation performance of the DBD reactor in removing the targeted pollutants was conducted in one of or all the water matrices; deionised water, final wastewater effluent, and tap water, using the setup reactor operated at continuous flow mode and under favourable operating conditions.
- e. Both quantitative and qualitative analyses were carried out to determine the residual concentration of the pollutants and their by-products, respectively.
- f. The degradation mechanism pathways were proposed based on the by-products observed and the reactive species investigated.

1.7 Thesis layout

This thesis consists of 6 chapters, of which all the results in the chapters are either published or submitted for publication. Each chapter has its methodology, results, conclusions, and appendices, providing a full report:

- Chapter 1 provides a brief introduction to the research study. It details the motivation behind the study, the aims and objectives, scope, including the structure of the thesis.
- Chapter 2 provides a comprehensive description of past literatures focusing on the occurrence and types of pharmaceutical residues in the environment, and the application of AOPs. The chapter also provides advances in non-thermal plasma technology research and the status of the technology in degrading the pollutant.
- Chapter 3 evaluates the performance of the DBD reactor for the removal of tramadol analgesic in deionised water and final wastewater effluent. The results from this chapter have been published in the Elsevier Journal of Water Process Engineering.
- Chapter 4 provides a mechanistic study on the degradation of cefixime antibiotic with the DBD reactor and the influence of radical scavengers as well as a metal ion catalyst.

- Chapter 5 provides an insight into the degradation of carbamazepine anti-epileptic with the continuous-flow DBD reactor and a comparison of the technology with UV-based systems in terms of degradation efficiency, energy efficiency, and the energy cost associated with the treatment processes.
- Chapter 6 summarises the results of the study and concludes with future recommendations.

Chapter 2: Literature review

This chapter provides a detailed review on the topic under investigation. An overview of the occurrence and categories of pharmaceutical pollution was presented to provide evidence of the fact that they have become contaminants of concern globally. The traditional treatment methods were discussed, and their limitations were reported. The common forms of advanced oxidation processes and their benefits were also highlighted; however, emphasis was placed on the application of non-thermal plasma processes in water treatment. The mechanisms behind the operations of the forms of non-thermal plasma categories were also discussed including a summary of the recent studies on their applications for water decontamination. Emphasis was placed on the configurations of dielectric barrier discharge (DBD) and their advantages. The factors generally affecting the performance of a non-thermal plasma technology were highlighted, and the chapter concluded with gaps identified with the use of a DBD technology which informed the direction of this study.

2.1 State of pharmaceutical pollution

The occurrence of pharmaceutical pollution in the environment is a multifaceted issue that has far-reaching implications. Over the last decades, there has been a surge in worldwide environmental research driven by the prevalence of pharmaceutical residues in water and wastewater as shown in Figure 2.1. Although the occurrence and build-up of these foreign substances in water is not new, their accumulation and treatment facilities have garnered more reports [10,33,34]. The presence of these harmful substances in water significantly impacts the availability of safe drinking water on a global scale. The buildup of pharmaceutical compounds within water and wastewater treatment plants has resulted in the treated wastewater becoming unsuitable for reuse due to the high toxicity and contamination of the generated sludge with PhCs. Also, the contaminants found in the treated wastewater indicate that conventional treatment methods are ineffective in their removal, often leading to the discharge of untreated effluents into the environment [35–37].

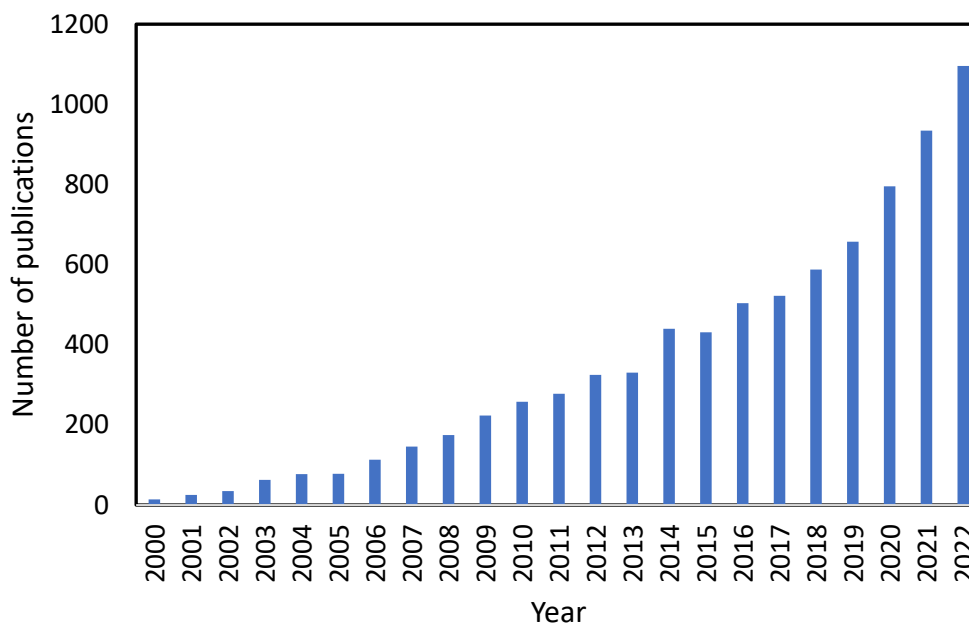


Figure 2.1: Statistics of publications on occurrence of PhACs in the water and wastewater (Scopus database for search “pharmaceuticals AND water AND wastewater,” accessed October 10, 2023 [38])

Globally, the consumption of pharmaceuticals is vast. For example, between 2000 and 2001, Germany alone produced millions of non-steroidal anti-inflammatory drugs like aspirin, paracetamol, ibuprofen, and diclofenac amounting to about 86 tonnes [39]. Countries like France and Switzerland have also been reported to have high rates of pharmaceutical consumption in Europe [40]. The prevalence of these compounds in water bodies differs across countries, possibly influenced by prescription habits.

In a study conducted in North-West, Denmark, Matamoros *et al.* [41] reported the existence of 17 emerging contaminants in water samples collected from a restored wetland and two rivers. According to the authors, the prevalent contaminants with the highest concentration were pharmaceuticals which included diclofenac and caffeine, reaching as high as 156 ng/L and 382 ng/L, respectively. Other pharmaceutical residues discovered in lower concentrations included ibuprofen (32 ng/L), and carbamazepine (95 ng/L). The authors also mentioned that the high concentration of these pollutants in the samples investigated must have been a result of discharge from sewer overflows as well as effluent from WWTPs. In South Carolina, USA, Melanie and her co-workers detected a total of 19 pharmaceutical and personal care products (PPCPs) in samples collected from two local WWTPs over a year [42]. 11 of these compounds were quantified in the influent stream, 9 in the effluent while 7 compounds were detected in surface water close to the plants. Of these compounds, the pharmaceutical residues with the highest frequency of detection were acetaminophen, caffeine, and cotinine. Ibuprofen had the highest concentration amongst the samples (11 ng/L) but with a lower frequency of detection. The authors also noted that the frequency of detection is a function of site differences, WWTPs removal efficiencies, and seasonality.

In France, Dinh *et al.* [43] discovered 23 persistent antibiotics in elementary river watersheds coming from domestic and hospital sources. Despite passing through WWTPs, the concentration of the pharmaceuticals from both hospital and domestic sources was as high as 12,850 ng/L, while the concentrations from the domestic stream reached a maximum of 550 ng/L. Antibiotics like ofloxacin, sulfamethoxazole, trimethoprim, ciprofloxacin, norfloxacin, and enoxacin, all had a very high detection frequency in the samples analysed. In an intensive study conducted by Meffe and Bustamante [44] in Italy, 15 pharmaceutical contaminants were reported in a total of 161 emerging contaminants investigated in surface and groundwater. The maximum concentration of the pharmaceuticals in the surface water was 3,590 ng/L, whereas

only josamycin antibiotic was encountered in groundwater with a minimum concentration of 100 ng/L. Also, estrogens and illicit drugs appeared in surface water with a concentration below 50 ng/L. Nieto-Juarez *et al.* [12] provided a study on the level of pharmaceutical pollutants seen in municipal WWTPs (MWWTPs) in Peru and their effect on surface waters receiving the treated wastewater effluent. According to the authors, a total of 38 pharmaceutical drugs were detected using a Liquid Chromatography coupled with Mass Spectrometry (LC-MS/MS), out of which about 60% and 75% could be found in surface water and the MWWTPs. The most prevalent drug in the MWWTP samples was acetaminophen in concentration above 100 µg/L. Next to this was the anti-epileptic drug – gabapentin (11.85 µg/L) and antibiotics – ciprofloxacin, sulfamethoxazole, azithromycin, clarithromycin, and trimethoprim (1.86 – 4.47 µg/L). Whereas, in surface water, the acetaminophen remained the most prevalent of the drug but reduced to 28.70 µg/L, while sulfamethoxazole followed with a concentration of 4.36 µg/L. This study suggests that antibiotics are perhaps more recalcitrant pollutants in WWTPs.

A study conducted by López-Serna *et al.* [45] in Spain reported the occurrence of 72 pharmaceuticals in groundwater and 23 by-products. Antibiotics dominated the pollutant category with concentrations reaching as high as 1,000 ng/L. The concentration of the by-products was much lower than their corresponding parent compounds. The authors also noted that the concentration of the compounds in groundwater was as high or higher than those in the river, due to natural bank filtration from the river that received large amounts of effluents from WWTPs. Also, Mohapatra *et al.* [46] analysed the concentration of 12 commonly reported pharmaceutical drugs from WWTP effluents in India and USA in their study. It was discovered that the yearly average concentration in the Indian WWTP effluent was 50% higher than that of the USA. Also, compounds like carbamazepine, ibuprofen, sulfamethoxazole, ciprofloxacin, erythromycin, naproxen, and fluoxetine had >80% frequency of detection in both the inlet and effluent streams of the WWTP. The influence of the physicochemical properties of pharmaceutical compounds on their removal efficiencies in WWTP was studied by Behera *et al.* [47] in Korea. While analgesic acetaminophen, stimulant caffeine, and hormone estriol had over 99% removal efficiency with WWTP, antibiotic sulfamethazine and anti-epileptic carbamazepine had removal efficiencies below 30%. Acetaminophen, tramadol, carbamazepine, ibuprofen, diclofenac, 17 β-estradiol, and caffeine were among the 20 PhACs detected in 167 bottled water collected in France and other European countries according to a study conducted by Lardy-Fontan *et al.* [48]. The detection of these compounds was possible

with the aid of the highly sensitive isotope dilution-solid phase extraction-liquid chromatography-mass spectrometry method.

In Africa, pharmaceuticals have also been detected in the environment thus necessitating their removal according to research studies. For example, Verlicchi and Grillini [7] investigated the concentration of pharmaceuticals in surface waters from both South Africa and Mozambique and noted that these values were significantly higher than the concentration of similar drugs found in most European rivers. The prevalent compounds reported in their study are ibuprofen (84,600 ng/L), acetylsalicylic acid (159,900 ng/L), clozapine (78,300 ng/L), phenacetin (68,300 ng/L) and estriol (46,200 ng/L). The study also showed that higher concentrations of the pollutants were detected in winter than in summer, depending on the consumption pattern. In another study conducted in South Africa, efavirenz, nevirapine, carbamazepine, methocarbamol, bromacil, and venlafaxine were discovered in a river body [49]. Also, the highest concentration of these pollutants was recorded in the winter season.

These studies underscore the fact that water contamination from pharmaceutical residues is a pressing global problem. Generally, the concentrations of pharmaceutical residues are higher in WWTP effluents compared to freshwater bodies or receiving water channels. This is due to natural attenuation processes such as dilution, hydrolysis, adsorption, and photolysis [50]. While the implications of these contaminants on human health are still being explored, their presence in water bodies can potentially pose health risks [4,51,52]. A comprehensive report on the occurrence of PhACs has been summarised in Table 2.1, indicating their widespread presence in global water sources. The trace occurrence of the pharmaceuticals in the African context as against other developed societies may have been due to the lack of extensive research and poor detection capabilities in this region. Also, the amount of funding directed to this area of research in other regions may exceed that of Africa. In general, the consumption of PhCs has risen over the last decade globally and so is their release and discovery in the environment.

Table 2.1: Reports on the global occurrence of pharmaceutical residues in the environment.

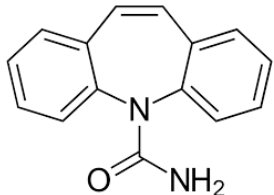
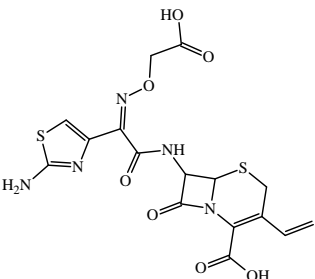
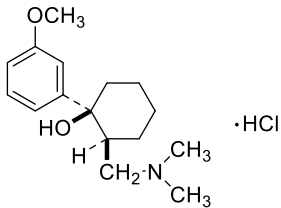
| Continent | Countries | Class of Pharmaceuticals | Pharmaceutical compounds/ metabolites | Concentration detected | Sources | References |
|-----------|--------------|---|--|------------------------|---|------------|
| Africa | South Africa | Antibiotics, antivirals, antiepileptic, stimulant | Ibuprofen, acetylsalicylic acid, caffeine, atenolol, phenacetin, carbamazepine, estriol, clozapine, nevirapine, efavirenz | 0.013 – 159 mg/L | Surface and ground water | [7,49] |
| | Mozambique | Antibiotics | Sulfamethizole, erythromycin, trimethoprim, clarithromycin | 0.005 – 53 mg/L | River | [53] |
| | Nigeria | Antibiotics, anti-inflammatory, antiepileptic, | Diclofenac, Azithromycin, carbamazepine, erythromycin, ibuprofen, sulfamethoxazole, naproxen | < 10 – 1100 µg/L | Domestic, industrial and hospital wastewater | [54] |
| Asia | Japan | Antibiotics, anti-inflammatory, antipsychotic, antiallergic agent, antiepileptic, analgesic, contrast agent, antiallergic | Tetracycline, carbamazepine, diclofenac, oseltamivir, iopamidol, epinastine, hydralazine hydrochloride, caffeine | NR | Drinking water | [55] |
| | China | Antibiotic, antipidemic, anti-inflammatory, anti-hypensive, anti-hypertensive, anticonvulsant, antipsychotic | Caffeine, N,N-Diethyl-meta-toluamide (DEET), diclofenac, clofibric acid, gemfibrozil, carbamazepine, ketoprofen, sulpiride, mefenamic, metoprolol, indometacin | 2.2 – 320 µg/L | Influent and effluent of WWTPs | [56] |
| | India | Antiepileptic, antihypertensive, antibacterials, analgesics, stimulant | Carbamazepine, atenolol, sulfamethoxazole, ibuprofen, acetaminophen, caffeine | NR | Activated sludge from WWTPs, hospital WWTPs, rivers and groundwater | [57] |
| | South Korea | Antibiotic, analgesics, antilipidemic, antihypertensive, | Acetaminophen, atenolol, lincomycin, sulfamethazine, metoprolol, carbamazepine, caffeine | > 10 µg/L | WWTPs | [47] |

| | | | | | | |
|---------------|---|--|--|-------------------|-----------------------|------|
| Europe | Malaysia | antiepileptic, stimulant, hormones, | Caffeine and diclofenac | 0 – 54 ng/L | River bodies | [18] |
| | France | Stimulants, NSAIDs Antibiotics, antiepileptic, anti-inflammatory, psychostimulants, non-steroidal drugs | Ciprofloxacin, diclofenac, ibuprofen, ketoprofen, naproxen, carbamazepine, norfloxacin, ofloxacin | NR | Surface water | |
| | Portugal | Anti-inflammatory | Acetaminophen, ketoprofen, hydroxyibuprofen, carboxyibuprofen | 89.7 – 1,227 ng/L | Seawater | [58] |
| | Spain | Anti-inflammatory, antiepileptic, lipid regulators, antibiotics | Acetaminophen, atenolol, bezafibrate, caffeine, carbamazepine, chlorpromazine, clofibrate, diclofenac, diphenyl hydantoin, fluoxetine, ibuprofen, ketoprofen, naproxen, salicylic acid, sulfadimetoxine, fluphenazine, trimethoprim and paraxanthine | 0.1 – 2,784 µg/L | Surface water | [59] |
| | Switzerland | Antibiotic | Clarithromycin | 57 – 330 ng/L | Treated WWTP effluent | [60] |
| North America | Croatia | Antibiotics | Sulfanomides, trimethoprim, fluoroquinolones, and macrolides | 2 – 20 µg/L | Municipal wastewater | [61] |
| | Hungary | Antidepressants, antiepileptics, anaesthetics, opioid, NSAIDs, stimulant | Carbamazepine, tiamotrigine, lidocaine, benzoylcegonine, tramadol, caffeine and cinolazepam | 2.6 – 38.41 ng/L | Drinking water | [62] |
| | United Kingdom | Antibiotics, anti-inflammatory | Clotrimazole, dextropropoxyphene, erythromycin, ibuprofen, propranolol, tamoxifen, and trimethoprim | 4 – 2,370 ng/L | Surface water | [63] |
| | USA | Anti-inflammatory, antiepileptics | Acetaminophen, carbamazepine, sulfadimetoxine, sulfamethoxazole, oxytetracycline, caffeine, tylosin | 24 – 1,340 ng/L | Surface water | [64] |
| | Canada | Stimulant | Caffeine | 0.2 – 5.9 ng/L | Lakes | [65] |
| Mexico | Anti-inflammatory, antiepileptics, lipid regulators | Ibuprofen, naproxen, diclofenac, acetaminophen, carbamazepine, gemfibrozil, ketoprofen | 0.4 – 123,000 µg/L | Raw wastewater | [66] | |
| Cuba | Antibiotics | Ampicillin, benzyl-penicillin, tetracycline | 1 – 11,400 µg/L | River | [67] | |

| | | | | | | |
|---------------|-------------|--|---|-----------------|----------------------------------|------|
| Oceania | Australia | Anti-inflammatory, antiepileptics, opioid | Codeine, paracetamol, tramadol, venlafaxine, fluoxetine, iopromide, carbamazepine | 0.9 – 67.1 µg/L | Marine water | [68] |
| South America | New Zealand | Anti-inflammatory | Acetaminophen and naproxen | 5.5 – 7.7 ng/g | Estuarine sites | [69] |
| | Brazil | Anti-inflammatory, lipid regulators | Gemfibrozil, bezafibrate, diclofenac and ibuprofen | 0.1 – 1 µg/L | Sewage treatment plant effluents | [70] |
| | Argentina | Anti-inflammatory, antiepileptics, stimulant | Diclofenac, ibuprofen, atenolol, carbamazepine, and caffeine | 0.03 – 42 µg/L | Wastewater effluent | [71] |

NR: Not Reported

Table 2.2: Physicochemical characteristics of the pharmaceutical compounds studied.

| Compound | Chemical structure | Molecular weight | Water solubility | Polarity | Acidity | Excretion | Toxicity report |
|---------------|---|------------------|------------------|----------|---------|---|---|
| | | g/mol | mg/L | Log P | pKa | | |
| Carbamazepine |  | 236.27 | 17.7 | 2.45 | 7.00 | 72% absorbed and metabolised in liver, 28% is excreted in faeces. | <ul style="list-style-type: none"> - Induces malformation in Zebra fish and larvae [72] - Carcinogenic in mice - Causes endocrine disruptions in human and aquatic animals - Affects the nervous system |
| Cefixime |  | 453.45 | 55.11 | 1.00 | 3.53 | 50% of the administered dose is excreted unchanged in urine [73] | <ul style="list-style-type: none"> - Antibiotic resistance may occur in humans - Can enhance the growth of antibiotic resistant bacteria [74] |
| Tramadol |  ·HCl | 263.38 | 20,000 | 1.35 | 9.41 | 70% metabolism by the body, 30% excreted as wastes [75]. | <ul style="list-style-type: none"> - Induces both genotoxic and cytotoxic effects on human lymphocytes [75]. - Affects the mobility of aquatic species, e.g. crayfish [76]. |

2.2 Classification of pharmaceutical residues found in water and wastewater sources

A list of the classes of some of the pharmaceutical residues commonly detected in the environment has been provided in Figure 2.2. Over the last decades, antibiotics have emerged as a novel category of contaminants causing concern due to their implications for both human health and aquatic ecosystems [53]. They are among the most dispensed drugs, playing a crucial role in both human and veterinary medicine. The global consumption of antibiotics is estimated to be between 100,000 and 200,000 tons annually [77]. Iran is tipped as one of the biggest consumers of this pharmaceutical class, consuming twice as much as Australia [78,79]. After consumption by humans or animals, these drugs undergo partial metabolism, with the resultant metabolites being excreted through urine and faeces. However, due to their high toxicity and persistence in the environment, both human beings and aquatic species can be exposed to antibiotics over a prolonged period. Another concern is their ability to promote antibiotic resistance in microbial communities which also inhibits their bacterial breakdown [80]. The common antibiotics have been reported in Figure 2.1. The presence of antibiotics in different water cycles has been extensively discussed in numerous studies [12,81,82]. Another significant class of pharmaceuticals that have been commonly investigated are the Non-Steroidal Anti-Inflammatory Drugs (NSAIDs). These are recognised for their pain relief and anti-inflammatory benefits [83]. Medications like ibuprofen, acetaminophen, diclofenac, and naproxen are some of the notable NSAIDS reported in literature and found to exist even in drinking water. Due to their immediate relief services, NSAIDS are sometimes purchased over the counter and abused, increasing their consumption rate and detection in the environment.

Additionally, clofibric acid, gemfibrozil, and bezafibrate used to regulate blood lipids, have been detected across water sources and this is attributed to their persistence and mobility in water. Antiepileptic drugs are a group of pharmaceuticals used to treat people with epilepsy, seizures, and other mental cases. Among the antiepileptic drug category, carbamazepine is considered the most consumed. According to Hai *et al.* [84], about 28% of the parent carbamazepine drug that is consumed is excreted through urine and faeces unchanged. Meanwhile, due to its high consumption rate, low biodegradability, and low removal efficiency in WWTPs, it is commonly detected in water sources. Some hormones and veterinary

medicines, including 17 β -estradiol and estrone, have been identified in several water bodies [66]. This has also raised concerns about their potential impact on aquatic life. The other classifications are mentioned in Figure 2.2.

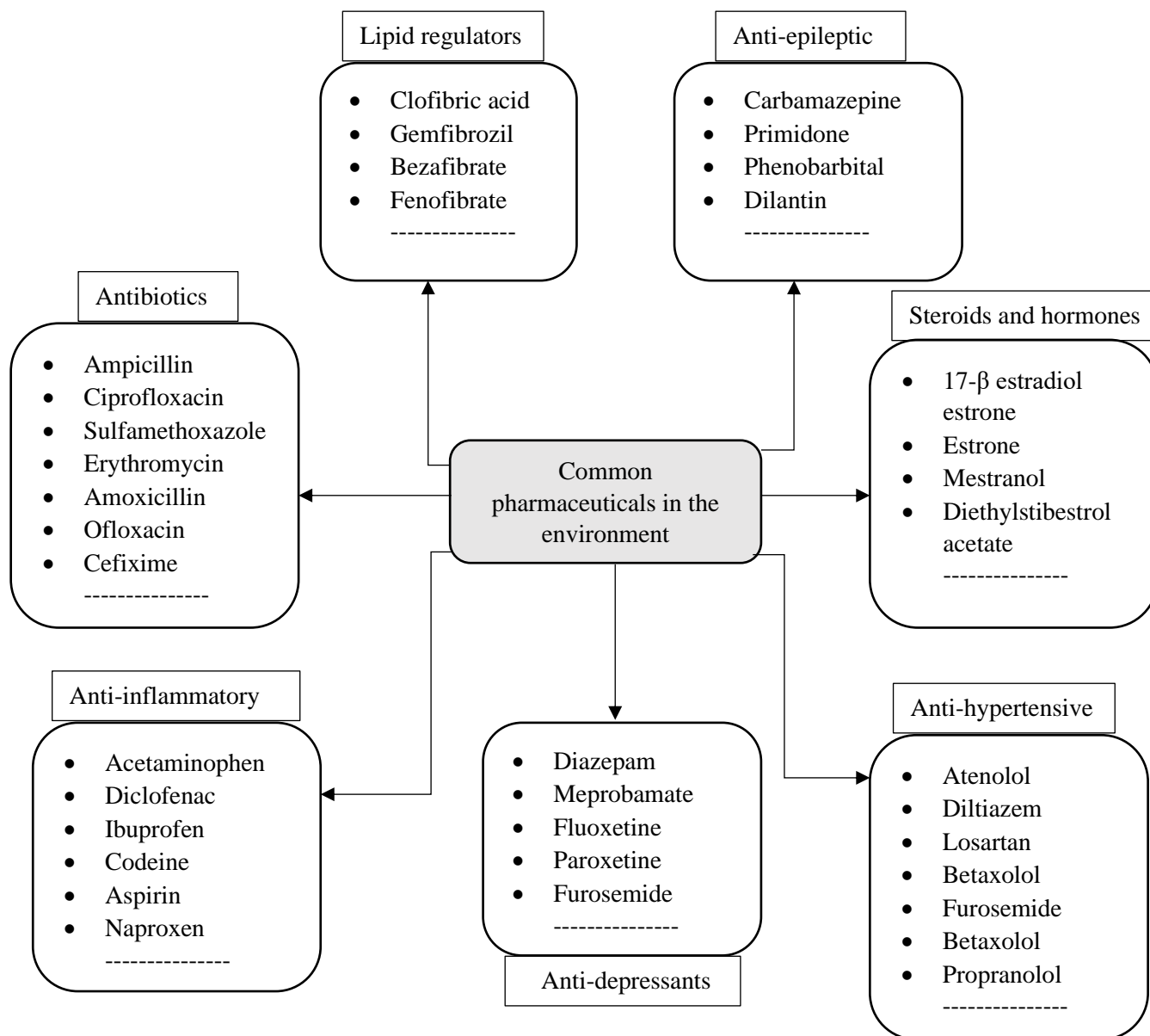


Figure 2.2: Common classifications of pharmaceuticals found in water and wastewater [85].

2.3 Pharmaceuticals considered in this study

Tramadol is an opioid, used primarily to alleviate moderate to severe pains. Only about 70% of the parent compound is used up, yielding metabolites like N-desmethyl-tramadol (N-DES-) and O-desmethyl-(O-DES-)[75]. Tramadol comes in white or almost white, crystalline powder. It is freely soluble in water and in methanol, but slightly soluble in acetone. It has a dissociation constant, pKa of 9.41. The chemical structure of tramadol and some details on its toxicity are provided in Table 2.2. Concentrations up to 1,116 ng/L and 100 ng/L have been detected in WWTPs and surface water, respectively [75]. Chapter 3 has been dedicated to its removal with various technologies including the DBD developed for this study.

Cefixime is a third-generation cephalosporin antibiotic. It works against gram-positive microbes and shows effectiveness against certain gram-negative bacteria like *Escherichia coli* [86]. CFX is prescribed for ear infections, upper and lower respiratory tract infections, urinary tract infections, and gonorrhoea. Cefixime is a white to light yellow, crystalline powder. It has a molecular weight of 453.454 with a chemical structure shown in Table 2.2. CFX is insoluble in water, but slightly soluble in alcohol. Due to its indiscriminate usage, continuous input, and persistence in various environmental matrices, it has become an emerging pollutant being monitored in water [74]. Chapter 4 provides more details on the removal of the contaminant in water with the DBD reactor.

Carbamazepine is commonly prescribed for treating various seizures and pain resulting from trigeminal neuralgia. It is also effective in managing partial onset seizure epilepsy, mixed episodes of mania and depression, alcohol withdrawal symptoms, and restless legs syndrome. The chemical structure of CBZ can be found in Table 2.2. The appearance of CBZ is a white or near-white crystalline powder. Its solubility in water is quite low, with reported values ranging from 0.112 – 35 mg/L, and being a nonpolar substance, its acid dissociation constant stands at pKa = 7.0 [87]. While it remains stable in environmental conditions and isn't highly soluble in substances like ethanol or acetic acid, it does dissolve in methanol, chloroform, dimethylformamide, and ethylene glycol monomethyl ether. Typical concentrations of CBZ include 1,075 – 6,300 ng/L in WWTP effluent [88], 81 – 1,100 ng/L surface water [89], and 425 – 3,600 ng/L [90]. The common metabolites of CBZ include CBZ-epoxide, CBZ-diol, CBZ-acridan, 2-OH-CBZ, 3-OH-CBZ [84]. Chapter 5 provides more details on the removal of

the CBZ with the DBD reactor and a comparison of the performance of the reactor with UV-based systems.

2.4 Challenges affecting the detection of pharmaceutical contaminants.

It is critical to detect and quantify pharmaceutical pollutants for effective risk assessment, regulatory compliance, and the development of mitigation methods. However, due to their low concentrations, various chemical characteristics, and the complexity of environmental matrices, pharmaceutical pollutants pose significant obstacles to detection. This section dives into the complexity of detecting pharmaceutical pollutants in water and the environment, focusing on the technical, analytical, and logistical issues encountered by regulatory authorities and researchers. Also, advanced analytical techniques which have been recently used are discussed.

2.4.1 Low concentrations

The existence of pharmaceutical pollutants at trace levels in environmental samples is one of the most difficult issues affecting their detection [48,91]. Many drugs permeate the environment at amounts far lower than those seen in medical applications. As a result, existing analytical methods may be insufficiently sensitive to detect these chemicals. Also, the low concentration of pharmaceutical pollutants can lead to a diminished signal-to-noise ratio in analytical measurements [92]. This can result in the potential for false positives or the inability to distinguish between the target compound and background noise. Background interference is mostly caused by the presence of other organic and inorganic compounds in water samples during analysis. To minimise this interference and enhance detection accuracy, proper sample preparation and pre-treatment steps are essential [93].

2.4.2 Chemical properties

Also, pharmaceutical contaminants in water exhibit a wide range of chemical properties that significantly influence their detection and removal processes. These properties, which include solubility, polarity, stability, and reactivity, also play a crucial role in determining the efficacy of analytical techniques and treatment methods [17]. Understanding how these chemical

properties impact detection is essential in creating tailored solutions to address pharmaceutical pollution in water systems.

The solubility of pharmaceuticals increases their detectability. Highly water-soluble chemicals may be present in greater amounts in water samples making their identification easier. Conversely, poorly water-soluble compounds might require specialised extraction methods to transport them from the solid phase to the liquid phase for analysis. The solubility also affects the sensitivity of detection methods, as compounds with low solubility might be present at lower concentrations and thus require more sensitive procedures. Also, solubility influences the extent to which pharmaceutical contaminants are partitioned between the aqueous and solid phases during treatment operations. Highly water-soluble contaminants are more likely to remain in the treated water effluent, whereas less soluble compounds might be adsorbed on solid particles and removed via sedimentation or filtration processes.

Polar drugs are more easily detected by utilizing chromatographic procedures that rely on interactions with polar stationary phases [70]. Techniques like high-performance liquid chromatography (HPLC) can effectively separate and quantify polar compounds. Hydrophobic compounds, on the other hand, might require reverse-phase chromatography or solid-phase extraction to improve retention and separation [70]. Coagulation, flocculation, and traditional activated sludge treatment can all be used to successfully remove polar contaminants [94]. These approaches, however, may be less effective at removing hydrophobic substances. Because of their heightened affinity for hydrophobic surfaces or increased susceptibility to oxidative breakdown, advanced treatment procedures such as adsorption onto activated carbon or advanced oxidative processes may be more suitable for eliminating hydrophobic pharmaceuticals.

The stability of pharmaceutical substances affects their detectability over time. Compounds that degrade quickly may require rapid sample collection and analysis to ensure accurate quantification. The choice of detection methods is also influenced by stability, as chemicals prone to degradation may require sensitive and rapid techniques like the LC-MS or GC-MS to identify their presence before they degrade. In addition, the reactivity of pharmaceuticals influences their susceptibility to degradation during treatment processes. Compounds with high reactivity might transform into breakdown products that are less harmful or more easily

removed. Thus, AOPs such as ozonation, photocatalysis, and plasma, take advantage of the reactivity of pharmaceuticals to break them down into simpler and less persistent compounds.

2.5 Detection methods for pharmaceutical residues

The technical chemistry community faces challenges in developing dependable and verified quantitative methods and resources to detect PhACs, aiming for global laboratory applicability. The primary approach to analysing these organic pollutants in various environmental matrices revolves around chromatographic separation and mass spectrometry identification. Before any analysis, preliminary treatment steps like filtration, pH adjustments, structural separation, and sample intensification are usually essential [95]. In the next subsections, some of the commonly used advanced analytical tools used for the detection of PhACs are discussed. A detailed overview of the method development for commonly reported pharmaceuticals has been reported by Kang [96].

2.5.1 Liquid Chromatography-Mass Spectrometry (LC-MS)

The LC-MS is a versatile instrument used for the identification and quantification of pharmaceutical pollutants in various environment matrices, including water, soil, sediments, and biota [96]. It combines the separation capabilities of liquid chromatography (LC) with the sensitive and selective detection of mass spectrometry (MS). In the LC component, a liquid mobile phase carries the sample through a stationary phase packed inside a chromatographic column. The different compounds in the sample interact differently with the stationary phase, leading to their separation based on their chemical properties, such as polarity, size, and affinity. After separation by LC, eluent (liquid exiting the LC column) is introduced into the mass spectrometer. In the MS, molecules ionised into charged particles (ions) and separated based on their mass-to-charge (m/z). The detector then records the intensity of these ions, generating mass spectra.

The LC-MS has been coupled with MS in the detection of various PhACs with high sensitivity (even at parts per trillion) in complex environmental matrices. For instance, Patel *et al.* [97] coupled LC-MS/MS to detect tramadol metabolite in the human plasma, measuring as low as 0.5 ng/mL concentration. However, some challenges exist with its operation. For example,

complex environmental matrices can lead to matrix effects, which may interfere with the ionization and detection of target pharmaceuticals. Also, method development is required for each pharmaceutical compound in most cases, and this can be time-consuming, as it may require optimization.

2.5.2 Gas Chromatography-Mass Spectrometry (GC-MS)

The GC-MS is a highly sensitive instrument capable of detecting PhACs at low concentrations, often in the parts per billion (ppb) or even more. It combines two analytical techniques, Gas Chromatography (GC) and Mass Spectrometry (MS). In the GC component, a gaseous mobile phase carries the sample through a capillary column with a stationary phase [98]. Compounds in the sample are separated based on their volatilities and interactions with the column, resulting in a chromatogram that represents the distribution of compounds over time. After separation by GC, the effluent is introduced into the mass spectrometer. The MS ionises the separated molecules into charged ions, which are then sorted and detected based on their mass-to-charge ratio. The resulting mass spectrum provides information about the molecular structure and identity of the compounds. GC-MS is mostly suitable for non-polar pharmaceutical compounds, as polar compounds may not efficiently partition into the gas phase. Also, it requires sample preparation which includes extraction of compounds into suitable solvents before analysis.

2.5.3 High-Performance Liquid Chromatography (HPLC)

The HPLC is a widely used analytical technique for the detection and quantification of pharmaceutical pollutants in environmental samples. It offers several advantages and has specific applications in monitoring and studying the presence and behaviour of pharmaceutical contaminants in the environment. Its mechanism is based on the LC technique, described in the previous section but in this case without the MS. The separation of the compounds occurs based on their differential interaction with the stationary phase. The key components in the HPLC system are a high-pressure pump, injector, column, detector, and data acquisition system. Unlike the LC-MS, it is capable of analyzing a wide range of PhACs, including polar and non-polar compounds. It also requires less extensive sample preparation compared to GC-MS systems. However, just like the LC-MS it requires method development and optimization for

specific analytes and sample types. Also, some compounds may require specialised detectors for enhanced detection sensitivity. Generally, the detectors coupled with a HPLC can be broadly classified into bulk property and solute property detectors, and their key distinction lies in whether the detector is measuring properties that represent the entire sample (bulk property) or properties specific to individual components within the sample (solute property) [99].

Bulk property detectors like refractive index detectors and electrical conductivity detectors assess alterations in both solute and mobile phase collectively. These detectors exhibit variations in readings even with minor adjustments in the mobile phase composition. However, despite their broad applicability, they are utilised less frequently due to inadequate sensitivity and restricted range. On the hand, solute property (or selective) detectors offer responses based on the specific physical or chemical properties of the analyte [99,100]. These detectors are designed to be independent of the mobile phase and are particularly useful when specific identification and quantification of individual solutes are required. Common examples of solute property detector include UV-Visible detectors, diode array detectors, fixed wavelength detectors, fluorescence detectors, infrared detectors, and mass spectrometry detectors [101].

2.5.4 Ultra-Performance Liquid Chromatography (UPLC)

UPLC operates on the same fundamental principles as the HPLC, but the notable difference is that it has a high resolution and faster analysis. Like the HPLC, it uses a liquid mobile phase to convey the sample through a column packed with a stationary phase. The separation of the compounds is based on their differential interactions with the stationary phase. However, the UPLC employs columns with smaller sizes, which results in reduced plate heights, leading to higher efficiency than the chromatographic resolution. In addition to its high sensitivity and efficiency, UPLC offers very quick analysis which aids high sample throughput in environmental monitoring. The major challenge however with this instrument is its high cost, which is usually more than conventional HPLC systems.

2.6 Conventional wastewater treatment

It is important to examine the series of methods that make up conventional WWTPs because they are the primary channels through which PhACs enter the environment. A typical WWTP is made up of a series of primary, secondary, and occasionally tertiary treatment procedures that can remove a variety of impurities from wastewater streams. These processes have been effective in treating traditional contaminants such as suspended and colloidal particulate matter, nutrients, dissolved organic matter, and pathogens [102]. The WWTP treatment process is usually a combination of physical separations, as well as chemical and biological reactions. Generally, the performance of water treatment technologies largely depends on the nature of the targeted contaminants and their physicochemical characteristics some of which include the hydrophobicity, dissociation constant, and so on, as described in the previous section [17]. In most cases, WWTP faces significant limitations in handling emerging water contaminants like pharmaceuticals because they are neither designed nor optimised to handle such micropollutants [21,103,104]. In some cases, a negative removal efficiency has been reported for some pharmaceuticals (like sulfamethoxazole) where the concentration in the effluent surpasses the influent stream concentrations [105]. The reason for this is that drugs are excreted via urine and faeces as either the parent compound or their metabolite and some metabolites return to the parent form within the WWTP process.

Usually, a typical conventional WWTP setup begins with primary treatment such as screening and sedimentation. These only remove the large solids and particulate matter contained in wastewater. Some researchers like Boiteux *et al.* [106] and Sun *et al.* [107] have observed an unsatisfactory removal of micropollutants like perfluoroalkyl and polyfluoroalkyl substances at the primary treatment stage of a WWTP. Even with the addition of a flocculant, Ternes *et al.* [108] also reported that the removal efficiency for pharmaceuticals like diclofenac, clofibrac acid, carbamazepine, and bezafibrate was insignificant. To improve the efficiency of ECs in the primary treatment section, a physicochemical process like the sorption method has been adopted, considering that the existing setup is only able to remove less than 10% of most compounds in the influent wastewater stream [109]. The mechanism for sorption involves both the absorption of the compounds onto the lipid fraction of the primary sludge via hydrophobic interactions and the adsorption of the compounds onto the surface of the sludge through electrostatic interactions [110]. The sorption of ECs is largely dependent on the

physicochemical properties of the contaminants, characteristics of the adsorption media, and operating environmental conditions [17].

The challenge with sorption however is that it is only a phase-changing technology, where the contaminant in the liquid phase (wastewater) is transferred into a solid phase (sludge) providing temporary water purification [111]. There is a need to further treat the sludge as this could create secondary pollution if not properly handled. Therefore, sorption-based treatment methods can only be sustainable if or when integrated with other contaminant degradation technologies. Also, the adsorbent often becomes saturated and requires regeneration or replacement over time. Some adsorbents can be selective, limiting their applications to a broad range of contaminants.

The secondary treatment stage is aimed at removing organics and nutrients through biological degradations. In this case, the contaminants undergo a series of processes like biodegradation, sorption, dispersion, dilution, photodegradation, and volatilization. Of these, the most significant mechanism aiding the removal of ECs is biodegradation [112]. The photodegradation process is dependent on adequate light exposure, and it is affected by the blockage of sunlight by highly concentrated particulate matter [113]. Also, the volatilization of contaminants is controlled by Henry's law constant (k_H) [114]. A high k_H in the range of 10^{-2} – 10^{-3} atm m³/mol signifies high volatilization, whereas k_H values less than 10^{-7} like those reported for pharmaceuticals like azithromycin, erythromycin, diclofenac, ibuprofen, carbamazepine, indicate insignificant volatilization [115].

Generally, biological treatment involves the use of microorganisms like algae, fungi, and bacteria to degrade high molecular weight substances into smaller substances. In this process, the microbes consume the organic substances for their cell growth thus enhancing the biodegradation of pollutants. Different secondary wastewater treatment technologies like activated sludge process, trickling filters, moving bed biological reactor (MBBR), biological aerated filters (BAF), fungal bioreactor, and microalgal bioreactor, have been employed in literatures [12,116,117]. The activated sludge process (ASP) is the most common and promising biological method used for the removal of ECs from wastewater [118]. It involves the microbial biodegradation of contaminants in an aeration tank [119]. A study by Ahmed *et al.* [109] reported above 65% removal efficiency for pharmaceuticals using ASP.

Kasprzyk-Hordern *et al.* [90] investigated the removal of 55 pharmaceuticals, personal care products, endocrine disruptors, and other illicit drugs using ASP and trickling bed filters. The authors observed <70% removal efficiency for all 55 compounds with trickling bed filters and >85% removal efficiency for the ASP. About 30 – 75% of anti-inflammatory drugs and antibiotics have been removed through biological treatment [120]. However, there have been reports that Carbamazepine cannot be removed by WWTPs [10,121]. Despite its huge potential, the challenge with the biological degradation process is that it depends on the toxicity of the contaminants being consumed or that of their byproducts. These reasons necessitate a tertiary treatment technology to completely degrade organic pollutants into less toxic byproducts.

2.7 Advanced oxidation processes as a tool for the removal of pharmaceuticals

Advanced oxidation processes (AOP) encompass a diverse array of activation techniques and oxidant generation methods, each employing unique mechanisms for organic pollutant breakdown. A comprehensive overview of the existing and emerging AOPs is illustrated in Figure 2.3 [122]. Among the processes listed, there is a varying range of maturity, spanning from widely accepted AOPs to those still in the exploratory phase. The core of all AOPs can be distilled into two phases: in situ generation of reactive species and their subsequent interactions with the targeted organic pollutants. The mechanisms underpinning radical generation are influenced by specific process parameters and can be further optimised based on system design and the quality of the water being treated. Apart from radical scavenger influences, other factors like radical mass transfer in surface-focused AOPs and fluid dynamics significantly impact the efficiency of the pollutant elimination process. In the subsequent sections, a few of the commonly reported AOPs used for pharmaceutical degradation will be discussed (the categories highlighted in Figure 2.3) including their mechanisms and the principles driving their radical formation. Some of the limitations of the existing AOPs will also be highlighted.

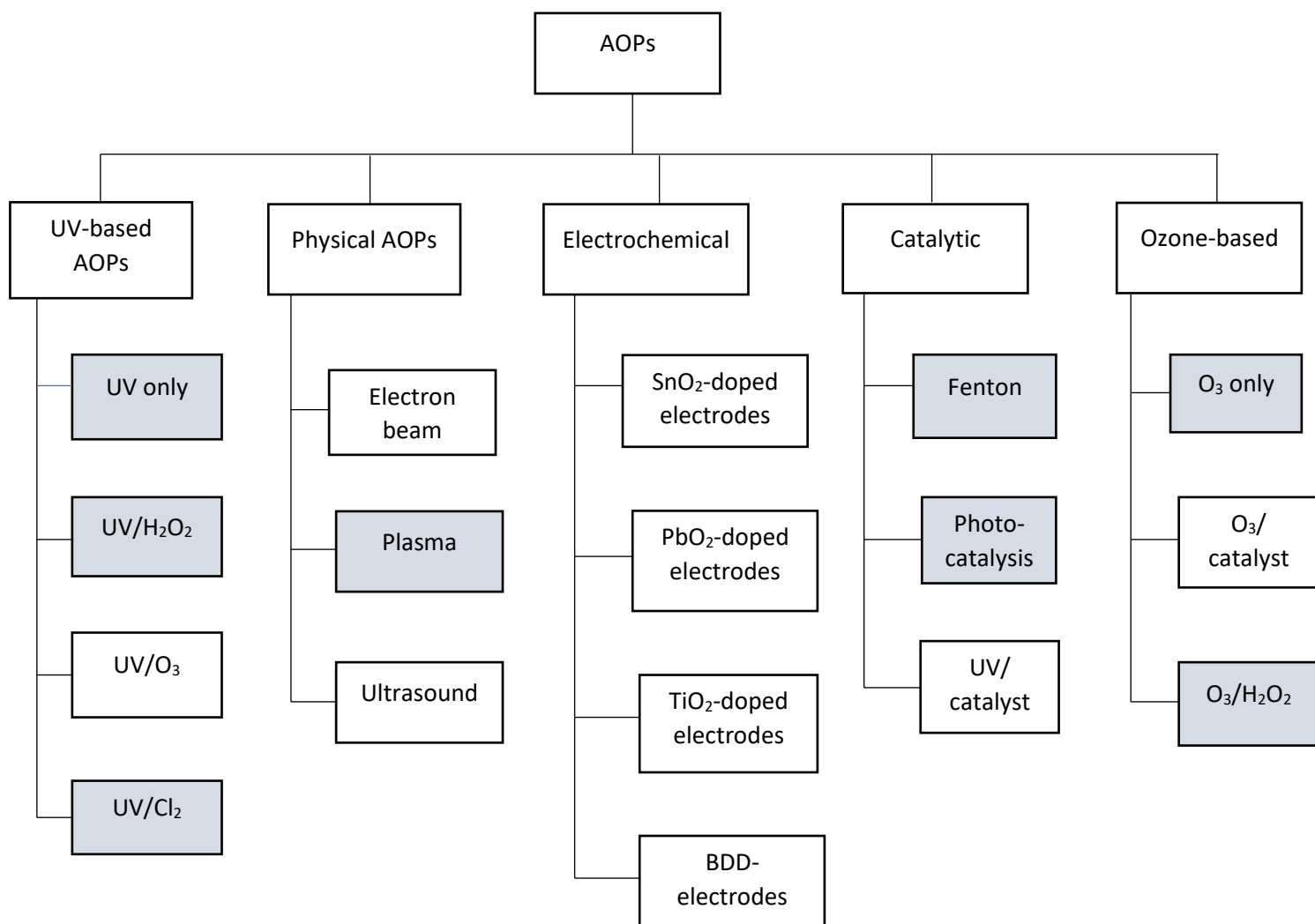


Figure 2.3: Classification of advanced oxidation processes [122].

2.7.1 UV and UV-assisted processes

UV photolysis involves the use of ultraviolet light to break down pharmaceutical contaminants in water. During this process, pharmaceutical pollutants absorb UV light (usually UV-C with wavelength 254 nm), which provides the energy needed to break chemical bonds within the molecules [123]. As a result, reactive intermediates are formed, which can break down into simpler, less hazardous chemicals. The UV procedure is however selective because it seeks molecules with chromophoric groups that can absorb UV light. In other words, compounds with weak or no UV absorbance may not be efficiently degraded. According to Luo *et al.*

[124], the crucial parameters that influence the degradation kinetics under direct photolysis are rate constants, quantum yield, and molar extinction. There are however AOPs that combine UV with oxidizing species like Cl_2 , H_2O_2 , O_3 , and so on.

The combination of UV/ Cl_2 offers a synergistic approach to addressing pharmaceutical contaminants in water. By enhancing the individual strengths of both UV and chlorine, this process delivers enhanced oxidation capabilities, making it an effective and versatile solution. UV light initiates the photodegradation of the contaminants, while chlorine acts as a powerful oxidant, contributing to the degradation process. The interaction between UV light and chlorine generates $\bullet\text{OH}$ along with reactive species like Cl^\bullet and Cl_2^\bullet [125]. Cl^\bullet is, however, a more selective oxidant than $\bullet\text{OH}$ since it favours electron-rich contaminants. The UV/ Cl_2 process is effective against a diverse range of pharmaceutical contaminants, regardless of their chemical structures or properties. In addition to the removal of the contaminants, chlorine also acts as a disinfectant in this process, eliminating microbial organisms in the water. This process, however, is favoured at lower pH values [126]. UV/ Cl_2 has been successfully used in improving the degradation of PhACs like chloramphenicol [127], carbamazepine [128], ronidazole [129], and some lipid regulators [130]. These studies highlighted the important role of chlorine oxide radical formed in the UV/ Cl_2 process.

The UV/ H_2O_2 process is used in a variety of applications, such as municipal water treatment plants, industrial effluent treatment, and advanced water purification systems. It also represents a dynamic and efficient approach to tackling the challenge of pharmaceutical contamination in water. The UV light activates H_2O_2 by initiating its photolysis to generate $\bullet\text{OH}$ which oxidises the pharmaceutical compounds. For example, a UV/ H_2O_2 system was applied to completely degrade cyclophosphamide drug in tap water within 60 mins treatment time [131].

Some studies have compared UV-based systems based on their performance and operating costs. For instance, Cobo-Golpe *et al.* [132] compared the performance of UV-only, UV/ H_2O_2 , and UV/ Cl_2 systems in the removal of tramadol and their transformation products. At neutral pH, the authors reported that UV in combination with free chlorine proved to be the most effective removal method, with a rate constant of 0.3785 min^{-1} compared to 0.2005 min^{-1} recorded for UV/ H_2O_2 . This was said to be due to the higher molar absorptivity of chlorine compared to H_2O_2 . Meanwhile, direct photolysis of tramadol had the lowest rate of removal

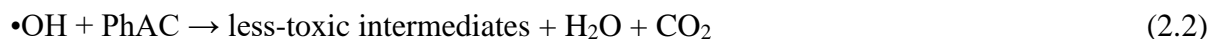
(0.045 min⁻¹). However, the transformation product from UV/Cl₂ appeared to be more toxic than those of UV/H₂O₂. Miralles-Cuevas *et al.* [133] also noted from an economic point of view that a UV/H₂O₂ system has a lower operating cost compared to other UV-based systems like UV/S₂O₈²⁻, solar/Fe²⁺/H₂O₂ and solar/Fe²⁺/S₂O₈²⁻ for the elimination of pharmaceuticals like carbamazepine, antipyrine, caffeine, ciprofloxacin and sulfamethoxazole.

2.7.2 Fenton process

The Fenton process is a highly effective and widely used AOP for removing pharmaceutical toxins and other organic pollutants from water and wastewater. It involves the generation of hydroxyl radicals (•OH) through the reaction between Ferrous iron (Fe(II)) and hydrogen peroxide (H₂O₂) under acidic conditions [134,135]. The generated •OH are highly reactive and can initiate both homogenous and heterogeneous reactions. In a homogeneous Fenton reaction, both the reactants (Fe (II) and H₂O₂) and the •OH are present in the aqueous phase [136]. Whereas, in a heterogeneous Fenton reaction, the Fe (II) catalyst is adsorbed on a solid surface while both H₂O₂ and the contaminant are present in the liquid phase. In this case, the surface-bound Fe (II) therefore catalyses the decomposition of H₂O₂ to generate on the catalyst surface, which then reacts with the contaminants present in the liquid phase [137].

The mechanism for Fenton reaction is represented in Eq. (2.1) and (2.2). The efficiency of this process is strongly influenced by pH, initial concentration of the pollutant, temperature, H₂O₂ dose, and amount of catalyst, amongst others [134,138,139]. To start with, the ratio of Fe (II) and H₂O₂ is essential for the efficient generation of •OH. Excess concentration of H₂O₂ can lead to the reduction of Fe³⁺ to Fe²⁺. Also, studies have reported the efficiency of a Fenton reaction to be between 3 and 4 [140]. It was reported that the optimal pH for which Fe can effectively function as a catalyst during antibiotic degradation reaction is 3 [141]. A similar observation was reported for paracetamol [142]. At higher pH, precipitation of ferric oxyhydroxide may occur. Thus, in most cases, Fenton reaction is restricted to acidic conditions to avoid precipitation. Also, Houtman [143] noted that the degradation efficiency of a Fenton-based reaction increased with temperature, but not beyond 40 °C. One intrinsic advantage of the Fenton process is its low cost and easy recovery of the residual iron. For these reasons, it has gained interest in industrial applications. However, more research studies are needed to overcome the low acidic conditions required for the Fenton as well as photo-Fenton processes.

By finding a solution to the ‘traditional’ conditions required, the kinetics and degradation efficiency will be significantly enhanced. Thus, more studies are required in various water matrices and over a wide range of pH.



2.7.3 Ozonation and O₃-assisted processes.

Ozone (O₃) has been traditionally employed in water treatment as both an oxidizing agent and disinfectant. As an oxidant, O₃ primarily attacks electron-rich functional groups such as double bonds, amines, and activated aromatic structures [122]. Considering that its reaction in real solutions typically results in the generation of hydroxyl radicals (•OH), it can also offer degradation benefits over a range of pharmaceutical contaminants [34]. The production of •OH can arise from ozone’s reaction with hydroxyl ions (OH⁻), although this is a relatively slow process with a second-order rate constant (70 M⁻¹s⁻¹) [122]. Nevertheless, it should be noted that the decomposition of ozone into •OH can significantly enhance the degradation of pollutants because •OH has about 10⁶ to 10¹² times more oxidizing strength than ozone [144].

Ozone and its combinations with H₂O₂ (O₃/H₂O₂) and UV light (O₃/UV) have been utilised to address pharmaceutical pollution in water either as standalone treatment methods or as a preparatory step preceding other procedures. O₃/H₂O₂ is otherwise called peroxone process and it produces •OH. A study conducted by Wang *et al.* [145] reported the application of conventional O₃ conventional peroxone (O₃/H₂O₂) for the removal of 5 common pharmaceuticals (diclofenac, clofibric acid, ibuprofen, bezafibrate, p-CBA, and gemfibrozil) in various water matrices. Initially, O₃ was able to decompose faster in the surface water (SW) because it had more dissolved organic matter than groundwater (GW) and secondary effluent (SE). Meanwhile, at specific O₃ dosages (maximum of 1.5 mg O₃/mg) the addition of H₂O₂ increased the yield of •OH by about 5 – 12% decomposition of O₃ in the GW and 5 – 7% in SW and negligibly in the SE. This ozone-assisted method enhanced the degradation of ozone-resistant pharmaceuticals (ibuprofen and clofibric acid) in both GW and SW. The advantage of the peroxone process is that less ozone would be consumed, thus decreasing the operating cost.

The addition of metal iron foam to the conventional ozonation process in the treatment of pharmaceutical wastewater was explored by Huang *et al.* [146]. Within a reaction time of 2 h, the iron foam combined with ozonation yielded a 53% removal rate for the dissolved organic carbon which was about 21% higher than the conventional ozonation system. Iron in this medium acted as a catalyst to facilitate the generation of free radicals ($\bullet\text{OH}$) and some O-based species which can rapidly mineralise the targeted organic contaminants. In the process, iron was oxidised into iron oxides and oxyhydroxides. Another study on catalytic ozonation was reported by Pelalak and co-workers using iron-based goethite nanoparticles [147]. Meanwhile, heterogeneous catalysts like ZnO, TiO₂, and MnO₂ can also be used to improve an ozonation process.

While ozonation is possible with pharmaceutical parent compounds, in some cases, ozone has been unable to further degrade the metabolites formed. For example, Kharel *et al.* [148] reported the difficulty in the degradation of Epoxy-carbamazepine, Di-OH-carbamazepine, and *N*-desmethyl tramadol metabolites compared to their parent compounds. To get rid of the transformation products, the authors used a granulated activated carbon (GAC) filter. Aziz *et al.*, [149] also reported a poor mineralization efficiency for the ozonation system used in the degradation of diclofenac and ibuprofen, compared to other AOPs investigated. Therefore, one of the major challenges with the use of an ozonation system is that the parent compounds are usually not completely mineralised in the aqueous solution, so there could be a need to add other removal techniques to enhance their applications in water treatment. However, the economic viability of such combined methods needs to be examined for wider acceptance. Also, ozone is a selective oxidant, meaning it doesn't equally oxidise all compounds. Factors such as pH, ozone dosage and temperature play vital roles in ozone application in water treatment. Due to its short half-life, high dosage of ozone is usually necessary to react with the target contaminants. From an industrial perspective, ozonation methods are energy intensive and this makes their deployment commercially challenging.

2.7.4 Photocatalytic processes

A photocatalysis process uses semiconductors with minimal energy gaps that become excited upon exposure to photons from a light source (e.g. visible, UV, LED) [150]. When these photons have energy surpassing the semiconductor's energy gap, they induce the formation of

electron-hole pairs [151]. Subsequently, these produced holes (h^+) interact with water to produce $\bullet OH$, which then engages with organic pollutants breaking them down into less toxic byproducts [152]. Research into the utilization of photo-activated catalysts for water purification has gained significant attention in the past years [153–155]. While a variety of photocatalysts exists, most studies have focused on two primary reactions: homogeneous photo-Fenton process and heterogeneous photocatalysis. Also, the degradation or mineralization efficiency depends on the efficiency of a catalyst, light variety, pH of the solution, and water composition.

The photocatalytic degradation of carbamazepine, acetaminophen, and ibuprofen was compared using TiO_2 under UV light and UV-vis light as reported by Dudziak *et al.* [156]. This study showed that the rate constant for carbamazepine was highest under the UV-vis light but next to ibuprofen in the UV light. Meanwhile, acetaminophen had the lowest rate constants under these two light sources. Gao *et al.* [157] reported the photocatalytic degradation of the antiepileptic drug carbamazepine using bismuth oxychlorides (BiOCl). The rate of the reaction was dependent on the pH, catalyst dosage, and initial concentration of the pollutant investigated. Meanwhile, Meribout *et al.* [158] compared the efficacy of BiOCl and BiOCl/AgCl composites in the degradation of carbamazepine in water. BiOCl/AgCl was observed to be more efficient in the degradation of carbamazepine due to its higher photocatalytic activity under visible light than BiOCl.

A study on the photocatalytic degradation of cefixime trihydrate was reported by Shooshtari and Ghazi [159] using nano $\alpha Fe_2O_3/ZnO$. Under optimised conditions of $8 W/m^2$ UV-vis light intensity and $0.41 g/L$ catalyst concentration, 99.1% degradation of the pharmaceutical contaminant was recorded in 127 min irradiation time. Rahman *et al.* [160] applied a CuO-NiO nanocomposite photocatalyst to degrade cefixime in water. The degradation efficiency recorded was 90% with a rate constant of $7.4 \times 10^{-3} min^{-1}$. Meanwhile, the degradation of cefixime was greatly enhanced by catalyst dosage and at lower pH. In a recent study by Kazemi *et al.* [161], the performance of three photocatalysts (bismuth ferrite, cobalt-doped bismuth ferrite, and $\alpha-Fe_2O_3@phosphotungstic$) was compared for the degradation of tramadol in water. The degradation efficiency recorded for bismuth ferrite, cobalt-doped bismuth ferrite, and $\alpha-Fe_2O_3@phosphotungstic$ was 81.1% at 120 min, 90.63% at 80 min, and 92.32% at 80

min, respectively. Thus, the efficacy of cobalt-doped bismuth ferrite and α - Fe_2O_3 @phosphotungstic in the degradation of tramadol were demonstrated.

Despite the intense research focus on photocatalysis, its application in large-scale industrial or urban water treatment systems remains limited, primarily due to its suboptimal efficiency in generating $\bullet\text{OH}$. Also, the recovery of the catalyst from the solution after treatment is usually an issue of concern.

2.7.5 An overview of the plasma process

For decades, the fundamental states of matter have been universally acknowledged as solid, liquid, gas, and plasma. Plasma, often regarded as the fourth state of matter, is generated when atoms and molecules within a gas are subjected to ionization, dissociation, and excitation, resulting in the release of energetic electrons, ions, and other species. Plasma exhibits unique characteristics, notably the existence of charged particles and the conduct electricity. It consists of a diverse mixture of components such as gaseous molecules, free radicals, metastable species, and UV photons, which contribute to its complex behaviour and potential applications [162,163].

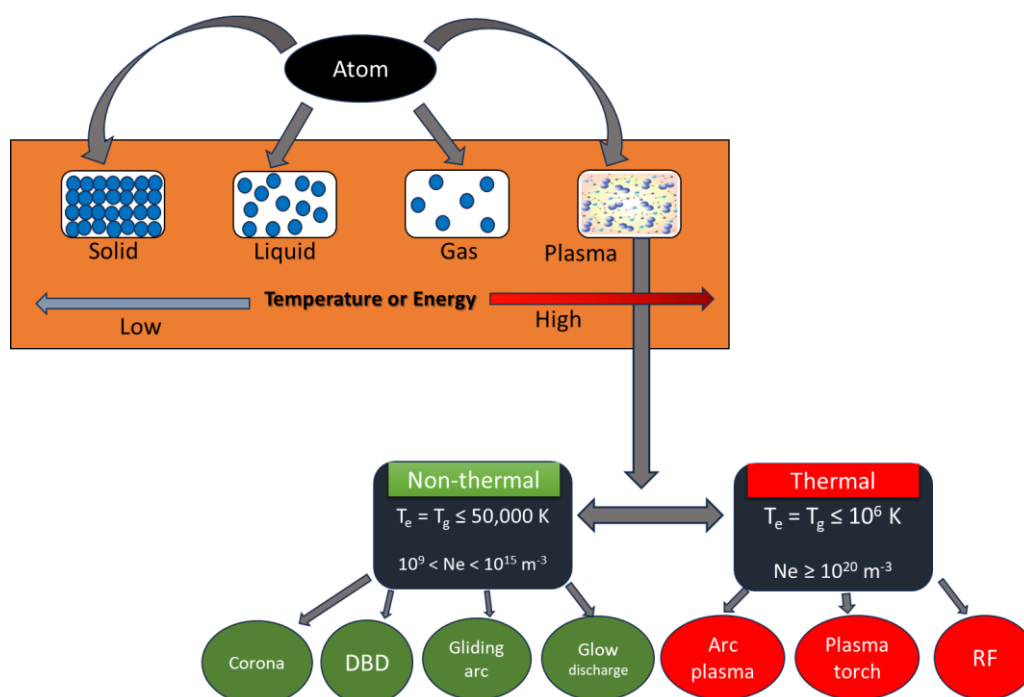


Figure 2.4: Common plasma configurations [164].

The classification of plasma types is shown in Figure 2.4. From a broad point of view, plasma can be divided into two major categories, namely: thermal plasma (TP) and non-thermal plasma (NTP), based on the temperature between the electrons, ions, and neutrals [164]. Thermal plasma (usually arc discharges, torches, or radio frequency) is generated at a high gas pressure and can be attributed to the frequent collisions occurring between the high-energy electrons and neutral species [103]. As a result, the electron temperature (T_e) and gas temperature (T_g) are identical or exist in thermal equilibrium ($T_e = T_g \leq 10^6$ K) and the electron density (n_e) is greater than 10^{20} m⁻³ [165]. Meanwhile, at low pressures (e.g., atmospheric pressure), the reduced frequency of collision between the free electrons and the neutral species inhibits thermal equilibrium and the energy supplied favours the electrons. Therefore, T_e is considerably higher than T_g ($T_e > T_g \leq 10^6$ K). In this case, the electron density falls to $10^9 - 10^{15}$ m⁻³ [165].

Thermal plasma has been applied extensively in metallurgy processes like the smelting of metals and refining due to its high energy density and ability to reach extremely high temperatures. It also finds application in material synthesis and waste disposal. Non-thermal plasma, on the other hand, has been deployed over a wide range of fields and have been used for applications like biomedicine, environmental cleanup/water purification, microelectronics, surface modifications, and textile amongst others. One of the key advantages of NTP is its ability to work at lower temperatures, making it suitable for temperature-sensitive materials and biological applications. Also, it consumes less energy than the TP, making it cost-effective for certain applications. In most cases, maintaining stable thermal plasmas over extended periods can be technically challenging [103].

2.8 Application of non-thermal plasma in water treatment

Non-thermal plasma can be described as electrical discharges occurring in the temperature range of 300 – 50,000 K [2]. While thermal plasma is maintained by introducing high electrical energy so that a high flux of heat is created to degrade recalcitrant contaminants by incineration, an NTP (or cold plasma or non-equilibrium) on the other hand operates at low temperatures, reducing the energy consumption and still achieving effective contaminant removal [166]. As a result, they have attracted significant attention as promising water treatment technologies

within the plasma space [20,167–169]. Considering their plasma-phase distribution, electrical discharges from the NTP methods can be commonly divided into three: direct discharges in the liquid phase, indirect discharge in the gas phase above the liquid, and hybrid gas-liquid system, as shown in Fig. [170].

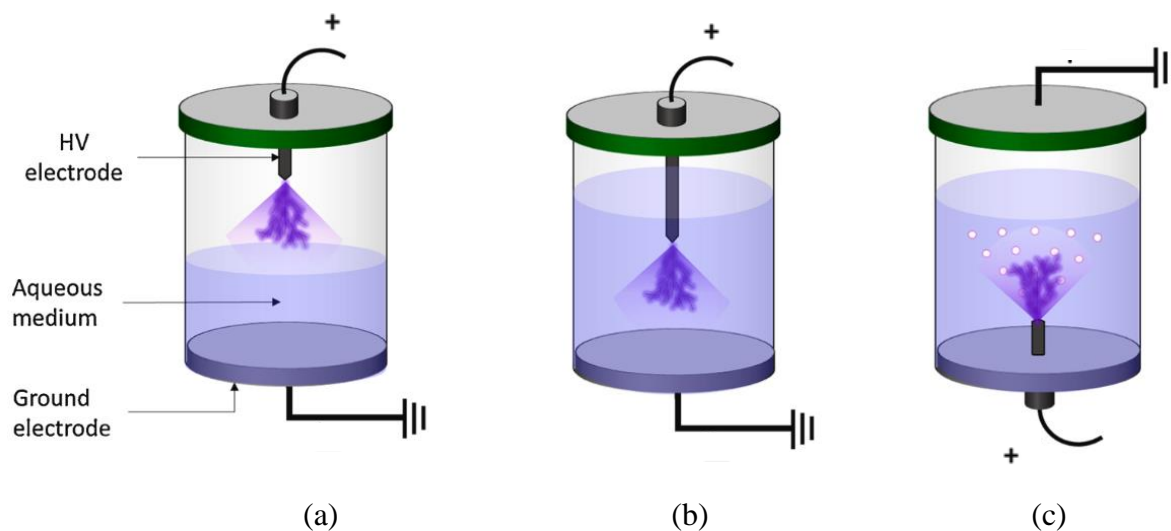


Figure 2.5: Forms of electrical discharges. (a) discharge in gas phase above liquid (b) direct gas discharge in the liquid (c) hybrid gas-liquid discharge. (Adapted from [163]).

Plasma generated in the gas phase above the liquid (indirect discharge) releases reactive oxygen and nitrogen species which eventually diffuse into water to initiate chemical reactions, as shown in Figure 2.5 (a) [171]. Meanwhile, the reactions occurring in the liquid can be influenced by the plasma formed at the gas-liquid interface. Due to their equivalent breakdown intensity in the atmospheric gas, plasma formation, and gas phase breakdown above liquid surface are mostly identical to glow electrical discharges [172]. For electrical discharges above liquid using the liquid as an electrode, the presence of the liquid surface impacts both the physical characteristics of the discharge and the chemical reactions that occur at the gas-liquid interface. The reason for this is that the discharge current is conveyed through the water electrode by ions, which have far lower mobility than electrons in metals. Also, in this discharge type, a considerable amount of the discharge power is lost in the liquid creating high evaporation rates [173].

Direct discharge in liquid involves a simple system in which chemically active species are generated directly in the aqueous medium to degrade contaminants as shown in Figure 2.5 (b). This process, however, presents complicated challenges due to the unique properties of water as a discharge medium. Water being significantly denser than gases lacks the extended periodic structure of atoms and molecules found in most solids. Also, for electrical discharges within liquid, the flow of current relies on the slow movement of the molecules and ions present which is also susceptible to the conductivity of the solution [174]. As a result, more energy is required to generate discharges in the liquid compared to discharges above the liquid, and the temperature of the liquid is increased [175]. Other impact factors that affect the breakdown of pollutants in a direct discharge include the purity level of the solution and the presence of microbubbles from the presence of dissolved gas.

Electrical discharges at the gas-liquid interface (also known as discharges in bubbles/vapour) are usually characterised by a large contact surface area. This allows the gaseous species to diffuse more effectively inside the liquid with less energy required to form the plasma. The chemistry of the process is however similar to that of the gas discharge above liquid, where the liquid is acting as the electrode [176]. Also, its energy requirement is lower than that of the direct electrical discharge in water.

2.9 Reactive species in a non-thermal plasma

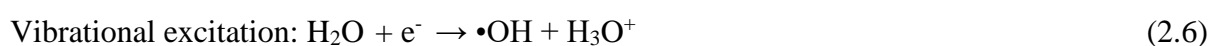
The electrical discharges mentioned above all have certain common chemical reaction mechanisms and physical phenomena, including the formation of molecular and reactive species. The most common reactive species generated in a non-thermal plasma include both reactive oxygen species (O_3 , $\bullet OH$, H_2O_2 , etc) and reactive nitrogen species (RNS). Other reactions facilitate the production of UV light and shockwaves which also aid the degradation of an organic pollutant in water. To understand the reaction mechanism by which pollutants degrade in aqueous solution, it is necessary to understand the reactions that lead to the generation of reactive species as well as their individual properties. This is the focus of this section.

2.9.1 Reactive oxygen species (ROS)

ROS encompasses a range of active species including free radicals, ions, atoms, and excited molecules. They are prevalent and predominant in virtually all kinds of gas plasma, with a longer half-life compared to other reactive species in the gas phase. The relatively lower dissociation energy of oxygen molecules (5.2 eV) amplifies its presence in plasma gas over the other reactive species [177]. The ROS spectrum comprises both radical and non-radical forms of oxygen. The radicals include species like $\bullet\text{OH}$, peroxy ($\text{ROO}\cdot$), and superoxide, whereas non-radical forms consist of components like ozone, singlet oxygen, and hydrogen peroxide [178]. Some of the common ROS are briefly discussed in the next sections, and their properties have been summarised in Table 2.3.

2.9.1.1 Hydroxyl radical

The hydroxyl radical ($\bullet\text{OH}$, $E_0 = 2.8$ eV) is a highly reactive specie with a short half-life (10^{-9} s) [177]. It is generated by the reaction between water molecules and high-energy electrons in a dissociation, ionization, and vibrational process according to Eq. (2.3) – (2.9) [179,180].



Hydroxyl radicals play a crucial role in the removal of organic pollutants due to their high oxidation potential and non-selectivity [181]. Their primary actions with organic contaminants include the abstraction of hydrogen atoms, electrophilic addition to an unsaturated bond, and electron transfer [175].

2.9.1.2 Hydrogen peroxide

Considering the short half-life of $\bullet\text{OH}$ radicals as mentioned above and their diffusion distance (approximately 6×10^{-9} m), their transfer from the plasma zone into aqueous medium in most cases becomes difficult [182]. As a result, they may recombine into long-lived product called hydrogen peroxide (H_2O_2 , $E_0 = 1.78$ V) according to Eq. (2.10). Hydrogen peroxide is a stable, neutral non-radical with a longer half-life than other ROS. While H_2O_2 typically doesn't rapidly react with many organic substances, making it less immediately effective for water treatment, its presence can amplify the overall oxidative capacity of the plasma and profoundly influence its chemistry [175]. In environments rich in H_2O_2 , a greater quantity of $\bullet\text{OH}$ can be formed through a range of processes including dissociation, photolysis, and metal-driven catalytic reactions.



2.9.1.3 O-based specie

The exposure of O_2 to electrical discharge results in the formation of atomic oxygen (O , $E_0 = 2.42$ V) by the dissociation of O_2 molecules. This specie can further enhance the formation of $\bullet\text{OH}$ according to Eq. (2.11).



Atomic oxygen can directly react with contaminants in an aqueous medium and also facilitate the production of ozone (O_3 , $E_0 = 2.07\text{V}$) by its reaction with oxygen molecules as seen in Eq. (2.12) :



Ozone is perhaps the most prominent neutral species in plasma, exhibiting a strong oxidizing power in the liquid phase, compared to Cl_2 , ClO_2 , and even H_2O_2 [183]. Being a potent oxidative variant of oxygen, it is most effective when it serves as an electron acceptor during the oxidation of metal ions, or as an electrophile in oxidizing compounds like phenol and other aromatic compounds. For carbon-carbon multiple bonds, it could act as an additive agent. However, due to high instability, O_3 can easily dissociate into oxygen. Whereas, in neutral and

basic conditions it is unstable and breaks down through a repetitive chain process to form $\bullet\text{OH}$ [184].

2.9.2 Reactive nitrogen species (RNS)

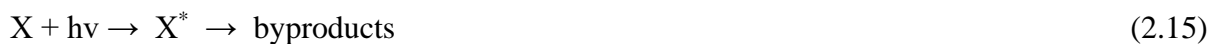
RNS comprises a group of chemical intermediates originating from nitric oxide; a predominant reactive compound produced in plasma. When N_2 is energised, excited species like N and N_2^+ are generated according to Eq. (2.13) and (2.14) [185].



These excited nitrogen species react with oxygen and some ROS such as O_3 and superoxide to produce additional RNS. The formation and destruction of RNS are significantly influenced by ROS. The common RNS commonly reported include nitric oxide (NO), nitrogen dioxide (NO_2), nitrate (NO_3), peroxyxynitrite (ONOO^-). These nitrogen species play a role in oxidizing biological molecules, with NO , NO_2 , and ONOO^- (often referred to as N_xO_y) being the most extensively researched among them [186].

2.9.3 Ultraviolet light

The UV light emitted in all water-containing plasma processes is a result of excited species returning to lower energy states after being generated by collisions between electrons and neutral molecules. The typical mechanism for UV degradation is described in Eq (2.15). When an organic molecule (X) is exposed to UV light, it absorbs the radiation and becomes promoted to an excited state (X^*) [175]. However, due to its short lifetime ($10^{-9} - 10^{-8}$ s), the excited molecule quickly returns to its ground state where it can be degraded into new molecules.



In addition to degrading the organic compound, UV light also facilitates some other important reactions like the dissociation of O_3 and H_2O_2 , thereby producing $\bullet\text{OH}$ in the plasma system which is a strong oxidizing agent.

2.9.4 Shockwave

In processes involving electrical discharges, shockwaves are created upon the rapid expansion of the plasma channel within the surrounding water [187,188]. This means that high electrical energy can generate shockwaves, either by directly introducing them into the liquid or bubbles within the liquid [189]. For instance, discharges that resemble streamers in liquid can create shock fronts, while discharges in bubbles within the liquid can produce weaker shockwaves when the bubbles collapse [190,191]. In contrast, gas-phase plasmas typically don't generate shockwaves in the liquid. However, they can influence the motion of the liquid in three specific scenarios: cold plasma jets or plumes, ionic wind, and the formation of Talyor cones at the interface between the plasma and water [192]. The resulting shockwave can directly trigger pyrolytic and chemical reactions within the liquid through electrohydraulic cavitation. For example, shockwaves can lead to the production of more •OH and H₂O₂ in the liquid by causing water dissociation [192].

Table 2.3: Chemical properties of the common reactive oxygen species in a non-thermal plasma reactor [193,194]

| Specie | Half-life (s) | Density (cm ⁻³) | Oxidation potential (V) |
|-------------------------------|-------------------------------------|-------------------------------------|-------------------------|
| •OH | 10 ⁻⁹ | 10 ¹⁵ – 10 ¹⁷ | 2.80 |
| H ₂ O ₂ | 60 | 10 ¹⁵ – 10 ¹⁷ | 1.78 |
| O• | 10 ⁻⁶ | 10 ¹⁴ – 10 ¹⁶ | 2.42 |
| O ₃ | 1.2 × 10 ³ | 10 ¹⁵ – 10 ¹⁷ | 2.07 |
| HO ₂ • | NA | NA | 1.70 |
| •O ₂ ⁻ | 10 ¹⁰ – 10 ¹² | 10 ¹⁰ – 10 ¹² | 1.44 |

NA: Not available

Table 2.4: Studies on the application of NTP in the degradation of pharmaceutical residues.

| PhACs | Plasma type | Solution matrix | Solution volume (mL) | Initial concentration (mg/L) | Treatment time (min) | Removal efficiency (%) | Reference |
|-------------------------------|--------------------------------|----------------------|----------------------|------------------------------|----------------------|------------------------|-----------|
| Methylparaben | Metal-wire-plate Corona | Tap water | 330 | 10 | 5 | 100 | [195] |
| Acetamiprid | DBD | Deionised water | | 50 | 200 | 83.48 | [196] |
| Sulfasalazine | Water falling DBD | Ultrapure water | 100 | 10 | 15 | 96 | [197] |
| Carbamazepine | Pulsed corona | Milli-Q water | 300 | 0.5 | 66 | 90 | [198] |
| Diatrizoate | | | | | | 45 | |
| Diazepam | | | | | | 47 | |
| Diclofenac | | | | | | 99 | |
| Ibuprofen | | | | | | 86 | |
| 17 α -ethinylestradiol | | | | | | 96 | |
| Trimethoprim | | | | | | 84 | |
| 17 β -estradiol | DBD | Ultrapure water | 500 | 0.1 | 30 | 100 | [199] |
| Verapamil | Gliding arc | | 25 | 24.5 | 80 | 97 | [200] |
| Ibuprofen | Cylindrical wetted-wall corona | Milli-Q water | 500 | 60 | 80 | 91.7 | [26] |
| Pentoxifylline | Coxial DBD | Tap water | 200 | 100 | 60 | 92.5 | [201] |
| Metronidazole | DBD | Synthetic wastewater | 140 | 50 | 45 | 90.3 | [202] |
| Cephalexin | Multi-pin-to-liquid Corona | | 15 | 40 | 15 | 96.1 | [203] |
| Cefazolin | Corona | | | | | 95.2 | |
| Diclofenac | Multi-needle-plane Corona | Milli-Q water | 50 | 1 | 10 | 100 | [204] |
| Carbamazepine | Corona | | | | | 96 | |
| Ciprofloxacin | | | | | | 92 | |
| Ampillicin | Floating electrode DBD | Deionised water | 1 | 7 | 5 | 100 | [205] |
| Metronidazole | Glow discharge (with | Drinking water | 10,000 | 51,348 | 15 | 90 | [188] |

| | | | | | | | | |
|----------------|--------------------------|-----------------------------|-------|------|----|--------------------------------------|--|-------|
| | | hydrodynamic cavitation) | | | | | | |
| Tramadol | | | | | | | | |
| Methylparaben | Corona | Tap water | 55 | 50 | 30 | | | [206] |
| Carbamazepine | Rotating drum corona | Ultrapure water | 1,000 | 23.6 | 90 | 98 (at 34 rpm), 95 (at 17 rpm) | | [207] |
| Clofibric acid | | | | 21.5 | | 97 (at 34 rpm), 93 (at 17 rpm) | | |
| Iopromide | | | | 79.1 | | 40 (at 34 rpm), 45 (at 17 rpm) | | |
| Pefloxacin | DBD | Deionised water | 100 | 120 | 25 | 97.7 | | [208] |
| Enrofloxacin | Nanopulsed DBD | Ultra-pure water | 8.5 | 40 | 20 | 100 | | [29] |
| Diclofenac | Plana falling film | Deionised water | 500 | 50 | 30 | 100 | | [149] |
| Ibuprofen | DBD | | | | 20 | 100 | | |
| Paracetamol | DBD | Tap water | 40 | 25 | 60 | 99 | | [209] |
| Paracetamol | Gliding arc | Milli-Q water | 180 | 200 | 60 | 62.6 | | [210] |
| Cefixime | Underwater bubble DBD | Deionised water | 50 | 100 | 30 | 94.8 | | [211] |
| Tetracycline | Surface DBD | Deionised water | 500 | 50 | 20 | 93.3 | | [212] |
| Sulfadiazine | | | | | | 81.2 | | |
| Ciprofloxacin | | | | | | 58.5 | | |
| Diclofenac | DBD | | 100 | 10 | 10 | 100 | | [213] |
| Carbamazepine | Ex situ DBD | Tap water | 100 | 20 | 3 | 100 | | [23] |
| | In situ DBD | | | | 60 | 90.7 | | |
| Caffeine | DBD | Ultrapure water | 100 | 50 | 24 | 41 | | [214] |

2.10 Types of non-thermal discharge

Table 2.4 provides a summary of the various types of NTP configurations that have been applied in the degradation of pharmaceutical residues as well as their efficiencies. Over the years, researchers have developed and tested different NTP reactors in water and wastewater treatment according to the discharge types (Corona, dielectric barrier discharge, glow, and gliding arc) as shown in Figure 2.4. The aim has always been to eliminate harmful organic compounds from water by oxidation. It is easy to notice a significant variation in removal efficiency and treatment duration for the same compound when comparing different reactor configurations within the same discharge type or across different types. Also, the reported concentrations of treated pollutants span a wide range, from a few milligrams to several hundred or even thousand milligrams.

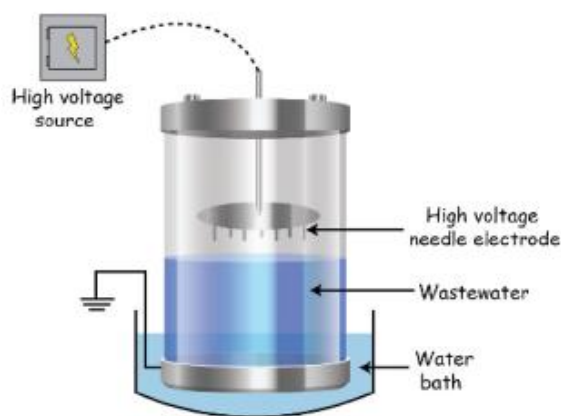
2.10.1 Corona discharge (CD)

In a pulsed electrical discharge system, a pulsed-based electric generator is employed which can generate sharp, high-voltage pulses within nano to microseconds. In this process, only free electrons gain significant energy, resulting in the creation of energetic electrons and subsequently, non-thermal plasma [215]. Common setups for pulsed electrical discharge employ two dissimilar electrodes: one with a high curvature, such as needles or wires, and the other, a low-curvature plate [216–218]. This design minimises the initial voltage required for discharge formation, given that the larger curved electrode can initiate a substantial potential gradient due to its uniform electric field. Figure 2.6 illustrates corona discharge arrangements.

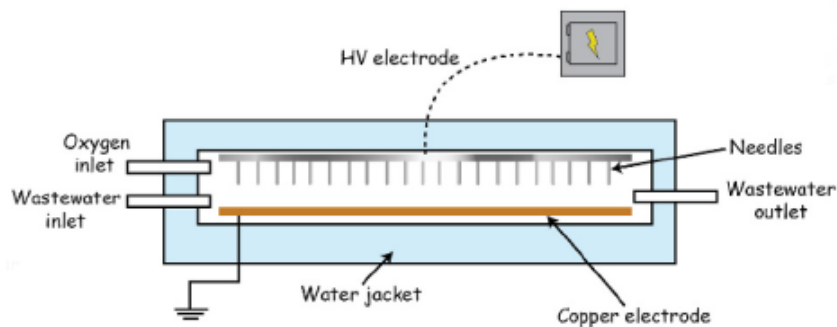
When it comes to pulsed voltage setups, the point-of-plate configuration is the most examined. This involves a high-voltage point electrode positioned at a fixed distance from a grounded plate electrode [218–220]. One of the key advantages of this setup is its ability to allow generated active species in the liquid to directly engage with pollutants. However, the slower transport rates within the liquid phase can cause notable disparities in temperature and concentration between the plasma area and the main solution. This can eventually lead to the recombination and suppression of active radicals within the discharge regions. Similarly, pronounced boundary transitions can be observed at the gas-liquid intersection in the gas discharge reactor [175].

The innovative efforts by B.R Locke’s team in designing point-plate reactors deserve special mention [221–223]. Recognizing the distinct characteristics of both gas and liquid discharges, the authors introduced a hybrid gas-liquid reactor. In this arrangement, the high-voltage electrode is submerged in the liquid, while the ground electrode is set in the gas phase. This reactor design promotes the generation of short-lived radicals and H₂O₂ in the liquid phase for organic pollutant degradation. Moreover, electrical discharge can also manifest above the liquid surface, enhancing the production of active species and enabling ozone generation in an oxygen-rich environment. This, in turn, facilitates pollutant elimination by diffusion into the liquid phase [216,224].

Despite the efficacy of a needle matrix and other forms of CD in wastewater treatment, its scalability presents challenges. Also, the high-voltage electrodes are prone to rapid electrode wear and deterioration, which affects the longevity of the reactor and may necessitate frequent maintenance. Also, despite termed “non-thermal” plasma, there can be localised heating in CD reactors, which may affect certain sensitive applications. Some studies on the application of CD in the degradation of pharmaceutical residues are presented in Table 2.4.



(a)



(b)

Figure 2.6: A schematic illustration of a corona discharge. (Adapted from [225]).

2.10.2 Glow discharge (GD)

Glow discharge arises when an electric current reacts with a gas confined within a barrier. For example, when voltage is applied between two electrodes housed within a gas-filled enclosure at a reduced pressure, glow discharge can be observed as shown in Figure 2.7 [225]. The ionised gas emits a glow when the necessary voltage is attained, and this depends on the gas composition. Researchers have developed various reactor configurations to produce glow discharge, and these fall into two primary categories based on the position of the discharge [226–228]. In the first design, the metal anode either touches or is submerged within the liquid where the glow discharge is generated. In the alternative setup, as described by Wang *et al.* 2012 [226], a porous substance divides the anode and cathode, both submerged in the liquid, into separate chambers.

Zhang *et al.* [229] designed a GD plasma reactor for the degradation of microcystin-LR in water. The authors used a stainless steel plate and a stainless steel needle as cathode and anode, respectively. The anode was positioned at about 5 mm above the solution, while the cathode was submerged within it. The electrodes were connected to a DC power source. The discharge was created when the voltage surpassed the specific threshold, creating plasma at the gas-liquid interface. Then the discharge was maintained at a reduced voltage. Argon gas was supplied in the reactor before and during the discharge process. A combination of a hydrodynamic cavitation unit with a glow plasma discharge (HC-GPD) was used by Pereira *et al.* [188] in the degradation of metronidazole antibiotic in drinking water. The synergistic effect of the HC-

GPD system enhanced the production of OH, UV light, and shockwaves which aided the degradation of the persistent pollutant with 90% efficiency in 15 min.

The complexity of setting up a glow discharge, however, may pose a challenge in its deployment. This coupled with other operational intricacies may necessitate precise control over parameters like voltage, gas type, and electrode material. Also, the effect of gas discharge is more pronounced near the electrode surfaces. For larger volume solutions, ensuring effective treatment may be challenging.

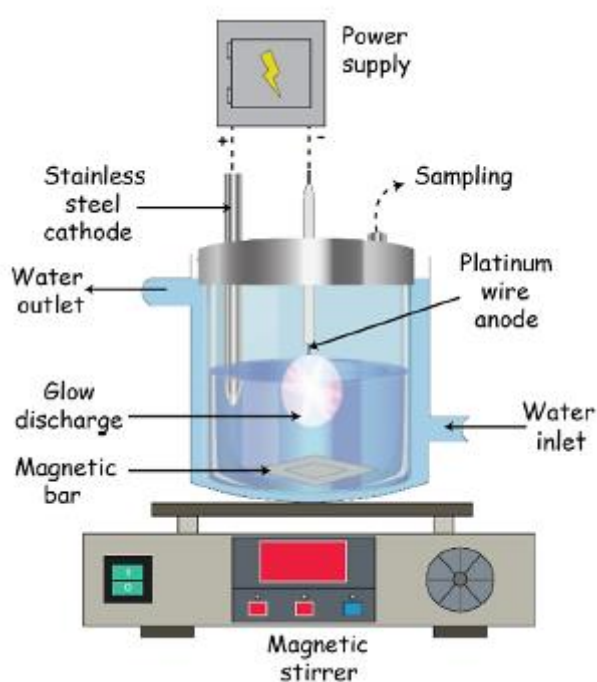


Figure 2.7: A schematic illustration of the glow discharge arrangement. (Adapted from [225]).

2.10.3 Gliding arc discharge (GAD)

The gliding arc discharge stands out as an innovative method that showcases both thermal and non-thermal plasma properties. A typical GAD reactor is shown in Figure 2.8. It incorporates an insulating shield, “knife-edge” diverging electrodes, a high-voltage power source, a nozzle, and an impedance [230]. During the GAD procedure high voltage is applied between two or more “knife-edge” diverging electrodes. The thinnest gap between these electrodes undergoes electric breakdown, forming an arc discharge when the electric field hits about 3 kV/mm in the

air [175]. As gas rushes through the nozzle at high speed, the arc (which is essentially thermal plasma) extends in length, while the ionised gas cools down. This results in a transformation into a non-thermal plasma, eventually fragmenting into a plasma. Unlike pulsed corona discharge, GAD offers a method for introducing high electrical power, leading to greater production of transient active species.

A study conducted by Krishna *et al.* [200] reported the degradation of verapamil hydrochloride in water by gliding arc discharge. The GAD was generated using a 750 W power source between two diverging copper electrodes of a half-circle shape with minimal gap distance of 5 mm. Meanwhile, compressed air was used as the working gas. The setup gave a maximum degradation efficiency of 97% for the pharmaceutical contaminant in 80 min treatment time and a first-order rate constant of 0.01 min^{-1} . The enhanced discolouration of methyl violet 10B in a GAD was studied by Tiya-Djowe *et al.* [231]. In this case, an initial degradation efficiency of 6.7% for 100 mg/L of the pollutant increased to 55.6% with the addition of maghemite ($\gamma\text{-Fe}_2\text{O}_3$). Similarly, Slamani *et al.* [210] added an iron catalyst to a GAD process to initiate a Fenton reaction, thus improving the degradation of paracetamol. The authors observed that with the iron catalyst, the pollutant was completely degraded with >92% mineralization degree.

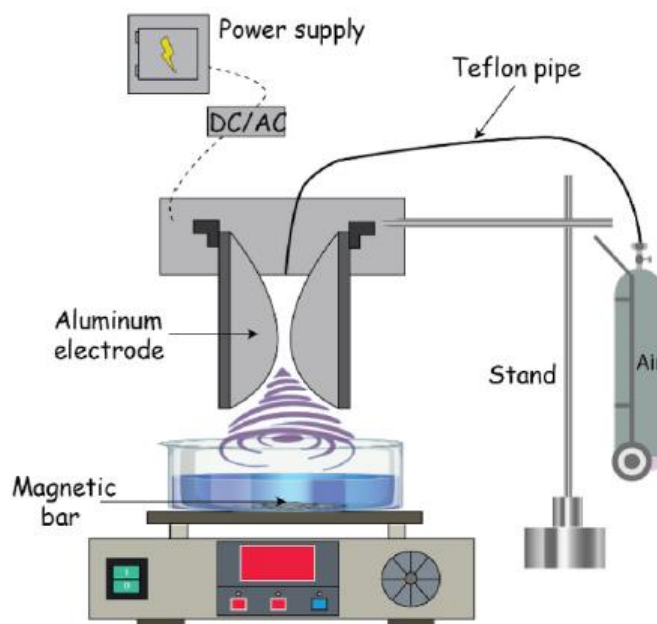


Figure 2.8: A schematic illustration of the typical gliding arc discharge. (Adapted from [225]).

2.10.4 Dielectric barrier discharge (DBD)

Dielectric barrier discharge, otherwise called silent discharges, has emerged as a cutting-edge solution for water treatment applications, as well as in this present study [232]. The DBD is generated between two electrodes with at least one of the electrodes coated with a dielectric barrier as seen in Figure 2.9. This barrier can be made of materials such as ceramics, quartz, or glass. When high voltage is applied to the electrodes, a series of micro discharges or plasma filaments form without transitioning into an arc, owing to the presence of the dielectric barrier. The electrical discharge from the DBD system is a plethora of radical species with high oxidizing potentials. In addition to generating $\bullet\text{OH}$, the DBD system also produces UV rays, O_3 , $\text{O}\bullet$, $\bullet\text{O}_2^-$, H_2O_2 amongst other species, which combine in water solutions to facilitate pollutant degradation without additional chemical additives.

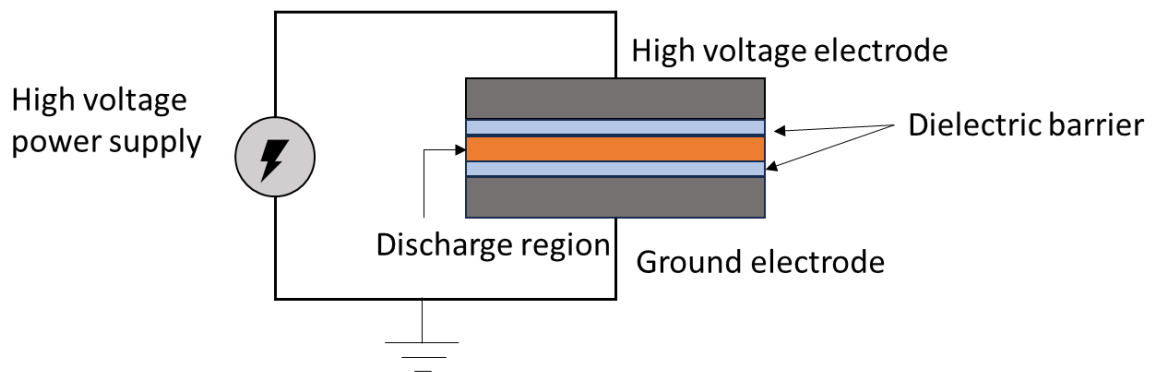
The DBD plasma system was previously crafted for ozone production in the industry and applied for wastewater treatment [233]. However, implementing this treatment method necessitated ozone-production steps, which required significant capital expenditure. In water treatment applications, DBD offers several benefits. Typically, they are straightforward to set up and function across a wide pressure range using different discharge gases. Their operating temperature is relatively low compared to direct discharges [234]. Moreover, the dielectric barrier ensures that there is minimal contamination of the sample by electrode materials since the electrodes are shielded by an inert dielectric barrier. With power usage being just a few Watts, DBDs are energy efficient while achieving electron densities up to 10^{15} cm^{-3} [235–237]. The low energy consumption of a DBD also provides significant benefits to its cost of water treatment. The next section has been dedicated to an in-depth discussion of the various configurations of the DBD plasma system.

2.11 Configurations of the dielectric barrier discharge

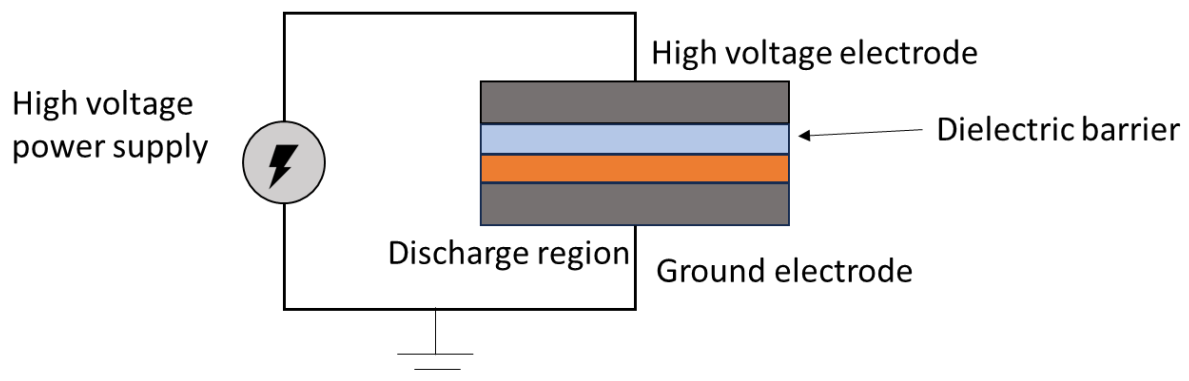
Multiple DBD configurations have been utilised for the breakdown of organic pollutants in various aqueous mediums and their efficiency is influenced by the configurations of their electrodes. Each configuration and principle are described by the existence of an insulating material in the discharge path. To generate the DBD plasma at normal pressure with moderately

high voltage amplitudes, the range specified for the discharge gap is between 0.1 – 10 mm. The common designs of DBD (as seen in Figure 2.9) include (a) planar and (b) cylindrical. Other geometries like surface, volume, and needle-to-pin have been reported in this section as well.

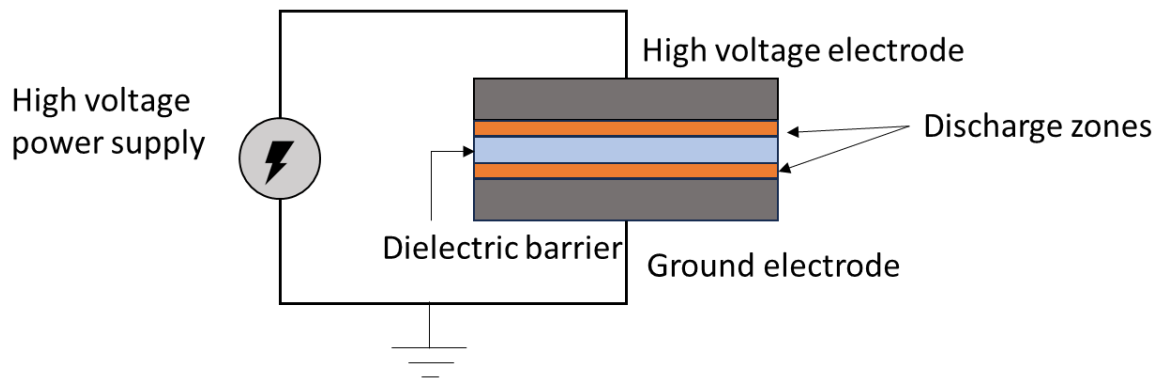
In a planar-shaped DBD, both electrodes are generally flat and are parallel to each other as shown in Figure 2.9 (a1) – (a3). One or more of these electrodes are covered with a dielectric barrier. The choice of dielectric material can influence the efficiency and characteristics of the discharge. When a high voltage is applied across the electrodes, the electric field generated leads to the ionization of the gas present between the electrodes, producing the discharge. However, because of the barrier, the discharge generated is not continuous but consists of numerous tiny, short-lived discharge filaments or microdischarges. These are bright and thin filaments that are distributed unevenly across the electrode's surface. According to Brandenburg, there are two basic planar configurations of DBD which include the surface and volume DBD [238].



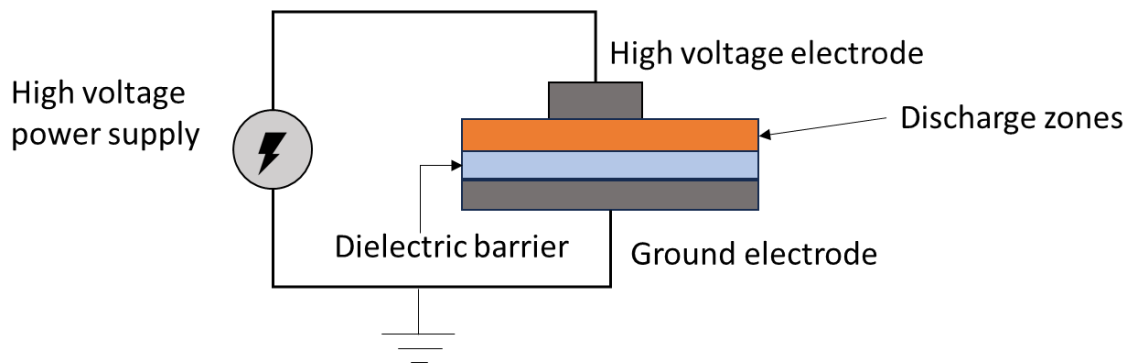
(a1)



(a2)



(a3)



(b)

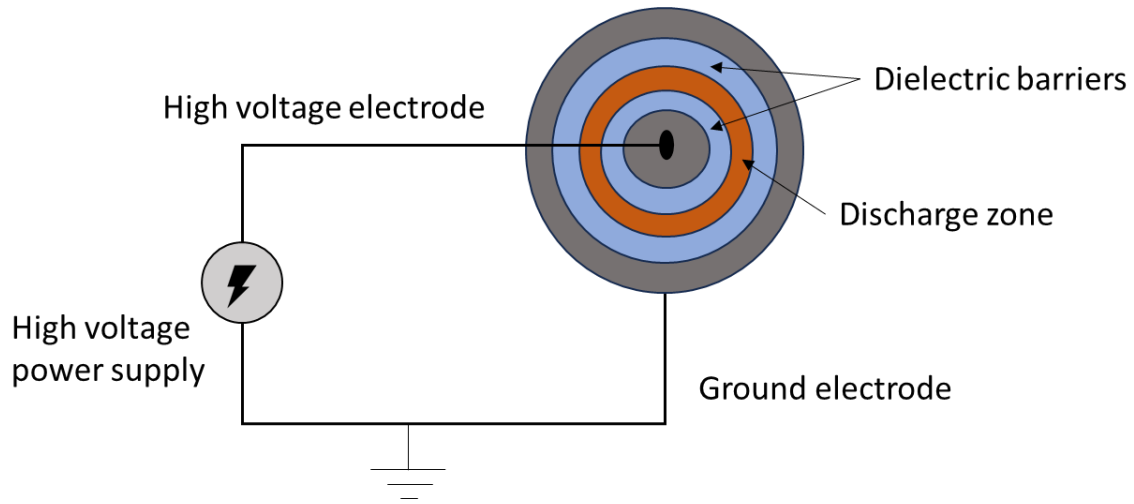
Figure 2.9: Planar DBD configurations: (a) volume DBD (1-symmetric, 2-asymmetric, 3-floated dielectric) (b) surface DBD [239].

In the volume DBD setup, either one or both electrodes are shielded by dielectric barriers (a1 and a2) or there is a dielectric layer dividing the gas gap into two parts (a3) [240]. In the a1 design, both metallic electrodes are shielded from potentially reactive particles originating in the plasma. In the a2 and a3 designs, one or both metallic electrodes come in direct contact with the plasma, which could cause erosion or corrosion. However, the plasma can function at a reduced high voltage amplitude in these setups compared to a because a larger percentage of the voltage is used across the gas gap. This allows for a greater charge per unit of electrode

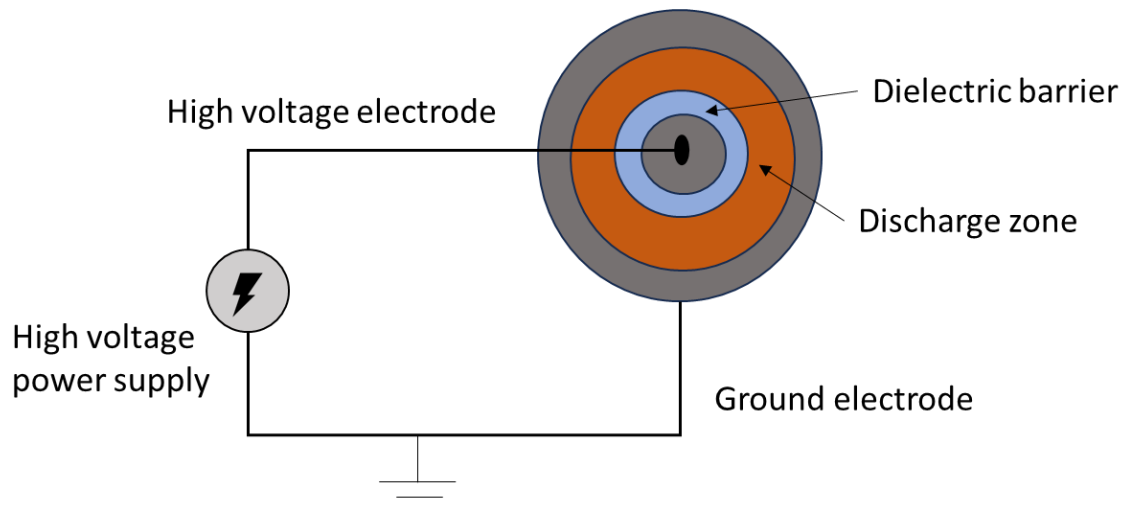
area. In a3, the dielectric remains unconnected. This doesn't affect its primary operation but merely offers an alternative for treating gases using DBDs.

For surface DBDs shown in Figure 2.9 (b), both electrodes come in direct contact with the barrier [239]. In this setup, the plasma is formed at the exposed electrode and moves across the dielectric surface, while the counter-electrode is housed within another dielectric layer. This arrangement has been implemented using mesh wire electrodes beneath the plate [241], by employing patterned metal films on insulating plates, or by the strategic etching of circuit boards [162]. The asymmetrical design (b2) is extensively discussed in plasma actuator studies, for example [242].

The cylindrical DBD shown in Figure 2.10 consists of one or two concentric tubes serving as insulating mediums (commonly made of quartz). The electrode at the centre is a metal wire or rod. In the design with two dielectric layers, the rod or wire is encased within an inner dielectric tube. An outer electrode may be a metal body or foil secured to the tube's exterior. The central electrode is subject to a high voltage while the outer one is grounded for safety. Plasma discharge occurs in the space between the tubes. The process of micro-discharge formation, quenching, and re-ignition (especially with AC sources) mirrors that of the planar DBD but radially takes place, emanating from the central electrode outward or vice-versa, depending on the setup. A capillary DBD can have either a ring-ring or pin-ring configuration as represented in Figure 10 (a) and (b). The ring-ring design forms plasma in a glass capillary with two separate electrodes encircling it. The formation of the plasma jet is influenced by the high voltage electrode's distance from the capillary opening. For the pin-ring geometry, the DBD occurs between a metallic pin within the capillary and an external ring, separated by the capillary wall.



(a)



(b)

Figure 2.10: Cylindrical DBD configurations (a) ring-ring (b) pin-ring [239].

Another DBD configuration is the needle-to-plate. This design employs a hollow stainless-steel needle as the discharge electrode with gases like helium being introduced through it. A copper sheet serves as the counter electrode. Between these electrodes, a glass slide maintains a typical distance of 5 to 10 mm, and a stable plasma is created when an alternating voltage. For a surface DBD setup, a set of linear electrodes are mounted onto a pure alumina ceramic base. This ceramic base can adopt a flat or cylindrical shape. Within the ceramic base, there is a film-like

opposing electrode acting as an inducing agent. When AC voltage is supplied across the electrodes, the discharge emerges from each electrode's outer limits and travels across the ceramic's surface.

2.12 Factors affecting the electrical discharges from an NTP during water treatment.

The NTP process has been extensively investigated and deployed as an effective water and wastewater treatment technology. However, its efficacy depends on several factors, including the type of gas used in generating the plasma, gas flow rate, applied voltage and frequency, mode of exposure, and water flow rate for a continuous flow process. Other variables such as the pH, and conductivity can also significantly affect the reaction mechanism, kinetics, and overall performance of the reactor.

2.12.1 Input power

The power used in generating plasma discharges plays a pivotal role in the degradation of pharmaceutical pollutants. This is because the more power applied, the more active species are produced, leading to quicker degradation of the substances [213,243]. Power calculations are a function of voltage and frequency, and so the dissipated power increases when either the applied voltage or frequency increases. For example, Dong *et al.* [244] observed a 41.4% increase in the degradation efficiency of benzohydroxamic acid when the applied voltage applied to a dielectric barrier discharge increased from 10 kV to 14.5 kV. Similarly, the degradation of anti-inflammatory ibuprofen increased from 71.4% to 85.4% when the pulse frequency applied to a DBD system was changed from 150 Hz to 225 Hz [245]. A linear increase in the first-order reaction kinetics was reported by Li *et al.* [212] for three antibiotics (tetracycline, sulfadiazine, and ciprofloxacin) as the voltage applied to the reactor increased from 11 kV to 19 kV. In this study, the reactive oxygen species ($\bullet\text{OH}$, O_2 , and $\bullet\text{O}_2^-$) investigated on a resonance spectrometer increased with the applied voltage. Meropoulis *et al.* [203] also reported an increase in the concentration of long-lived species (H_2O_2) as the voltage increased from 19 kV to 24.2 kV while degrading cephalosporins in water. This study also showed that a significant change in degradation efficiency was observed with the applied voltage rather than frequency.

The impact of voltage and frequency on the energy yield (mass of pollutant degraded per kWh energy consumed) has also been studied by some researchers. However, the reports on energy yield and input power have been inconsistent in literatures. While some researchers claim that the energy yield increased with dissipated power [246,247], others found contrary results [248–250]. As a result, it is necessary to investigate the individual parameters of a reactor to understand their effects on energy yield.

2.12.2 Initial concentration of pollutants

Many studies conducted to date have examined pharmaceutical concentrations ranging from a few mg/L to several magnitudes in mg/L. While these figures significantly exceed environmental levels and typical wastewater samples, they simplify the analysis process for diluted samples. This approach facilitates the tracking of the degradation of the primary pollutant and its by-products over the observed duration. Several authors have reported that the initial concentration of organic pollutants affects their rate of degradation with plasma. The degradation efficiency decreased with an increase in the initial concentration of the contaminant.

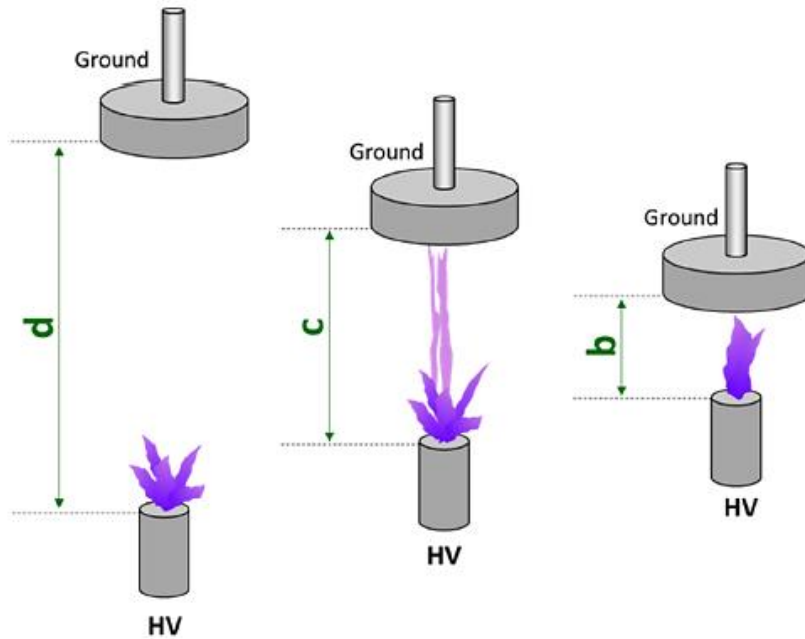
Zeng *et al.*[26] reported the influence of the initial concentration of ibuprofen on its rate of degradation with a wetted-wall corona discharge. Four initial concentrations (10, 20, 40, and 60 mg/L) were considered in this study, and the results showed that the rate constant dropped sharply from 143.6×10^3 to 30.3×10^3 (min^{-1}) as the initial concentration went from 10 to 60 mg/L. Similar observations have been reported for ciprofloxacin [251], metronidazole [202], sulfadiazine [247], estadiol, [199], amongst others. To explain the reason for this phenomenon, it is important to understand the intricate environment arising from plasma-liquid interactions. As the plasma produces reactive species, these oxidizing agents methodically break down the parent compound, generating intermediate products. This dynamic introduces a competition between the primary substance and its degradation derivatives. Therefore, a higher initial concentration will only mean more degradation byproducts will be formed which in turn will result in an increased consumption of the active species and a reduced degradation efficiency eventually.

2.12.3 Composition of feed gas

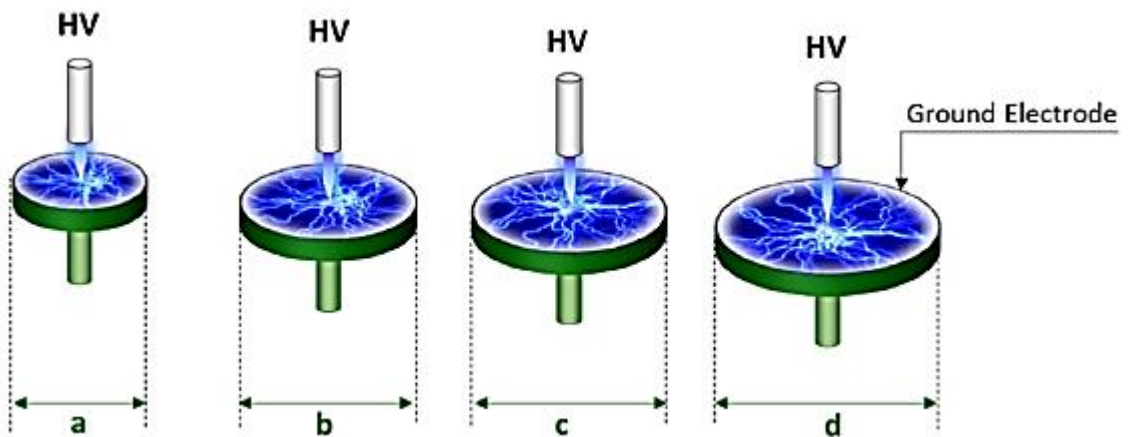
The working gas used in the plasma plays a vital role in determining the resulting chemical reactions. For typical gas-phase plasma interactions with liquid, the type of gas has a direct impact on the production of reactive species, which in turn affects the breakdown of the pollutants. In attempting to reduce the cost of treatment, studies have investigated the possibility of using air as the working gas in the degradation of pollutants in water. On the other hand, gases like oxygen, nitrogen, argon, and helium have also been explored in the generation of active species. Meropoulos *et al.* [203] compared the degradation efficiency of cephalosporins with plasma generated in air, oxygen, and nitrogen. The authors reported the degradation efficiency for the pharmaceutical compound in the order oxygen (over 99%) > air (96.1%) > nitrogen (69.8%). A similar observation was recorded in another study for the removal of cefixime [211]. Hu and Wang [208] generated a higher concentration of H₂O₂ in the liquid phase and O₃ in the gas phase for pure oxygen compared to air. Rezaei *et al.* [252] compared the concentration of H₂O₂ and NO₂⁻ generated with argon, helium, and nitrogen in a plasma-liquid system. Their results showed that the highest concentration of the two species was generated in argon, followed by helium. The superiority of oxygen over other forms of working gases has been commonly reported especially in the production of reactive oxygen species. In addition, the gas flow rate affects the rate of degradation of pollutants in water.

2.12.4 Reactor design and discharge gap

The gap between electrodes, or the discharge gap, is a critical factor in the effective degradation of contaminants. This is because altering the distance between the electrodes can modify the intensity of the electric field. Various electrical discharge types have been explored as shown in Figure 2.6, as also reported by [217]. Chen *et al.* [253] observed that a wider electrode gap prolongs the time required to effectively degrade pollutants. On the other hand, Sano *et al.* [254] noted that for the degradation of organic compounds in water, there is an optimal cathode-anode gap at certain voltage levels to maximise pollutant degradation [254]. Similarly, Stratton *et al.* reported that the plasma discharge area expands as the grounded electrode diameter or surface increases, given a constant electrode distance [255]. Therefore, electrode design should ensure even plasma distribution and a sufficiently large discharge area.



Where: $b < c < d$



Where: $a < b < c < d$

Figure 2.11: Effect of reactor design on the plasma discharge characteristics. (a) electrode distance (b) Surface of electrode (Adapted from [256]).

2.12.5 pH of the solution

The pH of the solution markedly influences the plasma's chemical properties during electrical discharge. Optical emission spectrum analysis has shown that the emission intensity of $\bullet\text{OH}$ produced by pulsed streamer discharge varies with pH, being more pronounced under neutral

and alkaline conditions [257]. Another study highlighted that the creation of H_2O_2 in either gas or liquid phase is pH dependent [258]. The initial pH of the solution affects the balance between various plasma species, which in turn has a significant impact on the degradation reactions of organic pollutants. Hydroxyl radicals, among other potent oxygen-based oxidisers, can quickly transform into O^- under alkaline conditions. These species display chemical activity that is considerably different from $\bullet\text{OH}$. For instance, when reacting with organic compounds $\bullet\text{OH}$ functions as an electrophile, while O^- operates as a nucleophile. This difference results in the formation of unique intermediates, leading to varied reaction pathways [180].

The effect of initial pH has often been studied by researchers but the results clearly show that the degradation of an organic pollutant can either be favoured in an acidic medium or basic medium, depending on the production and distribution of the reactive oxygen species and the molecular structure of the chemical compound [259]. For example, Yu *et al.* [260] investigated the degradation of DEET (N,N-diethyl-meta-toluamide) with a water-falling plasma system under different pH conditions (2.92, 6.48, 9.02, and 11.04) and reported that the degradation efficiency decreased with increase in pH values. Feng *et al.* [261] made a similar observation and reported that at low pH values. Some studies have mentioned that the lower degradation efficiency observed in some cases is due to the deprotonation of the molecule, which can result in either the stability of the compound or an increase their hydrophilicity. Other researchers like He *et al.* [262], however, have noted the increased degradation efficiency as the pH containing tetracycline increased, suggesting that the negatively charged compound may have been attacked by the electrophilic $\bullet\text{OH}$.

In general, for plasma generated in air, the solution acidifies rapidly to about 3-4 usually in the first few minutes of treatment. This drastic drop in pH can be attributed to the formation of inorganic acids (e.g., HNO_2 , HNO_3) in the solution. Meropoulis *et al.* [203] observed that the pH of the solution from an air-induced plasma reduced quickly compared to that of a nitrogen plasma. While the pH of simulated wastewater can influence the rate of degradation of contaminants, its impact is less pronounced in natural wastewater due to the presence of multiple organic compounds and synthetic chemicals that stabilise the solution.

2.12.6 Conductivity of the solution

Based on the type of NTP reactor used and the position of the plasma discharge, liquid conductivity could play a major role in the treatment efficiency. This is because the conductivity of a solution can directly influence the characteristics of an electrical discharge and the generation of reactive species [257]. The effect of solution conductivity on the discharge type is shown in Figure 2.7 [263].

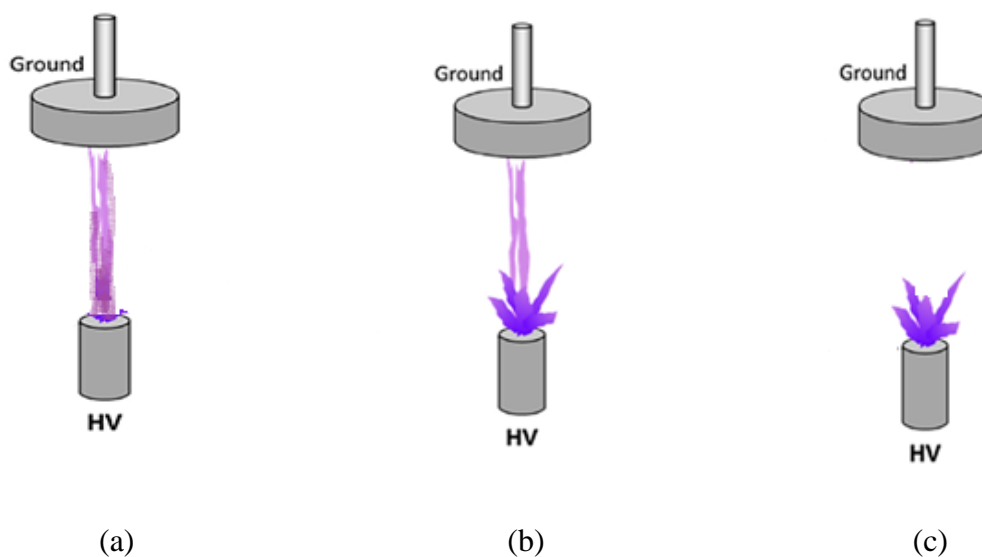


Figure 2.12: (a) Spark discharge with conductivity of $14 \mu\text{S}/\text{cm}$ (b) Streamer discharge with conductivity of $70 \mu\text{S}/\text{cm}$ (c) Corona discharge with conductivity of $300 \mu\text{S}/\text{cm}$. (Adapted from [263]).

Different conductivities can lead to various discharge modes: spark, spark-streamer, and corona discharges. For example, in a pulsed liquid discharge, as the conductivity rises, the discharge mode transitions from a spark discharge to a streamer and eventually to a corona discharge [263]. Meanwhile, at low conductivity, the length of the streamer is elongated, triggering a spark discharge. Spark discharge offers a more reactive environment compared to a streamer corona discharge, given the presence of high-energy particles, UV radiation, shockwaves, and supercritical water, which collectively induce pyrolytic and free radical reactions around the plasma region. At high solution conductivity, the discharge current rises with more potent UV emissions and elevated temperatures [170]. This, unfortunately, reduces the production rate of active species and inhibits degradation. For instance, Yang *et al.* [263] observed a decrease in the OH generated from $11.57 \mu\text{mol}/\text{L}$ to $6.01 \mu\text{mol}/\text{L}$ as the solution conductivity increased

from 14 $\mu\text{S}/\text{cm}$ to 300 $\mu\text{S}/\text{cm}$ after a 30 min discharge treatment. However, this phenomenon is not generally applicable to all cases where the plasma discharge is generated entirely in the gas phase. For instance, Dong *et al.* [244] reported only a 3.4% reduction in degradation efficiency as the conductivity of the solution increased from 86 $\mu\text{S}/\text{cm}$ to 224 $\mu\text{S}/\text{cm}$ their NTP.

For electrical discharges generated directly above the water surface, the conductivity of the solution also impacts the discharge behaviour. In this case, as the conductivity increases in a fixed discharge gap setting, the discharge path on the liquid surface might become denser, more luminous, and shorter [264]. The presence of ions like CO_3^{2-} , HCO_3^- , PO_4^{3-} , NO_2^- and Cl^- , have been confirmed to control the liquid conductivity and also act as radical scavengers in the solution, quenching the effect of $\bullet\text{OH}$ [229,265,266]. Therefore, their presence in the solution will inhibit the degradation of pollutants.

2.13 Plasma combined with catalysts

As discussed above, plasma systems are efficient alternatives for the degradation of PhACs in an aqueous solution by the generation of active species in situ. Several efforts have been made to improve the performance of a plasma reactor. Some of these include the optimization of the process conditions and reactor designs, as previously discussed. Another important strategy is the use of catalysts. Plasma combined with catalysts, often referred to as plasma catalysts, is a promising approach for water contamination. This synergetic process enhances the efficiency of pollutant removal by leveraging the strengths of both plasma and catalysis. The major catalyst categories commonly reported in literature include metal oxide and metal ion catalysts.

2.13.1 Metal oxide catalysts

One of the most widely used metal oxide catalysts is titanium dioxide (TiO_2) due to its easy accessibility, affordability, chemical stability, and non-toxic nature [267]. Usually, the photocatalyst is activated within the high-voltage discharge area of the plasma reactor. For instance, Ching *et al.*, [268] measured the UV light intensity arising from the pulsed electrohydraulic discharges to be about $10^6 \text{ W}/\text{cm}^2$ and noted its role in the activation of TiO_2 which helped in the decolourization of dye and removal disinfection of *Escherichia coli*.

In a typical plasma-catalysis process, the intense electric field most likely inhibits the merging of electrons and holes on the surface of the TiO₂, thus amplifying the photocatalyst's quantum effect [269]. Additionally, the shockwaves and ultrasound formed during the electric discharge process can clean and restore the catalyst's surface and boost the transportation of reactants to it, enabling a higher number of active catalyst sites to engage in the reactions. Thus, merging plasma technologies with photocatalysis will potentially amplify the strengths of both AOPs significantly, while addressing their drawbacks.

Strong UV emissions can be obtained in arc discharges, while spark and gliding arcs and dielectric barrier discharges can also generate useful UV light for plasma-catalytic actions. Therefore, the presence of a metal oxide photocatalyst like TiO₂ will enhance the removal of organic substances in water with either of the NTP configurations. The role of the catalyst can be affirmed by examining the concentration of the concentration of reactive species such as OH, H₂O₂, and O radicals, generated in the plasma [270]. For instance, reported that the emission intensities of OH and O radicals in distilled water containing TiO₂ were 1.7 and 3.8 respectively times those of a solution without the catalyst [271]. An investigation of the pollutant intermediates also confirmed the dominance of OH radicals in a plasma-TiO₂ catalyst process. Meanwhile, Jiang *et al.* [175] note that infusing an O₂-rich gas into a plasma catalysis is essential. This is because the dissolved O₂, acting as electron receptors, interacts with e⁻ to produce superoxide, which can further undergo one-electron reduction to yield the desired OH for non-selective oxidations and then H₂O₂. These processes are described in Eq. (2.16) – (2.20).



Plasma-photocatalysis featuring TiO₂ has been applied extensively in literatures. For example, the degradation efficiency of a model contaminant like phenol increased to 98% in 60 min with the addition of TiO₂, compared to 60% without the catalyst using a pulsed plasma system [272].

Similarly, Wang *et al.* [270] obtained an increased efficiency for the degradation of phenol by combining a pulsed corona discharge with TiO₂. Li *et al.* [273] synthesised a La/Ce-TiO₂ catalyst for the degradation of perfluorooctanoic acid in a DBD reactor. In 280 min, the authors recorded 97.5% degradation of the recalcitrant pollutant (100mg/L) and as high as 37 g/kWh energy yield during this process. Guo *et al.* [274] combined graphene-TiO₂ nanocomposites to aid the degradation of fluoroquinolone antibiotics in a pulsed discharge plasma system. In their study, the combination of graphene and TiO₂ helped to further boost the generation of •OH and H₂O₂ in the reactor system, thus enhancing the degradation of the antibiotic. The composite catalyst yielded a degradation efficiency of 99.4%, while TiO₂ catalyst-alone and the plasma system-without catalyst gave 75.7% and 64.8%, respectively. Graphene, in this case, was added due to its unique physical properties, such as high specific surface area, excellent conductivity, and favourable optical properties [275].

However, it should be noted that the degradation efficiency positively correlates with the concentration of TiO₂ slurry up to a certain level. Extreme concentrations of the catalyst can result in high turbidity which can obstruct the UV light from the discharge area from reaching the organic molecules in the solution. The other metal oxides reported in literatures include: ZnO [276], SnO₂ [277], WO₃ [278] so on, which are less popular in wastewater treatment applications than TiO₂.

2.13.2 Metal ion catalyst

An alternative approach used in improving the efficiency of a plasma system is the addition of metal ion catalysts like ferrous salt. This stems from the understanding that the incorporation of iron salts can catalytically convert the generated H₂O₂ into •OH through Fenton reactions as previously discussed in Section 2.8.2. Fenton reaction is also shown in Eq. (2.1) and (2.2). Moreover, Fenton process within the plasma system can be triggered by self-emitted “white light” which spans wavelengths from 200 nm in the UV range to 1000 nm in the infrared range [175].

2.14 Summary of knowledge gaps

This literature review has provided substantial evidence of the widespread pharmaceutical pollution in the environment. With the use of advanced analytical techniques, several researchers around the world have been able to monitor and identify various PhACs in different water matrices, indicating that this is a global issue. Meanwhile, the lack of a robust toxicity report and release guidelines for PhACs has been a major excuse to ignore these compounds during wastewater effluent discharge. However, with the recent endocrine disruptions observed among aquatic species, and traces of genetic toxicities in humans, environmental monitoring bodies around the world have begun to ask questions on the undiscovered effects of prolonged exposure to PhACs, seeing that some (like carbamazepine) have already been discovered in drinking water consistently.

This review also provides an in-depth insight into the NTP methodology as an emerging AOP for the breakdown of pharmaceutical pollutants. When compared with traditional wastewater treatment methods and other advanced oxidation processes, NTP methods are highly effective in decontaminating pharmaceutical wastewater with significant energy efficiency and less toxic by-products to deal with after treatment. Initially, the mechanisms of the NTP technology were discussed, along with an explanation of plasma discharge patterns. Following that, various NTP reactor models were discussed and supported with specific examples in which they have been applied. Most studies have leaned towards the use of corona discharges and DBD, due to their high energy efficiency, low-temperature requirement, safety, and ease-of-use. Thereafter, the study focused on DBD reactors, and their various configurations commonly found and reported in literatures. The prospects of using DBD in future wastewater treatments are very promising, yet it is vital to recognise and address certain inherent challenges.

1. Throughput: The majority of the studies reported in Table 2.4 have been conducted in batch mode. This makes it difficult for these studies to be thought of beyond the laboratory scale. For wastewater remediation, it is necessary to develop continuous reactors rather than batch reactors to be able to handle large volumes of contaminated solutions.
2. Identification of reactive species and their roles: When generating plasma discharges (e.g. with air), multiple reactive species emerge. Grasping their role in breaking down pollutants demands a detailed knowledge of each species and their concentration.

3. Working gas: Most NTP studies utilise oxygen in generating plasma discharge. While this has resulted in a significant degradation of the pollutant, the challenge is that this gas must be regularly supplied to the reactor at a cost which adds to the expense of running the treatment process. It would be interesting to see how the reactor performs with natural atmospheric air used as working gas without an aerodynamic device.
4. Influence of natural radical scavengers: The efficacy of a DBD reactor has been established in highly pure solutions. Here, the reactive species generated have no interference with possible scavenging agents. In real life cases, this is not attainable as the presence of some natural ions may potentially inhibit the performance of the oxidative species. Although there are a few studies on this perspective, there are no detailed studies on how the naturally occurring ions affect the plasma species during treatment.
5. Energy efficiency: A typical NTP reactor consumes only a portion of the overall energy supplied to it in generating reactive species, the rest goes unutilised. Therefore, knowing an application's energy needs before developing an NTP reactor helps optimise energy and reduce the associated cost of treatment.
6. Toxicity analysis: Most NTP studies focus on the primary pollutant. Testing the toxicity of the NTP-treated effluent is seldom done, which could impact its wider adoption. Therefore, understanding the safety of the resultant effluent through toxicity studies is essential.
7. Analysis of byproducts: Standard methods might be insufficient in identifying the byproducts after NTP use. This shortcoming limits a detailed toxicity investigation especially on treated wastewater. Enhanced chromatography tailored for intermediate product identification is essential.
8. Catalyst application: While the use of metal oxide and metal ion catalysts has been noted to enhance the effectiveness of a DBD plasma system, there is an area which remains unexplored and that is how these catalysts perform in the presence of radical scavengers.

Chapter 3: An investigation on the removal of tramadol analgesic in deionised water and final wastewater effluent using a novel continuous flow dielectric barrier discharge reactor.

In this chapter, the degradation of tramadol (TRA) was studied for the first time in deionised water (D.I) and final wastewater effluent (FWWE) using a dielectric barrier discharge reactor operated in a continuous flow mode. Initially, the reactor was optimised for voltage and initial concentration conditions. After 60 min treatment, the degradation efficiency of TRA was 93% in D.I and only 27% in FWWE. Also, the pseudo-first-order rate constant in D.I (0.056 min^{-1}) was an order of magnitude higher than the FWWE (0.0056 min^{-1}). To understand the reasons for this disparity, experiments were conducted to investigate the impact of conductivity, pH, and certain natural radical scavengers present in the wastewater. The results revealed that the rate of degradation and kinetics of TRA in the presence of HCO_3^- was comparable to those observed in FWWE due to the scavenging of the $\bullet\text{OH}$ radicals. Fenton reaction with TRA was confirmed with the synthetic solution based on the increased production of H_2O_2 . Toxicity tests showed that the treated TRA solution did not inhibit the growth of *Escherichia coli* as opposed to the untreated solution. This chapter has been published in the Journal of Water Process Engineering (doi: 10.1016/j.jwpe.2023.104294), and a copy of the title page is shown in Appendix A5.

3.1 Introduction

The occurrence of residual pharmaceuticals in the water cycle has been linked to their increased production, consumption, and decrease in their prices over the last two decades [279]. Although they are detected in very low concentrations (ngL^{-1} and μgL^{-1}), these emerging contaminants have become a concern to both the scientific community and the public due to their persistence in the environment and toxicity reports [62]. One of the pharmaceutical compounds of interest is Tramadol (TRA), an opioid that is widely used for treating moderate to severe pains. Its global consumption surged from 290 tons in 2006 to 424 tons in 2012 [280], with Germany alone prescribing 24 tons in 2012 [281]. Meanwhile, only about 70% of TRA dosage is metabolised by the human system, leaving the remaining 30% to be excreted as waste [97]. Given its high hydrophilicity and low biodegradability, TRA has been classified as one of the extremely recalcitrant water micropollutants [282]. This characteristic renders its elimination through conventional wastewater treatment setups very challenging. Furthermore, documented reports have surfaced detailing the adverse impacts of TRA on aquatic life, including Zebra fish [283], Crayfish [284], Tilapia [285], Common carp [286], among others. These findings underscore the urgency for the development of technologies that can effectively deal with the micropollutant in water sources.

Various methods have been proposed to address the challenge of recalcitrant micropollutants like pharmaceuticals in water, with advanced oxidation processes (AOPs) gaining more attention in recent times [26,287,288]. These innovative methods encompass the generation of highly potent reactive species such as ozone (E_0 : 2.07 V) and hydroxyl radicals (E_0 : 2.8 V), that can potentially oxidise toxic pharmaceutical compounds into harmless by-products [289]. Hydroxyl radicals ($\cdot\text{OH}$) are particularly desirable because they are not only strong oxidisers but also non-selective towards various types of micropollutants. A variety of AOPs, such as ozonation [290], ozone-assisted process with Fe [291], ultraviolet irradiation with chlorine and H_2O_2 [132], photocatalysis [75,161,292], Fenton-like process [293] have demonstrated successful TRA degradation with notable removal efficiencies. Among emerging AOPs, non-thermal plasma technology (NTP) has garnered significant interest due to its simplicity, versatility, high energy efficiency, environmental suitability, and minimal reliance on additional chemical reagents. NTP treatment capitalises on the synergy of reactive species – ($\text{H}\cdot$, $\cdot\text{OH}$, $\text{O}\cdot$, $^1\text{O}_2$), molecules (H_2O_2 , O_3 , etc.), ultraviolet light, and shock waves [175]. Within

NTP configurations, the Dielectric barrier discharge (DBD) stands out for its operation at low/atmospheric pressure conditions and near-ambient temperatures. This configuration offers distinct advantages such as low energy consumption, thereby contributing to a cost-effective treatment solution. Alternate NTP configurations for water treatment have been reported by Cui *et al.* [294], and their efficiencies have been extensively discussed by Malik [237].

Several factors affect the effectiveness of an AOP in eliminating micropollutants, including the mode of operation (batch, continuous, etc), solution conductivity, and the presence of natural radical scavengers, among others. Typically, studies on TRA removal have been conducted in batch mode where the generated reactive species have adequate mass transfer in the solution and contact with the pollutant. While this mode yields rapid and energy-efficient degradation, its drawback lies in limited throughput, curtailing potential applicability beyond the laboratory-scale [295]. Also, the conductivity of the solution can influence the rate of reactive species generated in certain AOPs. While a Surface Dielectric Barrier Discharge (SDBD) reactor remains unaffected by water conductivity because the discharge has no direct contact with the liquid [296], initiating a discharge in a Volume Dielectric Barrier Discharge (VDBD) system necessitates low conductivity in the order of a few $\mu\text{S}/\text{cm}$ [297]. Elevated solution conductivity in VDBD systems reduces the length of the discharges, thereby decreasing the intensity of the reactive species generated and ultimately impacting pollutant degradation. For instance, Karoui *et al.* [251] observed varying degradation efficiencies for ciprofloxacin across various water matrices: ultra-pure water $15.12 \mu\text{S}/\text{cm}$), tap water ($492.2 \mu\text{S}/\text{cm}$), and pharmaceutical water ($2454 \mu\text{S}/\text{cm}$) in a VDBD treatment. The degradation efficiencies observed were 100%, 76%, and 60%, respectively. Also, natural ions in raw aqueous solutions are acknowledged as potential scavenger for the reactive species. These dynamics elucidate the rationale behind majority of DBD studies concentrating on solutions characterised by low conductivity and high purity. However, there are unanswered questions on how the degradation of micropollutants are prohibited in real wastewater effluent.

Therefore, this study not only examined the performance of a flow-through VDBD-type reactor in the degradation of TRA but also probes the divergences in pollutant removal between synthetic water and final wastewater effluent. To date, micropollutant investigations in this specific context remain scarce, prompting the development of multiple assumptions in this study. The first hypothesis was based on the influence of solution property, particularly the

conductivity of the wastewater effluent, given its potential to affect the length of the discharges as mentioned earlier. The second hypothesis considered the influence of cross-interference reactions between natural ions (Cl^- , HCO_3^-) and the ROS generated by the reactor. The influence of naturally occurring ions in the wastewater effluent was used in elucidating their impact on the reactive species available for contaminant degradation. Finally, a simple toxicity investigation was performed with *Escherichia coli*.

3.2 Experimental method

3.2.1 Materials

Tramadol hydrochloride ($\text{C}_{16}\text{H}_{25}\text{NO}_2\cdot\text{HCl}$, purity >99%) was purchased from Sigma-Aldrich Co. (Johannesburg, South Africa). The molecular structure of this compound is shown in Figure A1. Sodium hydroxide (NaOH), sulphuric acid (H_2SO_4), potassium chloride (KCl), and sodium chloride (NaCl) were purchased from Glassworld (Johannesburg, South Africa). Other chemicals like Sodium hydrogen carbonate (NaHCO_3), and Iron (II) sulphate heptahydrate ($\text{FeSO}_4\cdot 7\text{H}_2\text{O}$) were supplied by Merck Chemicals (PTY) Ltd. (Germiston, South Africa). All the chemicals were used without further purification because of their high purity. The synthetic TRA solutions were prepared in deionised water which had a resistivity of about $18.2 \text{ M}\Omega/\text{cm}$. Final wastewater effluent was collected from a local municipality in Pretoria West, South Africa, at the effluent discharge point.

3.2.2 Experimental procedure

5 mg/L TRA solution was prepared in a litre of deionised water, final wastewater effluent, and in solutions containing NaOH (2 M), H_2SO_4 (2 M), NaCl (2 mg/L), NaHCO_3 (236 mg/L), KCl (0.3 M), $\text{FeSO}_4\cdot 7\text{H}_2\text{O}$ (2 mg/L). These solutions were subjected to plasma treatment individually. The experimental setup, shown in Figure 3.1 (a), featured a DBD plasma reactor composed of borosilicate glass with wall thickness and outer diameters of 0.23 cm and 4 cm, respectively. The length of the glass tube is 30 cm, and it incorporated a stainless-steel rod of 1.27 cm in diameter and 29 cm in length, serving as the high-voltage (HV) electrode. A conductive copper tape, 1 mm width, and 0.1 mm thickness constituted the ground electrode,

encircling the glass both radially and laterally as shown in Figure 3.1 (b). Air was introduced naturally into the reactor as the working gas without an aerodynamic device. The plasma discharge was initiated and maintained by an alternating current (AC) power source (built by Jeenel Technologies Pty, Boksburg, South Africa) operated between 6 – 8 kV input voltage and a constant frequency of 20 kHz. According to Figure 3.1 (a), the high voltage line was connected to the HV multi-pin inner stainless-steel electrode, positioned centrally within the reactor. The HV electrode was hollow, facilitating the passage of water from the storage into the reactor, while the discharges are generated at the multi-pin edges. The contaminated water was sprayed out evenly at the upper section of the reactor through a micro jet spray positioned in a spacer at the top of the HV electrode. The spacer also helps to hold the electrode centrally within the reactor. As the water descended, it contacts the purple-coloured discharges at the multi-pin edges, subsequently flowing back into the storage. This cyclic process persisted for the designated treatment duration, with the water being pumped back into the reactor using a peristaltic pump operated at 400 mL/min flow rate. To ensure uniform solution mixing in the storage container, a magnetic stirrer was employed. Additionally, the pH of the solution was adjusted with aqueous NaOH and H₂SO₄ solutions.

Unless otherwise specified, the input voltage from the AC power supply was set at 8 kV, while the actual discharge current and voltage measurements were monitored with a digital oscilloscope (Rigol DS1074 Zplus, 70 MHz 1 GSa/s). The dissipated power for the reactor was calculated via Eq. (3.1). Optical emissions spectra were captured with a spectrometer (manufactured by StellarNet Inc) to investigate the reactive species generated in the DBD reactor.

$$P (W) = \frac{1}{T} \int_0^T V(t) \times I(t) dt \quad (3.1)$$

Where P is the average dissipated power, while V(t) and I (t) are the waveforms of voltage and current at time t, respectively.

3.2.3 Analytical measurements

The pH and conductivity of the solution were measured with a HANNA Multiparameter HI98194 meter. The concentration of hydrogen peroxide and ozone were obtained by

spectrophotometry using a Lovibond® Spectrodirect water testing instrument (Tintometer® Group, Germany) after the contaminated solution was exposed to plasma treatment. To achieve this, each of the reagents assigned to the different molecules were added to the samples withdrawn from the storage in a designated vial without dilution. The removal of TRA was monitored by measuring TRA concentration as a function of time during plasma treatment. To achieve this, 1 mL aliquot of the treated solution was withdrawn from the storage at 5 minutes intervals and analyzed on a High-Performance Liquid Chromatography (HPLC). The HPLC used is an Alliance Waters 2695 with a UV-Vis Waters detector equipped with Waters C18 5µ column which has 4.6 by 250 mm dimensions. The mobile phase used consisted of 50% acetonitrile and 50% water (with 1% acetic acid) at a flow rate of 1 mL/min. The injection volume was set at 10 µL while the UV detector was operated at 272 nm. TRA degradation efficiency in the solution was estimated using Eq. (3.2):

$$\eta (\%) = \frac{(TRA_o - TRA_t)}{TRA_o} 100 \quad (3.2)$$

Meanwhile, TRA degradation kinetics was confirmed as pseudo first-order according to Eq. (3.3):

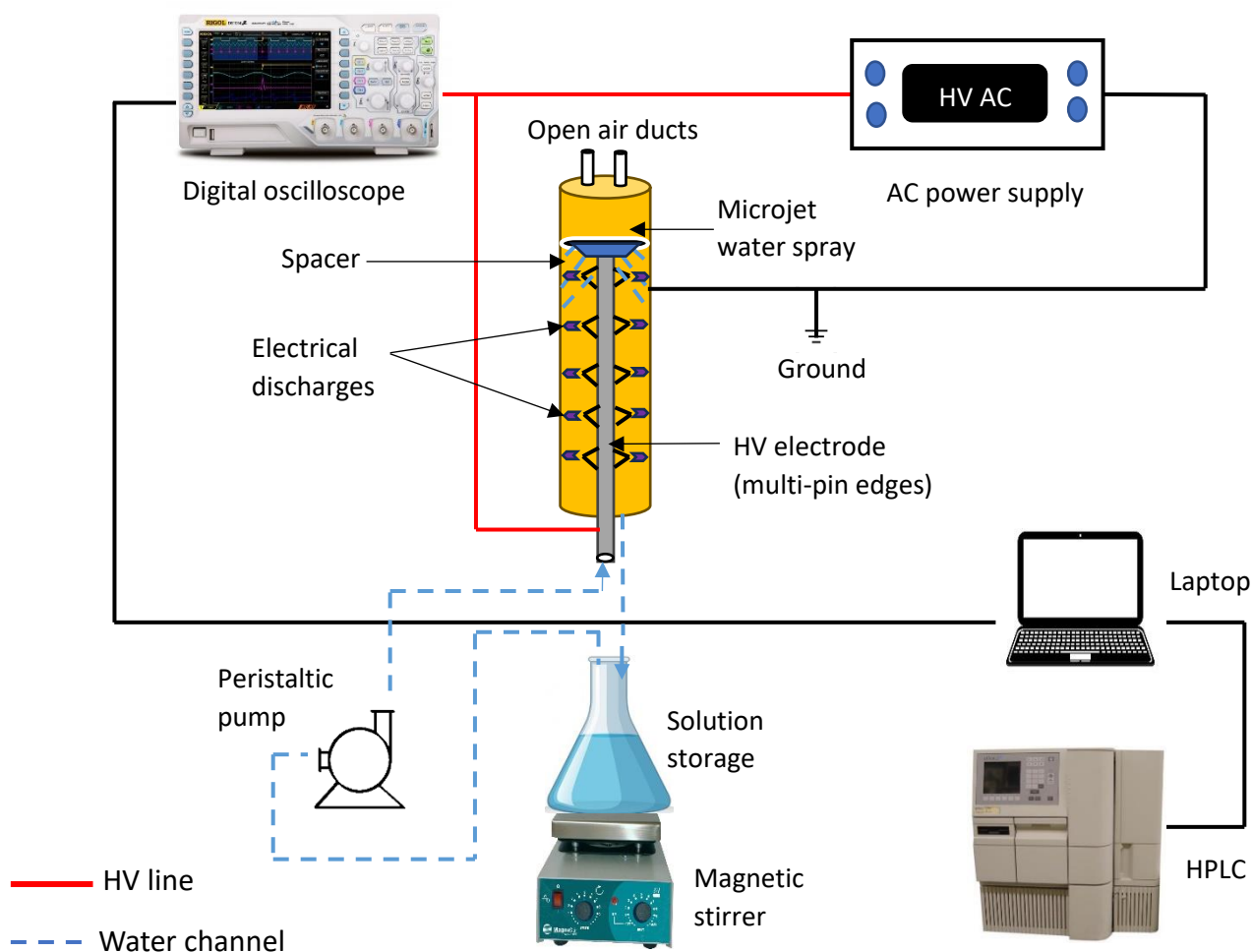
$$\ln \left(\frac{TRA_o}{TRA_t} \right) = kt \quad (3.3)$$

TRA_o and TRA_t (mg) represent the initial tramadol concentration and concentration at a predetermined time, t (min), respectively. η represents tramadol degradation efficiency and the rate constant is defined as k (min^{-1}). All inorganic ions present in the water matrices were quantified using a 940 professional Ion Chromatography (IC) variable chromatography (Metrohm, Switzerland), with a Metrosep C6-250/4.0 separation column and C6 eluent 8 mM oxalic acid (Metrohm, Switzerland) and the results are summarised in Table 3.1. Also, the energy yield, Y (g/kWh), is defined as the amount of TRA decomposed per unit of energy consumed. This was calculated with Eq. (3.4):

$$Y (g/kWh) = \frac{TRA_o \times V \times \frac{\eta}{100}}{P \times t} \quad (3.4)$$

where V is the volume of the treated water (L), η the degradation efficiency (%), P is the average power dissipated in the DBD reactor (W) and t represents the treatment time (h). Y_η describes the energy yield at a specific degradation efficiency, η (%).

To investigate the toxicity of the solution, an American Type Collection strain of Gram-negative *Escherichia coli* (ATCC 10536™) was purchased from Sigma Aldrich (Johannesburg, South Africa), and grown on Luria Bertani (LB) medium under incubation conditions for batch-batch reproducibility. The antibacterial activity of plasma-treated and untreated solutions containing TRA was tested by diffusion bioassay to determine zones of inhibition. Prior to the toxicity investigation, the bacterium was inoculated in nutrient broth at 37 °C for 24 h after which it was overlaid on the surface of nutrient agar plates. The tests were conducted in triplicate for untreated, plasma-treated TRA solutions respectively, and a control. After incubation, the presence of inhibition zones was used to confirm antibacterial activity.





(b)

Figure 3.1: Experimental arrangement for the tramadol degradation process (a) Schematic illustration of the setup (b) DBD plasma reactor showing purple streamer discharges at the edges of the multi-pin electrode.

3.3 Results and discussion

3.3.1 Electrical and optical characteristics of the dielectric barrier discharge reactor

The electrical properties of a plasma system directly influence its degradation efficiency. Therefore, voltage and current the variations during plasma discharge were captured with the digital oscilloscope and used in the calculation of the dissipated power. Figure A2 provides the characteristic current-voltage waveforms of the gas-liquid DBD plasma discharges with air. As shown, the peak value of discharge voltage and current were approximately 8.0 kV and 44.8 mA. In this study, the average dissipated power was estimated as 77 W.

To understand the reaction mechanism facilitated by the reactive species present, emission spectroscopy was conducted on the plasma generated as presented in Figure 3.2 in a range of 270 – 450 nm and 600 – 850 nm. Each specie was identified by comparing the peak positions with the atomic line database obtained in literature references [211,289,298]. As expected in

atmospheric air non-equilibrium discharges, the spectra were dominated by the excited N_2 molecules, then N_2^+ , OH, and O. These were generated primarily by energetic electron collisions with N_2 , O_2 , and H_2O molecules [211]. The N_2 spectrum ($C^3\Pi_u - B^3\Pi_g$) was followed by the N_2 spectrum ($B^3\Pi_g - A^3\Sigma_u^+$), indicating the formation of N_2 ($A^3\Sigma_u^+$) states. According to Lu *et al.* [232], N_2 ($B^3\Pi$ and $C^3\Pi$) and N_2^+ ($x^2\Sigma_g^+$) states are products of the electron impact excitation of the molecular ground state N_2 ($x^1\Sigma_g^+$). Meanwhile, OH radicals found at 297 and 309 nm [298] could be formed by the dissociation of water molecules caused by an electronic impact, as described in Eq. (3.5). Whereas O radicals at 777 nm might have been formed by energetic collisions of electrons with O_2 molecules, as described in Eq. (3.6) [299].



The analysis of the optical emission spectra revealed the generation of nitrogen, hydroxyl radicals, and atomic oxygen in the DBD reactor. These active species were found to be transferred into the liquid phase, where they further facilitated the production of secondary oxidative species, including H_2O_2 , O_3 , NO_3 , and NO_2 within the aqueous solution.

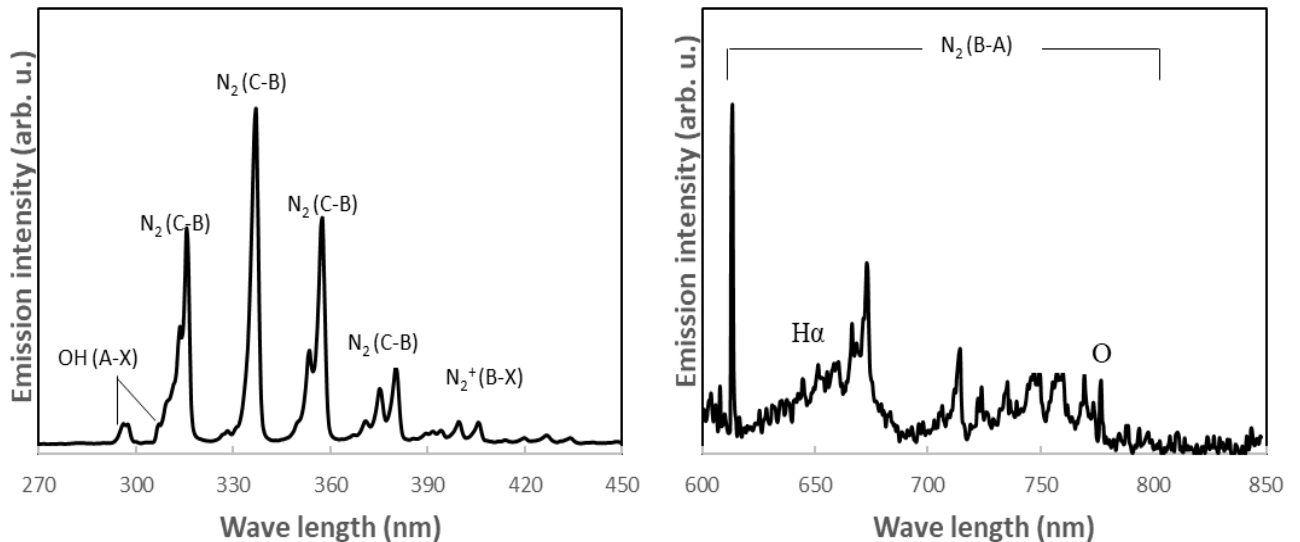


Figure 3.2: Optical emission spectrum of the plasma generated in the dielectric barrier discharge reactor at 20 kHz and 8 kV.

3.3.2 Influence of operating conditions on the removal TRA

Initially, the impact of applied voltage and initial concentration on TRA degradation efficiency was assessed. The parameters yielding the highest TRA conversion were subsequently considered as the optimal conditions.

Table 3.1: Ion chromatography analysis of the final wastewater effluent obtained from Daspoort Municipality, South Africa.

| Parameter | Unit | Measured value |
|-----------------------------|-------|----------------|
| Active hydrogen ions (pH) | | 7.53 |
| Conductivity | μS/cm | 548 |
| Total Suspended Solid (TSS) | mg/L | 10.4 |
| Chemical oxygen demand | mg/L | 10 |
| <i>Ortho</i> -Phosphate | mg/L | 0.06 |
| Chloride | mg/L | 56.26 |
| Sulphate | mg/L | 95.52 |
| Nitrite | mg/L | 1.42 |
| Nitrate | mg/L | 12.40 |
| Iron | mg/L | 0 |
| Bicarbonate | mg/L | 236 |
| Lithium | mg/L | 0.03 |
| Sodium | mg/L | 58.24 |
| Manganese | mg/L | 0.52 |
| Magnesium | mg/L | 24.74 |
| Bromide | mg/L | 5.42 |
| Calcium | mg/L | 44.43 |

3.3.2.1 Effect of input voltage

The input voltage is one of the significant parameters showing a great influence on the degradation of micropollutants with DBD reactors [22]. An increase in the input voltage is expected to increase the concentration of the reactive species formed in the reactor which will simultaneously increase the rate of degradation of the pollutant. From the results in Figure 3.3 (a), as the voltage increased from 6 to 8 kV, the rate of conversion of TRA also increased from 71% to 93% respectively during the plasma treatment. Similarly, the reaction kinetics more than doubled from 0.022 to 0.056 min⁻¹ respectively, as shown in Figure A3. This confirms that there is a positive relationship between the applied voltage and the rate of the reaction for TRA degradation with the DBD reactor. Comparable observations surfaced during the plasma-induced removal of pharmaceuticals like cephalosporins [203], Ibuprofen [245] amongst others.

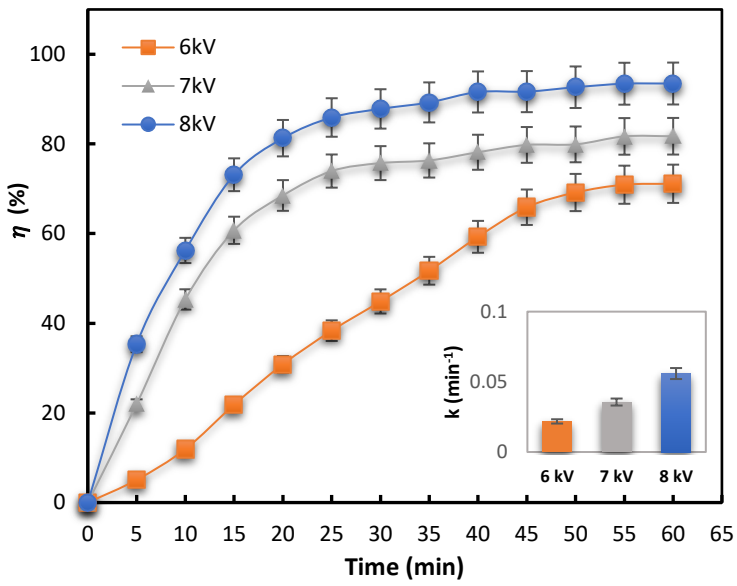
During the initial 20 min period, the degradation of TRA at 8 kV and 7 kV voltage inputs proceeded rapidly reaching 81% and 73% conversions respectively. Conversely, the rate of conversion was lower 6 kV. However, after 20 min, TRA degradation at 6 kV showed a consistent linear trend, while at 7 kV and 8 kV, the degradation proceeded at a notably slow rate. This divergence could potentially stem from a decline in available reactive species over extended durations. Another plausible explanation is the heightened competition between TRA and its intermediate products for the reactive species at 7 kV and 8 kV. Thus, the impact of applied voltage after 20 minutes on the removal of the actual contaminant was limited. Furthermore, the energy yield for TRA increased with the applied voltage as shown in Figure 3.3 (b). For example, at 50% TRA degradation, the energy yield (Y_{50}) computed at 6 kV, 7 kV, and 8 kV was approximately 0.07 g/kWh, 0.2 g/kWh, and 0.23 g/kWh, respectively. For each voltage, the energy yield decreased with an increase in the rate of TRA degradation. This is because, under a constant input voltage, the degradation rate of the target pollutant increases up to a point in which further energy input no longer contributes to pollutant removal.

The performance of the DBD plasma used in this work was compared with other AOPs in Table 2.2. As mentioned earlier, most of the studies were conducted in batch modes with small solution volumes. A commercialised pulsed corona discharge reactor used in the degradation of TRA achieved 91% degradation efficiency of the contaminant in 2 h [300]. Photocatalysis

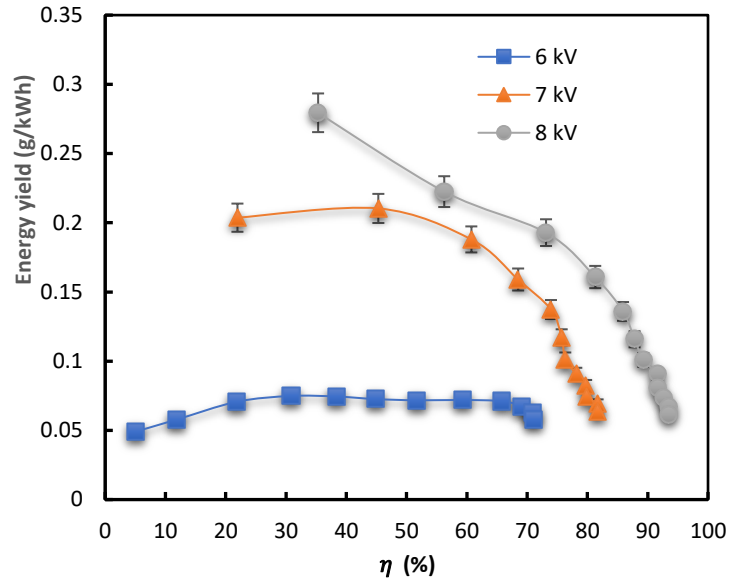
experiments conducted in 25 mL TRA solution gave 81.1% and 90.63% degradation efficiencies in 80 min and 120 min with bismuth ferrite and cobalt doped-bismuth ferrite catalysts, respectively.

Table 3.2: Degradation of TRA in water with selected AOPs.

| Methods | Operating conditions | Mode | Degradation efficiency | Treatment time | Rate constant | References |
|--|---|-----------------|------------------------|----------------|---|------------|
| Pulsed corona discharge | 33.4 μ M TRA prepared in 10 L and pH 6 | Continuous flow | 91% | 120 min | $3.10 \text{ m}^3 \text{ kW}^{-1} \text{ h}^{-1}$ | [300] |
| Photocatalysis | 10 mg/L TRA with 100 mg/L TiO_2 catalyst | Batch | 95% | 20 min | 0.153 min^{-1} | [292] |
| Electro-Fenton | 26.3 mg/L TRA in 250 mL solution at 500 mA | Batch | 100% | 10 min | $5.59 \times 10^9 \text{ M}^{-1} \text{ s}^{-1}$ | [293] |
| Photocatalysis | Bismuth ferrite in 25 mL TRA solution cobalt-doped bismuth ferrite in 25 mL TRA solution Fe_2O_3 phosphotungstic acid in 25 mL TRA solution | Batch | 81.1% | 120 min | 0.0145 min^{-1} | [161] |
| | | | 90.63% | 80 min | 0.0329 min^{-1} | |
| | | | 91.32% | 80 min | 0.0312 min^{-1} | |
| UV/Chlorine | 5 μ g/L TRA in 25 mL solution buffered to pH 7 | Batch | 100% | 10 min | 0.3785 min^{-1} | [132] |
| UV/ H_2O_2 | 5 μ g/L TRA in 25 mL solution buffered to pH 7 | | 100% | 15 min | 0.2005 min^{-1} | |
| Gamma irradiation combined with nanofiltration | 20 mg/L TRA in ultrapure water with 5 kGy | Batch | 100% | 12 min | - | [301] |
| Electrochemical oxidation | 100 μ M TRA in 100 mL under 30 mA electrolysis | | 100% | 90 min | - | [281] |
| DBD plasma treatment | 5 mg/L TRA in 1 L solution operated in continuous flow mode | Continuous flow | 93% | 60 min | 0.056 min^{-1} | This work |

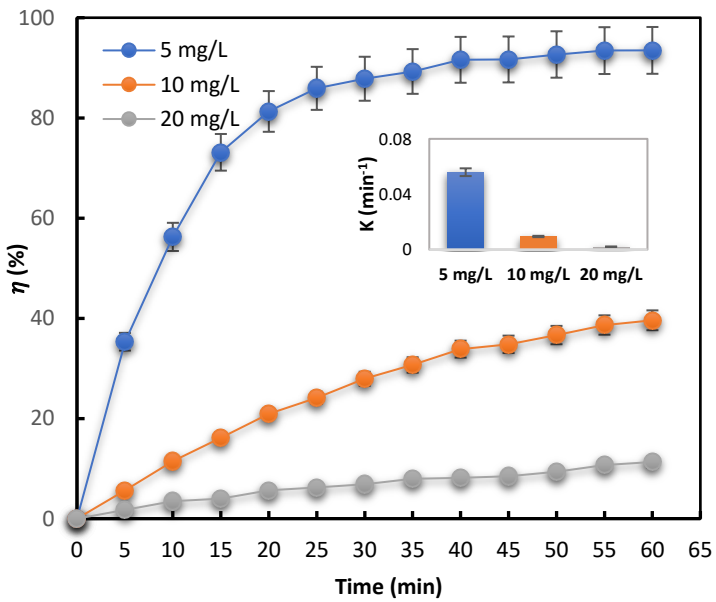


(a)

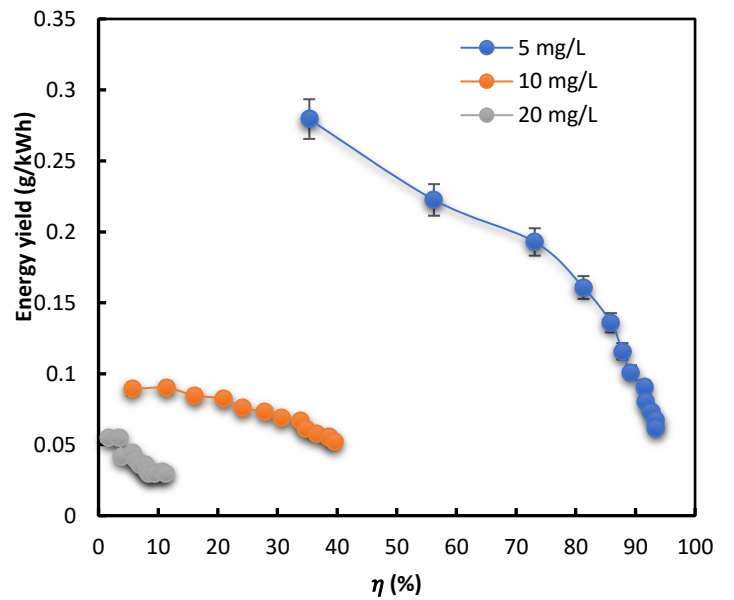


(b)

Figure 3.3: Effect of voltage on 5 mg/L TRA degradation. (a) Degradation efficiency and kinetics. (b) Energy yield.



(a)



(b)

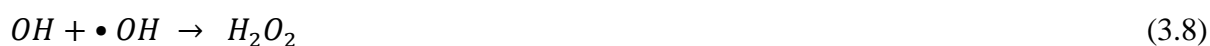
Figure 3.4: Effect of concentration on TRA degradation at 8 kV. (a) Degradation efficiency and kinetics; (b) Energy yield.

3.3.2.2 Effect of initial concentration

Using the optimum voltage of 8 kV, the effect of initial concentration on the degradation of TRA was examined. The results provided in Figure 4 (a) showed that the degradation efficiency of the pollutant decreased from 93% to 11% with an increase in the initial concentration from 5mg/L to 20 mg/L. Similarly, the reaction kinetics reduced from 0.056 to 0.002 min⁻¹, respectively, as shown in Figure S3. This result can be explained by the increase in the molecules of TRA caused by an increase in its initial concentration. As TRA molecules increase, not only does the consumption of the reactive species intensifies, but cross-reactions between the intermediate products and the reactive species also escalates. This limits further degradation of the pollutant itself. It is noteworthy that the concentration of TRA considered in this study surpasses what is typically encountered in the environment [8]. This suggests that at a much lower initial concentration of TRA than what was reported in this study, the degradation efficiency with our DBD system will be higher. Figure 4 (b) shows that at lower degradation efficiencies, the energy yield decreased as the initial concentration increased. A similar observation was reported for the removal of sulfadiazine antibiotics in water [197].

3.3.3 Contribution of active species: Generation of O₃, H₂O₂, NO₃⁻ and NO₂⁻ during the DBD discharge

The production of secondary oxidative species like ozone, hydrogen peroxide, nitrate and nitrite were examined in this study. Among these, the reactive oxygen species (O₃ and H₂O₂) have received significant attention due to their pivotal role in oxidizing micropollutants. The production of O₃ is based on Eq. (3.7), as derived from Eq. (5) and (6), while H₂O₂ is produced according to Eq. (3.7) – (3.9), respectively.



During the initial 20 min treatment period, the concentration of both O₃ and H₂O₂ increased simultaneously under the air-plasma treatment, with H₂O₂ having more presence in the solution and reaching as high as 2.2 mg/L. However, over extended durations, a sharp decline in the

concentration of H_2O_2 was observed plummeting to as low as 0.24 mg/L after one hour. The decline in the concentration of H_2O_2 provides another important explanation for the degradation rate of TRA after 20 min as seen in Figure 3.5 (a). This is because H_2O_2 is a direct product of the combination of short-lived OH radicals. Therefore, a decrease in its concentration means that less $\bullet\text{OH}$ is generated within the plasma. The generation of O_3 , on the other hand, quadrupled within the first 20 minutes of TRA removal and subsequently diminished. This result also verifies that O_3 played an important role in the elimination of TRA. Figure 3.5 (b) shows that the concentration of NO_3^- in the solution increased from 10 mg/L in the first 22 min to 76 mg/L after an hour, while NO_2^- increased from 4.8 mg/L in the first 30 min then decreased to 4.05 mg/L after an hour. An increase in the concentrations of the reactive nitrogen species in the solution will potentially increase acidity, especially in the absence of a pH buffer.

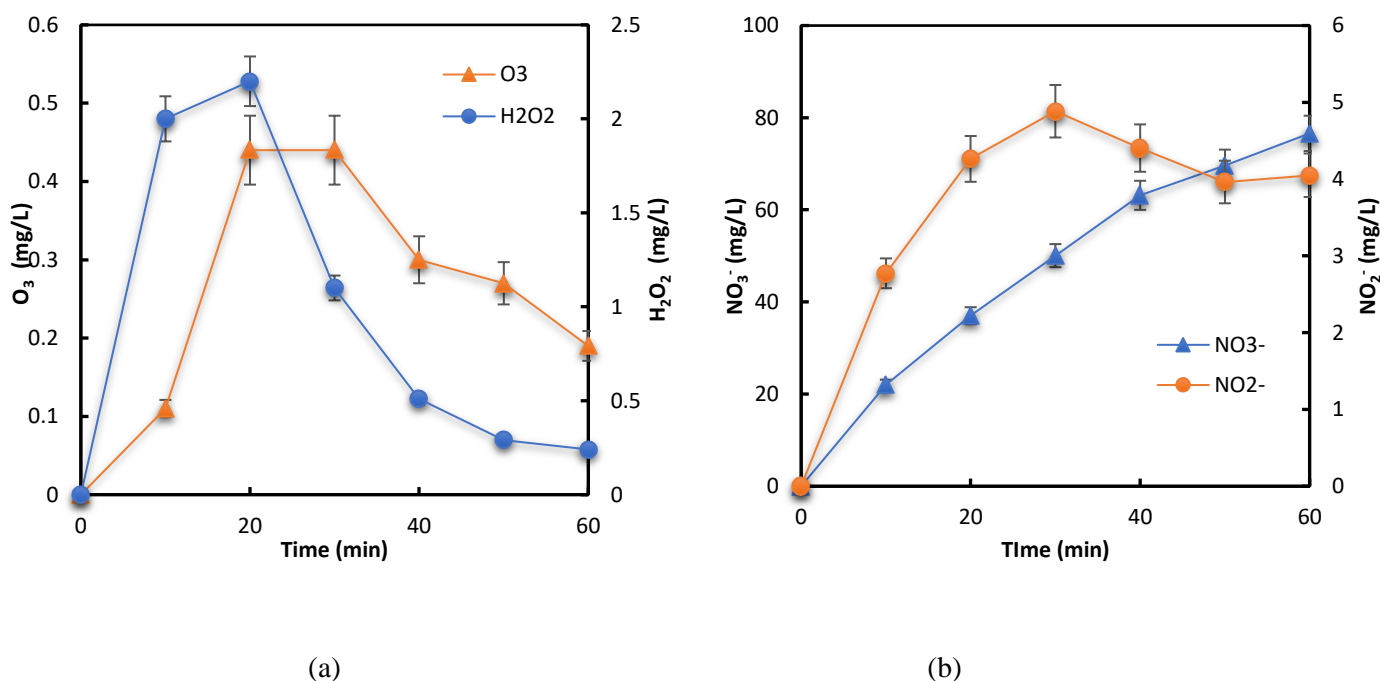


Figure 3.5: Reactive species formed during TRA degradation (5 mg/L initial concentration and 8 kV). (a) O_3 and H_2O_2 concentration; (b) NO_3^- and NO_2^- concentration.

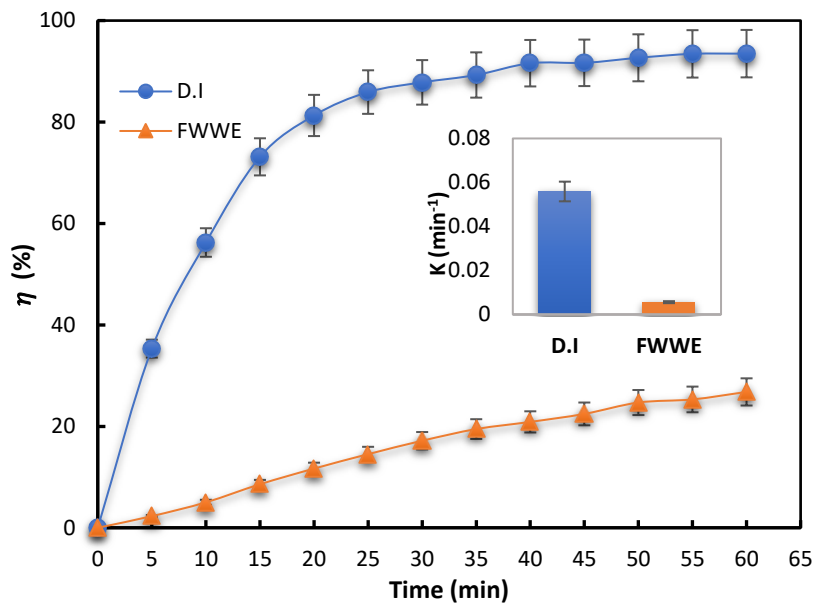
3.3.4 Comparison of the degradation of TRA in deionised water and final wastewater effluent

Based on the optimum initial concentration and voltage obtained, the degradation of TRA in deionised water and final wastewater effluent matrices was compared as shown in Figure 3.6 (a). After an hour of plasma treatment, the degradation efficiency of TRA was only 27% in the wastewater compared to 93% observed in deionised water. Also, the rate constant for TRA degradation in FWWE was 0.0056 min^{-1} which is an order of magnitude lower than that of the D.I matrix. The maximum energy yield was also markedly different, with the D.I yielding 0.28 g/kWh and the effluent matrix showing only 0.02 g/kWh , as illustrated in Figure 3.6 (b).

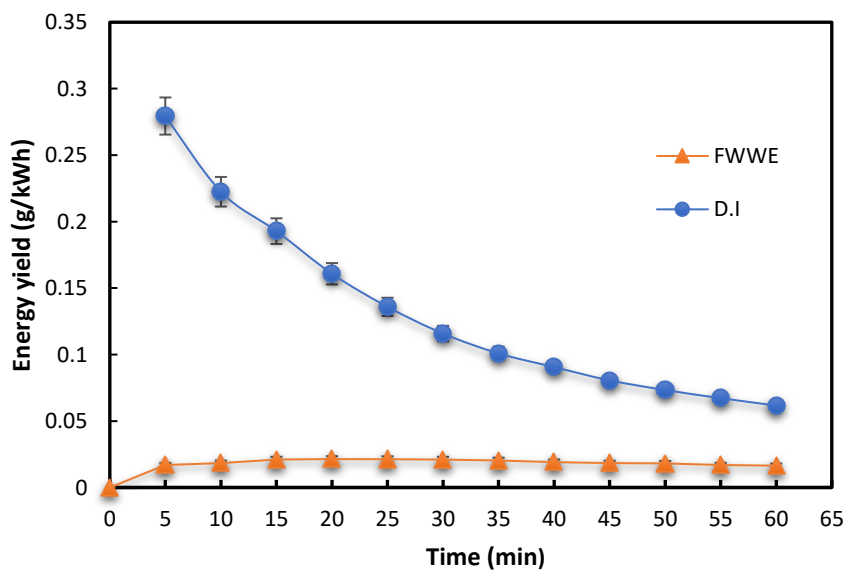
The pH and conductivity variations within the solution matrices during treatment are illustrated in Figure 3.6 (c). During the initial 5 min of treatment, the pH of the synthetic TRA solution decreases rapidly then continued at a steady value of about 0.11 in the next 55 mins. This observation can be attributed to the increased formation of nitrogen ions (NO_3^- and NO_2^-) within the solution as described in Figure 3.5 (b). The presence of NO_3^- and NO_2^- ions in the solution enables the formation of HNO_3 and HNO_2 compounds, subsequently resulting in increased acidity. Also, an increased formation of ions can be directly correlated with the linear increase in the conductivity of the solution as illustrated in Figure 3.6 (c). This further imposes limitations on the continued degradation of TRA. The presence of nitrogen ions and increased solution acidity may be attributed to the use of atmospheric air plasma system, as opposed to pure synthetic oxygen gas for plasma generation [203]. On the other hand, the pH of the wastewater solution remained fairly constant, while the conductivity only increased slightly. This is largely due to the buffering properties of the carbonate ion present in the wastewater effluent.

To examine the other factors responsible for the disparity in the degradation of TRA in the water matrices, some hypotheses were made. Firstly, considering that the wastewater effluent had a conductivity of more than two orders higher than deionised water ($2 \mu\text{S/cm}$) in magnitude, we hypothesised that conductivity might potentially influence the degradation of TRA in the wastewater. To verify this, KCl was added to the deionised TRA solution to increase its conductivity to that of wastewater ($548 \mu\text{S/cm}$). From the result provided in Table A1, the degradation rate constant at this result (0.0036 min^{-1}) defers from that of the final wastewater effluent (0.0056 min^{-1}). These results suggest that conductivity was not the sole

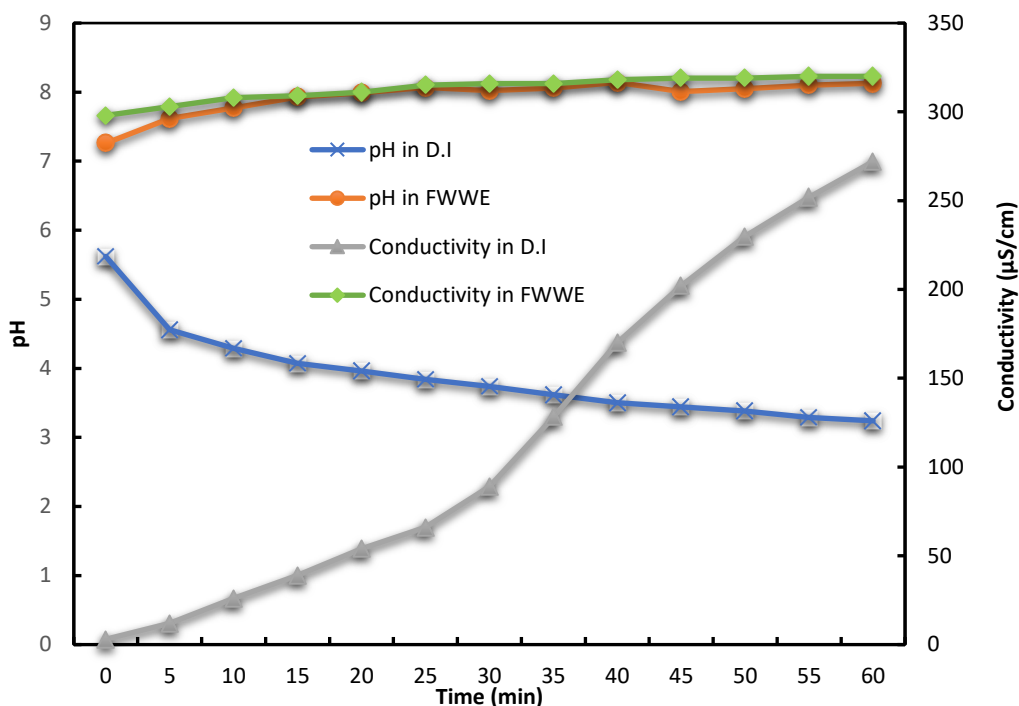
determinant of the disparity. To further investigate other possible limiting factors, control experiments were conducted for TRA in deionised water to examine (i) the effect of chloride ions, as chlorine is always used at the disinfection stage before final effluent discharge, (ii) the effect of carbonate ions, as sodium bicarbonate salts are added during treatment procedures to control pH. (iii) An in-depth investigation of the effect of pH variations was also conducted. Furthermore, a possible effect of the Fenton reaction, linked to the presence of Fe^{2+} ion was explored, despite their absence in the wastewater based on Table 3.1.



(a)



(b)



(c)

Figure 3.6: (a) Degradation of tramadol in deionised water and final wastewater effluent as a function of time; (b) Energy yield comparison; (c) pH and conductivity of the solution matrices as a function of time (Initial TRA concentration: 5 mg/L; Voltage: 8 kV).

3.3.4.1 Effect of chloride ions

Following the investigation into conductivity, the subsequent aspect explored was the potential influence of chloride ions. Chloride ions are primarily introduced into wastewater via hypochlorite chemicals, often used at the final effluent treatment phase for microbial disinfection. According to Table 3.1, the concentration of chloride ions measured in the wastewater was 56.26 mg/L. Therefore, to investigate the effect of chloride ions, 92.9 mg of sodium chloride was added into a deionised TRA solution and subjected to an hour of plasma treatment. The results, as depicted in Figure 3.7, revealed that the degradation of TRA in wastewater and TRA in D.I with sodium chloride exhibited similar trend during the initial 25 min. Subsequently, the degradation of TRA in D.I with sodium chloride continued linearly up to 52% efficiency. Table S1 showed that the final rate constant for the TRA with chloride ions was almost double that of the final wastewater effluent. Therefore, while the addition of

chloride ions initially impacted TRA degradation similar to the trend observed in the wastewater, it does not completely elucidate the observations for TRA in the effluent reaction medium. This is because chlorine gas ($E_0: 1.36 \text{ V}$) also has the potential to oxidise TRA in the solution. Another study has reported that the addition of chlorine to a UV system improved the removal efficiency of TRA in just 10 minutes compared to UV/H₂O₂ [132]. The interaction between chloride ions and $\bullet\text{OH}$ is explained in Eq. (3.10) – (3.13) [302]. However, the presence of NaCl as a chloride source was reported to harm the degradation efficiency of dye [303], due to the abstraction of $\bullet\text{OH}$ radicals.

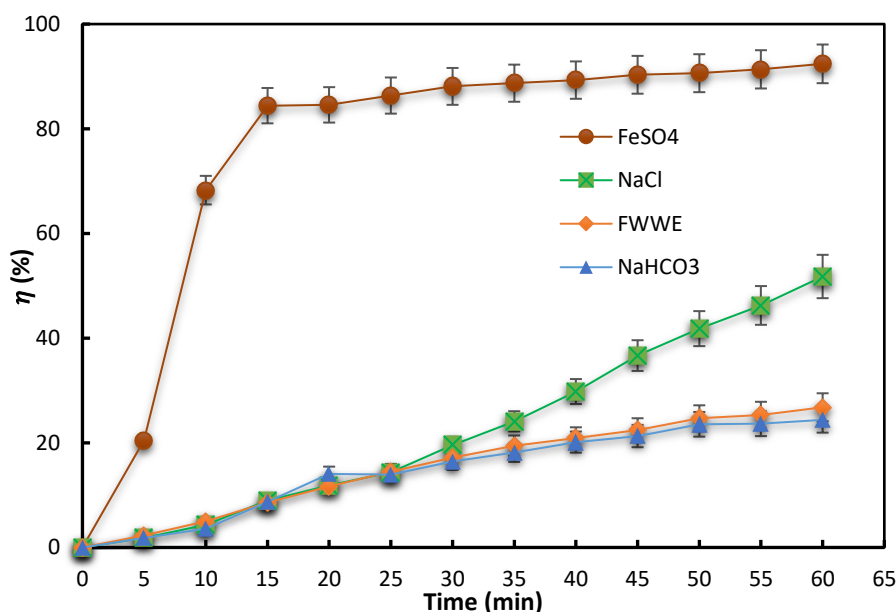


Figure 3.7: Degradation of tramadol in different reaction solutions (Initial TRA concentration: 5 mg/L; Voltage: 8 kV).

3.3.4.2 Effect of bicarbonate ions

The concentration of bicarbonate ions in the wastewater was 236 mg/L as provided in Table 3.1. To examine the influence of this potential radical scavenger on TRA degradation, 325 mg

of NaHCO_3 , equivalent to the concentration of the ion in the wastewater, was added to TRA deionised water solution. The solution was then subjected to an hour plasma treatment. The results obtained are provided in both Figure 3.7 and Table A1. In comparison with the wastewater dataset, these results revealed identical values for both degradation efficiency (27%) and rate constant (0.0056 min^{-1}). This implies that the presence of bicarbonate ions in the FWWE primarily accounts for its diminished degradation efficiency. However, this observation may be different for other organic compounds and different water matrices. For instance, a study reported that the presence of bicarbonate ions in tap water improved the degradation efficiency of phenol compared to a deionised (Milli-Q) water matrix [304]. In this case, the carbonate radical ($\text{CO}_3^{\cdot-}$) generated appeared to be a good oxidizing agent for phenol. Meanwhile, $\text{CO}_3^{\cdot-}$ is known to have a longer half-life than $\cdot\text{OH}$ [305]. The oxidation of some selected organic compounds has also been found to be facilitated by the presence of $\text{CO}_3^{\cdot-}$ [306]. In this present study, bicarbonate ions scavenged the hydroxyl radicals generated by the DBD plasma reactor which was the primary specie responsible for TRA degradation. $\text{CO}_3^{\cdot-}$ was generated according to Eq. (3.14) [307].



Also, despite the nitric compounds present in the solution, the pH recorded in Table S1 remained constant for the bicarbonate reaction solution. As explained earlier, the presence of bicarbonate ions in the solution helps to stabilise and maintain the pH level.

3.3.4.3 Effect of pH

The impact of pH on TRA degradation was examined by adding H_2SO_4 and NaOH to the deionised water matrix to adjust the pH levels. The experiments were carried out at pH levels of 3, 7, and 11, respectively, and compared with TRA deionised water solution. According to the results provided in Figure A4, an increase in pH reduces the rate of the reaction and consequently the efficiency of tramadol removal with the DBD reactor. Also, the reaction is unfavourable at extremely low pH values like 2. Meanwhile, a study on the removal of sulfadiazine with DBD reported that the degradation efficiency of the contaminant increased with the pH of the treated solution [197], as well as another study on phenol [304]. The reason for this can be explained by the fact that under basic pH conditions, ozone is further decomposed into more powerful oxidants like hydroxyl radicals and superoxide ions [256].

However, this is not the case for this study as ozone is not the key driver for the removal of TRA.

3.3.4.4 Effect of iron ions

While Fe^{2+} was not detected in the wastewater effluent at specific sampling time, prior researches [122,149,210,308] have reported that the degradation efficiency of micropollutants contaminants with a plasma reactor can be improved by the addition of Fe^{2+} as a metal ion catalyst. This is because Fe^{2+} reacts with H_2O_2 in the reactor to produce hydroxyl radicals as described in Eq. (3.15) – (3.17) [309]. Therefore, this study examined the possible effect of Fe^{2+} in the DBD tramadol treatment. To do this, $FeSO_4 \cdot 7H_2O$ was added into the deionised solution of tramadol to potentially increase the oxidizing potential of generated H_2O_2 by its conversion into $\bullet OH$ from the Fenton reaction. Figure 3.7 and Table A1 illustrate the effect of the addition of Fe^{2+} on the degradation of TRA. The experiment was performed at a concentration of 0.3 mg/L Fe^{2+} which represents the legal limit for wastewater discharge [310]. With the addition of iron, the degradation of tramadol was enhanced significantly such that in just 15 minutes, 84% of the pollutant had been removed compared to 73% recorded for the solution without iron. Also, after 60 minutes the rate constant of the Fe-enhanced solution was 0.061 min^{-1} compared to 0.056 min^{-1} for the synthetic solution. Unlike, the solution without iron, with Fe^{2+} the concentration of H_2O_2 was 1.18 mg/L in 20 min. This suggested that H_2O_2 was used up quickly during the process to facilitate the production of more $\bullet OH$. Based on these results, it may be inferred that the presence of Fe^{2+} in TRA solution could potentially influence its degradation efficiency with DBD plasma. Also, considering that the concentration of iron in wastewater could vary per time and season, it is recommended that future studies try to consider the possible effect of Fe^{2+} variation.



3.3.5 Elimination of antibacterial activity

An investigation of the effect of plasma exposure on the inhibition of bacterial activity in the pre-treated and treated TRA solutions was conducted and compared, as shown in Figure 3.8. The assessment of antibacterial activity in the TRA solution was based on the inhibition of *E. coli* growth, serving as an indicator of the solution's potential harm to the microorganism. It was observed that the untreated TRA solution showed clear inhibition zones on the agar plates as seen in Figure 3.8 (a), while the plasma-treated solution had no inhibition zones after 60 min as shown in Figure 3.8 (b). This indicated that the plasma-treated TRA solution was non-toxic to *E. coli*. As a baseline for comparative analysis, a third plate containing solely deionised water was included as a control within the experiment as seen in Figure 3.8 (c). The observed zones, in this case, were similar to those of the plasma-treated plate in Figure 3.8 (b).

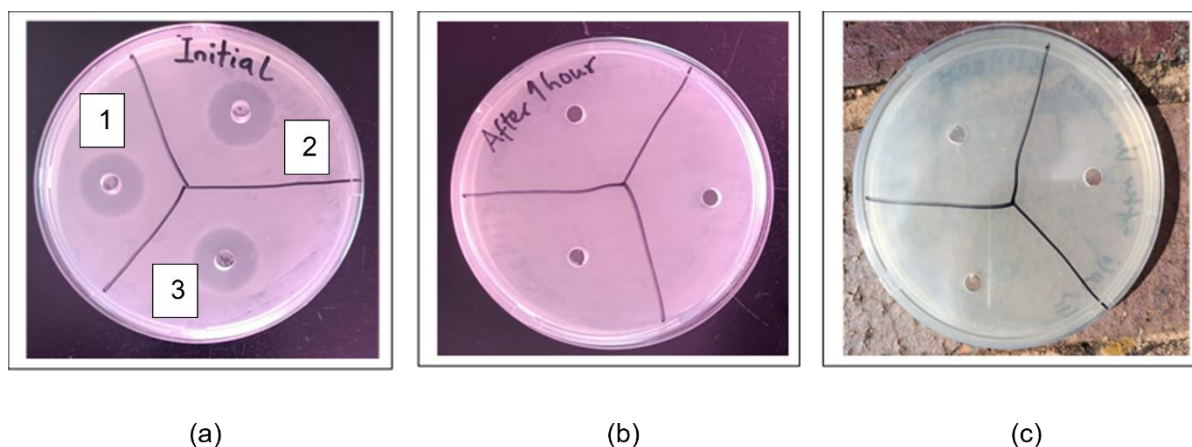


Figure 3.8: Bioassay to study the antibacterial activity of TRA samples against Gram-negative *E. coli* strain. (a) untreated tramadol solution with three zones of inhibition; (b) plasma-treated tramadol solution showing no inhibition zones; (c) is the control.

3.4 Conclusion

An investigation of tramadol degradation in deionised and final wastewater effluent matrices was carried out in this study with a newly developed water-falling dielectric barrier discharge reactor. Initially, the reactor was optimised for applied voltage and initial concentration of the pollutant. An increase in voltage directly led to an increase in the concentration of the reactive species, which in turn improved the degradation of tramadol. Meanwhile, an increase in the

concentration of the pollutant was a setback to the conversion process as the available molecules quickly scavenged the reactive species and inhibited further degradation. The optimum degradation of tramadol occurred at a combination of 8 kV and 5 mg/L. At these conditions, degradation efficiency and rate constant in deionised water were 93% and 0.056 min^{-1} , respectively. Contrarily, in the final wastewater matrix, tramadol degradation reached only 27% with 0.0056 min^{-1} rate constant. To elucidate this discrepancy, the authors investigated the effect of the significant radical scavengers present in the effluent solution through control experiments carried out in deionised water. Among all ions examined, CO_3^{2-} in deionised water exhibited the closest resemblance with the final wastewater effluent with a similar rate constant (0.0056 min^{-1}). This is because the HCO_3^- ion scavenged $\bullet\text{OH}$ radicals that could have oxidised the organic pollutant to generate $\text{CO}_3^{\bullet-}$ in the solution. Fenton reaction was also observed for the degradation of tramadol with a slightly higher degradation and kinetics than the TRA synthetic solution. Also, an increase in pH reduced the efficiency of the degradation. A toxicity test was used to confirm that the plasma-treated solution did not affect a Gram-negative *E. coli*. Considering that the addition of inorganic compounds that act as radical scavengers change the properties of water and treatment performances, the effect of their concentration should be investigated in future studies.

Chapter 4: Mechanistic study of cefixime degradation with an atmospheric air dielectric barrier discharge and influence of metal ion catalyst

This chapter addresses objectives one and three of the study and has been submitted to Elsevier Separation and Purification Technology Journal. The evidence of submission is provided in Appendix B7. The chapter details the application of a plasma generated by an atmospheric air DBD for the degradation of cefixime (CFX). Cefixime was investigated because it is an antibiotic with very few plasma-based degradation reports. The results indicated a complete degradation of CFX in a synthetic solution in 8 min treatment time with 6 kV and 20 kHz applied voltage and frequency, respectively. The energy yield recorded was 420 mg/kWh at the treatment time. Five intermediates were identified and a possible degradation pathway for the pollutant was proposed based on these using mass spectrum analysis. Also, radical scavenger experiments were used to understand the specific chemical species facilitating the pollutant's degradation. The effects of metal ion catalysts on the degradation of CFX were investigated in the aqueous solution. Fe^{2+} has been known to improve the degradation of organic compounds by facilitating the oxidizing power of H_2O_2 . A new idea was examined in this study, which was to examine the degradation of an organic pollutant in the presence of both metal ion catalyst and some selected hydroxyl radical scavengers (iso-propyl alcohol, tert-butyl alcohol, and sodium hydrogen carbonate). The results showed significant improvement in the degradation of CFX and energy yield in the presence of Fe^{2+} and the radical scavengers investigated which are due to the consumption of H_2O_2 .

4.1 Introduction

Cefixime (CFX), an antibiotic belonging to the cephalosporin class, has been included in some lists of emerging contaminants that are being monitored by regulatory agencies in water and wastewater [311]. It is widely prescribed for the treatment of bacterial infections in humans, including respiratory tract infections, urinary tract infections, and sexually transmitted infections. Due to its frequent use and incomplete absorption in the body, a significant amount of CFX is excreted through urine, and this ends up in wastewater [312]. Meanwhile, conventional wastewater treatment processes have been ineffective in the removal of most antibiotics [74]. As a result, significant quantities of CFX pass through these treatment systems and enter the environment through effluent discharge. Due to their poor solubility, CFX exhibits moderate to high persistence in the environment, leading to their long-term presence. At the same time, prolonged exposure to CFX and other similar persistent antibiotics has been linked to developmental abnormalities, reduced reproductive success, disruptions in the balance of microbial ecosystems in aquatic environments, and the development of antibiotic resistance [313].

As emerging technologies like advanced oxidation processes (AOPs) continue to gain interest in the degradation of refractory organic pollutants, plasma generated in electrical discharges has also been investigated as a possible degradation method for antibiotics since it leaves less toxic by-products. Plasma formation occurs through the introduction of energy into the gaseous phase, initiating inelastic collisions that lead to ionization and dissociation processes [314]. As a collective entity, plasma demonstrates macroscopic neutrality and exhibits group behaviour. The most captivating aspect of plasma lies in its capacity to establish a dynamic environment where photons, electrons, positive ions, reactive species (excited molecules and atoms), and radicals can coexist simultaneously to effect the degradation of organic compounds [235]. Already, non-thermal plasma (NTP) reactor designs like corona discharges [206,300,315,316], dielectric barrier discharge (DBD) [29,196,299], gliding arc [303,317], glow discharges [147], have been used in the degradation of similar persistent micro-organic compounds in water with significant efficiencies. In each geometry, the plasma is generated either within the liquid or in the gas phase above the liquid, or in some cases, in both the liquid and gas phases. Discharges generated in the liquid or gas phase result in different physical and chemical effects, which include the formation of shock waves, UV radiation, active radicals ($\bullet\text{H}$, $\bullet\text{O}$, $\bullet\text{OH}$), and molecular species (H_2O_2 , O_3 , etc.) [201]. A DBD plasma technology provides a novel means by which all these species can be generated at relatively

low temperatures and with high energy efficiency. Non-biodegradable pharmaceutical pollutants like pentoxifylline [201], ibuprofen [26], ciprofloxacin [251], norfloxacin [30], diclofenac [198], carbamazepine, [23] amongst others have been significantly degraded using a DBD reactor.

While DBD plasma is known for its energy efficiency, it is worth noting that the plasma characteristics can be significantly influenced by the initial conditions of the sample. In an attempt to improve the efficiency of a DBD plasma-based water treatment process, several efforts have been made by researchers. Some of these include the combination of a DBD plasma with other technologies like an ultrafiltration system for low energy degradation [318], increasing the mass transfer of the reactive species from the gas to the liquid phase through underwater bubbles [319], and the use of innovative power sources to improve energy efficiency [320,321]. To increase the chances of deploying the DBD system beyond lab-scale applications, some studies have examined the effect of water recirculation for increased throughput [206]. The use of heterogeneous catalysts like TiO_2 and CeO_2 has also been widely used to increase the generation of reactive species by leveraging on their activation with UV radiation and conversion of long-lived species into highly reactive ones ($\bullet\text{OH}$) [322–325]. However, these catalysts impose a high cost of treatment and the need to add a catalyst-recovery step all of which make their industrial applications a challenge to date. On the other hand, some studies have noted that the inclusion of a metal ion catalyst could potentially improve degradation efficiency with low associated cost [308,326,327].

In attempting to understand the controlling effect of active radicals, the degradation of pollutants in the presence of radical scavengers has also been explored, and the results have shown that radical scavengers could impede or enhance the degradation of a pollutant [29,255,328]. Also, the feed gas composition shows a remarkable effect on the treatment process during plasma treatment. For instance, Zhang et al . [211] compared the degradation efficiency of antibiotic CFX with oxygen, synthetic air, nitrogen, and argon using DBD technology. The authors reported that in the presence of synthetic air, the removal of CFX reached as high as 94.8%, next to oxygen (99.8%), in 30 min treatment time. Argon and Nitrogen gases gave a degradation efficiency of 73.4% and 45.3%, respectively. Besides this being the only available literature on CFX degradation with NTP, the degradation experiments in this study were conducted in a batch reactor which held a small volume of solution. To the

best of our knowledge, there is no study on the removal of CFX with a continuous-flow of DBD plasma generated by atmospheric air without an aerodynamic device. The intrinsic advantage of running a plasma experiment with natural air lies in the reduction of its cost of treatment which boosts its potential for commercial deployment. Also, there is an underexplored area in plasma water treatment and AOPs in general which is the investigation of the technology's performance in the presence of low-cost metal ion catalysts and radical scavengers.

Therefore, the contribution of this study is threefold. First, a continuous-flow atmospheric air DBD plasma was used to study the degradation of CFX for the first time. Secondly, after optimizing the factors that affect the degradation of the pollutant, an investigation of the reactive species facilitating this process was conducted. The intermediate products identified during the degradation process with the key reactive species provided a hint on the possible removal mechanism for CFX. Lastly, the influence of catalytic metal ion (Fe^{2+}) was studied as well as its effect in enhancing the degradation of CFX in the presence of various OH radical scavengers. Considering the interrelationship between OH and H_2O_2 , the concentration of H_2O_2 was monitored in the synthetic solutions containing OH radical scavengers and the metal ion catalyst. Overall, the main results from this study suggest a method for significantly increasing the efficiency of a DBD plasma technology in handling persistent micropollutants like antibiotic cefixime whilst also potentially reducing the cost of treatment.

4.2 Experimental section

4.2.1 Materials and chemicals

Cefixime ($\text{C}_{16}\text{H}_{15}\text{N}_5\text{O}_7\text{S}_2$ and MW = 453.50 g/mol) was purchased from Sigma-Aldrich Company (Germany). The physicochemical properties and chemical structure of CFX are summarised in Table B1 and Figure B1, respectively. Iron (II) sulphate heptahydrate ($\text{FeSO}_4 \cdot 7\text{H}_2\text{O}$) used as the source of Fe^{2+} was purchased from Merck, Germany. The chemical reagents used as radical scavengers include iso-propyl alcohol ($(\text{CH}_3)_2\text{CHOH}$) supplied by Radchem (PTY) LTD (South Africa), tert-butyl alcohol ($(\text{CH}_3)_3\text{COH}$), sodium hydrogen carbonate (NaHCO_3), sodium pyruvate ($\text{C}_3\text{H}_3\text{NaO}_3$), p-Benzoquinone ($\text{C}_6\text{H}_4\text{O}_2$) and uric acid ($\text{C}_5\text{H}_4\text{N}_4\text{O}_3$) which were supplied by Sigma-Aldrich (USA). The pH of the solution was altered

using sodium hydroxide (NaOH) and sulphuric acid (H₂SO₄) which were purchased from Glassworld (South Africa). All the chemicals used were of high-purity analytical grade and therefore required no further purification. The working solutions were prepared in deionised water obtained using an Elga LabWater Chorus 1 device.

4.2.2 Experimental procedure

The experimental setup for this study is provided in Figure 2.1. The major instruments consist of a DBD plasma reactor with water-falling film, high voltage AC power supply, high-performance liquid chromatography (HPLC), and a digital oscilloscope as shown in the setup, while ultra-performance liquid chromatography-mass spectrometry (UPLC-MS) system using a quadrupole time of flight (qToF) detector was added in this case. The reactive species generated by the DBD plasma reactor under atmospheric air include N₂, •OH, N₂⁺ and O, as was extensively discussed in the previous chapter (Section 3.4.1). The DBD reactor itself consists of a high-voltage electrode made of a multi-pin stainless steel rod of 29 cm in length and 1.27 cm in diameter. This was placed in a 30 cm long borosilicate glass tube which has 0.23 cm wall thickness and 4 cm outer diameter. The outer electrode was made of conductive copper tape with a 1 mm width and a thickness of 0.1 mm. The DBD plasma discharge was generated with natural atmospheric air in the absence of any aerodynamic device. The CFX solution was circulated in and out of the reactor by a peristaltic pump operated at a 500 mL/min flow rate. The contaminated solution enters the reactor through the hollow HV electrode and is sprayed via a micro jet spray centrally positioned at the top of the reactor. As the solution falls within the reactor, it contacts the plasma discharge generated at the multi-pins where the reactive species can act on the contaminant.

A stock solution of CFX was prepared by dissolving 100 mg of the compound first in methanol, then made up to 1 L in deionised water and subjected to sonication for about 20 min. Subsequently, 5 mg/L of CFX in 500 mL working solutions were derived from the stock solution. The experiments were conducted in continuous flow mode and at predetermined time intervals, samples of the treated solution were withdrawn from the water storage for both quantitative and qualitative analysis. The AC input voltage considered are 4,5, and 6 kV and at

a frequency of 20 kHz. Each experiment was conducted either in duplicate or triplicate, and the reported values represent the mean along with their error bars.

4.2.3 Analytic methods

An Alliance Water (2695 series) HPLC system equipped with Waters C18 5 μ column (4.6 mm \times 250 mm) was used to analyze the concentration of CFX during the experiments. The mobile phase consisted of 25% acetonitrile and 75% water (with 1% acetic acid) and a flow rate of 1 mL/min was used. The injection volume was 10 μ L while the column temperature was set at 30 \pm 5 $^{\circ}$ C. A UV-Vis Waters detector was used, and this was set at 289 nm. The degradation efficiency was calculated as:

$$\eta = \frac{C_o - C_t}{C_o} \times 100 \quad (4.1)$$

where η is the degradation efficiency of CFX, C_o is the initial concentration of CFX (mg/L) and C_t is the concentration of CFX (mg/L) at treatment time t (min). The kinetic analysis of CFX with DBD plasma was fitted according to the following first-order kinetic Eq. (4.2):

$$\ln \left(\frac{C_o}{C_t} \right) = kt \quad (4.2)$$

Where k is the reaction rate constant, t is the treatment time (min). The efficiency of the pollutant degradation was represented by yield (Y , g/kWh) which is defined as the amount of CFX degraded per unit energy consumed in the discharge according to Eq. (4.3) [201,329].

$$(Y, \text{g/kWh}) = \frac{C_o V \eta}{P t} \quad (4.3)$$

Where V is the volume of the solution treated (mL); P is the average power dissipated in the discharge (W) computed using Eq. (3.1).

The pH measurements were taken with a HANA multiparameter H198194 meter. The concentrations of H₂O₂ and O₃ generated in the plasma discharge were measured with a Lovibond spectrodirect water testing instrument (Tintometer Group, Germany), while an ion chromatography (IC) with a metrosep C6-250/4 separation column and C6 eluent 8 mM oxalic

acid was used to determine the concentrations of both NO_2^- and NO_3^- in the aqueous solution during DBD treatment. To investigate the roles of the active species generated in the plasma, scavenger experiments were set up with individual solutions of CFX containing uric acid (UA), tert-butyl alcohol (TBA), p-benzoquinone (BQ), and sodium pyruvate (SP) to trap O_3 , $\bullet\text{OH}$, $\bullet\text{O}_2^-$ and H_2O_2 , respectively.

4.2.3.1 Byproduct analysis

A Waters UPLC coupled in series to a Waters SYNAPT G1 HDMS mass spectrometer was used to generate accurate mass data. Optimization of the chromatographic separation was done utilizing a Waters HSS T3 C18 column (150 mm x 2.1 mm, 1.8 μm), and the column temperature was controlled at 60 °C. A binary solvent mixture was used consisting of water (Eluent A) containing 10 mM formic acid (pH of 2.4) and acetonitrile (Eluent B) containing 10 mM formic acid. The initial conditions were 98%A at a flow rate of 0.4 mL/min and were maintained for 1 minute, followed by a linear gradient to 10%A at 6 minutes. The conditions were kept constant for 1 minute and then changed to the initial conditions. The runtime was 10 minutes and the injection volume was 1 μL . Samples were kept cool at 8 °C in the Waters Sample Manager during the analysis.

The SYNAPT G1 mass spectrometer was used in V-optics and operated in electrospray mode to enable the detection of all ESI-compatible compounds. Leucine enkephalin (50 pg/mL) was used as a reference calibrant (Lock Mass) to obtain typical mass accuracies between 1 and 5 mDa. The mass spectrometer was operated in both ESI positive and negative modes with a capillary voltage of 2.5 kV, the sampling cone at 30 V, and the extraction cone at 4.0 V. The scan time was 0.2 seconds covering the 50 to 1000 Dalton mass range with an interscan time of 0.02 seconds. The source temperature was 120 °C and the desolvation temperature was set at 450 °C. Nitrogen gas was used as the nebulisation gas at a flow rate of 550 L/h and cone gas was added at 50 L/h. The software used to control the hyphenated system and do all data manipulation was MassLynx 4.1 (SCN 872).

4.3 Results and discussion

4.3.1 Impact of solution water flowrate

In a continuous-flow scenario, the flow rate of the treated solution influences the circulation time of the solution as well as the thickness of the liquid film. Therefore, in this study, the impact of solution flow rate on the removal of CFX was investigated as shown in Figure 4.1 (a) and (b). An increase in the flow rate from 300 mL/min to 500 mL/min favoured the removal of CFX from 94% to over 99%, and the kinetic constant (k) increased from 0.32 min⁻¹ to 0.58 min⁻¹, respectively. This is because an increase in the rate of recirculation of the treated solution in the reactor increased the thickness of the liquid film thus reducing the loss of reactive species. Also, increasing the flow rate of the liquid also increased the number of possible cycle times of the solution within the reactor thus enhancing the degradation of the targeted pollutant by adequate contact with the reactive species. This observation was also reported in the removal of Ibuprofen [245] and N, N-diethyl-m-toluamide (DEET) [260] by a water falling film DBD plasma. In practical applications, a high flow rate will be necessary for treating high volume of solution. However, at a very high flow rate, the liquid film might become too thick for the formation of the discharge and distribution of the reactive species. This can reduce the degradation efficiency and kinetics as was observed in Figure 4.1 (a) and (b) with 600 mL/min flow rate. Considering the degradation efficiency and rate constant shown by the k value, the water flow rate for later experiments was set at 500 mL/min.

4.3.2 Impact of applied voltage

The influence of applied voltage is an important factor in plasma treatment, particularly because it influences the generation of reactive species that oxidise pollutants in water. Typically, an increase in the applied voltage leads to the production of more reactive species which will enhance the rate of pollutant removal. The effect of applied voltage on CFX removal is shown in Figure 4.2 under the influence of the optimised flow rate (500 mL/min) and initial CFX concentration of 5 mg/L. With an increase in the input voltage from 4 kV to 6 kV, the degradation efficiency for the pollutant rose from 40% to over 99% within the 8 minutes of treatment, respectively as shown in Figure 4.2 (a). Also, the kinetic constant, as shown in Figure 4.2 (b) increased by an order of magnitude (from 0.05 min⁻¹ to 0.58 min⁻¹) as the applied

voltage increased from 4 kV to 6 kV. An increase in the intensity of the reactive species was confirmed by a change in the short purple discharge becoming long streamers as the voltage increased from 4 kV to 6 kV. The long streamers generated at 6 kV led to a faster degradation of CFX. During the treatment, the temperature of the electrode and that of the solution remained between 25 ± 3 °C, indicating that the degradation occurred at a low temperature.

The relationship between energy yield and treatment time is shown in Figure B3. Across specific voltages, the energy yield decreased over the treatment period. After 8 min plasma treatment, the energy yields recorded for 4 kV, 5 kV, and 6 kV were 0.19 g/kWh, 0.34 g/kWh, and 0.42 g/kWh, respectively. The degradation efficiency and energy yields for different AOPs used in the removal of CFX were compared in Table 4.1. The DBD plasma used in this study had the shortest treatment time taken to attain over 90% degradation efficiency among the technologies. Also, the energy yield recorded in this study far surpassed what was reported in most of the studies presented. Zhang *et al.* [211] reported a 1.5 g/kWh energy yield for CFX degradation using an underwater plasma bubble reactor in 50 mL solution after 30 min.

4.3.3 Impact of CFX concentration

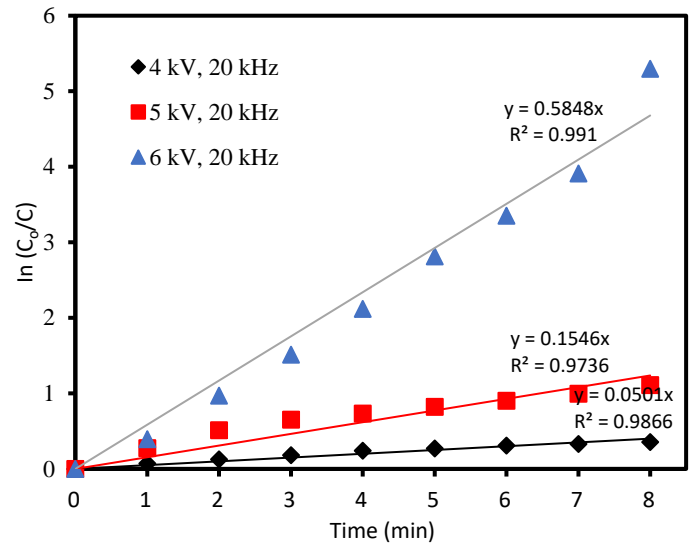
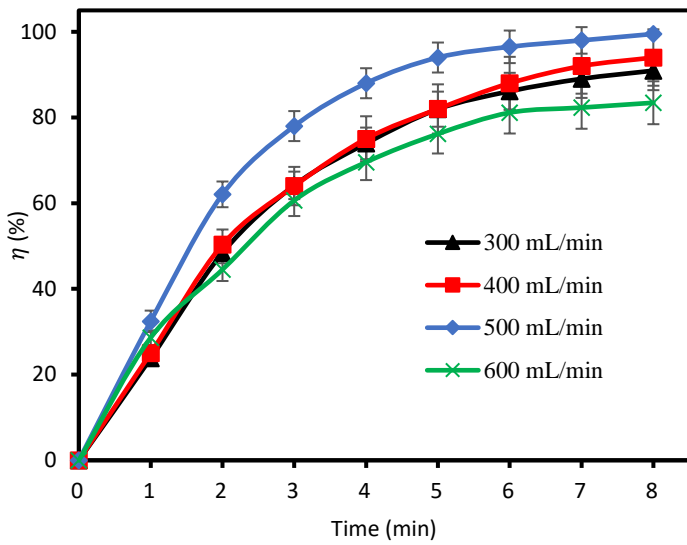
Typically, the concentration of organic pollutants in the environment varies over time due to various reasons as discussed in study [7]. Therefore, it is necessary to examine the effect of different CFX concentrations on its degradation. The concentration of CFX is related to the number of molecules of the compound in the solution which in turn affects its reaction with the active species generated by the DBD plasma reactor. The effect of the initial concentration of CFX was investigated at an optimum flow rate of 500 mL/min and an applied voltage of 6 kV. From Figure 4.3 (a) and (b), a lower initial concentration of CFX aided the degradation of the pollutant and its reaction kinetics. While the concentration considered in this study may be several magnitudes higher than what is naturally found in the environment, the results obtained have shown that as the concentration of the pollutant increases the degradation efficiency will reduce. For CFX, at initial concentrations of 5 mg/L, 10 mg/L, and 20 mg/L the removal efficiencies were >99%, 63%, and 50% after 8 min as illustrated in Figure 4.3 (a). Also, the kinetic constant reduced from 0.58 min^{-1} to 0.09 min^{-1} as the concentrations increased from 5 mg/L to 20 mg/L as shown in Figure 4.3 (b).

Meanwhile, the relationship between the initial concentration of CFX and energy yield showed an opposite trend as seen in Fig B3 (b). At the same treatment time, the energy yield increased with the initial concentration of the pollutant. After 8 min plasma treatment, the energy yield observed for 20 mg/L CFX was about 1.04 g/kWh, while 10 mg/L and 5 mg/L gave energy yields of 0.56 g/kWh and 0.42 g/kWh, respectively. Therefore, in this study, as the initial concentration of CFX increased from 5 mg/L to 20 g/mL, the degradation efficiency reduced by half its value while the energy yield increased by more than two times. This is because as the voltage remained at 6 kV, the quantity of oxidative species, including active particles, was constant per unit time at the same discharge conditions.

Therefore, as the rate of collisions among CFX molecules increases at higher initial concentrations, the consumption rate of reactive species rises significantly, thereby imposing a limit on degradation efficiency over a prolonged time. However, at low initial concentrations, the degradation efficiency is enhanced since fewer molecules are reacting with the species. This explanation elucidates why the degradation efficiency of CFX exhibited an inverse relationship with an increase in the initial concentration. A similar observation was reported by Wang *et al.* [202] for the degradation of metronidazole antibiotic by a DBD plasma configuration. Based on the analysis provided above, the initial concentration of 5 mg/L was selected for subsequent experiments.

Table 4.1: Comparison between selected AOPs used in the degradation of cefixime.

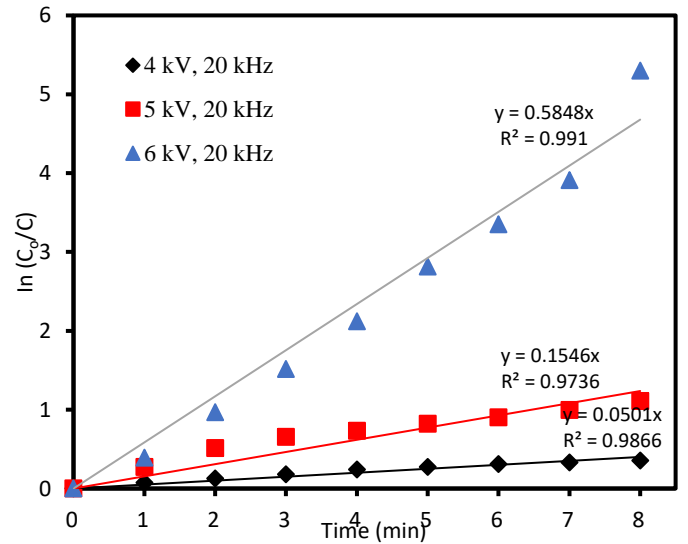
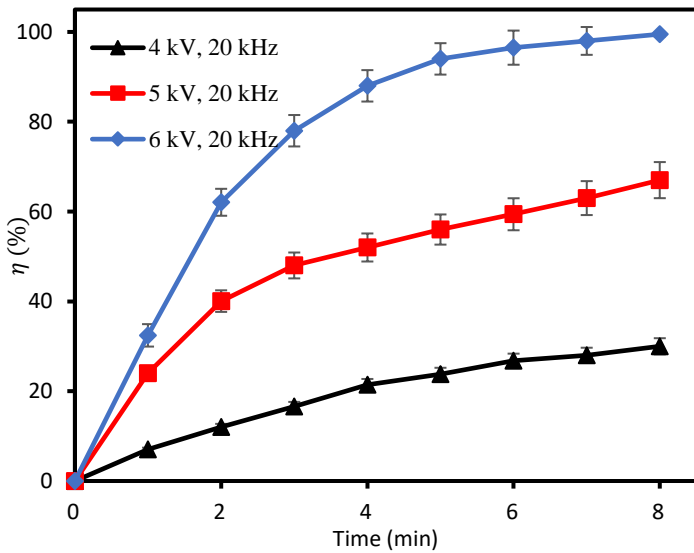
| Technology | Operating conditions | Initial concentration (mg/L) | Treatment time (min) | Degradation efficiency (%) | Energy yield (g/kWh) | Reference |
|---|---|------------------------------|----------------------|----------------------------|----------------------|-----------|
| SWCNT/ZnO/Fe ₃ O ₄ catalyst under UV-A irradiation | 0.46 g/L of the photocatalyst at pH 5.93 | 10 | 180 | 94.19 | - | [330] |
| Photo-Fenton system | NiCu ₂ S ₄ QDs@Fe ₃ O ₄ nanocomposite using visible light | 20 | 180 | 81 | - | [331] |
| CuO-NiO nanocomposite | 1 g/L of the photocatalyst at pH 2 | 15.22 | 180 | 90 | - | |
| Nano α -Fe ₂ O ₃ /ZnO photodegradation | 0.41 g/L of the catalyst under 8 W/m ² UV-vis irradiation | 10.11 | 127 | 99.1 | 0.022 | [159] |
| NiO/nano-clinoptilolite (NiO/NCP) | 0.25 g/L of the photocatalyst at pH 5 | 20 | 300 | 80 | 0.043 | [332] |
| Visible-light photocatalysis using α -Fe ₂ O ₃ @TiO ₂ | 0.012 g/L of the catalyst at pH 4.76 and calcination temperature of 439.34 °C | 20.5 | 103 | 98.8 | - | [333] |
| Plasma bubbles generated under water | Batch operation with discharge power of 6.3 W | 100 | 30 | 94.8 | 1.5 | [211] |
| DBD plasma discharge with multi-pin electrode | Atmospheric DBD plasma operated in continuous flow mode | 5 | 8 | >99 | 0.42 | This work |



(a)

(b)

Figure 4.1: Effect of water flow rate (a) degradation efficiency; (b) kinetics (Input voltage: 6 kV, initial concentration of CFX: 5 mg/L).



(a)

(b)

Figure 4.2: Effect of applied voltage (a) degradation efficiency; (b) kinetics (flow rate: 500 mL/min, initial concentration of CFX: 5 mg/L).

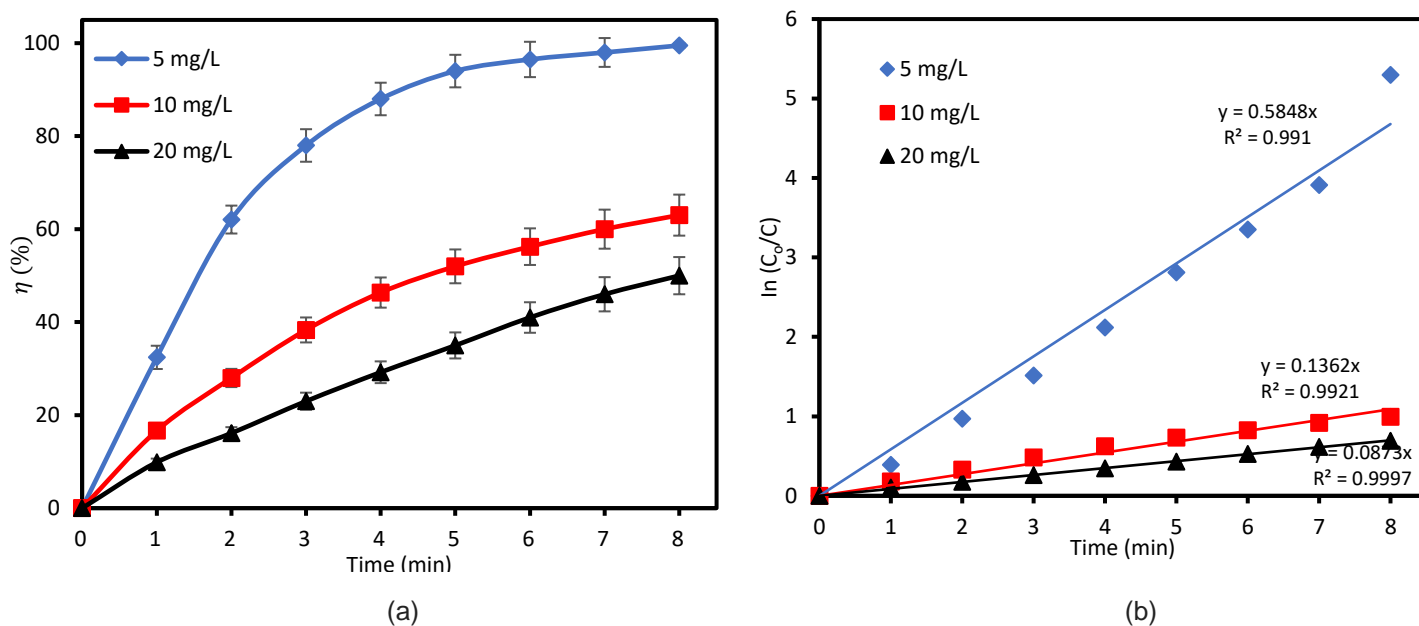


Figure 4.3: Effect of input concentration (a) degradation efficiency; (b) kinetics (flow rate: 500 mL/min, input voltage: 6 kV).

4.3.4 Impact of initial pH

The solution pH can influence the rate of degradation of an organic molecule in an aqueous medium [260]. To investigate the impact of solution pH on the removal of CFX, synthetic CFX solutions were subjected to treatment in the DBD plasma reactor, varying the initial pH values from 2.6 to 9. The relationship between the initial pH and the rate constant is presented in Figure 4.4. The results show that the rate of degradation of CFX is pH sensitive, progressing faster at higher alkaline conditions. In a strongly acidic medium (pH 2.6), the rate constant observed was about 0.1 min^{-1} , compared to 0.58 min^{-1} observed in the weak acidic medium (pH 5).

Meanwhile, as the initial pH increased from 5 to 9, the rate constant increased only slightly from 0.58 min^{-1} to 0.62 min^{-1} , respectively, within the treatment time considered. These findings indicate that the degradation of CFX was significantly impeded in a highly acidic condition but favoured in both neutral and alkaline conditions. The explanation for this is two-fold. Firstly, considering that the dissociation constant for CFX is 3.53 [334], when the initial

pH was below 3.53, CFX existed in the aqueous solution as molecules. Whereas it existed in the form of anions when the pH was higher than 3.53. Studies have shown that anions can readily react with the reactive species generated in a DBD system which will result in a rapid degradation of the organic compound [335]. Secondly, it has been reported that an increased $\bullet\text{OH}$ production is favoured under basic pH due to the presence of OH^- ions which could have increased the reaction rate [257].

Figure 4.4 (b) shows the change in pH values resulting from the initial pH variations. For the initial pH values of 5, 7, and 9, the final pH converged to approximately 4.7 ± 0.02 in all three conditions. However, at an initial pH of 2.6, the pH variation remained relatively constant for the entire treatment period. Generally, the pH of a solution during atmospheric air plasma treatment decreases due to the formation of nitrogen compounds [197].

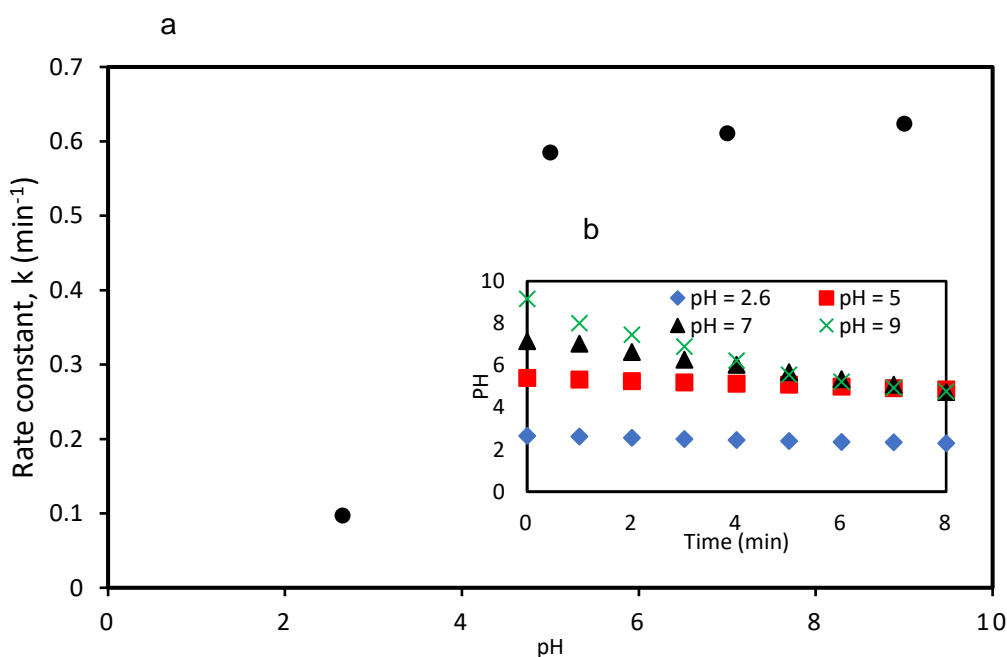
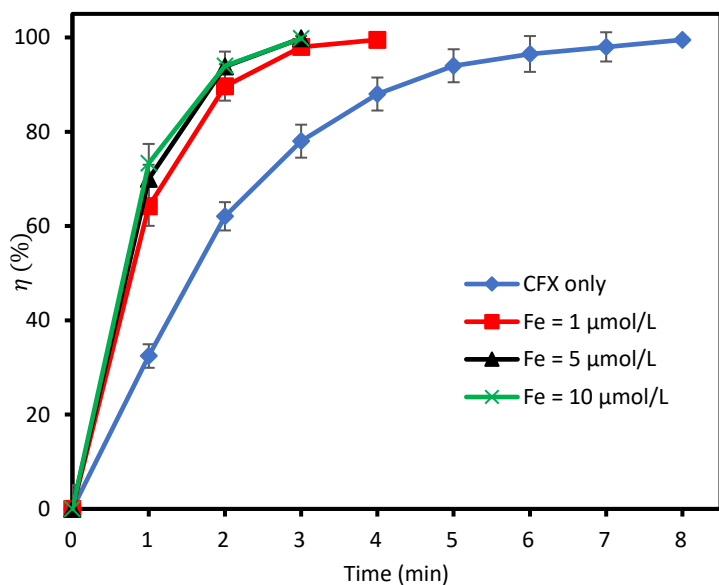
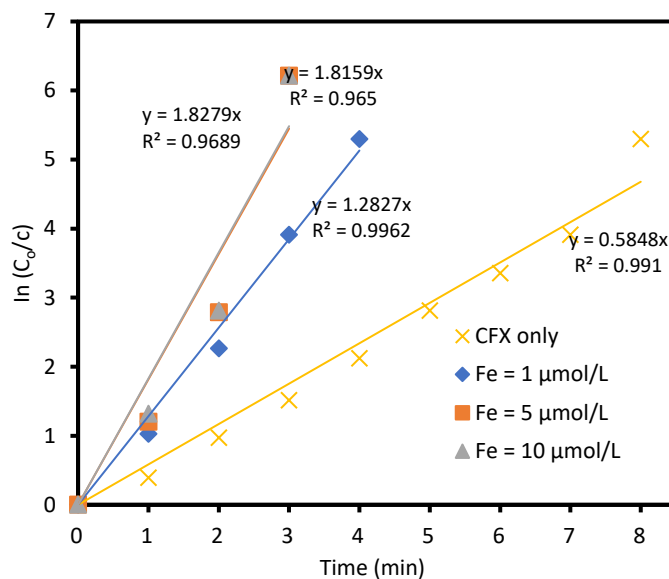


Figure 4.4: Effect of initial solution pH on CFX degradation (a) rate constant; (b) change in solution pH.



(a)



(b)

Figure 4.5: Effect of Fe^{2+} on the degradation of CFX (a) degradation efficiency; (b) kinetics.

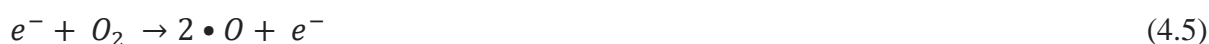
4.3.5 Effect of adding a metal ion catalyst

Several researchers have employed Fe^{2+} as a catalyst in plasma-based water treatment and observed significant improvement in the degradation efficiency of pollutants [24,210,308,327]. Therefore, this study investigated the possible influence of Fe^{2+} as a low-cost metal ion catalyst for the removal of CFX at different concentrations. As depicted in Figure 4.5, the addition of $\text{FeSO}_4 \cdot 7\text{H}_2\text{O}$ resulted in over 99% degradation of the pollutant in just 4 min. Meanwhile, in the absence of the catalyst, the degradation efficiency reached 88% at the same period. Furthermore, as the concentration of Fe^{2+} increased from 1 $\mu\text{mol/L}$ to 10 $\mu\text{mol/L}$, the rate constant also rose slightly from 1.28 min^{-1} to 1.83 min^{-1} after 8 min treatment. These observations can be attributed to Fenton reaction [336]. During the discharge process, both $\bullet\text{OH}$ and H_2O_2 are generated, but H_2O_2 reacts with Fe^{2+} according to Eq. (4.4) to produce more $\bullet\text{OH}$, thereby enhancing the removal of the pollutant. As this happens, the concentration of H_2O_2 is depleted.



4.3.6 Contribution of plasma reactive species and their roles

The efficacy of AOPs like plasma hinges on the generation of reactive chemical species. For an atmospheric air plasma, the spectra profile is primarily characterised by the presence of primary reactive species, including N_2 , N_2^+ , $\bullet OH$, and low intensity of O radicals [203]. In an aqueous medium, these reactive chemical species can further facilitate the production of secondary reactive species like H_2O_2 , O_3 , NO_2^- and NO_3^- . Both O_3 and H_2O_2 were formed from the bombardment of high energy electrons as seen in Eq. (4.5) – (4.9). These represent the long-lived reactive oxygen species (ROS) in the aqueous medium and their concentrations were monitored to explore their roles in the degradation of CFX. These species are also able to generate other highly reactive species, especially $\bullet OH$, which facilitates the degradation of the pollutant considering its high oxidation potential ($E_o = 2.8$ V) [337]. According to Figure 4.6 (a), the concentration of H_2O_2 is proportional to the treatment time, with an increased rate of H_2O_2 production observed between 6 to 8 min. The maximum H_2O_2 measured was about 1.45 mg/L at 8 min. Meanwhile, the formation of O_3 in the DBD plasma only began after 2 min and maintained a steady growth over the next 6 min reaching a maximum of 0.06 mg/L after 8 min.



The reactive nitrogen species present in the solution are NO_3^- and NO_2^- . These are generated from a series of reactions between excited N_2 with oxygen as presented in Eq. (10) to (15) [296]. The variation of NO_3^- and NO_2^- is shown in Figure 4.6 (b). The production of NO_2^- was only observed in the aqueous solution after 4 min of treatment reaching 2 mg/L after 8 min. Whereas, the formation of NO_3^- rose sharply in the first 2 min to 9.5 mg/L, continuing slowly over a prolonged time until 13.6 mg/L in 8 min. The production of the reactive nitrogen species can be linked to the increased acidity of the solution seen in Figure 4.4 (b), due to the formation of nitrous and nitric acid [296].



To investigate the individual contributions of the key reactive species to the degradation process, individual solutions of CFX containing species-specific scavengers were prepared and subjected to plasma exposure. Based on literature, we selected benzoquinone (BQ), tert-butyl alcohol (TBA), sodium pyruvate (SP), and uric acid (UA) as scavenging agents for $\bullet O_2^-$, $\bullet OH$, H_2O_2 , and O_3 , respectively [202,203,245]. The effect of the additions of these scavengers is shown in Figure 4.7 (a). In this study, 5 mg/L CFX concentration was considered with 0.5 mmol/L concentrations of BQ, TBA, TSP, and UA, separately. While this study has only focused on a single dose of the scavengers, further investigation of different concentrations of the quenchants might be necessary to provide an insight into the effect of variations of these scavengers as this could potentially affect the solution properties. After 8 min of DBD plasma treatment, the degradation efficiency of CFX reduced from over 99% (without scavenger) to 90%, 66%, 53%, and 51% in the presence of UA, TBA, BQ, and SP, respectively.

Likewise, the pseudo-first-order kinetic constant was reduced from 0.58 min^{-1} (without scavenger) to 0.33, 0.15, 0.11, and 0.10 min^{-1} upon the addition of UA, SP, TBA, and BQ, respectively. Comparing these results to the control (0.58 min^{-1}), it can be inferred that a significant difference in the degradation efficiency was observed for both TBA and BQ, which suggests that $\bullet O_2^-$ and $\bullet OH$ are the most critical reactive species for CFX degradation in this study. In contrast, O_3 played a minor role in the degradation of CFX, as seen in Figure 4.7 (a). Meanwhile, H_2O_2 may also have played a role in the degradation of the pollutant considering that $\bullet OH$ exists for a short time and they combine quickly to generate the species according to Eq. (4.9).

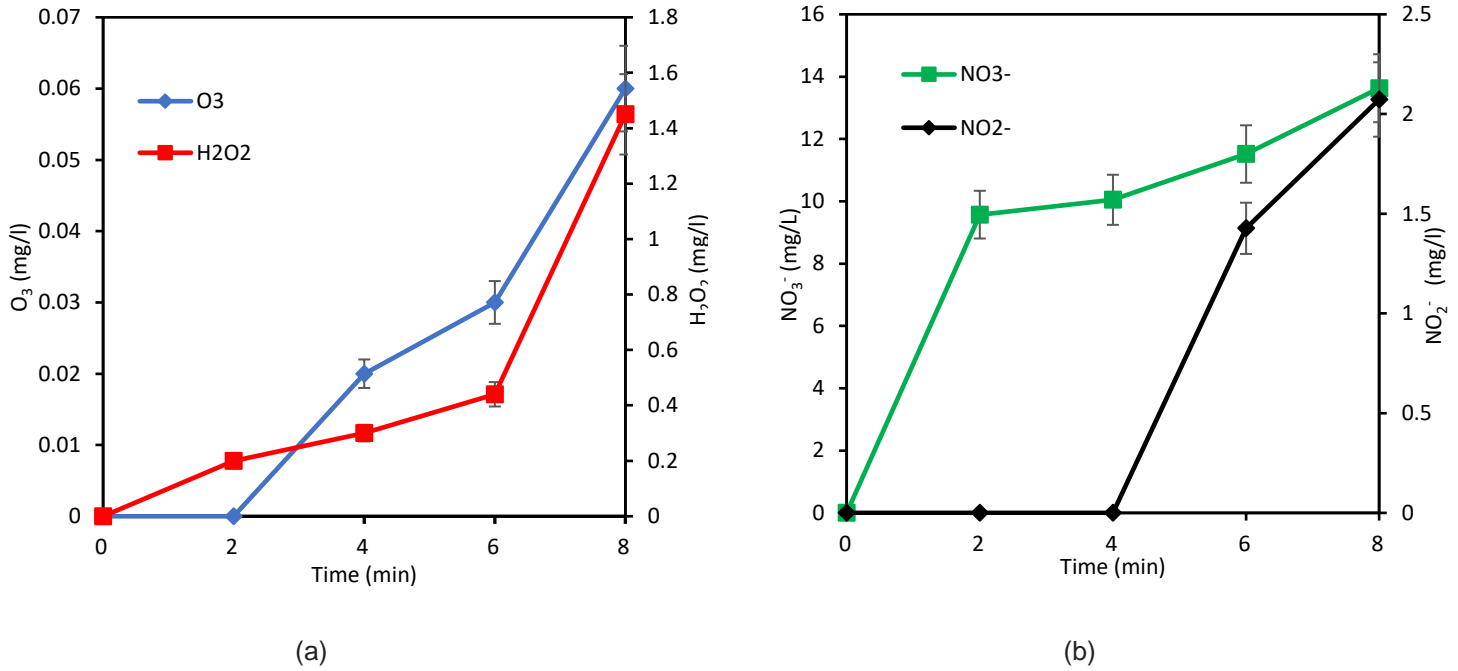


Figure 4.6: Contribution of reactive oxygen and nitrogen species during the degradation of CFX (a) O₃ and H₂O₂ (b) NO₃⁻ and NO₂⁻

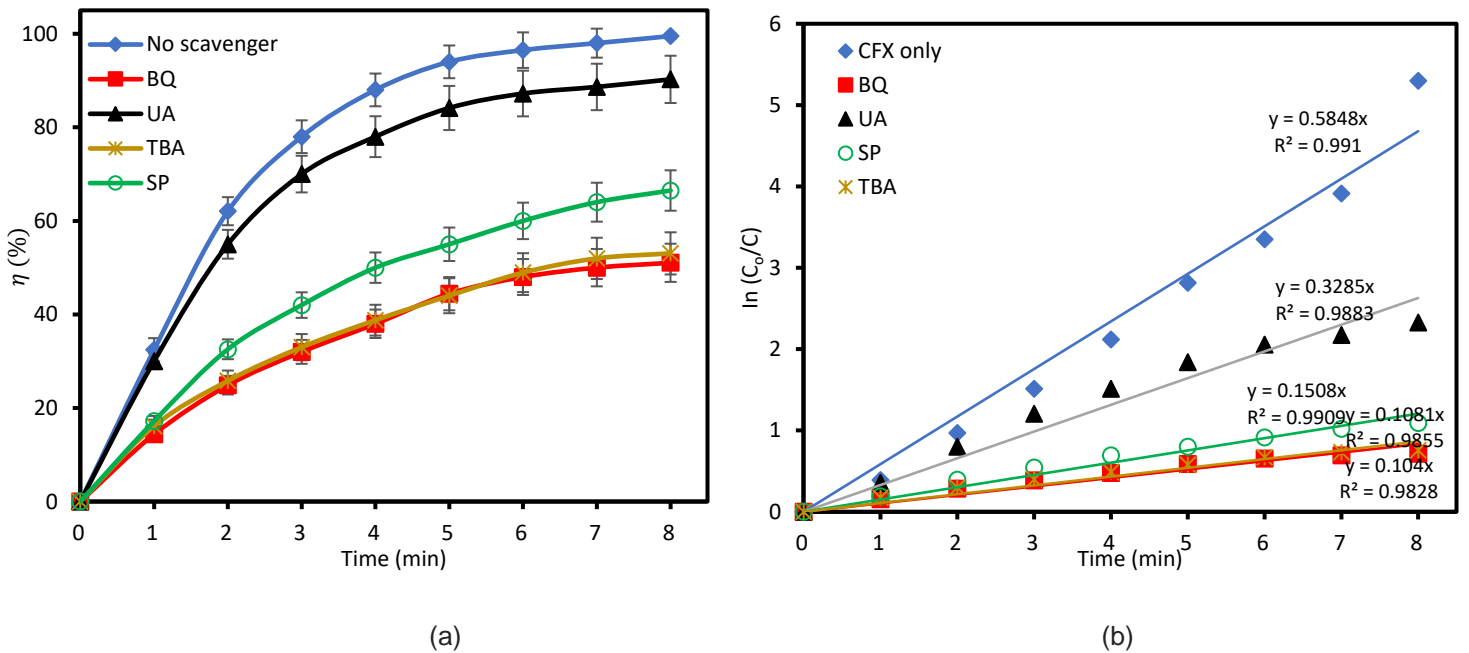
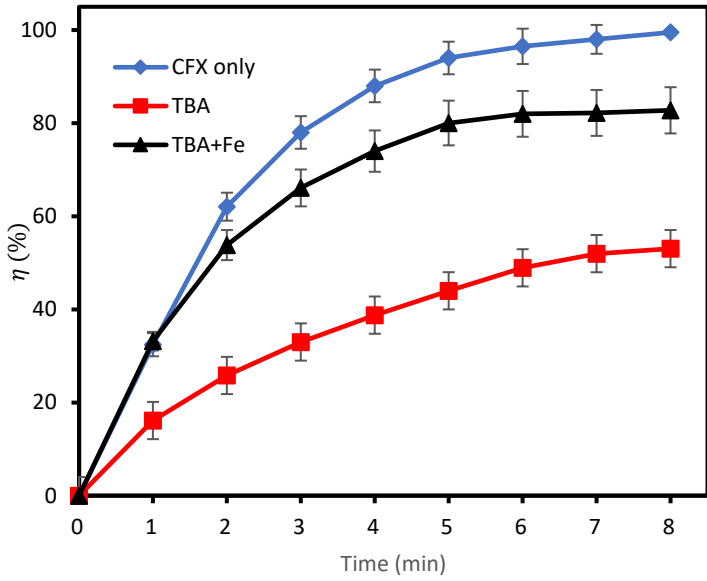
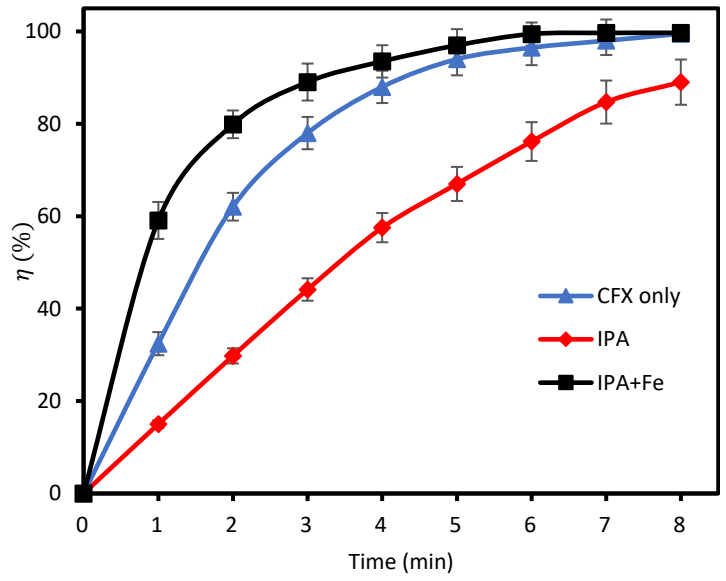


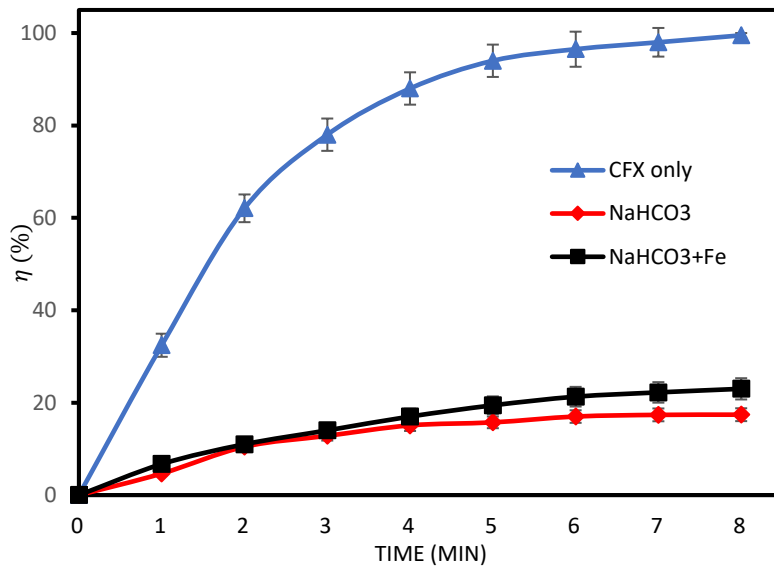
Figure 4.7: Effect of scavengers on CFX degradation in the DBD plasma system (a) degradation efficiency; (b) rate constants (Initial CFX concentration = 5 mg/L, Voltage = 5 kV, Frequency 20 kHz, Flow rate = 500 mL/min).



(a)

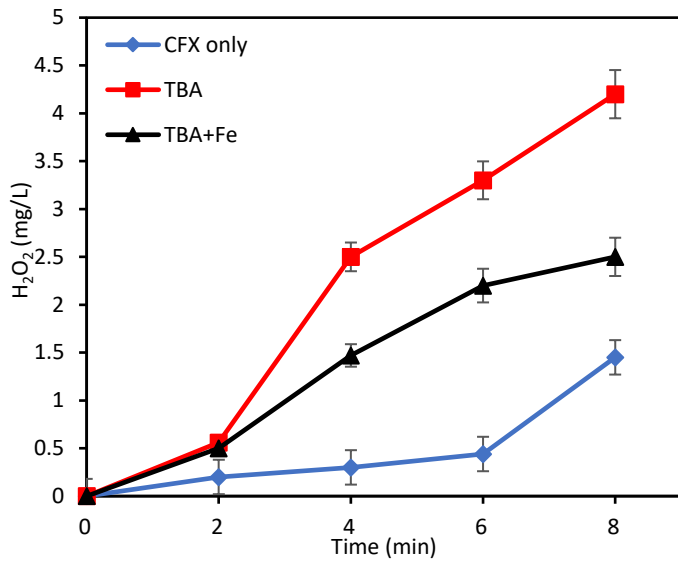


(b)

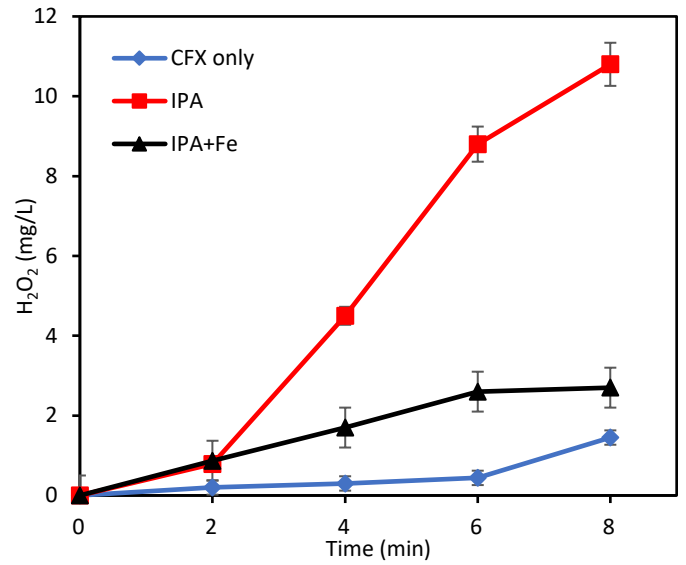


(c)

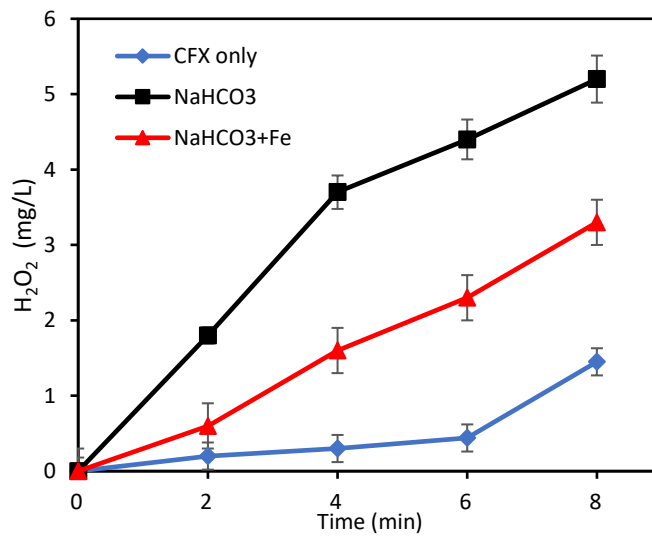
Figure 4.8: Effect of different additives on the degradation efficiency of CFX (a) TBA and Fe; (b) IPA and Fe; (c) NaHCO₃ and Fe (Initial CFX concentration = 5 mg/L, Voltage = 5 kV, Frequency 20 kHz, Flow rate = 500 mL/min).



(a)



(b)



(c)

Figure 4.9: Effect of various additives on H_2O_2 concentration (a) TBA and Fe; (b) IPA and Fe; (c) $NaHCO_3$ and Fe (Initial CFX concentration = 5 mg/L, Voltage = 5 kV, Frequency 20 kHz, Flow rate = 500 mL/min).

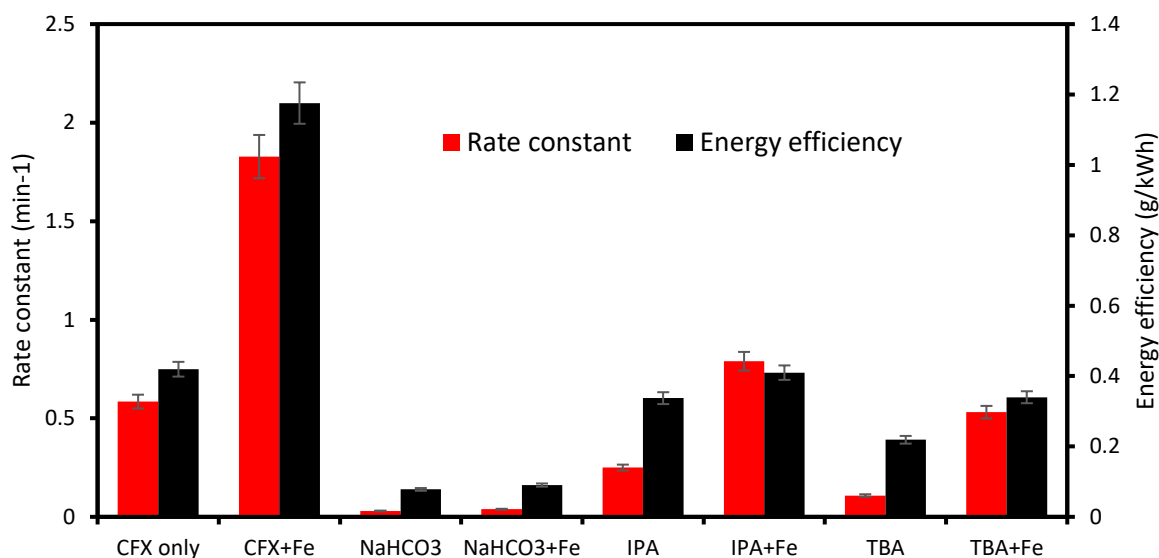


Figure 4.10: The rate constant and energy efficiency under different additives.

4.3.7 Investigating the combined effect of radical scavengers and metal ion catalyst

It has been established in this study that the degradation of the CFX pollutant with an atmospheric air DBD plasma can be related to the amount of H₂O₂ and •OH present. Also, the addition of Fe²⁺ as little as 1 μmol/L concentration was able to influence the rate of degradation of the pollutant through its reaction with H₂O₂ to generate more •OH species. Tert-butyl alcohol and iso-propyl alcohol are known •OH scavengers in aqueous solution which can react with the species according to Eq. (4.16) and (4.17), respectively. However, the scavenging effect of these species differs.

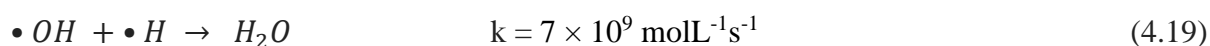
According to Figure 4.8 (a) and (b), the addition of 0.5 mmol/L of both TBA and IPA reduced the degradation efficiency of CFX in the aqueous solution to 53% and 89% within the treatment time, respectively. The result obtained for IPA in this case is interesting, as a previous study had reported a significant reduction in the degradation for CFX with the addition of the scavenger using a micro-bubble plasma technology [211]. Rong and Sun [338], on the other hand, observed that the addition of IPA improved the removal of triallyl isocyanurate (TAIC)

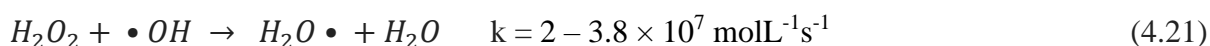
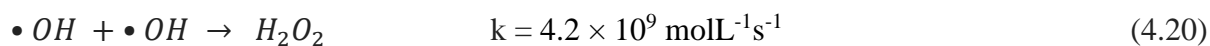
better than the case without the scavenger. In this case, the improved degradation efficiency of TAIC was due to the presence of other reactive species like $\bullet\text{H}$ and H_2O_2 even in the absence of $\bullet\text{OH}$. This result supports what was observed in this study because the presence of H_2O_2 was found to be perhaps another contributor to the degradation of CFX.

The difference in the degradation efficiency of IPA and TBA in this study can be explained by their reaction constants with $\bullet\text{OH}$. From Eq. (4.16) and (4.17), the rate at which IPA ($k = 1.9 \times 10^{10} \text{ molL}^{-1}\text{s}^{-1}$) reacts with $\bullet\text{OH}$ is faster than that of TBA ($k = 6.0 \times 10^8 \text{ molL}^{-1}\text{s}^{-1}$). This suggests that IPA has more potential to capture more $\bullet\text{OH}$ in the solution, leaving more H_2O_2 to appear in the solution. Also, NaHCO_3 , which is another other potential scavenger for $\bullet\text{OH}$ was considered in this study since it reacts with the reactive specie to form carbonate radical ($\text{CO}_3^{\bullet-}$) according to Eq. (4.18) [304]. However, despite that $\text{CO}_3^{\bullet-}$ has a lower oxidizing potential compared to $\bullet\text{OH}$, it can also be a good oxidizing agent. The addition of NaHCO_3 limited the degradation of CFX, yielding only 17% degradation efficiency after 8 min according to Figure 4.8 (c).



Figure 4.9 (a) – (c) shows the concentrations of H_2O_2 measured in the presence of the various chemical additives. Generally, it was observed that more H_2O_2 was detected in the presence of TBA, IPA, and NaHCO_3 . This signifies that all of these scavengers can enhance the formation of H_2O_2 indirectly in the aqueous solution. To explain this observation, first, we considered that the reaction rate constants for Eq. (4.20) and (4.21) are $4.2 \times 10^9 \text{ molL}^{-1}\text{s}^{-1}$ and $2 - 3.8 \times 10^7 \text{ molL}^{-1}\text{s}^{-1}$, respectively [224], indicating that the rate of recombination of $\bullet\text{OH}$ is about 100 times more than the consumption of H_2O_2 . Therefore, in the aqueous solution, H_2O_2 may be predominant. Secondly, when $\bullet\text{OH}$ is scavenged, the possibility of consuming H_2O_2 becomes minimal based on Eq. (4.21), leading to more H_2O_2 . Also, considering the effect of Fenton reaction described in Eq. (4.4), H_2O_2 becomes used up as Fe^{2+} catalyst was mixed with TBA, IPA, and NaHCO_3 as shown in Figure 4.10 (a) – (c).





Meanwhile, when the Fe^{2+} catalyst was mixed with the three scavengers individually, the degradation efficiency and kinetics increased according to Figure 4.8 and Figure 4.10, while the concentration of H_2O_2 dropped as shown in Figure 4.9. IPA again showed the most significant increase, even overlapping the solution without additives. This was because there was more H_2O_2 in the solution which could react with Fe^{2+} to generate more OH radicals. The degradation efficiency with the TBA solution increased from 53% to 83%, while $NaHCO_3$ only increased from 17% to 23 % in the presence of the Fe^{2+} .

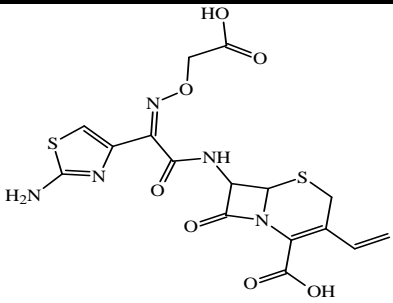
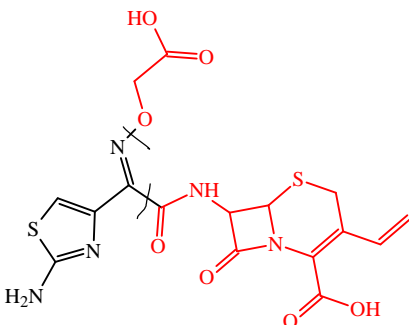
The rate of the reactions and energy yields in the presence of TBA, IPA, and $NaHCO_3$ were reduced according to Figure 4.10. However, when Fe^{2+} was introduced, the kinetics observed in the TBA solution had the highest growth of approximately 381%, while IPA and $NaHCO_3$ increased by 216% and 33%, respectively. For the energy yield (g/kWh), IPA and $NaHCO_3$ with Fe^{2+} increased by 21% and 12.5%, whereas TBA showed a 54% increase over the treatment period.

4.3.8 Identification of degradation intermediates and possible degradation pathways

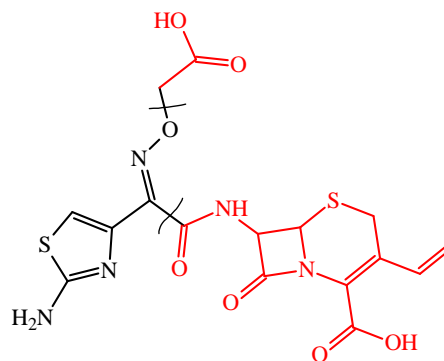
To clarify the degradation pathway of CFX using plasma, LC-MS analysis was employed to identify intermediate products in the process and the corresponding mass spectrum shown in Figure B6. A m/z value of 454 was observed at retention time 3.55 minutes which corresponds to the CFX parent compound and other five intermediate compounds with m/z values of 144, 118, 128, 287 and 288 were recognised at various retention times as shown in Table 4.2. The respective peaks have been low considering the concentrations analysed. However, the intensity of the CFX peak decreased with increase in the treatment times whereas the intensity of the intermediates increased at early stages and decreased thereafter, suggesting their mineralization at later stages of the reaction. The m/z values and possible molecular structures of intermediates (Figure 4.11) indicate that intermediates were generated mainly through loss

of functional groups and ring-open reactions with the main reaction sites as the sulfide in the thiazine ring, carboxylic, amide and imine groups. The cleavage of the azetidine ring is also suggested. Two degradation pathways have been suggested; one involves cleavage of the azetidine ring to form the first intermediate with m/z value of 287 followed by decarboxylation and cleavage of the imine-amide bond and breaking off of the thiazole ring to form m/z 144 and m/z 118 respectively. The second pathway involves opening of the thiazine ring and decarboxylation to form m/z value of 288 followed by cleavage at the amide functional group to form m/z 128. Out of the 5 intermediates, 4 had a shorter retention time than CFX implying that more polar intermediates were produced during degradation due to loss of some functional groups. After 8 min reaction time, some of the intermediates were eventually converted to H_2O , CO_2 , NO_3^- , NO_2^- , and SO_4^{2-} . At this reaction time, the spectra suggest that there might be an incomplete mineralization since small amounts of intermediates (m/z 144 and m/z 128) are still present but can fully be mineralised with longer degradation time.

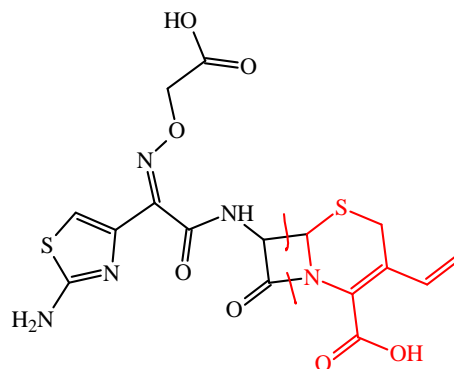
Table 4.2: Degradation by-products for cefixime with the DBD plasma reactor

| Identity | Chemical formula | Rt (min) | Characteristic ions (m/z) | Suggested structure |
|----------|-------------------------|----------|-------------------------------|--|
| C1 | $C_{16}H_{15}N_5O_7S_2$ | 3.55 | 453 |  |
| C2 | $C_4H_5N_3S$ | 0.80 | 128 |  |

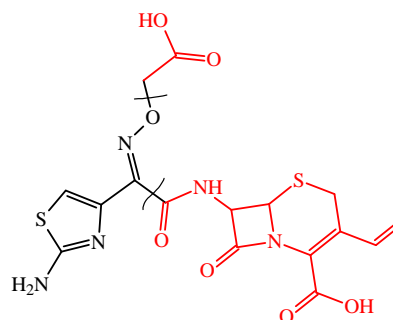
C3 C₄H₆N₃OS 1.06 144



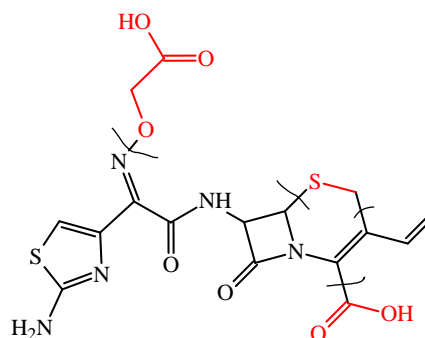
C4 C₉H₁₁N₄O₅S 1.80 287



C5 C₄H₆NO₃ 2.84 118



C6 C₁₂H₁₀N₅O₂S 5.56 288



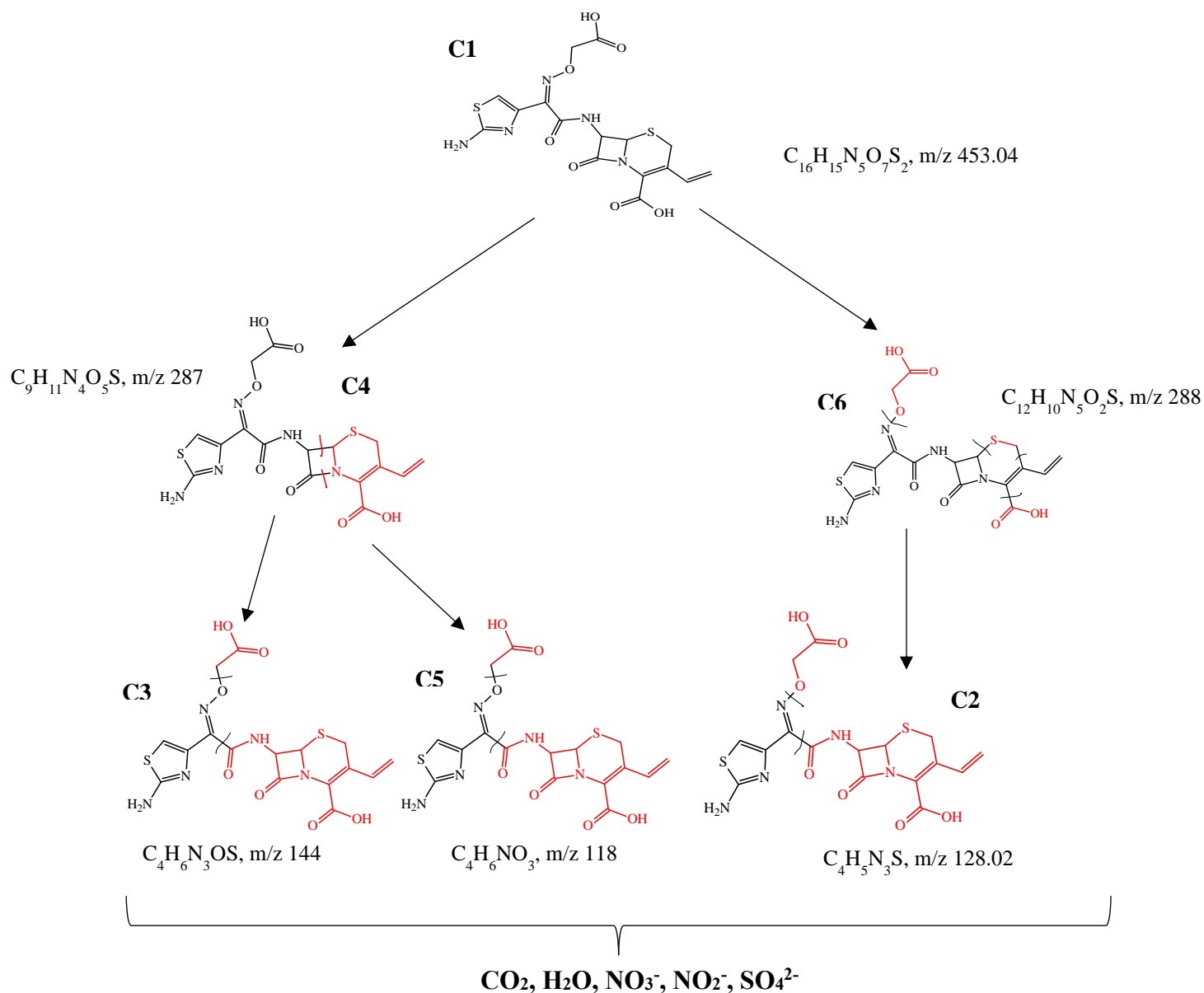


Figure 4.11: Proposed degradation pathway for the degradation of CFX using the DBD reactor.

4.4 Conclusion

An atmospheric air dielectric barrier discharge reactor was used in the degradation of cefixime antibiotics in this study. The results demonstrated that the pollutant can be almost completely removed by the technology in 8 min treatment time using an AC power supply operated at 6 kV applied voltage and 20 kHz frequency. An energy yield of 0.42 g/kWh was obtained with the reactor. The active species responsible for the degradation of this pollutant are primarily $\bullet\text{OH}$ and $\bullet\text{O}_2^-$ which were identified via radical scavenger experiments. H_2O_2 also played a minor role in the degradation of the pollutant. The influence of Fe^{2+} catalyst improved the oxidizing power of H_2O_2 generated by the reactor through its conversion to $\bullet\text{OH}$ which enhanced the degradation of CFX. A new contribution was also made with regards to the application of a DBD plasma reactor which is an investigation of the mixed additives of hydroxyl radical scavengers and the metal ion catalyst. From the degradation of cefixime, 5 intermediate products were observed which were used in proposing a degradation pathway.

Chapter 5: Insights into the degradation of carbamazepine using a continuous-flow non-thermal plasma reactor: mechanism and comparison with UV-based systems

This chapter addresses the first and fourth objectives of the study. It has been submitted to the Journal of Environmental Sciences. The evidence of submission is provided in Appendix C1. In addition to understanding the mechanism of degradation of carbamazepine (CBZ) with the DBD reactor, the key contribution of this chapter is the comparison of the technology used in this study with widely deployed advanced oxidation processes, like the UV-based systems. At first, the degradation of CBZ was studied using an atmospheric DBD reactor. Next, the influence of different operating parameters such as the initial concentration of the pollutant (10 – 30 mg/L), applied voltage (4 – 6 kV), pH (3 – 9), and conductivity (5 – 160 $\mu\text{S}/\text{cm}$) were investigated on the DBD performance based on the degradation efficiency of CBZ. The degradation efficiency recorded for CBZ was 92% at operating conditions of 10 mg/L, 6 kV, and 5 $\mu\text{S}/\text{cm}$. The degradation of the pollutant was inhibited in an acidic medium but was enhanced at both neutral and slightly alkaline pH conditions. The mechanism involved in the degradation of the pollutant with DBD was investigated by measuring the O_3 and H_2O_2 generated. Also, radical scavenger experiments were conducted to understand the contributions of reactive species like O_3 , H_2O_2 , $\cdot\text{OH}$ and $\cdot\text{O}_2^-$ produced in the treatment process. To understand the efficacy of the technology in real conditions, the DBD experiments were also performed in tap water (33% CBZ degradation and 0.01 min^{-1}) and in final wastewater effluent (showing 13% CBZ degradation and 0.004 min^{-1}) within 40 min treatment time. Lastly, the degradation efficiency of the DBD reactor, energy efficiency and energy cost were compared with those of UV-only, UV/ Fe^{2+} , UV/ H_2O_2 , and UV/ $\text{H}_2\text{O}_2/\text{Fe}^{2+}$ systems. In all the parameters investigated, the DBD plasma used in this work seemed to perform better than the UV-assisted systems, while UV-only system gave the worst performance.

5.1 Introduction

Active pharmaceutical contaminants are constantly being released into both surface and ground water through wastewater treatment plants (WWTP), run-off from agricultural fields, aquaculture facilities, and the application of bio-solids or manure to soils [10,33,339]. Additional pathways include release from manufacturing sites, hospital discharges, excretion of the parent compounds or their metabolites, and the disposal of unused or expired medicines into sewage. One of the pharmaceutical compounds that has garnered attention due to its extensive application and resistance to conventional and biological treatment is carbamazepine (CBZ) [340–342]. This compound, frequently prescribed for antiepileptic and mood-stabilizing medication, has a consumption rate of about 1,014 tons per year and it has been ubiquitously detected in diverse water sources including drinking water [87,343–345]. While specific reports on its human health impact are currently lacking, the widespread presence of CBZ in the environment raises questions about its potential impacts on non-target organisms and ecosystem dynamics.

In attempting to mitigate or eliminate pharmaceutical contaminants from the environment, some developed countries have tried to establish regulations for the proper and safe release of pharmaceutical substances [37,346]. Nevertheless, formulating these policies entails grappling with the intricate interplay between human health, environmental impact, regulatory frameworks, and public awareness. To strike a balance between effective environmental protection and access to essential medications, recommendations have been made on the inclusion of advanced oxidation processes (AOPs) into conventional WWTPs to enhance their efficacy [347]. The intrinsic advantage of AOP lies in their ability to produce active highly potent species like hydroxy radicals ($\bullet\text{OH}$) which can potentially oxidise pollutants into less toxic by-products. Thus, coupling an AOP with existing WWTP setups will help create a sophisticated system that can remove a myriad of pollutants regardless of their specific properties or concentrations.

Several AOP have been examined in the degradation of persistent pharmaceutical pollutants. For instance, with regards to CBZ, UV-assisted AOPs like UV/H₂O₂, UV/H₂O₂/Fe²⁺ and UV/H₂O₂/Fe³⁺ have yielded 60.2%, 90.6%, and 74.3% degradation efficiencies, respectively, when used to degrade the pollutant [348]. This study emphasised the roles of Fe²⁺ and Fe³⁺ in

the production of $\bullet\text{OH}$ in the solution which enhances degradation. Meanwhile, CBZ was said to be highly resistant to a direct photolysis system as only 7.5% degradation was achieved. In addition, the degradation byproducts reported for the UV-assisted AOP were less toxic than the parent compound. In another similar study, the role of Fe^{2+} was once again confirmed by Zou *et al.* [349] in the removal of CBZ using ferrous-activated sodium hypochlorite (NaOCl) on a soil system. In this case, the authors investigated the feasibility of $\text{Fe}^{2+}/\text{H}_2\text{O}_2$, $\text{Fe}^{2+}/\text{persulfate}$, and $\text{Fe}^{2+}/\text{NaOCl}$ systems in the degradation of CBZ under different initial soil pH conditions. A degradation efficiency of 94.5% was achieved with $\text{Fe}^{2+}/\text{NaOCl}$ with a 1:1 molar ratio in 4 h and this was reportedly due to the high yield of $\bullet\text{OH}$ in the system.

Other active radicals can potentially facilitate the degradation of CBZ. For example, Wang and Zhou [350] employed a combination of ultrasound and persulfate anions to achieve 89.4% degradation efficiency for CBZ in 120 min. This study demonstrated the potential of sulfate radicals ($\text{SO}_4^{\bullet-}$) in the oxidation of CBZ. Guo *et al.* [351] also used radical quenching experiments to confirm the superiority of $\text{SO}_4^{\bullet-}$ in the degradation of CBZ. Roy and Moholkar [352] developed a hybrid AOP system that can facilitate the production of both $\bullet\text{OH}$ and $\text{SO}_4^{\bullet-}$ radicals from hydrodynamic cavitation (HC) assisted UV/persulphate with composite $\text{ZnO}/\text{ZnFe}_2\text{O}_4$ particles. The hybrid system yielded 98.13% CBZ degradation in 60 min, compared to HC-only (7.7%), and HC/ $\text{Na}_2\text{S}_2\text{O}_8$ (65.73%). Photocatalysis is another well-known method used in the degradation of CBZ through the generation of active species using solar light irradiation and semiconductor materials. Ding *et al.* [353] reported a photocatalytic oxidation of CBZ using Bi^{3+} self-doped NaBiO_3 nanosheets with a nearly complete degradation efficiency (99.8%) in 60 min. Other catalysts used include TiO_2 [156], ZnIn_2S_4 [354], BiOCl and BiOCl/AgCl composite [158].

Ozone-based AOP has also been exploited for the degradation of CBZ. For example, Asghar *et al.* [355] reported the ozonation of CBZ in the presence of sulfur-doped graphene and completely degraded the pollutant with 0.08 mM. Meanwhile, Yang *et al.* [356] used an electro-peroxone process to generate both O_3 and H_2O_2 to achieve 99.8% degradation efficiency and 97.6% mineralization of the compound in 15 min and 90 min, respectively. The advantage of these two systems lies in the fact that O_3 generated in situ reacted with other species (H_2O_2) and catalyst (graphene) synergistically to produce $\bullet\text{OH}$ which is more potent than O_3 . Despite the suitability of all these technologies, limitations such as poor light

penetration and lamp fouling, high energy consumption, production of toxic by-products, catalyst activation, and recovery are some of the issues commonly reported in the literature about the AOP methods.

In this work, a non-thermal plasma (NTP) system was used in the degradation of CBZ. NTP systems have been remarked as highly effective and promising AOPs for the removal of persistent organic compounds because they are simple, effective, energy-efficient, scalable, and do not require additional chemical agents [174,299,357,358]. While other AOPs produce single active species, the discharge generated in the NTP system consists of UV radiation, O₃, •OH, H₂O₂, shock waves, and lots more. All of these produce a synergistic effect in degrading a wide range of pollutants with little or no challenges about selectivity and less toxic by-products to deal with. Various NTP configurations exist, as reported in literatures [175,256]. For the removal of CBZ, the common methods reported are dielectric barrier discharge (DBD) [32] and corona discharge [359]. Yu *et al.* [360] combined Fe²⁺ with a DBD reactor to effectively degrade CBZ. While these studies may have reported a significant degradation of CBZ, the notable gap however is the low throughput which inhibits a large-scale water treatment application. Also, treatment studies that are based on the generation of plasma discharges with natural atmospheric air are still rare.

Therefore, the first aim of this study was to investigate the efficacy of a continuous-flow atmospheric DBD reactor in the degradation of CBZ under different conditions (pollutant concentration, applied voltage, conductivity, and pH of the solution). Secondly, the addition of radical quenchers was used to understand the contributions of the active species generated in the DBD plasma. The third objective was to investigate the degradation of CBZ in different water matrices (deionised water, tap water, and final wastewater effluent) under the optimum operating parameters. To the best of our knowledge, this is the first DBD plasma-based study that provides a concise description of the degradation of CBZ in different water matrices. Considering that several literatures have reported the efficacy of UV-based treatment, the last objective focused on the comparison of the DBD plasma with UV-based systems in terms of degradation performance, energy efficiency, and the energy cost of treatment.

5.2 Materials and methods

5.2.1 Chemicals

Carbamazepine (CBZ, $C_{15}H_{12}N_2O$) with >99% purity was purchased from Leapchem (China). Deionised water obtained from an Elga LabWater Chorus 1 device was used in preparing the working solutions used in this experiment. Tap water was collected from the University of Pretoria, South campus at building 4, while final wastewater effluent was collected from the Daspoort municipality in Pretoria. Isopropanol (IPA, C_3H_8O) was supplied by Radchem (PTY) Ltd (South Africa), p-benzoquinone (BZQ, $C_6H_4O_2$), sodium pyruvate (SP, $C_3H_3NaO_3$) and uric acid (UA, $C_5H_4N_4O_3$) were purchased from Sigma-Aldrich (USA). Iron (II) sulphate heptahydrate ($FeSO_4 \cdot 7H_2O$) and hydrogen peroxide (H_2O_2 , 30%) was obtained from Merck (Germany). The pH of the solution was adjusted with sodium hydroxide (NaOH) and sulphuric acid (H_2SO_4) obtained from Glassworld (South Africa). All chemicals are of analytical grade and were used without further purification.

5.2.2 DBD plasma experiments

The DBD plasma experiments were conducted in a continuous-flow reactor with characteristics described in Table 5.1. The experimental setup for this study is similar to that used in our previous work [361]. This consists of a high voltage (HV) AC power supply, a continuous-flow DBD reactor, a peristaltic pump, a digital oscilloscope, an optical emission spectroscopy (OES) system, and a high-performance liquid chromatography (HPLC) system. The plasma reactor itself is shown in Figure 3.1 of Chapter 3.

Atmospheric air was used as the working gas in this experiment to generate discharges at the edge of the pins of the HV electrode. The contaminated water is pumped upwards from the storage tank through the hollow HV electrode, and it is dispersed evenly via a microjet placed at the top of the HV electrode in the glass tube. The falling water film then contacts the discharge produced at the multi-pins and gets collected back into the storage container. Recirculation of water was ensured by a peristaltic pump (Integra, China). The required AC voltage is generated by a custom-made AC voltage power supply fabricated by Jeenel Technologies Pty, South Africa. The applied voltage and discharge current of the plasma reactor were measured with the digital oscilloscope (Rigol DS1074Z Plus, 70 MHz). An AC

voltage of 6 kV was maintained in the experiments as it was in Chapter 4, unless otherwise specified.

Scavenging experiments were set up using IPA, UA, BZQ, and SP to investigate the possible contributions of $\bullet\text{OH}$, O_3 , $\bullet\text{O}_2^-$, and H_2O_2 , respectively. The synthetic solutions containing each of these scavengers were prepared in deionised water at different concentrations. The DBD plasma degradation experiment was also performed in tap water and final wastewater effluent to examine the effect of water matrices on the degradation of CBZ. The key properties of the synthetic water, tap water and final wastewater effluent are summarised in Table 5.2.

Table 5.1: Technical characteristics and operating conditions for the DBD plasma reactor.

| Reactor information | Value/description |
|--|--------------------------|
| Type of glass | Borosilicate tube |
| Length of glass tube | 30 cm |
| HV electrode material | Stainless steel |
| Length of HV electrode | 29 cm |
| Diameter of HV electrode | 1.7 cm |
| Discharge length | 6.9 mm |
| AC Voltage applied | 4 – 6 kV |
| AC Frequency | 20 kHz |
| Estimated average dissipated power at 6 kV | 42.7 W |
| Concentration of CBZ examined | 10 – 30 mg/L |
| Treated volume | 1 L |
| Water flow rate | 500 mL/min |

5.2.3 UV experiments

The setup for the UV-based experiments (UV only, UV/ Fe^{2+} , UV/ H_2O_2 , and UV/ $\text{Fe}^{2+}/\text{H}_2\text{O}_2$) is shown in Figure 5.1. The degradation was performed in a photochemical reactor equipped with a UV lamp (supplied by Lelesil Innovation Systems) and operated in a batch mode [154,362]. The photoreactor used in this study is comprised of a 1 L volume quartz-jacketed tube hosting a 250 W high-pressure mercury vapour lamp (HPMVL) UV light lamp, a 4 L cooling tank, a magnetic stirrer, and a protective compartment. 500 mL CBZ solution was exposed to the UV

treatment for 40 min and the solution was stirred at 400 rpm. Samples of the treated solution were withdrawn using a syringe at every 5 min interval for analysis.

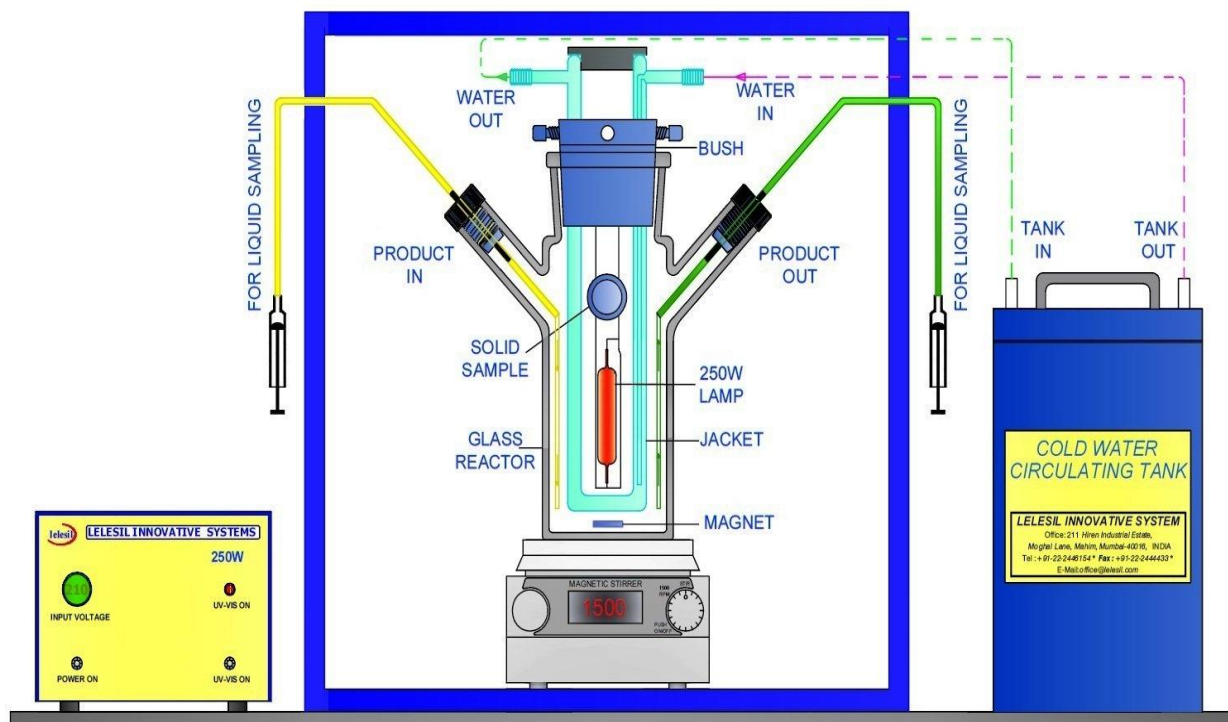


Figure 5.1: Setup for the UV-based experiments.

5.2.4 Analytical procedure

The residual CBZ concentrations in the aqueous solutions were monitored by an Alliance Waters 2695 high-performance liquid chromatography (HPLC) equipped with a 2489 Waters UV/Vis detector (285 nm) and a 4.6 mm × 250 mm C18 5 μ column. The mobile phase consisted of methanol and deionised water (50:50, v/v) with a flow rate of 1 mL/min and 10 μL injection volume. The degradation efficiencies for CBZ in the experiments were calculated using Eq. (5.1):

$$\eta (\%) = \frac{C_i - C_t}{C_i} (100) \quad (5.1)$$

Where η represents the degradation efficiency for CBZ (%), C_i represent the initial concentration of CBZ (mg/L) and C_t represent the concentration of CBZ at a particular

treatment time (min) in the solution (mg/L). The degradation efficiency provides an insight into the performance of the technology used in the degradation of the pollutant. Also, the kinetic analysis of CBZ fitted a pseudo-first order rate according to Eq. (5.2):

$$\ln \left(\frac{C_i}{C_t} \right) = k t \quad (5.2)$$

Where C_i and C_t have the same definitions as in Eq. (5.1), k is the reaction rate constant (min^{-1}) and the t remains the treatment time (min).

The pH and conductivity measurements were performed using a HANNA multiparameter H198194 meter. The concentration of hydrogen peroxide (H_2O_2) and ozone (O_3) in the solution was determined by spectrophotometry using a Lovibond spectrodirect water testing instrument (Tintometer Group, Germany) to investigate the yield of these species in the DBD plasma. Ion chromatography (940 Professional IC Vario, Metrohm, Germany) instrument was used to measure the anions in the solution.

Table 5.2: Characteristics of deionised water, tap water and final wastewater effluent.

| Parameters | Deionised water | Tap water | Final wastewater effluent |
|---|-----------------|-----------|---------------------------|
| pH | 5.72 | 7.53 | 7.3 |
| Conductivity ($\mu\text{S}/\text{cm}$) | 5 | 270 | 544 |
| Nitrates (NO_3^- , mg/L) | - | 12.2 | 15.2 |
| Nitrites (NO_2^- , mg/L) | - | 0.1 | 1 |
| Sulphate (SO_4^- , mg/L) | - | 23.3 | 57.5 |
| Chloride (Cl^- , mg/L) | - | 20.8 | 52.7 |
| Hydrogen carbonate (HCO_3^- , mg/L) | - | 99.6 | 150.5 |

5.3 Results and discussions

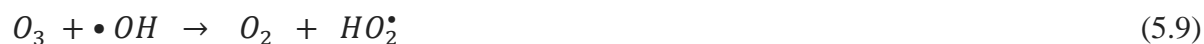
5.3.1 Investigation of the reactive species generated in the DBD plasma.

A typical DBD in the gas-liquid interface can prompt diverse chemical reactions which eventually result in the production of a broad range of highly reactive chemical species such as free radicals ($\bullet\text{OH}$, $\bullet\text{H}$, $\bullet\text{O}$, $\text{HO}_2\bullet$), neutral molecules (O_3 , H_2O_2) as well as other positive and

negative ions. These species have different oxidizing potentials and as mentioned earlier, they provide a combined effect in degrading organic pollutants in aqueous solutions. Also, the amount of the reactive species generated by a DBD plasma system, and their effectiveness is affected by certain factors such as input energy, type of gas used, and the flow rate, pH of the solution, and conductivity in some case, amongst others [22]. Some of these will be discussed in detail in the subsequent section.



Among the generated reactive species, $\bullet OH$ has been the most desired due to its strong oxidizing property ($E^\circ = 2.85$ V) and non-selectivity toward pollutants. It reacts with most organic matter by hydrogen abstraction with saturated aliphatic hydrocarbons or by electrophilic addition with unsaturated hydrocarbons [363]. The recombination of $\bullet OH$ produced in a gas-liquid plasma system generates H_2O_2 ($E^\circ = 1.77$ V) which is another important specie that facilitates the oxidation of organic pollutants [364]. The concentration of H_2O_2 can provide insight into the measure of $\bullet OH$ available in the aqueous solution. This is because $\bullet OH$ radicals have a short half-time while H_2O_2 is relatively stable. Therefore, to understand the mechanism and efficacy of the degradation of CBZ, the concentration of H_2O_2 was measured during CBZ (10 mg/L) degradation at an applied voltage of 6 kV and frequency of 20 kHz. According to Figure 5.2, the concentration of H_2O_2 increased with time reaching a peak of 6.7 mg/L in 30 min. Afterward, it decreased to 5.6 mg/L at the end of the treatment time. The decomposition of H_2O_2 after reaching its highest concentration can be explained by its reaction with the active species present in the discharge based on Eq. (5.3) – (5.5), and also by the effect of an increase in temperature as reported by [365].





Also, the presence of oxygen in the atmospheric air gas used induces a reaction between the highly energised electrons and oxygen, leading to the production of reactive oxygen species such as O_3 and $\bullet O$, according to Eq. (5.6) and (5.7). Meanwhile, O_3 ($E^{\circ} = 2.07$ V) is also a powerful oxidizing agent that can react effectively with organic pollutants through a series of reactions [256]. The concentration of O_3 produced in the DBD plasma system had a similar trend to that of H_2O_2 as shown in Figure 5.2. The decline in concentration observed after 30 min could also be attributed to the temperature increase observed in the solution. Also, O_3 can react with H_2O_2 to form $\bullet O_2^-$ according to Eq. (5.8) – (5.10). This specie is also important in the degradation of organic pollutants.

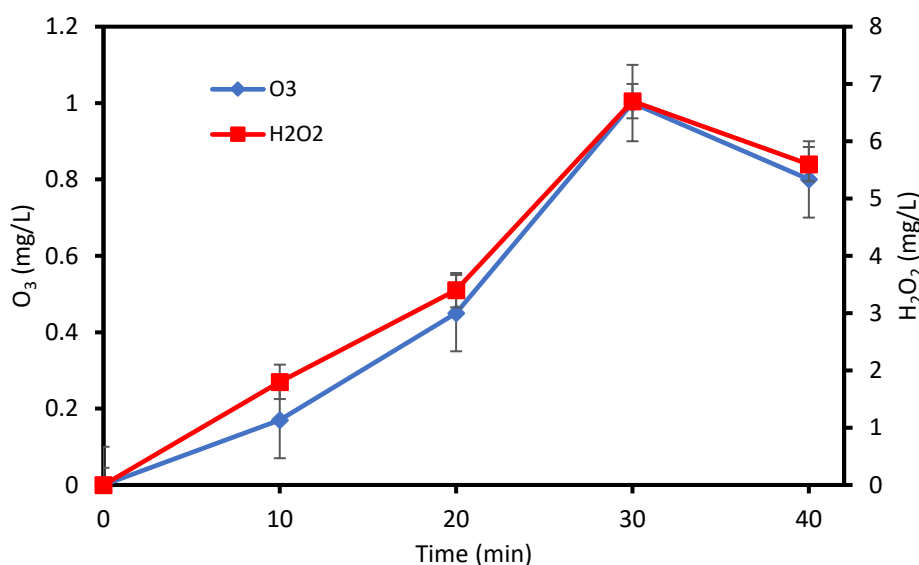


Figure 5.2: Variation in the concentration of O_3 and H_2O_2 during CBZ degradation.

5.3.2 Investigation of key operating parameters on CBZ degradation

5.3.2.1 Effect of initial concentration of CBZ

The effect of the initial concentration of CBZ on the degradation efficiency with DBD plasma system was studied at a voltage of 6 kV, frequency of 20 kHz and water flow rate of 500

mL/min. The results presented in Figure 5.3 showed that the degradation efficiency of the organic compound decreased from 92% to 39% with an increase in its initial concentration from 10 – 30 mg/L. This is because, at a constant voltage, a fixed amount of reactive species is generated by the DBD plasma system and transferred into the aqueous solution to degrade the pollutant. Therefore, a high CBZ molecule per reactive specie ratio will reduce the degradation efficiency observed and vice-versa. This implies that the degradation of the efficiency is significantly affected by the initial concentration of a pollutant at fixed applied power conditions.

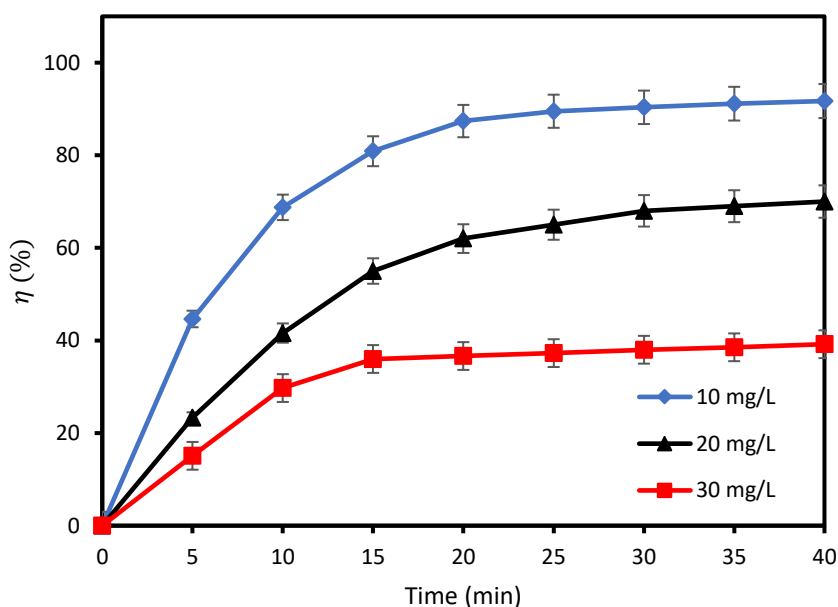
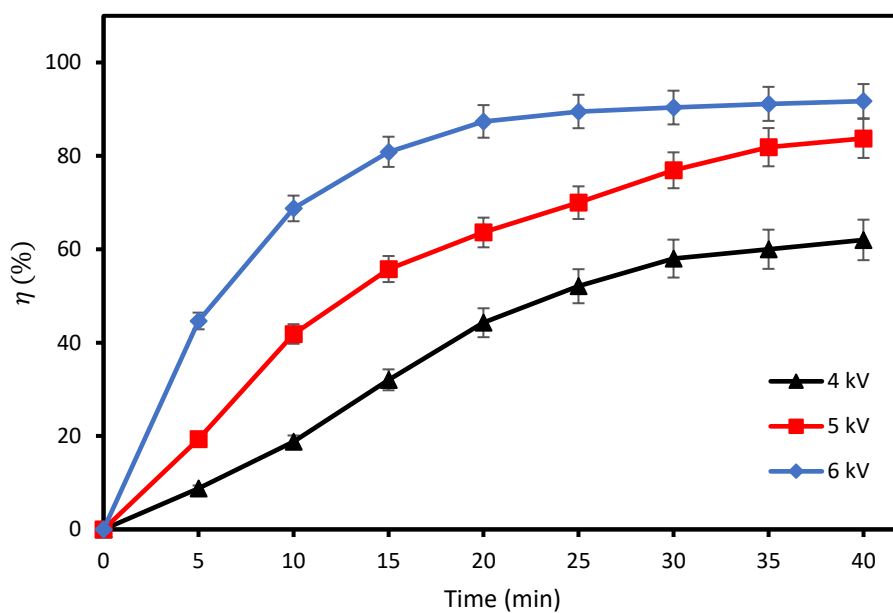


Figure 5.3: Effect of CBZ initial concentration on the degradation efficiency. (Experimental conditions: voltage 6 kV; frequency 20 kHz).

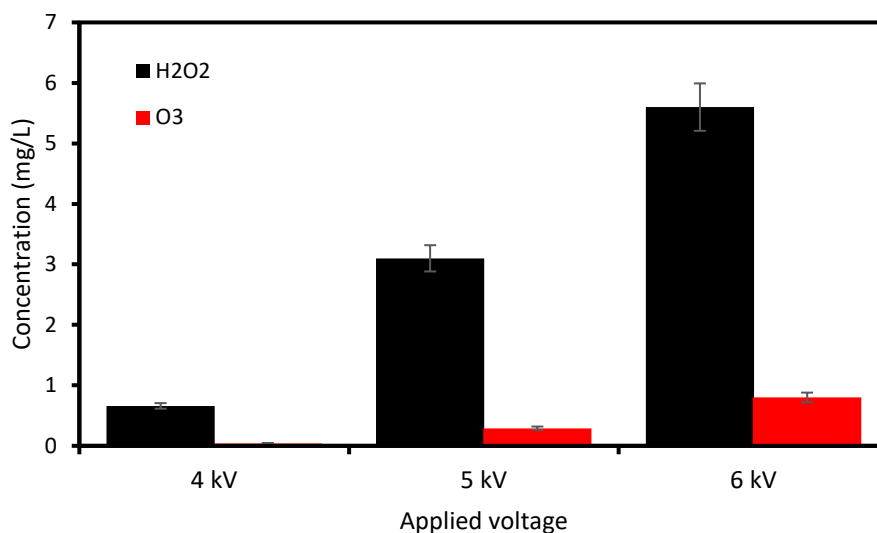
5.3.2.2 Effect of applied voltage

The generation of reactive species in a DBD plasma is a defining step during the degradation of organic pollutants. An important factor that influences the production of these species is the applied voltage. To establish the impact of applied voltage on the degradation efficiency of

CBZ, the DBD plasma experiments were conducted at different voltage conditions: 4, 5, and 6 kV. The degradation efficiency as a function of time is presented in Figure 5.4 (a) at an initial CBZ concentration of 10 mg/L. The degradation efficiency of CBZ increased from 62% to 92% as the voltage increased from 4 kV to 6 kV during the DBD plasma treatment. Previous literatures has attributed the increase in degradation efficiency per voltage to the spike in the concentration of active species in the solution [273,366,367]. This was confirmed in this study as seen in Figure 5.4 (b). An investigation of the production of H₂O₂ and O₃ showed that an increase in the applied voltage increased the concentration of both species measured in the aqueous solution. At 40 min, the concentration of H₂O₂ increased over 8 times when the voltage was increased from 4 kV to 6 kV, while the traces of O₃ only became noticed at 5 kV and increased by almost three times between 5 and 6 kV as illustrated in Figure 5.4 (b).



(a)



(b)

Figure 5.4: Effect of applied voltage on the degradation of CBZ. (a) degradation efficiency; (b) concentration of H₂O₂ and O₃ (Experimental conditions: CBZ initial concentration 10 mg/L; frequency 20 kHz).

5.3.2.3 Effect of solution conductivity

The conductivity of a solution has the potential to affect both the electric field intensity and ultraviolet radiation intensity of a typical NTP reactor [244]. However, this also depends on the type of reactor and position of the discharge with respect to the solution being treated [296]. In this work, a volume-based DBD was used and the conductivity of the solution was adjusted using KCl. Figure 5.5 shows the influence of solution conductivity on the degradation efficiency of CBZ at 6 kV and 10 mg/L initial concentration. Generally, an increase in the conductivity of the solution reduced the degradation efficiency. A significant reduction in the degradation efficiency from 92% to 5% was recorded as the conductivity increased from 5 $\mu\text{S}/\text{cm}$ to 160 $\mu\text{S}/\text{cm}$. Also, as the conductivity increased, the spark discharge transitioned into complete corona discharges (160 $\mu\text{S}/\text{cm}$), making degradation almost impossible. A very similar observation was noted by Yang *et al.* [263], and the impact of conductivity was said to be due to the contact the discharge has with the aqueous solution. Considering that the best

degradation efficiency for CBZ was observed at 5 $\mu\text{S}/\text{cm}$, other experiments were conducted at this conductivity.

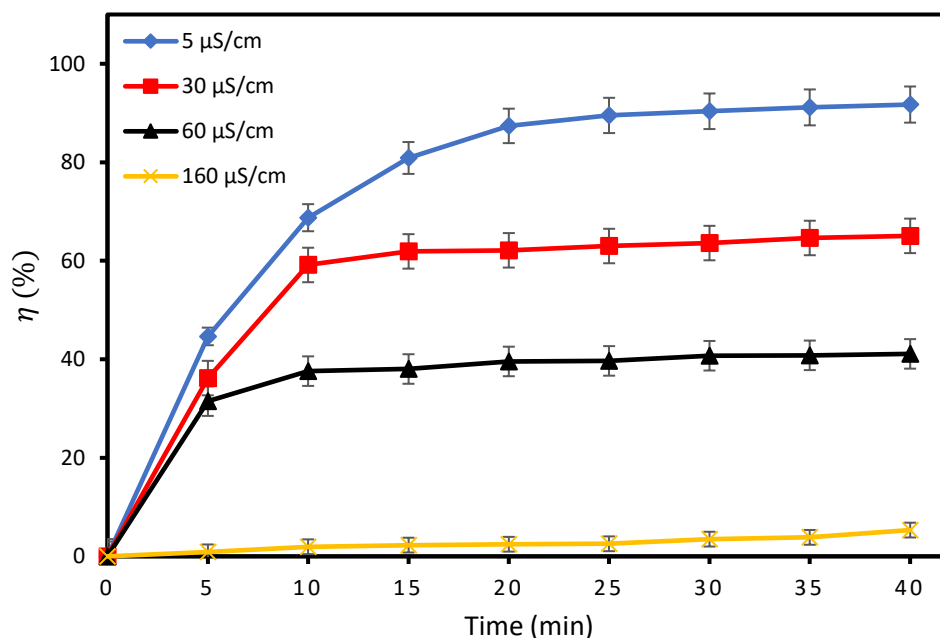


Figure 5.5: Effect of solution conductivity on the degradation efficiency of CBZ (Experimental conditions: CBZ initial concentration 10 mg/L; voltage 6 kV; frequency 20 kHz).

5.3.2.4 Effect of pH variation

Figure 5.6 shows the impact of different initial pH values on the degradation of CBZ, at an applied voltage of 6 kV and an initial concentration of 10 mg/L. The pH values of the solution were adjusted with NaOH and H₂SO₄ before plasma degradation. The trend observed shows that the degradation efficiency increased as the solution became more basic. An acidic medium was however inhibitive to the removal of CBZ in the solution. The degradation efficiency increased to 92% as the pH increased from 3 to 5.7 (pH of the synthetic solution), then continued to >99% as the pH increased further to 9.

During the DBD plasma treatment, the production of active species and other radicals in the aqueous solution affected the chemical properties of the solution like pH and conductivity. The variation of these parameters at optimum conditions of initial concentration of CBZ applied voltage, and conductivity are shown in Figure 5.7. As observed, the pH of the solution sharply decreased from 5.72 to 4.97 in the first 5 min of treatment, followed by a small steady decline over the next minutes. Meanwhile, the conductivity of the solution maintained a continuous rise over the 40-minute treatment time from 5 $\mu\text{S}/\text{cm}$ to 233 $\mu\text{S}/\text{cm}$. The decrease in pH can be linked to the dissolution of nitrogen oxides (NO_x) produced in the plasma by the reaction between N_2 and O_2 . This therefore means that the pH of the solution is reduced due to the formation of acidic HNO_2 and HNO_3 in the solution [251]. However, it should be noted that when using gases other than air or nitrogen, NO_x compounds may not be formed, and thus the pH may remain affected as confirmed by Meropoulis *et al.* [203]. The formation of nitrous acids was also confirmed by Aggelopoulos *et al.* [29], Rogli *et al.* [368], amongst others.

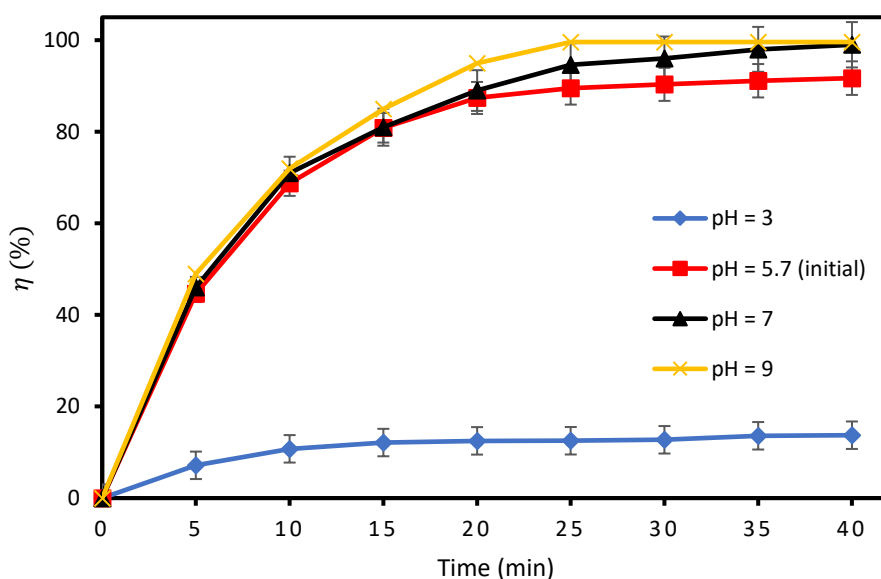


Figure 5.6: Degradation efficiency at different initial pH values (Experimental conditions: CBZ initial concentration 10 mg/L, voltage 6 kV; frequency 20 kHz).

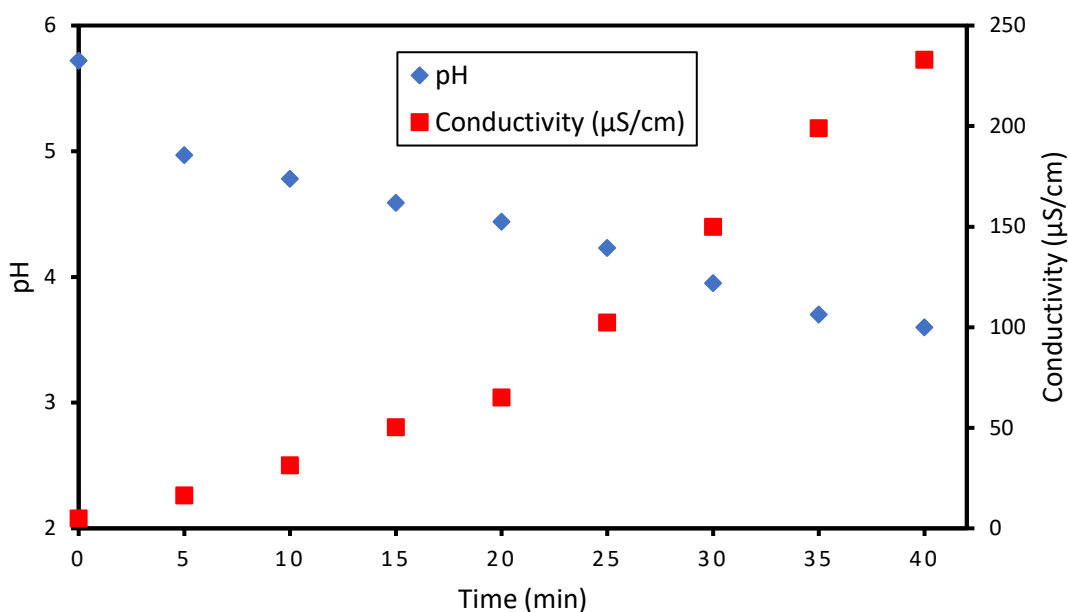


Figure 5.7: pH and conductivity trends for the control solution versus treatment time. (Experimental conditions: CBZ initial concentration 10 mg/L; voltage 6 kV; frequency 20 kHz).

5.3.3 Investigating the effect of radical scavengers

5.3.3.1 Role of •OH

The impact of •OH on the degradation of CBZ was investigated by adding isopropanol (IPA) into the aqueous solution to quench the reactive specie. Isopropanol was selected due to its ability to effectively react with •OH with a reaction rate of $1.9 \times 10^9 \text{ mol L}^{-1} \text{ s}^{-1}$, thus possible reactions with the active specie becomes inhibited [369]. According to Figure 5.8, the addition of IPA significantly reduced the degradation of CBZ. This inhibition effect was more obvious as the concentration of the radical scavenger increased. About 92% degradation of CBZ was achieved without IPA after 40 min plasma treatment and this reduced to 63% and 50% with the addition of 3 and 6 mmol/L IPA, respectively. Also, upon increasing the concentration of IPA from 3 mmol to 6 mmol/L, the rate of the reaction was reduced by 33%. Similarly, the reaction rate constant was reduced by a third as the concentration of IPA increased to 6 mmol/L

in the solution. These observations confirm that the $\bullet\text{OH}$ played a decisive role in the degradation of CBZ.

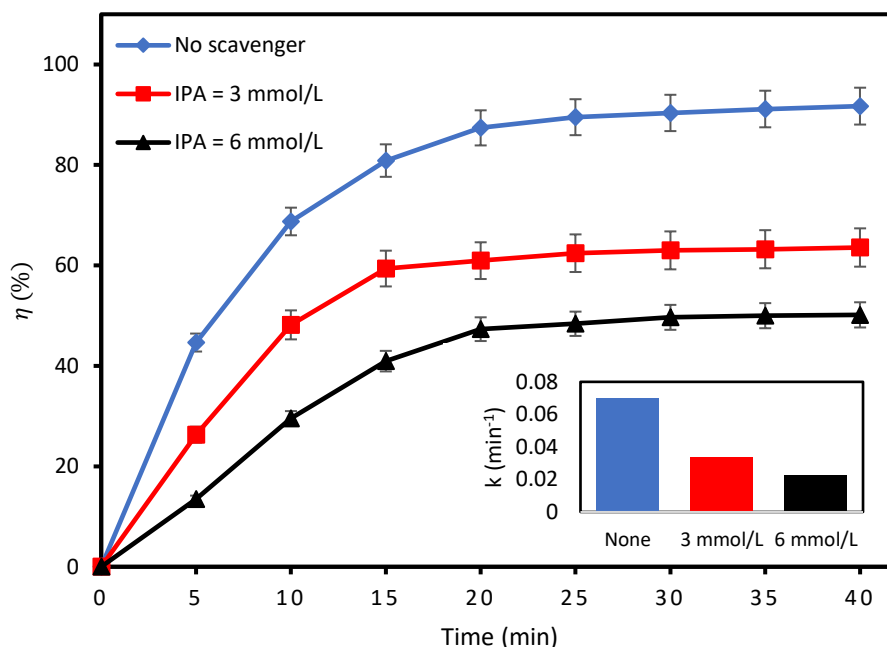


Figure 5.8: Influence of isopropanol on the degradation efficiency of CBZ (Experimental conditions: CBZ initial concentration 10 mg/L; voltage 6 kV; frequency 20 kHz).

5.3.3.2 Role of $\bullet\text{O}_2^-$

The formation of $\bullet\text{O}_2^-$ in the solution can be linked to the chain reaction occurring between O_2 and H_2O_2 as described earlier. This specie is also an important facilitator for the degradation of organic pollutants with a DBD process [245]. The impact of $\bullet\text{O}_2^-$ was examined in the presence of its scavenger which is commonly p-benzoquinone (BZQ) with a reaction rate of $2 \times 10^9 \text{ mol L}^{-1} \text{ s}^{-1}$ [211]. As seen in Figure 5.9, the degradation efficiency for CBZ was significantly inhibited by the addition of BZQ and the rate of inhibition increased with the concentration of the radical scavenger in the solution. When the concentration of BZQ was 0.5 mmol/L, the degradation efficiency observed for CBZ was reduced from 92% to 57% reducing the reaction rate by more than half in 40 min. A further increase in BZQ concentration to 1

mmol/L reduced the degradation efficiency further to 41% and the rate of the reaction reduced by 38%. The rate constant was reduced by 1/4th the value obtained without BZQ. These results therefore confirm that the $\bullet\text{O}_2^-$ generated in the DBD plasma must have played a role in the degradation of CBZ.

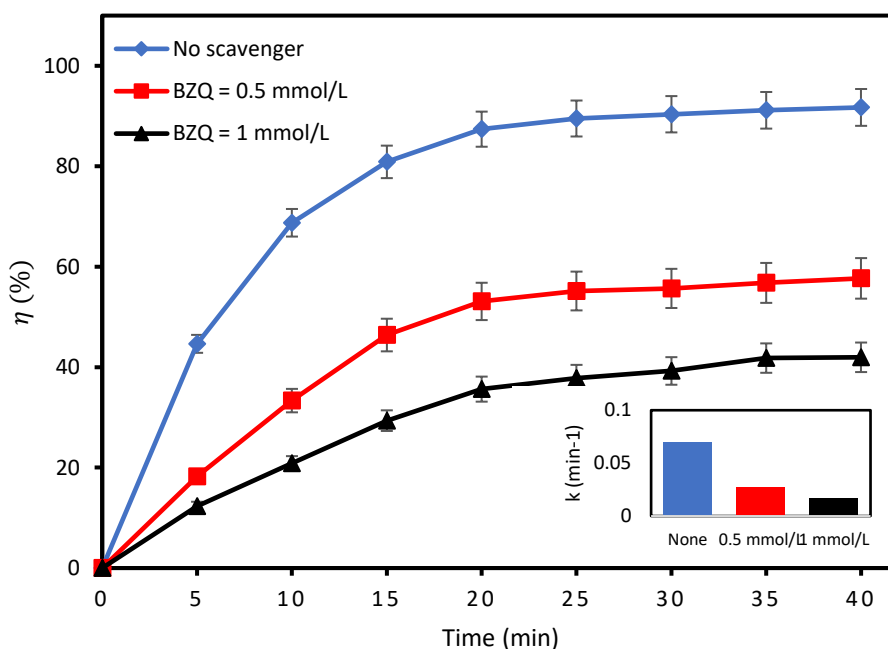


Figure 5.9: Influence of benzoquinone on the degradation efficiency of CBZ (Experimental conditions: CBZ initial concentration 10 mg/L; voltage 6 kV; frequency 20 kHz).

5.3.3.3 Role of O₃

Ozone (O₃) gas is one of the long-lived reactive species generated by an NTP reactor. Studies have reported its potency in the oxidation of organic compounds [149,336,370,371]. In this study, uric acid (UA) was used to quench the possible effect of O₃ in the system in order to investigate its role in the degradation of CBZ. The reaction rate for UA has been reported as $1.4 \times 10^6 \text{ mol L}^{-1} \text{ s}^{-1}$ [274,369]. With the addition of UA, the degradation efficiency of CBZ reduced significantly to about 18% from 92% to in 40 min as observed in Figure 5.10. A further increase in UA concentration in the solution had very little effect on the degradation efficiency. Also, the rate of the reaction in the presence of UA reduced by 92% compared to the control

solution, while an increase in UA concentration from 0.5 to 1 mmol/L had little effect on its kinetics. These results demonstrates that CBZ could be strongly oxidised by O_3 .

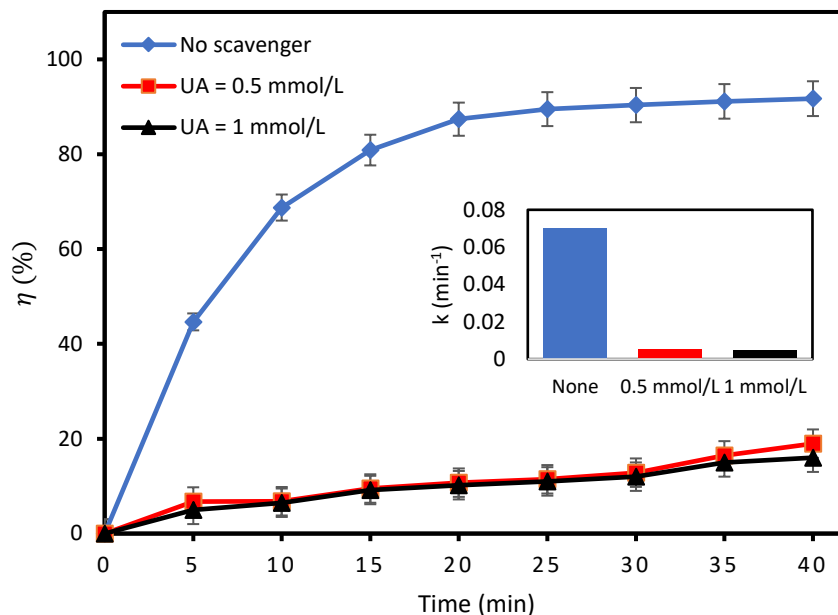


Figure 5.10: Influence of uric acid on the degradation efficiency of CBZ (Experimental conditions: CBZ initial concentration 10 mg/L; voltage 6 kV; frequency 20 kHz).

5.3.3.4 Role of H_2O_2

The last specie investigated in this study is H_2O_2 generated in the DBD plasma system. While this specie may be unstable in the solution, it also contributes to the overall degradation of organic pollutants due to its strong oxidation potential ($E^0 = 1.78$ V) and by its decomposition to OH radicals [256]. A previous study has reported that sodium pyruvate (SP) can be used to abstract H_2O_2 species in the solution with a reaction rate of $2.4 \text{ mol L}^{-1} \text{ s}^{-1}$ [211]. The addition of 0.5 mmol/L SP to the aqueous solution reduced the degradation efficiency of CBZ from 92% to 29% in 40 min as shown in Figure 5.11. This was further reduced to 7.5% when the SP concentration in the solution was doubled. Similarly, the rate of the reaction reduced by 83% with 0.5 mmol/L initial concentration of SP and by 78% when SP concentration was doubled. The rate constant dropped by 1/28th as the concentration of SP in the solution became 1

mmol/L. These results highlight the importance of H₂O₂ in the degradation of CBZ using the DBD plasma system.

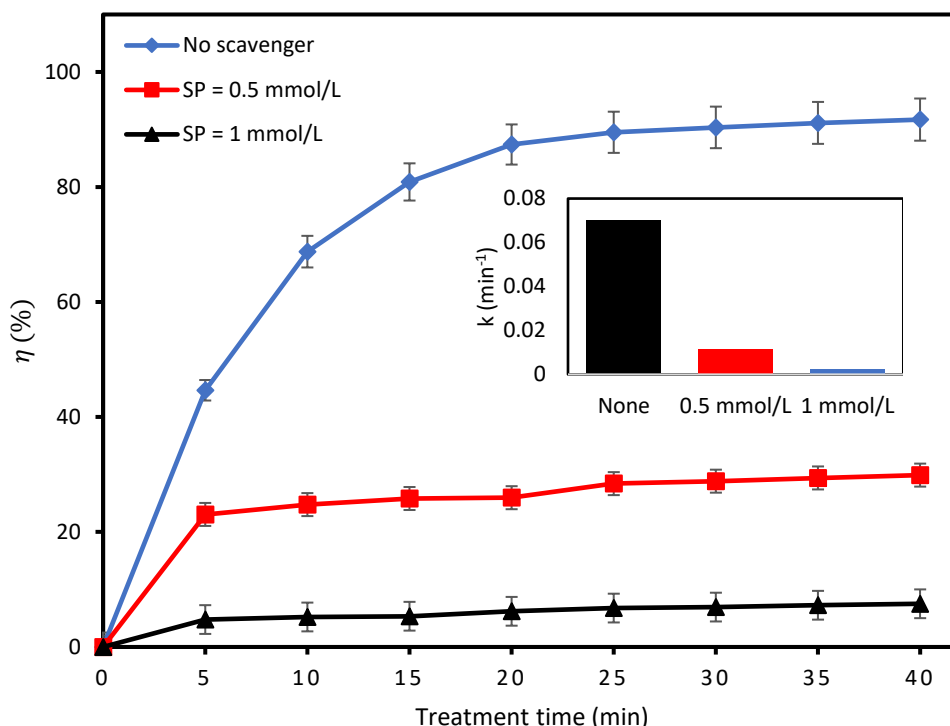


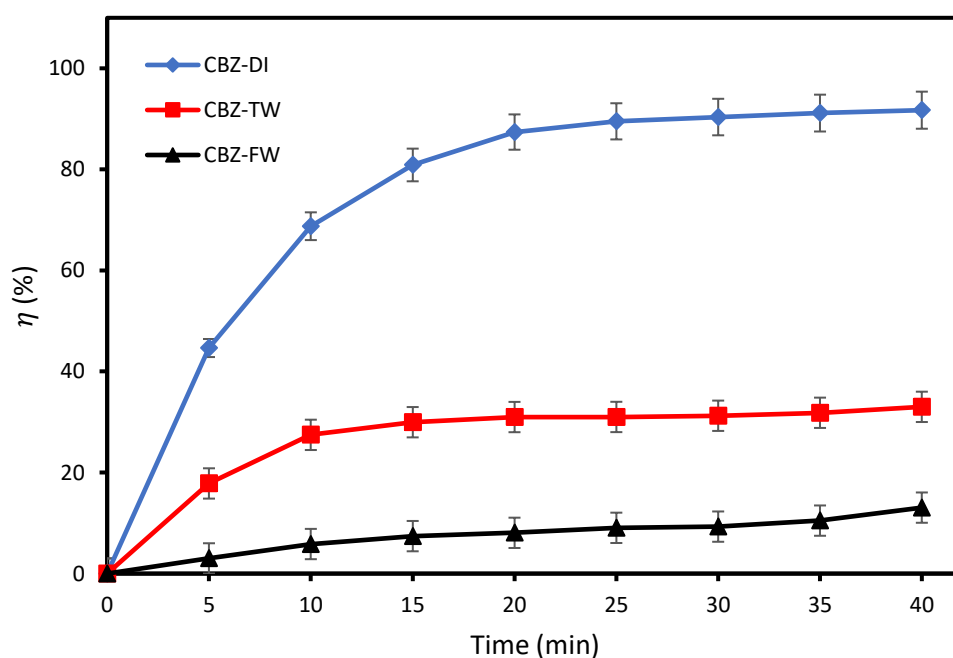
Figure 5.11: Influence of sodium pyruvate on the degradation efficiency of CBZ (Experimental conditions: CBZ initial concentration 10 mg/L; voltage 6 kV; frequency 20 kHz).

5.3.4 Effect of different water matrices on CBZ degradation

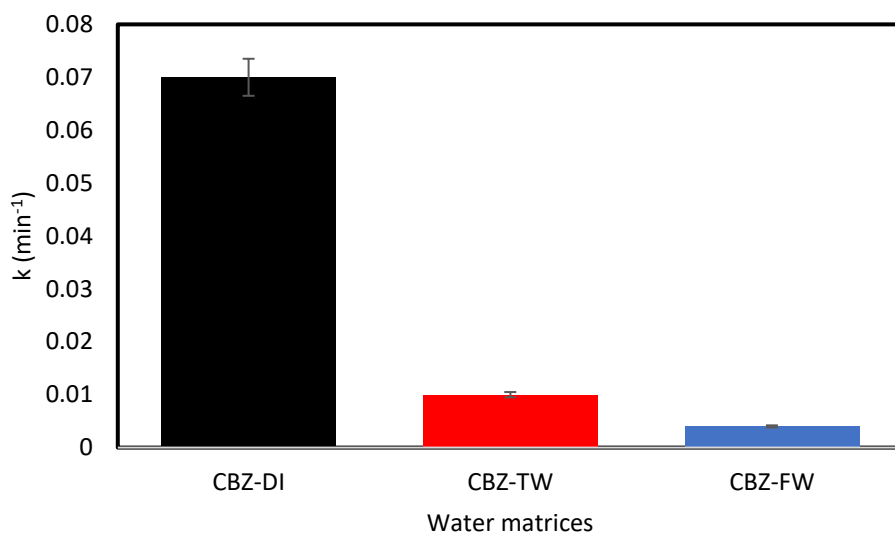
The chemical compositions of the different water matrices: deionised water, tap water, and final wastewater effluent are summarised in Table 1. The degradation efficiency and kinetics for CBZ are compared in the water matrices using the DBD reactor as shown in Figure 5.12. The degradation efficiency observed in TW and FW was 33% and 13%, respectively, compared to 92% in the DI. Similarly, a rate constant of 0.08 min⁻¹ observed in the DI was reduced to 0.01 min⁻¹ in TW and 0.004 min⁻¹ in the FW. These observations can be directly linked to the matrix compositions. The presence of inorganic ions such as chloride (Cl⁻), hydrogen carbonate (HCO₃⁻), nitrate (NO₃⁻), and sulphate (SO₄²⁻) may have a negative impact on the degradation

of CBZ with DBD plasma, leading to a significant reduction in the degradation efficiency. However, the most significant of these is Cl^- and HCO_3^- based on their concentrations in the matrices and their ability to react with $\bullet\text{OH}$ which is a significant specie facilitating the removal of the organic pollutants in NTP reactors. Nitrate has been reported to be an effective scavenger of aqueous electrons according to Palma *et al.* [103]. The reaction between Cl^- and $\bullet\text{OH}$ produces chlorine gas which is also a potential oxidant for organic pollutants. Also,

According to Table 5.3, there were no significant changes in the pH and conductivity for the TW and FW compared to the DI during the plasma treatment. In the TW, the pH range varied between 7.3 to 7.5, and 7.3 to 8.3 in the FW. Also, the conductivity for the TW increased slightly from 270 to 290 $\mu\text{S}/\text{cm}$, while the conductivity in FW increased from 544 to 617 $\mu\text{S}/\text{cm}$. Contrary to these observations, the pH and conductivity in the DI matrix increased significantly as was reported in previous studies with DBD plasma [251,304]. This is because the presence of inorganic ions like HCO_3^- acts as a pH buffer in both TW and FW, thus ensuring that their pH remains fairly constant during plasma treatment despite the nitrogen compounds present.



(a)



(b)

Figure 5.12: Effect of water matrices on (a) degradation efficiency of CBZ; (b) reaction rate for CBZ degradation. (Experimental conditions: CBZ initial concentration 10 mg/L; voltage 6 kV; frequency 20 kHz).

Table 5.3: Variation of pH and conductivity during the degradation of CBZ in TW and FW.

| Parameters | Deionised water | Tap water | Final wastewater effluent |
|------------------------------|-----------------|-----------|---------------------------|
| Initial pH | 5.7 | 7.5 | 7.3 |
| Final pH | 3.6 | 7.3 | 8.3 |
| Initial conductivity (μS/cm) | 5 | 270 | 544 |
| Final conductivity (μS/cm) | 233 | 290 | 617 |

5.3.5 Comparison of the removal of CBZ in DBD plasma and a UV-based system

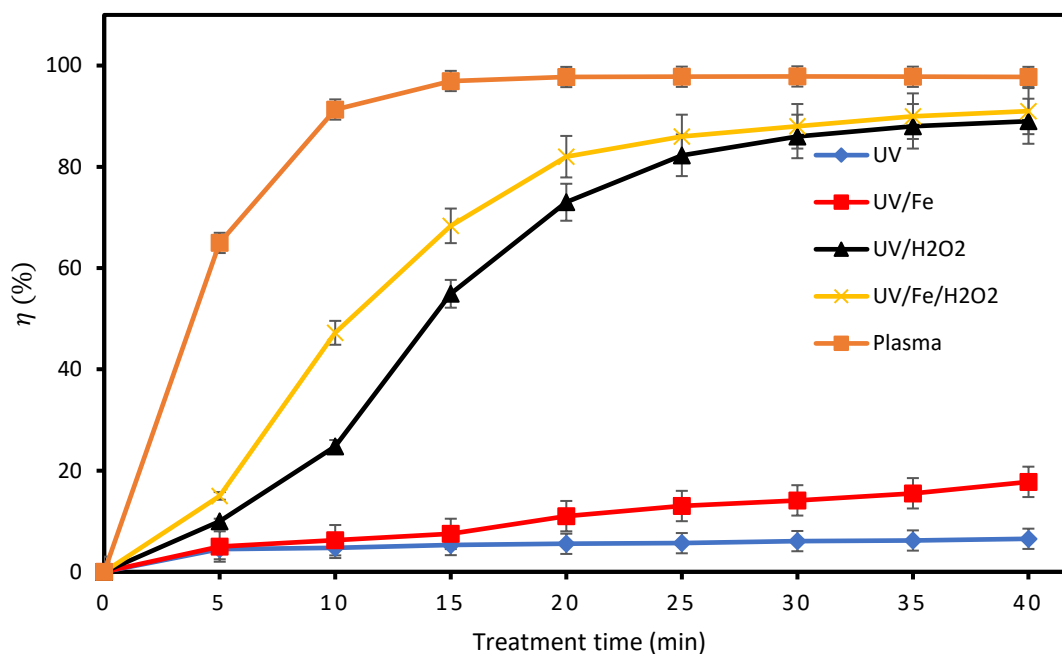
5.3.5.1 Degradation efficiency and kinetics

The most frequently studied AOPs for the degradation of CBZ is the application of photochemical oxidation, including UV/H₂O₂, photo-Fenton, and photocatalysis as mentioned in Section 5.2. However, it is often difficult to compare the reported results from literatures because of the different conditions (initial concentration, volume of solution, solvent matrix, input power, amongst others) in which the experiments were performed. Therefore, in this study, a UV-based system was used to treat a similar concentration of CBZ in the same water matrix (deionised water). The comparison between the performance of the atmospheric air DBD plasma used in this study with that of a similar AOP technology that has been developed to the point of full-scale commercialization helped to provide a fair basis to evaluate the effect of the technology. In this case, UV-based technology has been selected due to reports about its efficacy in removing organic pollutants, including CBZ [348,372]. The solution volume treated in all the UV experiments and plasma was 500 mL containing 10 mg/L CBZ.

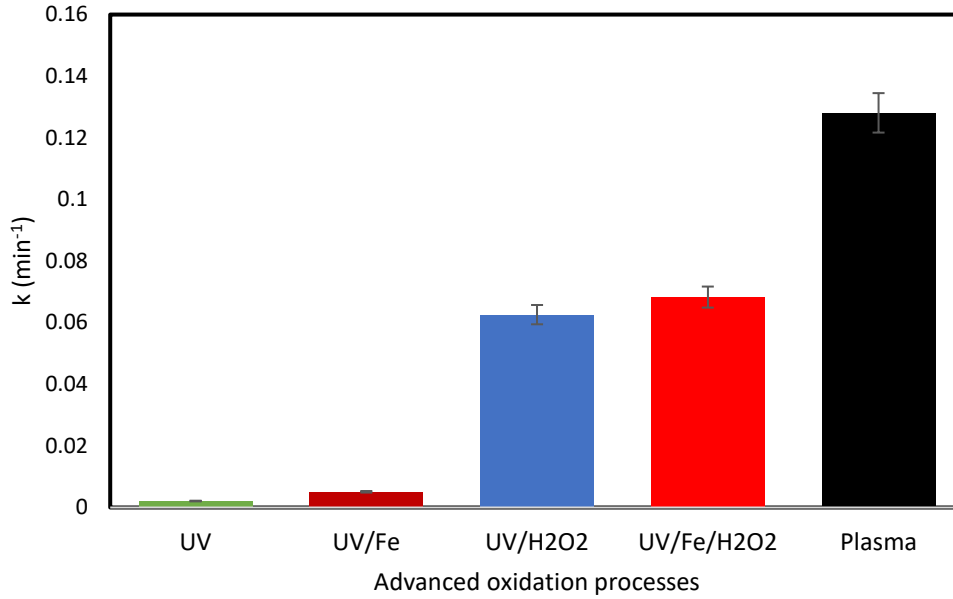
According to Figure 5.13 (a), a UV-only condition was able to achieve 6.5% CBZ degradation in 40 min. This result is consistent with previous findings [133,373,374]. The resistance of CBZ under a UV-only condition has been attributed to the presence of an amide group (RCONH₂) in the molecule [374]. Meanwhile, the addition of Fe²⁺ slightly increased the degradation efficiency to 17.7% in the same amount of time. UV/H₂O₂ is one of the most studied oxidation processes that has also been commercially deployed for the removal of organic pollutants. In this process, UV irradiates H₂O₂ to form •OH resulting in an increased degradation efficiency to about 90.3% in 40 min. Also, the addition of Fe²⁺ increased the rate of the reaction by a possible Fenton reaction occurring in the solution. An improvement in a UV-based reaction with the addition of H₂O₂ and Fe was also confirmed in a study by Ali *et al.* [348].

Table 5.4: Comparison of the degradation efficiency and kinetics for the different AOP setups used in this study.

| Technology | Fe [$\mu\text{mol/L}$] | H ₂ O ₂ [$\mu\text{mol/L}$] | Kinetics (min^{-1}) | CBZ solution (L) | η (%) |
|--------------------------------------|--------------------------|---|--------------------------------|------------------|------------|
| UV | 0 | 250 | 0.0021 | 0.5 | 6.5 |
| UV/Fe | 72 | 0 | 0.0051 | 0.5 | 17.8 |
| UV/H ₂ O ₂ | 0 | 250 | 0.0630 | 0.5 | 89 |
| UV/Fe/ H ₂ O ₂ | 72 | 250 | 0.0683 | 0.5 | 91 |
| Plasma | 0 | 0 | 0.1281 | 0.5 | 98 |



(a)



(b)

Figure 5.13: comparison of the different AOPs (a) degradation efficiency; (b) kinetics. Experimental conditions: Volume of solution = 500 mL; initial CBZ concentration = 10 mg/L

5.3.5.2 Energy efficiency

From an industrial-application perspective, another important factor necessary for comparing water treatment methods in addition to degradation efficiency is the energy efficiency which also directly affects the energy cost of treatment. The energy efficiency was estimated using the electrical energy per order (E_{EO}) figure-of-merit introduced by Bolton *et al.* [375]. The E_{EO} refers to the electrical energy (kWh) required to degrade a targeted pollutant by one order of magnitude in 1 m³ of water. This method has been reported to be suitable for conditions in which the concentration of the pollutant is low and for pseudo-first-order reactions. E_{EO} was calculated using the Eq. (5.11) [375–377]:

$$E_{EO} = \frac{P.t.1000}{V.60.\log\left(\frac{C_i}{C_f}\right)} \quad (5.11)$$

Where P is the power introduced into the system (kW), t is the treatment time (min), V is the volume of the solution (L), C_i is the initial concentration of CBZ and C_f is the final concentration of CBZ after 40 min treatment time. With the introduction of the first-order rate equation, Eq. (5.12) can be derived from (5.11):

$$E_{EO} = \frac{38.4 P}{V.k} \quad (5.12)$$

It should be noted that the power P mentioned in the equations and reflects the total power consumption of the AOPs considered. The vast majority of published literatures dealing with energy efficiency only specifies the power used in generating the chemical species, neglecting the energy consumed by the instrument itself and other possible energy losses. Thus, making comparisons between these technologies may be unfair. For the AOPs considered in this study, the power consumed was measured with an AC power meter (Schweitzer Engineering Laboratories, USA). The plasma and UV systems drew 125 W and 250 W, respectively, from the grid.

The energy cost of treatment, expressed in USD/m³ was estimated by multiplying the energy efficiency, E_{EO} , with the electricity price in the region (Tshwane, South Africa). Table 5.5 shows the energy efficiency and corresponding energy cost of treatment for the various AOPs examined in this study. The pseudo-first-order reaction rate constants needed to estimate EEO were taken from the kinetic data reported in Table 5.4. Furthermore, the average electricity tariff in Tshwane municipality for the category >650 kWh is approximately ZAR 3.32/kWh (equivalent to 0.17 USD/kWh according to Oanda rates) [378]. From the data in Table 5.5, the energy efficiency spans a wide range of 75.24 – 9142.86 kWh/m³, covering over two orders of magnitude. The energy efficiency for the UV systems (281.11 – 9142.86 kWh/m³) was significantly higher than that of the plasma system 75.24 kWh/m³. Meanwhile, a photolysis system without any additive is observed to be the most inefficient technology for treating CBZ. From the cost of treatment perspective, the UV systems were at least three times more than the plasma system. Again, it should be noted that the cost described in this study is not wholistic as it does not take the capital expense of the technology, operational, and maintenance costs into consideration. It only reflects the performance of the technology from an energy cost perspective.

Table 5.5: Comparison of the energy efficiency and associated costs of treatment for the AOPs considered in this work.

| AOP | E_{EO} (kWh/m ³) | Energy cost of treatment (USD/m ³) |
|--------------------------------------|--------------------------------|--|
| UV | 9142.86 | 1,554 |
| UV/Fe | 3764.71 | 640 |
| UV/H ₂ O ₂ | 306.70 | 52 |
| UV/Fe/ H ₂ O ₂ | 281.11 | 48 |
| Plasma | 75.24 | 13 |

5.4 Conclusions

In this study, an atmospheric DBD plasma was used for the treatment of CBZ-polluted water. The influence of several key operating parameters such as initial concentration, applied voltage, pH, and conductivity of the solution on the DBD performance in terms of CBZ degradation efficiency ($\% \eta$) was investigated. It was noted that an increase in the concentration of CBZ before the DBD treatment resulted in a lower ratio of the active species/CBZ molecule, which then reduced the degradation efficiency. Meanwhile, increasing the applied voltage into the system favoured the production of reactive species which enhanced the degradation efficiency simultaneously. The degradation of the pollutant was favoured at neutral pH as well as slightly alkaline conditions, whereas an increase in the conductivity of the solution changed the discharge scheme from spark to corona, thus reducing the degradation efficiency. Approximately 92% CBZ degradation (10 mg/L) was achieved by applying 6 kV voltage, 20 kHz frequency, and 5 μ S/cm conductivity. Also, the degradation mechanism for CBZ with the atmospheric DBD plasma was studied by investigating the concentration and role of the active species present in the aqueous solution and the effect of radical scavengers at different concentrations. Results showed that O₃ played a significant role in CBZ degradation followed by OH, H₂O₂, and O₂. In addition to the ROS present, RNS were also measured which played a role in the acidification of the solution during plasma treatment. To get closer to real conditions, the DBD experiments were also conducted in tap water and final wastewater effluent from a municipality. Significant inhibitions were observed in the effluent matrix, followed by tap water as compared to the deionised water used as control during the 40 min

treatment. This was due to the presence of naturally occurring organic and inorganic molecules in the water matrices. The DBD system was also compared with a commercialised UV system in terms of degradation efficiency and associated energy cost of treatment. The degradation results obtained were 6.5%, 17.8%, 89%, 91%, and 98% for UV-only, UV/Fe, UV/H₂O₂, UV/Fe/H₂O₂, and plasma systems, respectively in 40 mins. The plasma system also had the highest energy efficiency (75.24 kWh/m³) and the least required energy cost of treatment (13 USD/m³) compared to the UV-systems considered.

Chapter 6: General conclusion and Recommendations

Although each study chapter ended with a conclusion, in this final present chapter, the major results of the study and answers to the research questions are summarised. The chapter also identifies some limitations in the study and concludes with future recommendations to further extend the scope of work done.

6.1 Significant findings

This study has demonstrated the effectiveness of a dielectric barrier discharge plasma reactor, an advanced oxidation process, in the degradation of tramadol (TRA), cefixime (CFX), and carbamazepine (CBZ) pharmaceuticals. Initially, an attempt was made to contribute to two key challenges identified with the deployment of the DBD system, which include: the need to increase the throughput of a typical plasma treatment process, and the need to reduce the cost associated with the use of the working gas. To address these, this study was conducted with an atmospheric air DBD operated in a continuous-flow mode. Also, four research questions were proposed in this study, and these include: (1) what is the influence of operating parameters on the degradation efficiency of a continuous-flow atmospheric air DBD for degrading tramadol, cefixime and carbamazepine?(2) what is/are the specific ion(s) responsible for the difference in the degradation of a pharmaceutical pollutant in deionised water and final wastewater effluent? (3) how does a metal ion catalyst influence the degradation performance of a DBD reactor in the presence of radical scavengers? (4) how does a continuous-flow atmospheric air DBD compare with a UV-based system in terms of degradation efficiency, energy efficiency, and energy cost?

Generally, the results obtained in the study have shown that about 93% TRA degradation (5 mg/L) can be achieved in 60 min, >99% CFX degradation (5 mg/L) in 8 min, and 92% CBZ degradation (10 mg/L) in 40 min with the reactor. The applied voltage was within the range of 6 to 8 kV, and at a constant frequency of 20 kHz. In each case, the effects of various operating conditions (applied voltage, initial pollutant concentration, pH and conductivity of solution, water flow rate, and water matrices) were studied to understand the performance of the reactor and select a favourable condition for subsequent investigations. For instance, the influence of applied voltage revealed that the concentration of both reactive oxygen and nitrogen species (O_3 , H_2O_2 , NO_3^- , NO_2^-) can be increased as the voltage was increased. On the other hand, when the initial concentrations of the pollutants were increased, the degradation performance of the reactor dropped as a result of the increased ratio of the number of molecules of the pollutant to the reactive species available in the aqueous solution. The role of pH was not consistent, as both CFX and CBZ degradation increased with pH, while the degradation of TRA was partially inhibited at higher pH values. Conductivity also played a significant role in the degradation of the pollutant both in the synthetic solution and in real water solutions (tap water and final wastewater effluent). The reason is that the reactor is of the volume planar type. The influence

of metal ion catalysts (Fe^{2+}) was verified by a Fenton reaction, thus enhancing the degradation of the pollutants, specifically for CFX and TRA.

A deeper investigation on the chemical species responsible for the degradation of CFX and CBZ was conducted using radical scavenger experiments, and the results showed a significant impact of $\bullet\text{OH}$ on the two pharmaceuticals. However, O_3 was more important in the degradation of CBZ than in CFX. In the case of CFX, the reactor performance was enhanced when Fe^{2+} was mixed with $\bullet\text{OH}$ radical scavengers. This was due to the increased production of H_2O_2 in the aqueous solution. The degradation pathway for CFX was also investigated.

Meanwhile, the degradation of TRA was studied in deionised water and final wastewater effluent. In this case, the presence of HCO_3^- was found to play a limiting role in the degradation of TRA in the FWWE as the ion reacted with $\bullet\text{OH}$ to form $\text{CO}_3^{\bullet-}$. Also, an investigation of antibacterial activity revealed that the plasma-treated TRA solution was less toxic to *Escherichia coli* as opposed to the untreated solution. The performance of the DBD reactor was compared with a UV-based system at similar experimental conditions (volume of solution and initial concentration). It was noted that the degradation results obtained in plasma (98%) was more than the values for the UV setups 6.5%, 17.8%, 89%, 91% for UV-only, UV/Fe, UV/ H_2O_2 , UV/Fe/ H_2O_2 , respectively in 40 mins. The plasma system also had the highest energy efficiency (75.24 kWh/m³) and the least required energy cost of treatment (13 USD/m³) compared to the UV-systems considered.

Overall, the results from this present study have been able to provide answers to the research questions posed in section 1.3.

6.2 Recommendation for future studies

The results obtained in this study have shown the potential of a continuous flow atmospheric air DBD reactor in the degradation of a varied classification of pharmaceuticals that have been commonly reported in the environment. One key thing that has been observed is the efficiency of the reactor in dealing with mono-component solutions. However, considering that pharmaceutical pollutants always exist as mixtures and not as a single component in solution, future studies should consider the efficacy of the reactor in degrading a mixture of the pollutants in different water matrices, including real pharmaceutical waste samples. Toxicity

tests on organisms such as water fleas, could also be conducted to investigate the impact of the plasma-treated solution on complex organisms.

Also, having successfully examined the influence of a single operating parameter per time on the degradation efficiency, further studies may examine the interrelationship between the operating conditions of the reactor and how these impacts the degradation efficiency, energy yield, and the total organic compound present in the aqueous solution.

Meanwhile, it has been observed that the current reactor geometry is significantly affected by the conductivity of the solution due to the contact of the plasma species with the falling water film. Therefore, to realise its benefit for real wastewater treatment, it is necessary to dilute the solutions to reduce their conductivities before treatment. Also, the formation of nitrogen species does affect the degradation process, therefore reactive nitrogen species generated could be avoided by adopting an oxygen concentrator to filter natural air.

References

- [1] Botero-Coy AM, Martínez-Pachón D, Boix C, Rincón RJ, Castillo N, Arias-Marín LP, et al. ‘An investigation into the occurrence and removal of pharmaceuticals in Colombian wastewater.’ *Sci Total Environ* 2018;642:842–53. <https://doi.org/10.1016/j.scitotenv.2018.06.088>.
- [2] Massima Mouele ES, Tijani JO, Badmus KO, Perea O, Babajide O, Zhang C, et al. Removal of pharmaceutical residues from water and wastewater using dielectric barrier discharge methods—a review. *Int J Environ Res Public Health* 2021;18:1–42. <https://doi.org/10.3390/ijerph18041683>.
- [3] Grabicová K, Grabic R, Fedorova G, Vojs Staňová A, Bláha M, Randák T, et al. Water reuse and aquaculture: Pharmaceutical bioaccumulation by fish during tertiary treatment in a wastewater stabilization pond. *Environ Pollut* 2020;267. <https://doi.org/10.1016/j.envpol.2020.115593>.
- [4] Naidu R, Arias Espana VA, Liu Y, Jit J. Emerging contaminants in the environment: Risk-based analysis for better management. *Chemosphere* 2016;154:350–7. <https://doi.org/10.1016/j.chemosphere.2016.03.068>.
- [5] Khetan SK, Collins TJ. Human Pharmaceuticals in the Aquatic Environment: A Challenge to Green Chemistry. *Chem Rev* 2007;107:2319–64. <https://doi.org/https://doi.org/10.1021/cr020441w>.
- [6] World Health Organization (WHO). *Pharmaceuticals in Drinking-water*. 2011.
- [7] Verlicchi P, Grillini V. Surface Water and Groundwater Quality in South Africa and Mozambique — Analysis of the Most Critical Pollutants for Drinking Purposes and Challenges in Water Treatment Selection. *Water* 2020. <https://doi.org/doi:10.3390/w12010305>.
- [8] Wales S, Kasprzyk-hordern B, Dinsdale RM, Guwy AJ. The occurrence of pharmaceuticals , personal care products , endocrine disruptors and illicit drugs in surface water in South Wales, UK. *Water Res* 2008;42:3498–518. <https://doi.org/10.1016/j.watres.2008.04.026>.

- [9] Halling-Sorensen B, Nors Nielsen S, Lanzky PF, Ingerslev F, Holten Lutzhoft HC, Jorgensen SE. Occurrence, Fate and Effects of Pharmaceutical Substances in the Environment - A Review. *Chemosphere* 1998;36:357–93.
- [10] Ternes TA. Occurrence of drugs in German sewage treatment plants and rivers. *Water Res* 1998;32:3245–60. [https://doi.org/10.1016/S0043-1354\(98\)00099-2](https://doi.org/10.1016/S0043-1354(98)00099-2).
- [11] Jiang X, Zhu Y, Liu L, Fan X, Bao Y, Deng S, et al. Occurrence and variations of pharmaceuticals and personal-care products in rural water bodies: A case study of the Taige Canal (2018–2019). *Sci Total Environ* 2021;762:143138. <https://doi.org/10.1016/j.scitotenv.2020.143138>.
- [12] Nieto-Juárez JI, Torres-Palma RA, Botero-Coy AM, Hernández F. Pharmaceuticals and environmental risk assessment in municipal wastewater treatment plants and rivers from Peru. *Environ Int* 2021;155. <https://doi.org/10.1016/j.envint.2021.106674>.
- [13] Subedi B, Codru N, Dziewulski DM, Wilson LR, Xue J, Yun S, et al. A pilot study on the assessment of trace organic contaminants including pharmaceuticals and personal care products from on-site wastewater treatment systems along Skaneateles Lake in New York State, USA. *Water Res* 2015;72:28–39. <https://doi.org/10.1016/j.watres.2014.10.049>.
- [14] United States Geological Survey (USGS). Organic Compounds Assessed in Chattahoochee River Water Used for Public Supply near Atlanta , Georgia , 2004 – 05. n.d.
- [15] Hoppe-Jones C, Dickenson ERV, Drewes JE. The role of microbial adaptation and biodegradable dissolved organic carbon on the attenuation of trace organic chemicals during groundwater recharge. *Sci Total Environ* 2012;437:137–44. <https://doi.org/10.1016/j.scitotenv.2012.08.009>.
- [16] Miralles-Cuevas S, Oller I, Pérez JAS, Malato S. Removal of pharmaceuticals from MWTP effluent by nanofiltration and solar photo-Fenton using two different iron complexes at neutral pH. *Water Res* 2014;64:23–31. <https://doi.org/10.1016/j.watres.2014.06.032>.
- [17] Rout PR, Zhang TC, Bhunia P, Surampalli RY. Treatment technologies for emerging contaminants in wastewater treatment plants: A review. *Sci Total Environ*

- 2021;753:141990. <https://doi.org/10.1016/j.scitotenv.2020.141990>.
- [18] Salamatinia B AP. A Short Review on Presence of Pharmaceuticals in Water Bodies and the Potential of Chitosan and Chitosan Derivatives for Elimination of Pharmaceuticals. *J Mol Genet Med* 2015;s4:1–7. <https://doi.org/10.4172/1747-0862.s4-001>.
- [19] Sikosana ML, Sikhwivhilu K, Moutloali R, Madyira DM. Municipal wastewater treatment technologies: A review. *Procedia Manuf* 2019;35:1018–24. <https://doi.org/10.1016/j.promfg.2019.06.051>.
- [20] Palma D, Papagiannaki D, Lai M, Binetti R, Sleiman M, Minella M, et al. PFAS degradation in ultrapure and groundwater using non-thermal plasma. *Molecules* 2021;26:1–13. <https://doi.org/10.3390/molecules26040924>.
- [21] Rivera-Utrilla J, Sánchez-Polo M, Ferro-García MÁ, Prados-Joya G, Ocampo-Pérez R. Pharmaceuticals as emerging contaminants and their removal from water. A review. *Chemosphere* 2013;93:1268–87. <https://doi.org/10.1016/j.chemosphere.2013.07.059>.
- [22] Magureanu M, Bilea F, Bradu C, Hong D. A review on non-thermal plasma treatment of water contaminated with antibiotics. *J Hazard Mater* 2021;417. <https://doi.org/10.1016/j.jhazmat.2021.125481>.
- [23] Liu Y, Mei S, Iya-Sou D, Cavadias S, Ognier S. Carbamazepine removal from water by dielectric barrier discharge: Comparison of ex situ and in situ discharge on water. *Chem Eng Process Process Intensif* 2012;56:10–8. <https://doi.org/10.1016/j.cep.2012.03.003>.
- [24] Hama Aziz KH, Mahyar A, Miessner H, Mueller S, Kalass D, Moeller D, et al. Application of a planar falling film reactor for decomposition and mineralization of methylene blue in the aqueous media via ozonation, Fenton, photocatalysis and non-thermal plasma: A comparative study. *Process Saf Environ Prot* 2018;113:319–29. <https://doi.org/10.1016/j.psep.2017.11.005>.
- [25] Vanraes P, Ghodbane H, Davister D, Wardenier N, Nikiforov A, Verheust YP, et al. Removal of several pesticides in a falling water film DBD reactor with activated carbon textile: Energy efficiency. *Water Res* 2017;116:1–12. <https://doi.org/10.1016/j.watres.2017.03.004>.
- [26] Zeng J, Yang B, Wang X, Li Z, Zhang X, Lei L. Degradation of pharmaceutical

- contaminant ibuprofen in aqueous solution by cylindrical wetted-wall corona discharge. *Chem Eng J* 2015;267:282–8. <https://doi.org/10.1016/j.cej.2015.01.030>.
- [27] Vanraes P, Willems G, Daels N, Van Hulle SWH, De Clerck K, Surmont P, et al. Decomposition of atrazine traces in water by combination of non-thermal electrical discharge and adsorption on nanofiber membrane. *Water Res* 2015;72:361–71. <https://doi.org/10.1016/j.watres.2014.11.009>.
- [28] Shirmardi M, Alavi N, Lima EC, Takdastan A, Mahvi AH, Babaei AA. Removal of atrazine as an organic micro-pollutant from aqueous solutions: a comparative study. *Process Saf Environ Prot* 2016;103:23–35. <https://doi.org/10.1016/j.psep.2016.06.014>.
- [29] Aggelopoulos CA, Meropoulis S, Hatzisymeon M, Lada ZG, Rassias G. Degradation of antibiotic enrofloxacin in water by gas-liquid nsp-DBD plasma: Parametric analysis, effect of H₂O₂ and CaO₂ additives and exploration of degradation mechanisms. *Chem Eng J* 2020;398:125622. <https://doi.org/10.1016/j.cej.2020.125622>.
- [30] Zhang Q, Zhang H, Zhang Q, Huang Q. Degradation of norfloxacin in aqueous solution by atmospheric-pressure non-thermal plasma: Mechanism and degradation pathways. *Chemosphere* 2018;210:433–9. <https://doi.org/10.1016/j.chemosphere.2018.07.035>.
- [31] Iervolino G, Vaiano V, Palma V. Enhanced removal of water pollutants by dielectric barrier discharge non-thermal plasma reactor. *Sep Purif Technol* 2019;215:155–62. <https://doi.org/10.1016/j.seppur.2019.01.007>.
- [32] Liu Y, Mei S, Iya-Sou D, Cavadias S, Ognier S. Carbamazepine removal from water by dielectric barrier discharge: Comparison of ex situ and in situ discharge on water. *Chem Eng Process Process Intensif* 2012;56:10–8. <https://doi.org/10.1016/j.cep.2012.03.003>.
- [33] Daughton CG, Ternes TA. Pharmaceuticals and Personal Care Products in the Environment : Agents of Subtle Change? *Environ Health Perspect* 1999;107:907–38. <https://doi.org/10.1289/ehp.99107s6907>.
- [34] Majumder A, Gupta B, Gupta AK. Pharmaceutically active compounds in aqueous environment: A status, toxicity and insights of remediation. *Environ Res* 2019;176:108542. <https://doi.org/10.1016/j.envres.2019.108542>.
- [35] Edwards QA, Sultana T, Kulikov SM, Garner-O’Neale LD, Yargeau V, Metcalfe CD.

- Contaminants of Emerging Concern in Wastewaters in Barbados, West Indies. *Bull Environ Contam Toxicol* 2018;101:1–6. <https://doi.org/10.1007/s00128-018-2346-0>.
- [36] Luo Y, Yang Y, Lin Y, Tian Y, Wu L, Yang L, et al. Low-Temperature and Atmospheric Pressure Sample Digestion Using Dielectric Barrier Discharge. *Anal Chem* 2018;90:1547–53. <https://doi.org/10.1021/acs.analchem.7b04376>.
- [37] Sophia A. C, Lima EC. Removal of emerging contaminants from the environment by adsorption. *Ecotoxicol Environ Saf* 2018;150:1–17. <https://doi.org/10.1016/j.ecoenv.2017.12.026>.
- [38] Statistics of publications on occurrence of pharmaceuticals in water and wastewater based on scopus publications from 2000 to 2022 n.d. <https://www.scopus.com/results/results.uri?sort=plf-f&src=s&st1=degradation+of+carbamazepine+with+plasma&sid=fc6404efc4a2270c8fb1d72562ea9a20&sot=b&sdt=cl&sl=55&s=TITLE-ABS-KEY%28pharmaceuticals+AND+water+AND+wastewater%29&origin=resultslist&editSaveSearc> (accessed October 10, 2023).
- [39] Mompelat S, Le Bot B, Thomas O. Occurrence and fate of pharmaceutical products and by-products, from resource to drinking water. *Environ Int* 2009;35:803–14. <https://doi.org/10.1016/j.envint.2008.10.008>.
- [40] Goossens H, Ferech M, Stichele R Vander, Elseviers M. Outpatient antibiotic use in Europe and association with resistance: a cross-national database study. *Lancet* 2009;365:579–87. https://doi.org/10.1007/978-3-211-89836-9_1109.
- [41] Matamoros V, Arias CA, Nguyen LX, Salvadó V, Brix H. Occurrence and behavior of emerging contaminants in surface water and a restored wetland. *Chemosphere* 2012;88:1083–9. <https://doi.org/10.1016/j.chemosphere.2012.04.048>.
- [42] Hedgespeth ML, Sapozhnikova Y, Pennington P, Clum A, Fairey A, Wirth E. Pharmaceuticals and personal care products (PPCPs) in treated wastewater discharges into Charleston Harbor, South Carolina. *Sci Total Environ* 2012;437:1–9. <https://doi.org/10.1016/j.scitotenv.2012.07.076>.
- [43] Dinh QT, Moreau-Guigon E, Labadie P, Alliot F, Teil MJ, Blanchard M, et al. Occurrence of antibiotics in rural catchments. *Chemosphere* 2017;168:483–90.

<https://doi.org/10.1016/j.chemosphere.2016.10.106>.

- [44] Meffe R, de Bustamante I. Emerging organic contaminants in surface water and groundwater: A first overview of the situation in Italy. *Sci Total Environ* 2014;481:280–95. <https://doi.org/10.1016/j.scitotenv.2014.02.053>.
- [45] López-Serna R, Jurado A, Vázquez-Suñé E, Carrera J, Petrović M, Barceló D. Occurrence of 95 pharmaceuticals and transformation products in urban groundwaters underlying the metropolis of Barcelona, Spain. *Environ Pollut* 2013;174:305–15. <https://doi.org/10.1016/j.envpol.2012.11.022>.
- [46] Mohapatra S, Huang CH, Mukherji S, Padhye LP. Occurrence and fate of pharmaceuticals in WWTPs in India and comparison with a similar study in the United States. *Chemosphere* 2016;159:526–35. <https://doi.org/10.1016/j.chemosphere.2016.06.047>.
- [47] Behera SK, Kim HW, Oh JE, Park HS. Occurrence and removal of antibiotics, hormones and several other pharmaceuticals in wastewater treatment plants of the largest industrial city of Korea. *Sci Total Environ* 2011;409:4351–60. <https://doi.org/10.1016/j.scitotenv.2011.07.015>.
- [48] Lardy-Fontan S, Le Diouren V, Drouin C, Lalere B, Vaslin-Reimann S, Dauchy X, et al. Validation of a method to monitor the occurrence of 20 relevant pharmaceuticals and personal care products in 167 bottled waters. *Sci Total Environ* 2017;587–588:118–27. <https://doi.org/10.1016/j.scitotenv.2017.02.074>.
- [49] Rimayi C, Odusanya D, Weiss JM, Boer J De, Chimuka L. Contaminants of emerging concern in the Hartbeespoort Dam catchment and the uMngeni River estuary 2016 pollution incident, South Africa. *Sci Total Environ* 2018;627:1008–17. <https://doi.org/10.1016/j.scitotenv.2018.01.263>.
- [50] Pal A, Gin KYH, Lin AYC, Reinhard M. Impacts of emerging organic contaminants on freshwater resources: Review of recent occurrences, sources, fate and effects. *Sci Total Environ* 2010;408:6062–9. <https://doi.org/10.1016/j.scitotenv.2010.09.026>.
- [51] Englade AJ, Krenkel P, Shamas J. *Wastewater Treatment & Water Reclamation*. Elsevier Inc.; 2015. <https://doi.org/10.1016/b978-0-12-409548-9.09508-7>.

- [52] Christensen FM. Pharmaceuticals in the Environment — A Human Risk ? Regul Toxicol Pharmacol 1998;221:212–21. <https://doi.org/10.1006/rtph.1998.1253>.
- [53] Segura PA, Takada H, Correa JA, El K, Koike T, Onwona-agyeman S, et al. Global occurrence of anti-infectives in contaminated surface waters : Impact of income inequality between countries. Environ Int 2015;80:89–97. <https://doi.org/10.1016/j.envint.2015.04.001>.
- [54] Oluwatosin O, Adekunle B, Obih U, Arne H. Quantification of pharmaceutical residues in wastewater impacted surface waters and sewage sludge from Lagos, Nigeria. J Environ Chem Ecotoxicol 2016;8:14–24. <https://doi.org/10.5897/jece2015.0364>.
- [55] SIMAZAKI D, HIRAMATSU S, FUJIWARA J, AKIBA M, KUNIKANE S. Monitoring Priority of Residual Pharmaceuticals in Water Sources and Drinking Water in Japan. J Water Environ Technol 2014;12:275–83. <https://doi.org/10.2965/jwet.2014.275>.
- [56] Sui Q, Huang J, Deng S, Yu G, Fan Q. Occurrence and removal of pharmaceuticals, caffeine and DEET in wastewater treatment plants of Beijing, China. Water Res 2010;44:417–26. <https://doi.org/10.1016/j.watres.2009.07.010>.
- [57] Balakrishna K, Rath A, Praveenkumarreddy Y, Guruge KS, Subedi B. A review of the occurrence of pharmaceuticals and personal care products in Indian water bodies. Ecotoxicol Environ Saf 2017;137:113–20. <https://doi.org/10.1016/j.ecoenv.2016.11.014>.
- [58] Lolić A, Paíga P, Santos LHMLM, Ramos S, Correia M, Delerue-Matos C. Assessment of non-steroidal anti-inflammatory and analgesic pharmaceuticals in seawaters of North of Portugal: Occurrence and environmental risk. Sci Total Environ 2015;508:240–50. <https://doi.org/10.1016/j.scitotenv.2014.11.097>.
- [59] Fernández C, González-Doncel M, Pro J, Carbonell G, Tarazona J V. Occurrence of pharmaceutically active compounds in surface waters of the henares-jarama-tajo river system (madrid, spain) and a potential risk characterization. Sci Total Environ 2010;408:543–51. <https://doi.org/10.1016/j.scitotenv.2009.10.009>.
- [60] McArdell CS, Molnar E, Suter MJF, Giger W. Occurrence and Fate of Macrolide Antibiotics in Wastewater Treatment Plants and in the Glatt Valley Watershed,

- Switzerland. *Environ Sci Technol* 2003;37:5479–86. <https://doi.org/10.1021/es034368i>.
- [61] Senta I, Terzic S, Ahel M. Occurrence and fate of dissolved and particulate antimicrobials in municipal wastewater treatment. *Water Res* 2013;47:705–14. <https://doi.org/10.1016/j.watres.2012.10.041>.
- [62] Kondor AC, Molnár É, Vancsik A, Filep T, Szeberényi J, Szabó L, et al. Occurrence and health risk assessment of pharmaceutically active compounds in riverbank filtrated drinking water. *J Water Process Eng* 2021;41. <https://doi.org/10.1016/j.jwpe.2021.102039>.
- [63] Roberts PH, Thomas K V. The occurrence of selected pharmaceuticals in wastewater effluent and surface waters of the lower Tyne catchment. *Sci Total Environ* 2006;356:143–53. <https://doi.org/10.1016/j.scitotenv.2005.04.031>.
- [64] Reif AG, Crawford KJ, Loper CA, Proctor A, Manning R, Titler R. Occurrence of Pharmaceuticals , Hormones , and Organic Wastewater Compounds in Pennsylvania Waters , 2006 – 09 Scientific Investigations Report 2012 – 5106. 2012.
- [65] Liu YY, Ptacek CJ, Groza LG, Staples R, Blowes DW. Occurrence and distribution of emerging contaminants in mine-impacted lake water and potential use as co-tracers of anthropogenic activity in the subarctic region, Northwest Territories, Canada. *Environ Res* 2022;207:112034. <https://doi.org/10.1016/j.envres.2021.112034>.
- [66] Vázquez-Tapia I, Salazar-Martínez T, Acosta-Castro M, Meléndez-Castolo KA, Mahlknecht J, Cervantes-Avilés P, et al. Occurrence of emerging organic contaminants and endocrine disruptors in different water compartments in Mexico – A review. *Chemosphere* 2022;308. <https://doi.org/10.1016/j.chemosphere.2022.136285>.
- [67] Graham DW, Olivares-Rieumont S, Knapp CW, Lima L, Werner D, Bowen E. Antibiotic resistance gene abundances associated with waste discharges to the Almendares river near Havana, Cuba. *Environ Sci Technol* 2011;45:418–24. <https://doi.org/10.1021/es102473z>.
- [68] Birch GF, Drage DS, Thompson K, Eaglesham G, Mueller JF. Emerging contaminants (pharmaceuticals, personal care products, a food additive and pesticides) in waters of Sydney estuary, Australia. *Mar Pollut Bull* 2015;97:56–66. <https://doi.org/10.1016/j.marpolbul.2015.06.038>.

- [69] Stewart M, Olsen G, Hickey CW, Ferreira B, Jelić A, Petrović M, et al. A survey of emerging contaminants in the estuarine receiving environment around Auckland, New Zealand. *Sci Total Environ* 2014;468–469:202–10. <https://doi.org/10.1016/j.scitotenv.2013.08.039>.
- [70] Stumpf M, Ternes TA, Wilken RD, Silvana Vianna Rodrigues, Baumann W. Polar drug residues in sewage and natural waters in the state of Rio de Janeiro, Brazil. *Sci Total Environ* 1999;225:135–41. [https://doi.org/10.1016/S0048-9697\(98\)00339-8](https://doi.org/10.1016/S0048-9697(98)00339-8).
- [71] Elorriaga Y, Marino DJ, Carriquiriborde P, Ronco AE. Human pharmaceuticals in wastewaters from urbanized areas of Argentina. *Bull Environ Contam Toxicol* 2013;90:397–400. <https://doi.org/10.1007/s00128-012-0919-x>.
- [72] Rodrigues P, Guimarães L, Carvalho AP, Oliva-Teles L. Carbamazepine, venlafaxine, tramadol, and their main metabolites: Toxicological effects on zebrafish embryos and larvae. *J Hazard Mater* 2023;448. <https://doi.org/10.1016/j.jhazmat.2023.130909>.
- [73] Physicians' Desk Reference. 59th ed. New Jersey: Thomson PDR, Montvale; 2005.
- [74] Das N, Madhavan J, Selvi A, Das D. An overview of cephalosporin antibiotics as emerging contaminants: a serious environmental concern. *3 Biotech* 2019;9:1–14. <https://doi.org/10.1007/s13205-019-1766-9>.
- [75] Antonopoulou M, Thoma A, Konstantinou F, Vlastos D, Hela D. Assessing the human risk and the environmental fate of pharmaceutical Tramadol. *Sci Total Environ* 2020;710. <https://doi.org/10.1016/j.scitotenv.2019.135396>.
- [76] Buřič M, Grabicová K, Kubec J, Kouba A, Kuklina I, Kozák P, et al. Environmentally relevant concentrations of tramadol and citalopram alter behaviour of an aquatic invertebrate. *Aquat Toxicol* 2018;200:226–32. <https://doi.org/10.1016/j.aquatox.2018.05.008>.
- [77] Zuccato E, Castiglioni S, Bagnati R, Melis M, Fanelli R. Source, occurrence and fate of antibiotics in the Italian aquatic environment. *J Hazard Mater* 2010;179:1042–8. <https://doi.org/10.1016/j.jhazmat.2010.03.110>.
- [78] Abdollahiasl A, Kebriaeezadeh A, Nikfar S, Farshchi A, Ghiasi G, Abdollahi M. Patterns of antibiotic consumption in Iran during 2000-2009. *Int J Antimicrob Agents*

- 2011;37:489–90. <https://doi.org/10.1016/j.ijantimicag.2011.01.022>.
- [79] Rahimpour M, Saremi K, Shirvani E, Gomari H, Rahimpour M, Niroumanesh A, et al. A survey on medicine consumption in the mega cities of Iran. *Ital J Public Health* 2011;8:255–60.
- [80] Buser HR, Poiger T, Müller MD. Occurrence and fate of the pharmaceutical drug diclofenac in surface waters: Rapid photodegradation in a lake. *Environ Sci Technol* 1998;32:3449–56. <https://doi.org/10.1021/es980301x>.
- [81] Biswas P, Vellanki BP. Occurrence of emerging contaminants in highly anthropogenically influenced river Yamuna in India. *Sci Total Environ* 2021;782:146741. <https://doi.org/10.1016/j.scitotenv.2021.146741>.
- [82] Malev O, Lovrić M, Stipaničev D, Repec S, Martinović-Weigelt D, Zanella D, et al. Toxicity prediction and effect characterization of 90 pharmaceuticals and illicit drugs measured in plasma of fish from a major European river (Sava, Croatia). *Environ Pollut* 2020;266. <https://doi.org/10.1016/j.envpol.2020.115162>.
- [83] Evgenidou EN, Konstantinou IK, Lambropoulou DA. Occurrence and removal of transformation products of PPCPs and illicit drugs in wastewaters: A review. *Sci Total Environ* 2015;505:905–26. <https://doi.org/10.1016/j.scitotenv.2014.10.021>.
- [84] Hai FI, Yang S, Asif MB, Sencadas V, Shawkat S, Sanderson-Smith M, et al. Carbamazepine as a Possible Anthropogenic Marker in Water: Occurrences, Toxicological Effects, Regulations and Removal by Wastewater Treatment Technologies. *Water (Switzerland)* 2018;10:1–32. <https://doi.org/10.3390/w10020107>.
- [85] Magureanu M, Mandache NB, Parvulescu VI. Degradation of pharmaceutical compounds in water by non-thermal plasma treatment. *Water Res* 2015;81:124–36. <https://doi.org/10.1016/j.watres.2015.05.037>.
- [86] Castle SS, Medical VA. *Cefixime* 2007:1–5.
- [87] Hai FI, Yang S, Asif MB, Sencadas V, Shawkat S, Sanderson-Smith M, et al. Carbamazepine as a Possible Anthropogenic Marker in Water: Occurrences, Toxicological Effects, Regulations and Removal by Wastewater Treatment Technologies. *Water (Switzerland)* 2018;10. <https://doi.org/10.3390/w10020107>.

- [88] Heberer T. Occurrence, fate, and removal of pharmaceutical residues in the aquatic environment: a review of recent research data. *Toxicol Lett* 2002;131:5–17. <https://doi.org/10.1111/j.1439-0388.1936.tb00094.x>.
- [89] Hummel D, Löffler D, Fink G, Ternes TA. Simultaneous determination of psychoactive drugs and their metabolites in aqueous matrices by liquid chromatography mass spectrometry. *Environ Sci Technol* 2006;40:7321–8. <https://doi.org/10.1021/es061740w>.
- [90] Kasprzyk-Hordern B, Dinsdale RM, Guwy AJ. The removal of pharmaceuticals, personal care products, endocrine disruptors and illicit drugs during wastewater treatment and its impact on the quality of receiving waters. *Water Res* 2009;43:363–80. <https://doi.org/10.1016/j.watres.2008.10.047>.
- [91] József T, Kiss SR, Muzslay F, Máté O, Stromájer GP, Stromájer-Rácz T. Detection and Quantification of Pharmaceutical Residues in the Pest County Section of the River Danube. *Water (Switzerland)* 2023;15. <https://doi.org/10.3390/w15091755>.
- [92] Rockwood AL, Kushnir MM, Clarke NJ. *Mass spectrometry*. Elsevier Inc.; 2018. <https://doi.org/10.1016/B978-0-12-816063-3.00002-5>.
- [93] Hansen F, Øiestad EL, Pedersen-Bjergaard S. Bioanalysis of pharmaceuticals using liquid-phase microextraction combined with liquid chromatography–mass spectrometry. *J Pharm Biomed Anal* 2020;189. <https://doi.org/10.1016/j.jpba.2020.113446>.
- [94] Sadri Moghaddam S, Alavi Moghaddam MR, Arami M. Coagulation/flocculation process for dye removal using sludge from water treatment plant: Optimization through response surface methodology. *J Hazard Mater* 2010;175:651–7. <https://doi.org/10.1016/j.jhazmat.2009.10.058>.
- [95] Rathi BS, Kumar PS, Show PL. A review on effective removal of emerging contaminants from aquatic systems: Current trends and scope for further research. *J Hazard Mater* 2021;409:124413. <https://doi.org/10.1016/j.jhazmat.2020.124413>.
- [96] Xia K. *Analytical Methods. Tomography* 2010;21–62. <https://doi.org/10.1002/9780470611784.ch2>.

- [97] Patel BN, Sharma N, Sanyal M, Shrivastav PS. An accurate , rapid and sensitive determination of tramadol and its active metabolite O -desmethyltramadol in human plasma by LC – MS / MS. *J Pharm Biomed Anal* 2009;49:354–66. <https://doi.org/10.1016/j.jpba.2008.10.030>.
- [98] Vivekanandan-Giri A, Byun J, Pennathur S. Quantitative analysis of amino acid oxidation markers by tandem mass spectrometry. vol. 491. 1st ed. Elsevier Inc.; 2011. <https://doi.org/10.1016/B978-0-12-385928-0.00005-5>.
- [99] Sunil A, Anju G, Rajat V. HPLC Detectors, Their Types and Use: A Review. *Org Med Chem Int J* 2018;6:3–6. <https://doi.org/10.19080/OMCIJ.2018.06.555700>.
- [100] Bhardwaj SK, Dwivedi K, Agarwal D. A Review : HPLC Method Development and Validation I. *Int J Anal Bioanal Chem* 2016.
- [101] Willard HH, Merritt, Jr LL, Dean JA, Settle, Jr FA. Instrumental methods of analysis. 7th ed. 1988.
- [102] Shah AI, Din Dar MU, Bhat RA, Singh JP, Singh K, Bhat SA. Prospectives and challenges of wastewater treatment technologies to combat contaminants of emerging concerns. *Ecol Eng* 2020;152:105882. <https://doi.org/10.1016/j.ecoleng.2020.105882>.
- [103] Palma D, Richard C, Minella M. State of the art and perspectives about non-thermal plasma applications for the removal of PFAS in water. *Chem Eng J Adv* 2022;10:100253. <https://doi.org/10.1016/j.ceja.2022.100253>.
- [104] Tran NH, Reinhard M, Khan E, Chen H, Nguyen VT, Li Y, et al. Emerging contaminants in wastewater, stormwater runoff, and surface water: Application as chemical markers for diffuse sources. *Sci Total Environ* 2019;676:252–67. <https://doi.org/10.1016/j.scitotenv.2019.04.160>.
- [105] Noguera-Oviedo K, Aga DS. Lessons learned from more than two decades of research on emerging contaminants in the environment. *J Hazard Mater* 2016;316:242–51. <https://doi.org/10.1016/j.jhazmat.2016.04.058>.
- [106] Boiteux V, Dauchy X, Bach C, Colin A, Hemard J, Sagres V, et al. Science of the Total Environment Concentrations and patterns of per fl uoroalkyl and poly fl uoroalkyl substances in a river and three drinking water treatment plants near and far from a major

- production source. *Sci Total Environ* 2017;583:393–400.
<https://doi.org/10.1016/j.scitotenv.2017.01.079>.
- [107] Sun M, Arevalo E, Strynar M, Lindstrom A, Richardson M, Kearns B, et al. Legacy and Emerging Perfluoroalkyl Substances Are Important Drinking Water Contaminants in the Cape Fear River Watershed of North Carolina. *Environ Sci Technol Lett* 2016. <https://doi.org/10.1021/acs.estlett.6b00398>.
- [108] Ternes TA, Meisenheimer M, McDowell D, Sacher F, Brauch H-J, Haist-Gulde B, et al. Removal of Pharmaceuticals during Drinking Water Treatment. *Environ Sci Technol* 2002;36:3855–63. <https://doi.org/10.1021/es015757k>.
- [109] Boshir M, Zhou JL, Hao H, Guo W, Thomaidis NS, Xu J. Progress in the biological and chemical treatment technologies for emerging contaminant removal from wastewater: A critical review. *J Hazard Mater* 2017;323:274–98. <https://doi.org/10.1016/j.jhazmat.2016.04.045>.
- [110] Alvarino T, Suarez S, Lema J, Omil F. Science of the Total Environment Understanding the sorption and biotransformation of organic micropollutants in innovative biological wastewater treatment technologies. *Sci Total Environ* 2018;615:297–306. <https://doi.org/10.1016/j.scitotenv.2017.09.278>.
- [111] Rodriguez-narvaez OM, Peralta-hernandez JM, Goonetilleke A, Bandala ER. Treatment technologies for emerging contaminants in water: A review. *Chem Eng J* 2017;323:361–80. <https://doi.org/10.1016/j.cej.2017.04.106>.
- [112] Kim M, Guerra P, Shah A, Parsa M, Alaei M, Smyth SA. Removal of pharmaceuticals and personal care products in a membrane bioreactor wastewater treatment plant. *Water Sci Technol* 2014;2221–9. <https://doi.org/10.2166/wst.2014.145>.
- [113] Norvill ZN, Shilton A, Guieysse B. Emerging contaminant degradation and removal in algal wastewater treatment ponds: Identifying the research gaps. *J Hazard Mater* 2016;313:291–309. <https://doi.org/10.1016/j.jhazmat.2016.03.085>.
- [114] Stenstrom MK, Cardinal L, Libra J. Treatment of Hazardous Substances in Wastewater Treatment Plants. *Environ Prog* 1989. <https://doi.org/10.1002/ep.3300080214>.
- [115] Tran NH, Reinhard M, Gin KY. Occurrence and fate of emerging contaminants in

- municipal wastewater treatment plants from different geographical regions-a review. *Water Res* 2018;133:182–207. <https://doi.org/10.1016/j.watres.2017.12.029>.
- [116] Roccaro P. Treatment processes for municipal wastewater reclamation : The challenges of emerging contaminants and direct potable reuse. *Curr Opin Environ Sci Heal* 2018;2:46–54. <https://doi.org/10.1016/j.coesh.2018.02.003>.
- [117] Awaleh MO, Soubaneh YD. Waste Water Treatment in Chemical Industries : The Concept and Current Technologies. *Hydrol Curr Res* 2014;5:1–12. <https://doi.org/10.4172/2157-7587.1000164>.
- [118] Viancelli A, Michelon W, Rogovski P, Dorighello R, Estêvão C, Souza B De, et al. A review on alternative bioprocesses for removal of emerging contaminants. *Bioprocess Biosyst Eng* 2020;43:2117–29. <https://doi.org/10.1007/s00449-020-02410-9>.
- [119] Xu Q, Huang Q, Wei W, Sun J, Dai X, Ni B. Improving the treatment of waste activated sludge using calcium peroxide. *Water Res* 2020;187:116440. <https://doi.org/10.1016/j.watres.2020.116440>.
- [120] Carballa M, Omil F, Lema JM, Llombart M, García-Jares C, Rodríguez I, et al. Behavior of pharmaceuticals, cosmetics and hormones in a sewage treatment plant. *Water Res* 2004;38:2918–26. <https://doi.org/10.1016/j.watres.2004.03.029>.
- [121] Strenn B, Clara M, Gans O, Kreuzinger N. Investigations on the Behaviour of Selected Pharmaceuticals During Wastewater Treatment. *Water Sci Technol* 2004;50:269–76.
- [122] Miklos DB, Remy C, Jekel M, Linden KG, Drewes JE, Hübner U. Evaluation of advanced oxidation processes for water and wastewater treatment – A critical review. *Water Res* 2018;139:118–31. <https://doi.org/10.1016/j.watres.2018.03.042>.
- [123] Kim I, Yamashita N, Tanaka H. Performance of UV and UV/H₂O₂ processes for the removal of pharmaceuticals detected in secondary effluent of a sewage treatment plant in Japan. *J Hazard Mater* 2009;166:1134–40. <https://doi.org/10.1016/j.jhazmat.2008.12.020>.
- [124] Luo S, Wei Z, Spinney R, Zhang Z, Dionysiou DD, Gao L, et al. UV direct photolysis of sulfamethoxazole and ibuprofen: An experimental and modelling study. *J Hazard Mater* 2018;343:132–9. <https://doi.org/10.1016/j.jhazmat.2017.09.019>.

- [125] Watts MJ, Linden KG. Chlorine photolysis and subsequent OH radical production during UV treatment of chlorinated water. *Water Res* 2007;41:2871–8. <https://doi.org/10.1016/j.watres.2007.03.032>.
- [126] Watts MJ, Rosenfeldt EJ, Linden KG. Comparative OH radical oxidation using UV-Cl₂ and UV-H₂O₂ processes. *J Water Supply Res Technol - AQUA* 2007;56:469–77. <https://doi.org/10.2166/aqua.2007.028>.
- [127] Dong H, Qiang Z, Hu J, Qu J. Degradation of chloramphenicol by UV/chlorine treatment: Kinetics, mechanism and enhanced formation of halonitromethanes. *Water Res* 2017;121:178–85. <https://doi.org/10.1016/j.watres.2017.05.030>.
- [128] Pan Y, Cheng SS, Yang X, Ren J, Fang J, Shang C, et al. UV/chlorine treatment of carbamazepine: Transformation products and their formation kinetics. *Water Res* 2017;116:254–65. <https://doi.org/10.1016/j.watres.2017.03.033>.
- [129] Qin L, Lin YL, Xu B, Hu CY, Tian FX, Zhang TY, et al. Kinetic models and pathways of ronidazole degradation by chlorination, UV irradiation and UV/chlorine processes. *Water Res* 2014;65:271–81. <https://doi.org/10.1016/j.watres.2014.07.041>.
- [130] Kong X, Wu Z, Ren Z, Guo K, Hou S, Hua Z, et al. Degradation of lipid regulators by the UV/chlorine process: Radical mechanisms, chlorine oxide radical (ClO•)-mediated transformation pathways and toxicity changes. *Water Res* 2018;137:242–50. <https://doi.org/10.1016/j.watres.2018.03.004>.
- [131] Graumans MHF, Hoeben WFLM, Russel FGM, Scheepers PTJ. Oxidative degradation of cyclophosphamide using thermal plasma activation and UV/H₂O₂ treatment in tap water. *Environ Res* 2020;182:109046. <https://doi.org/10.1016/j.envres.2019.109046>.
- [132] Cobo-Golpe M, Fernandez-Fernandez V, Arias T, Ramil M, Cela R, Rodríguez I. Comparison of UV, chlorination, UV-hydrogen peroxide and UV-chlorine processes for tramadol removal: Kinetics study and transformation products identification. *J Environ Chem Eng* 2022;10:1–10. <https://doi.org/10.1016/j.jece.2022.107854>.
- [133] Miralles-Cuevas S, Darowna D, Wanag A, Mozia S, Malato S, Oller I. Comparison of UV/H₂O₂, UV/S₂O₈²⁻, solar/Fe(II)/H₂O₂ and solar/Fe(II)/S₂O₈²⁻ at pilot plant scale for the elimination of micro-contaminants in natural water: An economic assessment. *Chem Eng J* 2017;310:514–24. <https://doi.org/10.1016/j.cej.2016.06.121>.

- [134] Moreira FC, Boaventura RAR, Brillas E, Vilar VJP. Electrochemical advanced oxidation processes: A review on their application to synthetic and real wastewaters. *Appl Catal B Environ* 2017;202:217–61. <https://doi.org/10.1016/j.apcatb.2016.08.037>.
- [135] Shemer H, Kunukcu YK, Linden KG. Degradation of the pharmaceutical Metronidazole via UV, Fenton and photo-Fenton processes. *Chemosphere* 2006;63:269–76. <https://doi.org/10.1016/j.chemosphere.2005.07.029>.
- [136] Lu C, Deng K, Hu C, Lyu L. Dual-reaction-center catalytic process continues Fenton’s story. *Front Environ Sci Eng* 2020;14. <https://doi.org/10.1007/s11783-020-1261-x>.
- [137] Sreeja PH, Sosamony KJ. A Comparative Study of Homogeneous and Heterogeneous Photo-fenton Process for Textile Wastewater Treatment. *Procedia Technol* 2016;24:217–23. <https://doi.org/10.1016/j.protcy.2016.05.065>.
- [138] Ahmed MB, Zhou JL, Ngo HH, Guo W, Thomaidis NS, Xu J. Progress in the biological and chemical treatment technologies for emerging contaminant removal from wastewater: A critical review. *J Hazard Mater* 2017;323:274–98. <https://doi.org/10.1016/j.jhazmat.2016.04.045>.
- [139] Mirzaei A, Chen Z, Haghghat F, Yerushalmi L. Removal of pharmaceuticals from water by homo/heterogonous Fenton-type processes – A review. *Chemosphere* 2017;174:665–88. <https://doi.org/10.1016/j.chemosphere.2017.02.019>.
- [140] Badawy MI, Ghaly MY, Gad-Allah TA. Advanced oxidation processes for the removal of organophosphorus pesticides from wastewater. *Desalination* 2006;194:166–75. <https://doi.org/10.1016/j.desal.2005.09.027>.
- [141] Alalm MG, Tawfik A, Ookawara S. Degradation of four pharmaceuticals by solar photo-Fenton process: Kinetics and costs estimation. *J Environ Chem Eng* 2015;3:46–51. <https://doi.org/10.1016/j.jece.2014.12.009>.
- [142] Oturan MA, Aaron JJ. Advanced oxidation processes in water/wastewater treatment: Principles and applications. A review. *Crit Rev Environ Sci Technol* 2014;44:2577–641. <https://doi.org/10.1080/10643389.2013.829765>.
- [143] Hartmann M, Kullmann S, Keller H. Wastewater treatment with heterogeneous Fenton-type catalysts based on porous materials. *J Mater Chem* 2010;20:9002–17.

<https://doi.org/10.1039/c0jm00577k>.

- [144] Ribeiro AR, Nunes OC, Pereira MFR, Silva AMT. An overview on the advanced oxidation processes applied for the treatment of water pollutants defined in the recently launched Directive 2013/39/EU. *Environ Int* 2015;75:33–51. <https://doi.org/10.1016/j.envint.2014.10.027>.
- [145] Wang H, Zhan J, Yao W, Wang B, Deng S, Huang J, et al. Comparison of pharmaceutical abatement in various water matrices by conventional ozonation, peroxone (O₃/H₂O₂), and an electro-peroxone process. *Water Res* 2018;130:127–38. <https://doi.org/10.1016/j.watres.2017.11.054>.
- [146] Huang Y, Jiang J, Ma L, Wang Y, Liang M, Zhang Z, et al. Iron foam combined ozonation for enhanced treatment of pharmaceutical wastewater. *Environ Res* 2020;183:109205. <https://doi.org/10.1016/j.envres.2020.109205>.
- [147] Pelalak R, Alizadeh R, Gharehabani E. Enhanced heterogeneous catalytic ozonation of pharmaceutical pollutants using a novel nanostructure of iron-based mineral prepared via plasma technology: A comparative study. *J Hazard Mater* 2020;392:122269. <https://doi.org/10.1016/j.jhazmat.2020.122269>.
- [148] Kharel S, Stapf M, Mieke U, Ekblad M, Cimbritz M, Falås P, et al. Removal of pharmaceutical metabolites in wastewater ozonation including their fate in different post-treatments. *Sci Total Environ* 2021;759. <https://doi.org/10.1016/j.scitotenv.2020.143989>.
- [149] Hikmat K, Aziz H, Miessner H, Mueller S, Kalass D, Moeller D, et al. Degradation of pharmaceutical diclofenac and ibuprofen in aqueous solution, a direct comparison of ozonation, photocatalysis, and non-thermal plasma. *Chem Eng J* 2017;313:1033–41. <https://doi.org/10.1016/j.cej.2016.10.137>.
- [150] Gora S, Sokolowski A, Hatat-Fraile M, Liang R, Zhou YN, Andrews S. Solar photocatalysis with modified TiO₂ photocatalysts: Effects on NOM and disinfection byproduct formation potential. *Environ Sci Water Res Technol* 2018;4:1361–76. <https://doi.org/10.1039/c8ew00161h>.
- [151] Belver C, Bedia J, Rodriguez JJ. Zr-doped TiO₂ supported on delaminated clay materials for solar photocatalytic treatment of emerging pollutants. *J Hazard Mater*

- 2017;322:233–42. <https://doi.org/10.1016/j.jhazmat.2016.02.028>.
- [152] Leong S, Razmjou A, Wang K, Hapgood K, Zhang X, Wang H. TiO₂ based photocatalytic membranes: A review. *J Memb Sci* 2014;472:167–84. <https://doi.org/10.1016/j.memsci.2014.08.016>.
- [153] Ma D, Yi H, Lai C, Liu X, Huo X, An Z, et al. Critical review of advanced oxidation processes in organic wastewater treatment. *Chemosphere* 2021;275. <https://doi.org/10.1016/j.chemosphere.2021.130104>.
- [154] Magaela BN, Ndlovu KS, Tshangana CS, Muleja AA, Mamba BB, Nyokong T, et al. Photodegradation of ibuprofen using 5-10-15-20-tetrakis(4-bromophenyl) porphyrin conjugated to graphene quantum dots. *Opt Mater (Amst)* 2022;134:113147. <https://doi.org/10.1016/j.optmat.2022.113147>.
- [155] Rizzo L, Malato S, Antakyali D, Beretsou VG, Đolić MB, Gernjak W, et al. Consolidated vs new advanced treatment methods for the removal of contaminants of emerging concern from urban wastewater. *Sci Total Environ* 2019;655:986–1008. <https://doi.org/10.1016/j.scitotenv.2018.11.265>.
- [156] Dudziak S, Fiszka Borzyszkowska A, Zielińska-Jurek A. Photocatalytic degradation and pollutant-oriented structure-activity analysis of carbamazepine, ibuprofen and acetaminophen over faceted TiO₂. *J Environ Chem Eng* 2023;11. <https://doi.org/10.1016/j.jece.2023.109553>.
- [157] Gao X, Zhang X, Wang Y, Peng S, Yue B, Fan C. Photocatalytic degradation of carbamazepine using hierarchical BiOCl microspheres: Some key operating parameters, degradation intermediates and reaction pathway. *Chem Eng J* 2015;273:156–65. <https://doi.org/10.1016/j.cej.2015.03.063>.
- [158] Meribout R, Zuo Y, Khodja AA, Piram A, Lebarillier S, Cheng J, et al. Photocatalytic degradation of antiepileptic drug carbamazepine with bismuth oxychlorides (BiOCl and BiOCl/AgCl composite) in water: Efficiency evaluation and elucidation degradation pathways. *J Photochem Photobiol A Chem* 2016;328:105–13. <https://doi.org/10.1016/j.jphotochem.2016.04.024>.
- [159] Shooshtari NM, Ghazi MM. An investigation of the photocatalytic activity of nano A-Fe₂O₃/ZnO on the photodegradation of cefixime trihydrate. *Chem Eng J* 2017;315:527–

36. <https://doi.org/10.1016/j.cej.2017.01.058>.
- [160] Ur Rahman Z, Shah U, Alam A, Shah Z, Shaheen K, Bahadar Khan S, et al. Photocatalytic degradation of cefixime using CuO-NiO nanocomposite photocatalyst. *Inorg Chem Commun* 2023;148:110312. <https://doi.org/10.1016/j.inoche.2022.110312>.
- [161] Kazemi F, Zamani HA, Abedi MR, Ebrahimi M. Synthesis and comparison of three photocatalysts for degrading tramadol as an analgesic and widely used drug in water samples. *Environ Res* 2022:114821. <https://doi.org/10.1016/j.envres.2022.114821>.
- [162] Shimizu S, Barczyk S, Rettberg P, Shimizu T, Klaempfl T, Zimmermann JL, et al. Cold atmospheric plasma - A new technology for spacecraft component decontamination. *Planet Space Sci* 2014;90:60–71. <https://doi.org/10.1016/j.pss.2013.10.008>.
- [163] Li Y, Dong H, Xiao J, Li L, Chu D, Hou X, et al. Advanced oxidation processes for water purification using percarbonate: Insights into oxidation mechanisms, challenges, and enhancing strategies. *J Hazard Mater* 2023;442:130014. <https://doi.org/10.1016/j.jhazmat.2022.130014>.
- [164] Fan J, Wu H, Liu R, Meng L, Sun Y. Review on the treatment of organic wastewater by discharge plasma combined with oxidants and catalysts. *Environ Sci Pollut Res* 2021;28:2522–48. <https://doi.org/10.1007/s11356-020-11222-z>.
- [165] Gleizes A, Gonzalez JJ, Freton P. Thermal plasma modelling. *J Phys D Appl Phys* 2005;38. <https://doi.org/10.1088/0022-3727/38/9/R01>.
- [166] Gomez E, Rani DA, Cheeseman CR, Deegan D, Wise M, Boccaccini AR. Thermal plasma technology for the treatment of wastes: A critical review. *J Hazard Mater* 2009;161:614–26. <https://doi.org/10.1016/j.jhazmat.2008.04.017>.
- [167] Mizuno A. Recent Progress and Applications of Non-Thermal Plasma. *Int J Plasma Environ Sci Technol* 2009;3:1–7.
- [168] Magureanu M, Mandache NB, Parvulescu VI. Degradation of pharmaceutical compounds in water by non-thermal plasma treatment. *Water Res* 2015;81:124–36. <https://doi.org/10.1016/j.watres.2015.05.037>.
- [169] Hashim SA, Samsudin FND binti, Wong CS, Abu Bakar K, Yap SL, Mohd. Zin MF. Non-thermal plasma for air and water remediation. *Arch Biochem Biophys*

- 2016;605:34–40. <https://doi.org/10.1016/j.abb.2016.03.032>.
- [170] Locke BR, Sato M, Sunka P, Hoffmann MR, Chang JS. Electrohydraulic discharge and nonthermal plasma for water treatment. *Ind Eng Chem Res* 2006;45:882–905. <https://doi.org/10.1021/ie050981u>.
- [171] Wang T, Jia H, Guo X, Xia T, Qu G, Sun Q, et al. Evaluation of the potential of dimethyl phthalate degradation in aqueous using sodium percarbonate activated by discharge plasma. *Chem Eng J* 2018;346:65–76. <https://doi.org/10.1016/j.cej.2018.04.024>.
- [172] Gubkin J. Electrolytische Metallabscheidung an der freien Oberfläche einer Salzlösung. *Ann Phys* 1887;268:114–5. <https://doi.org/10.1002/andp.18872680909>.
- [173] Bruggeman P, Ribel E, Maslani A, Degroote J, Malesevic A, Rego R, et al. Characteristics of atmospheric pressure air discharges with a liquid cathode and a metal anode. *Plasma Sources Sci Technol* 2008;17. <https://doi.org/10.1088/0963-0252/17/2/025012>.
- [174] Bruggeman P, Leys C. Non-thermal plasmas in and in contact with liquids. *J Phys D Appl Phys* 2009;42. <https://doi.org/10.1088/0022-3727/42/5/053001>.
- [175] Jiang B, Zheng J, Qiu S, Wu M, Zhang Q, Yan Z, et al. Review on electrical discharge plasma technology for wastewater remediation. *Chem Eng J* 2014;236:348–68. <https://doi.org/10.1016/j.cej.2013.09.090>.
- [176] Locke BR, Lukes P, Brisset JL. Elementary Chemical and Physical Phenomena in Electrical Discharge Plasma in Gas-Liquid Environments and in Liquids. *Plasma Chem Catal Gases Liq* 2012;185–241. <https://doi.org/10.1002/9783527649525.ch6>.
- [177] Phaniendra A, Jestadi DB, Periyasamy L. Free Radicals: Properties, Sources, Targets, and Their Implication in Various Diseases. *Indian J Clin Biochem* 2015;30:11–26. <https://doi.org/10.1007/s12291-014-0446-0>.
- [178] Ozcan A, Ogun M. Biochemistry of Reactive Oxygen and Nitrogen Species. *Basic Princ Clin Significance Oxidative Stress* 2015. <https://doi.org/10.5772/61193>.
- [179] Joshi AA, Locke BR, Arce P, Finney WC. Formation of hydroxyl radicals, hydrogen peroxide and aqueous electrons by pulsed streamer corona discharge in aqueous solution. *J Hazard Mater* 1995;41:3–30. [https://doi.org/10.1016/0304-3894\(94\)00099-](https://doi.org/10.1016/0304-3894(94)00099-)

3.

- [180] Joshi RP, Thagard SM. Streamer-like electrical discharges in water: Part II. environmental applications. *Plasma Chem Plasma Process* 2013;33:17–49. <https://doi.org/10.1007/s11090-013-9436-x>.
- [181] Wardenier N, Liu Z, Nikiforov A, Van Hulle SWH, Leys C. Micropollutant elimination by O₃, UV and plasma-based AOPs: An evaluation of treatment and energy costs. *Chemosphere* 2019;234:715–24. <https://doi.org/10.1016/j.chemosphere.2019.06.033>.
- [182] Roots R, Okada S. Estimation of Life Times and Diffusion Distances of Radicals Involved in X-Ray-Induced DNA Strand Breaks or Killing of Mammalian Cells. *Radiat Res* 1975;64:306–20. <https://doi.org/https://doi.org/10.2307/3574267>.
- [183] Mai-Prochnow A, Zhou R, Zhang T, Ostrikov K (Ken), Mugunthan S, Rice SA, et al. Interactions of plasma-activated water with biofilms: inactivation, dispersal effects and mechanisms of action. *Npj Biofilms Microbiomes* 2021;7:1–12. <https://doi.org/10.1038/s41522-020-00180-6>.
- [184] Glaze WH. Drinking-water treatment with ozone. *Environ Sci Technol* 1987;21:224–30. <https://doi.org/10.1021/es00157a001>.
- [185] Dharini M, Jaspin S, Mahendran R. Cold plasma reactive species: Generation, properties, and interaction with food biomolecules. *Food Chem* 2023;405:134746. <https://doi.org/10.1016/j.foodchem.2022.134746>.
- [186] Khlyustova A, Labay C, Machala Z, Ginebra MP, Canal C. Important parameters in plasma jets for the production of RONS in liquids for plasma medicine: A brief review. *Front Chem Sci Eng* 2019;13:238–52. <https://doi.org/10.1007/s11705-019-1801-8>.
- [187] Abramov VO, Abramova A V., Cravotto G, Nikonov R V., Fedulov IS, Ivanov VK. Flow-mode water treatment under simultaneous hydrodynamic cavitation and plasma. *Ultrason Sonochem* 2021;70:105323. <https://doi.org/10.1016/j.ultsonch.2020.105323>.
- [188] Pereira TC, Flores EMM, Abramova A V., Verdini F, Calcio Gaudino E, Buccioli F, et al. Simultaneous hydrodynamic cavitation and glow plasma discharge for the degradation of metronidazole in drinking water. *Ultrason Sonochem* 2023;95:106388. <https://doi.org/10.1016/j.ultsonch.2023.106388>.

- [189] Šunka P, Babický V, Člupek M, Fuciman M, Lukeš P, Šimek M, et al. Potential applications of pulse electrical discharges in water. *Acta Phys Slovaca* 2004;54:135–45.
- [190] An W, Baumung K, Bluhm H. Underwater streamer propagation analyzed from detailed measurements of pressure release. *J Appl Phys* 2007;101. <https://doi.org/10.1063/1.2437675>.
- [191] Tachibana K, Takekata Y, Mizumoto Y, Motomura H, Jinno M. Analysis of a pulsed discharge within single bubbles in water under synchronized conditions. *Plasma Sources Sci Technol* 2011;20. <https://doi.org/10.1088/0963-0252/20/3/034005>.
- [192] Bruggeman P, Graham L, Degroote J, Vierendeels J, Leys C. Water surface deformation in strong electrical fields and its influence on electrical breakdown in a metal pin-water electrode system. *J Phys D Appl Phys* 2007;40:4779–86. <https://doi.org/10.1088/0022-3727/40/16/007>.
- [193] Glaze WH. Reaction Products of Ozone: A Review. *Environ Health Perspect* 1986;69:151–7. <https://doi.org/10.1289/ehp.8669151>.
- [194] Buxton G V, Greenstock CL, Helman P, Ross AB. Critical Review of Rate Constants for Reactions of Hydrated Electrons, Hydrogen Atoms and Hydroxyl Radicals ($\cdot\text{OH}$ / O^-) in Aqueous Solution. *J Phys Chem Ref Data* 1988;17. <https://doi.org/https://doi.org/10.1063/1.555805>.
- [195] Magureanu M, Dobrin D, Bradu C, Gherendi F, Mandache NB, Parvulescu VI. New evidence on the formation of oxidizing species in corona discharge in contact with liquid and their reactions with organic compounds. *Chemosphere* 2016;165:507–14. <https://doi.org/10.1016/j.chemosphere.2016.09.073>.
- [196] Li S, Ma X, Jiang Y, Cao X. Acetamiprid removal in wastewater by the low-temperature plasma using dielectric barrier discharge. *Ecotoxicol Environ Saf* 2014;106:146–53. <https://doi.org/10.1016/j.ecoenv.2014.04.034>.
- [197] Rong SP, Sun YB, Zhao ZH. Degradation of sulfadiazine antibiotics by water falling film dielectric barrier discharge. *Chinese Chem Lett* 2014;25:187–92. <https://doi.org/10.1016/j.ccllet.2013.11.003>.
- [198] Banaschik R, Lukes P, Jablonowski H, Hammer MU, Weltmann KD, Kolb JF. Potential

- of pulsed corona discharges generated in water for the degradation of persistent pharmaceutical residues. *Water Res* 2015;84:127–35. <https://doi.org/10.1016/j.watres.2015.07.018>.
- [199] Gao L, Sun L, Wan S, Yu Z, Li M. Degradation kinetics and mechanism of emerging contaminants in water by dielectric barrier discharge non-thermal plasma: The case of 17 β -Estradiol. *Chem Eng J* 2013;228:790–8. <https://doi.org/10.1016/j.cej.2013.05.079>.
- [200] Krishna S, Maslani A, Izdebski T, Horakova M, Klementova S, Spatenka P. Degradation of Verapamil hydrochloride in water by gliding arc discharge. *Chemosphere* 2016;152:47–54. <https://doi.org/10.1016/j.chemosphere.2016.02.083>.
- [201] Magureanu M, Piroi D, Mandache NB, David V, Medvedovici A, Parvulescu VI. Degradation of pharmaceutical compound pentoxifylline in water by non-thermal plasma treatment. *Water Res* 2010;44:3445–53. <https://doi.org/10.1016/j.watres.2010.03.020>.
- [202] Wang B, Li X, Wang Y. Degradation of metronidazole in water using dielectric barrier discharge synergistic with sodium persulfate. *Sep Purif Technol* 2022;303:122173. <https://doi.org/10.1016/j.seppur.2022.122173>.
- [203] Meropoulis S, Giannoulia S, Skandalis S, Rassias G, Aggelopoulos CA. Key-study on plasma-induced degradation of cephalosporins in water: Process optimization, assessment of degradation mechanisms and residual toxicity. *Sep Purif Technol* 2022;298:121639. <https://doi.org/10.1016/j.seppur.2022.121639>.
- [204] Singh RK, Philip L, Ramanujam S. Rapid degradation, mineralization and detoxification of pharmaceutically active compounds in aqueous solution during pulsed corona discharge treatment. *Water Res* 2017;121:20–36. <https://doi.org/10.1016/j.watres.2017.05.006>.
- [205] Smith J, Adams I, Ji H-F. Mechanism of Ampicillin Degradation by Non-Thermal Plasma Treatment with FE-DBD. *Plasma* 2017;1:1–11. <https://doi.org/10.3390/plasma1010001>.
- [206] Dobrin D, Magureanu M, Bradu C, Mandache NB, Ionita P, Parvulescu VI. Degradation of methylparaben in water by corona plasma coupled with ozonation. *Environ Sci Pollut Res* 2014:12190–7. <https://doi.org/10.1007/s11356-014-2964-y>.

- [207] Krause H, Schweiger B, Prinz E, Kim J, Steinfeld U. Degradation of persistent pharmaceuticals in aqueous solutions by a positive dielectric barrier discharge treatment. *J Electrostat* 2011;69:333–8. <https://doi.org/10.1016/j.elstat.2011.04.011>.
- [208] Hu X, Wang B. Removal of pefloxacin from wastewater by dielectric barrier discharge plasma: Mechanism and degradation pathways. *J Environ Chem Eng* 2021;9:105720. <https://doi.org/10.1016/j.jece.2021.105720>.
- [209] Baloul Y, Aubry O, Rabat H, Colas C, Maunit B, Hong D, et al. Paracetamol degradation in aqueous solution by non-thermal plasma. *EPJ Appl Phys* 2017;79:1–7. <https://doi.org/10.1051/epjap/2017160472>.
- [210] Slamani S, Abdelmalek F, Ghezzar MR, Addou A. Initiation of Fenton process by plasma gliding arc discharge for the degradation of paracetamol in water. *J Photochem Photobiol A Chem* 2018;359:1–10. <https://doi.org/10.1016/j.jphotochem.2018.03.032>.
- [211] Zhang T, Zhou R, Wang P, Mai-prochnow A, Mcconchie R, Li W, et al. Degradation of cefixime antibiotic in water by atmospheric plasma bubbles : Performance , degradation pathways and toxicity evaluation. *Chem Eng J* 2021;421:127730. <https://doi.org/10.1016/j.cej.2020.127730>.
- [212] Li H, Li T, He S, Zhou J, Wang T, Zhu L. Efficient degradation of antibiotics by non-thermal discharge plasma: Highlight the impacts of molecular structures and degradation pathways. *Chem Eng J* 2020;395. <https://doi.org/10.1016/j.cej.2020.125091>.
- [213] Rong S, Sun Y, Zhao Z, Wang H. Dielectric barrier discharge induced degradation of diclofenac in aqueous solution. *Water Sci Technol* 2014;69:76–83. <https://doi.org/10.2166/wst.2013.554>.
- [214] Wang J, Sun Y, Jiang H, Feng J. Removal of caffeine from water by combining dielectric barrier discharge (DBD) plasma with goethite. *J Saudi Chem Soc* 2017;21:545–57. <https://doi.org/10.1016/j.jscs.2016.08.002>.
- [215] Malik MA, Ghaffar A, Malik SA. Water purification by electrical discharges. *Plasma Sources Sci Technol* 2001;10:82–91. <https://doi.org/10.1088/0963-0252/10/1/311>.
- [216] Grabowski LR, Van Veldhuizen EM, Pemen AJM, Rutgers WR. Corona above water reactor for systematic study of aqueous phenol degradation. *Plasma Chem Plasma*

- Process 2006;26:3–17. <https://doi.org/10.1007/s11090-005-8721-8>.
- [217] Sugiarto AT, Sato M. Pulsed plasma processing of organic compounds in aqueous solution. *Thin Solid Films* 2001;386:295–9. [https://doi.org/10.1016/S0040-6090\(00\)01669-2](https://doi.org/10.1016/S0040-6090(00)01669-2).
- [218] Jiang B, Zheng J, Liu Q, Wu M. Degradation of azo dye using non-thermal plasma advanced oxidation process in a circulatory airtight reactor system. *Chem Eng J* 2012;204–205:32–9. <https://doi.org/10.1016/j.cej.2012.07.088>.
- [219] Hoeben WFLM, Van Veldhuizen EM, Rutgers WR, Cramers CAMG, Kroesen GMW. The degradation of aqueous phenol solutions by pulsed positive corona discharges. *Plasma Sources Sci Technol* 2000;9:361–9. <https://doi.org/10.1088/0963-0252/9/3/315>.
- [220] Zhang Y, Zhou M, Lei L. Degradation of 4-chlorophenol in different gas-liquid electrical discharge reactors. *Chem Eng J* 2007;132:325–33. <https://doi.org/10.1016/j.cej.2007.01.040>.
- [221] Holzer F, Locke BR. Multistage gas-liquid electrical discharge column reactor for advanced oxidation processes. *Ind Eng Chem Res* 2008;47:2203–12. <https://doi.org/10.1021/ie071442n>.
- [222] Grymonpré DR, Finney WC, Clark RJ, Locke BR. Hybrid Gas-Liquid Electrical Discharge Reactors for Organic Compound Degradation. *Ind Eng Chem Res* 2004;43:1975–89. <https://doi.org/10.1021/ie030620j>.
- [223] Lukes P, Locke BR. Degradation of substituted phenols in a hybrid gas-liquid electrical discharge reactor. *Ind Eng Chem Res* 2005;44:2921–30. <https://doi.org/10.1021/ie0491342>.
- [224] Sahni M, Locke BR. Degradation of chemical warfare agent simulants using gas-liquid pulsed streamer discharges. *J Hazard Mater* 2006;137:1025–34. <https://doi.org/10.1016/j.jhazmat.2006.03.029>.
- [225] Gao J, Wang X, Hu Z, Deng H, Hou J, Lu X, et al. Plasma degradation of dyes in water with contact glow discharge electrolysis. *Water Res* 2003;37:267–72. [https://doi.org/10.1016/S0043-1354\(02\)00273-7](https://doi.org/10.1016/S0043-1354(02)00273-7).
- [226] Wang X, Zhou M, Jin X. Application of glow discharge plasma for wastewater

- treatment. *Electrochim Acta* 2012;83:501–12.
<https://doi.org/10.1016/j.electacta.2012.06.131>.
- [227] Shen C, Wu S, Chen H, Rashid S, Wen Y. Phthalate degradation by glowdischarge plasma enhanced with pyrite in aqueous solution. *Water Sci Technol* 2016;74:1365–75.
<https://doi.org/10.2166/wst.2016.316>.
- [228] Liu W, Zhao Q, Wang T, Duan X, Li C, Lei X. Degradation of Organic Pollutants Using Atmospheric Pressure Glow Discharge Plasma. *Plasma Chem Plasma Process* 2016;36:1011–20. <https://doi.org/10.1007/s11090-016-9714-5>.
- [229] Zhang H, Huang Q, Ke Z, Yang L, Wang X, Yu Z. Degradation of microcystin-LR in water by glow discharge plasma oxidation at the gas-solution interface and its safety evaluation. *Water Res* 2012;46:6554–62. <https://doi.org/10.1016/j.watres.2012.09.041>.
- [230] Yan JH, Du CM, Li XD, Cheron BG, Ni MJ, Cen KF. Degradation of phenol in aqueous solutions by gas-liquid gliding arc discharges. *Plasma Chem Plasma Process* 2006;26:31–41. <https://doi.org/10.1007/s11090-005-8723-6>.
- [231] Tiya-Djowe A, Acayanka E, Lontio-Nkouongfo G, Laminsi S, Gaigneaux EM. Enhanced discolouration of methyl violet 10B in a gliding arc plasma reactor by the maghemite nanoparticles used as heterogeneous catalyst. *J Environ Chem Eng* 2015;3:953–60. <https://doi.org/10.1016/j.jece.2014.11.016>.
- [232] Lu X, Naidis G V., Laroussi M, Reuter S, Graves DB, Ostrikov K. Reactive species in non-equilibrium atmospheric-pressure plasmas: Generation, transport, and biological effects. *Phys Rep* 2016;630:1–84. <https://doi.org/10.1016/j.physrep.2016.03.003>.
- [233] Siemens W. Ueber die elektrostatische Induction und die Verzögerung des Stroms in Flaschendrahten[As to the electrostatic induction and the delay of the current Bottled wires]. *Ann Der Phys Und Chemie* 1857;178:66–122.
- [234] Laroussi M. Plasma Medicine: A Brief Introduction. *Plasma* 2018;1:47–60. <https://doi.org/10.3390/plasma1010005>.
- [235] Adamovich I, Baalrud SD, Bogaerts A, Bruggeman PJ, Cappelli M, Colombo V, et al. The 2017 Plasma Roadmap: Low temperature plasma science and technology. *J Phys D Appl Phys* 2017;50. <https://doi.org/10.1088/1361-6463/aa76f5>.

- [236] Foster JE, Weatherford B, Yee B, Gupta M. Evolution of underwater DBD plasma jet. *IEEE Trans Plasma Sci* 2011;39:2666–7. <https://doi.org/10.1109/TPS.2011.2145006>.
- [237] Malik MA. Water purification by plasmas: Which reactors are most energy efficient? *Plasma Chem Plasma Process* 2010;30:21–31. <https://doi.org/10.1007/s11090-009-9202-2>.
- [238] Brandenburg R. Corrigendum: Dielectric barrier discharges: progress on plasma sources and on the understanding of regimes and single filaments (*Plasma Sources Science and Technology* (2017) 26 (053001) DOI: 10.1088/1361-6595/aa6426). *Plasma Sources Sci Technol* 2018;27. <https://doi.org/10.1088/1361-6595/aaced9>.
- [239] Pietsch GJ. Peculiarities of dielectric barrier discharges. *Contrib to Plasma Phys* 2001;41:620–8. [https://doi.org/10.1002/1521-3986\(200111\)41:6<620::AID-CTPP620>3.0.CO;2-H](https://doi.org/10.1002/1521-3986(200111)41:6<620::AID-CTPP620>3.0.CO;2-H).
- [240] Kogelschatz U. Collective phenomena in volume and surface barrier discharges. *J Phys Conf Ser* 2010;257. <https://doi.org/10.1088/1742-6596/257/1/012015>.
- [241] Morfill GE, Shimizu T, Steffes B, Schmidt HU. Nosocomial infections - A new approach towards preventive medicine using plasmas. *New J Phys* 2009;11. <https://doi.org/10.1088/1367-2630/11/11/115019>.
- [242] Moreau E, Sosa R, Artana G. Electric wind produced by surface plasma actuators: a new dielectric barrier discharge based on a three-electrode geometry. *J Phys D Appl Phys* 2008;115204. <https://doi.org/10.1088/0022-3727/41/11/115204>.
- [243] Magureanu M, Piroi D, Mandache NB, David V, Medvedovici A, Bradu C, et al. Degradation of antibiotics in water by non-thermal plasma treatment. *Water Res* 2011;45:3407–16. <https://doi.org/10.1016/j.watres.2011.03.057>.
- [244] Dong B, Wang P, Li Z, Tu W, Tan Y. Degrading hazardous benzohydroxamic acid in the industrial beneficiation wastewater by dielectric barrier discharge reactor. *Sep Purif Technol* 2022;299:121644. <https://doi.org/10.1016/j.seppur.2022.121644>.
- [245] Li Z, Wang Y, Guo H, Pan S, Puyang C, Su Y, et al. Insights into water film DBD plasma driven by pulse power for ibuprofen elimination in water: performance, mechanism and degradation route. *Sep Purif Technol* 2021;277:119415.

- <https://doi.org/10.1016/j.seppur.2021.119415>.
- [246] Sokolov A, Kråkström M, Eklund P, Kronberg L, Louhi-Kultanen M. Abatement of amoxicillin and doxycycline in binary and ternary aqueous solutions by gas-phase pulsed corona discharge oxidation. *Chem Eng J* 2018;334:673–81. <https://doi.org/10.1016/j.cej.2017.10.071>.
- [247] Rong S, Sun Y. Wetted-wall corona discharge induced degradation of sulfadiazine antibiotics in aqueous solution. *J Chem Technol Biotechnol* 2014;89:1351–9. <https://doi.org/10.1002/jctb.4211>.
- [248] Singh RK, Philip L, Ramanujam S. Rapid degradation, mineralization and detoxification of pharmaceutically active compounds in aqueous solution during pulsed corona discharge treatment. *Water Res* 2017;121:20–36. <https://doi.org/10.1016/j.watres.2017.05.006>.
- [249] Guo H, Jiang N, Wang H, Lu N, Shang K, Li J, et al. Degradation of antibiotic chloramphenicol in water by pulsed discharge plasma combined with TiO₂/WO₃ composites: mechanism and degradation pathway. *J Hazard Mater* 2019;371:666–76. <https://doi.org/10.1016/j.jhazmat.2019.03.051>.
- [250] Xu Z, Xue X, Hu S, Li Y, Shen J, Lan Y, et al. Degradation effect and mechanism of gas-liquid phase dielectric barrier discharge on norfloxacin combined with H₂O₂ or Fe²⁺. *Sep Purif Technol* 2020;230:115862. <https://doi.org/10.1016/j.seppur.2019.115862>.
- [251] Karoui S, Saoud WA, Ghorbal A, Fourcade F, Amrane A, Assadi AA. Intensification of non-thermal plasma for aqueous Ciprofloxacin degradation: Optimization study, mechanisms, and combined plasma with photocatalysis. *J Water Process Eng* 2022;50:103207. <https://doi.org/10.1016/j.jwpe.2022.103207>.
- [252] Rezaei F, Vanraes P, Nikiforov A, Morent R, Geyter N De. Applications of Plasma-Liquid Systems: A Review. *Materials (Basel)* 2019.
- [253] Chen H, Mu Y, Xu S, Xu S, Hardacre C, Fan X. Recent advances in non-thermal plasma (NTP) catalysis towards C1 chemistry. *Chinese J Chem Eng* 2020;28:2010–21. <https://doi.org/10.1016/j.cjche.2020.05.027>.

- [254] Sano N, Kawashima T, Fujikawa J, Fujimoto T, Kitai T, Kanki T, et al. Decomposition of organic compounds in water by direct contact of gas corona discharge: Influence of discharge conditions. *Ind Eng Chem Res* 2002;41:5906–11. <https://doi.org/10.1021/ie0203328>.
- [255] Stratton GR, Dai F, Bellona CL, Holsen TM, Dickenson ERV, Mededovic Thagard S. Plasma-Based Water Treatment: Efficient Transformation of Perfluoroalkyl Substances in Prepared Solutions and Contaminated Groundwater. *Environ Sci Technol* 2017;51:1643–8. <https://doi.org/10.1021/acs.est.6b04215>.
- [256] Zeghioud H, Nguyen-Tri P, Khezami L, Amrane A, Assadi AA. Review on discharge Plasma for water treatment: mechanism, reactor geometries, active species and combined processes. *J Water Process Eng* 2020;38:101664. <https://doi.org/10.1016/j.jwpe.2020.101664>.
- [257] Sun B, Sato M, Clements JS. Optical study of active species produced by a pulsed streamer corona discharge in water. *J Electrostat* 1997;39:189–202. [https://doi.org/10.1016/S0304-3886\(97\)00002-8](https://doi.org/10.1016/S0304-3886(97)00002-8).
- [258] Thagard SM, Takashima K, Mizuno A. Chemistry of the positive and negative electrical discharges formed in liquid water and above a gas-liquid surface. *Plasma Chem Plasma Process* 2009;29:455–73. <https://doi.org/10.1007/s11090-009-9195-x>.
- [259] Magureanu M, Bilea F, Bradu C, Hong D. A review on non-thermal plasma treatment of water contaminated with antibiotics. *J Hazard Mater* 2021;417:125481. <https://doi.org/10.1016/j.jhazmat.2021.125481>.
- [260] Yu Z, Sun Y, Zhang G, Zhang C. Degradation of DEET in aqueous solution by water falling film dielectric barrier discharge : Effect of three operating modes and analysis of the mechanism and degradation pathway. *Chem Eng J* 2017;317:90–102. <https://doi.org/10.1016/j.cej.2017.02.068>.
- [261] Feng J, Zheng Z, Luan J, Li K, Wang L, Feng J. Gas-liquid hybrid discharge-induced degradation of diuron in aqueous solution. *J Hazard Mater* 2009;164:838–46. <https://doi.org/10.1016/j.jhazmat.2008.08.085>.
- [262] He D, Sun Y, Li S, Feng J. Decomposition of tetracycline in aqueous solution by corona discharge plasma combined with a Bi₂MoO₆ nanocatalyst. *J Chem Technol Biotechnol*

- 2015;90:2249–56. <https://doi.org/10.1002/jctb.4540>.
- [263] Yang B, Lei LC, Zhou MH. Effects of the Liquid Conductivity on Pulsed High-voltage Discharge Modes in Water. *Chinese Chem Lett* 2004;15:1215–8.
- [264] Lukes P, Clupek M, Babicky V. Discharge filamentary patterns produced by pulsed corona discharge at the interface between a water surface and air. *IEEE Trans Plasma Sci* 2011;39:2644–5. <https://doi.org/10.1109/TPS.2011.2158611>.
- [265] Wang HJ, Chen XY. Kinetic analysis and energy efficiency of phenol degradation in a plasma-photocatalysis system. *J Hazard Mater* 2011;186:1888–92. <https://doi.org/10.1016/j.jhazmat.2010.12.088>.
- [266] Arslan-Alaton I. A review of the effects of dye-assisting chemicals on advanced oxidation of reactive dyes in wastewater. *Color Technol* 2003;119:345–53. <https://doi.org/10.1111/j.1478-4408.2003.tb00196.x>.
- [267] Sahel K, Perol N, Chermette H, Bordes C, Derriche Z, Guillard C. Photocatalytic decolorization of Remazol Black 5 (RB5) and Procion Red MX-5B-Isotherm of adsorption, kinetic of decolorization and mineralization. *Appl Catal B Environ* 2007;77:100–9. <https://doi.org/10.1016/j.apcatb.2007.06.016>.
- [268] Ching WK, Colussi AJ, Sun HJ, Neelson KH, Hoffmann MR. Escherichia coli disinfection by electrohydraulic discharges. *Environ Sci Technol* 2001;35:4139–44. <https://doi.org/10.1021/es010643u>.
- [269] Li J, Zhou Z, Wang H, Li G, Wu Y. Research on decoloration of dye wastewater by combination of pulsed discharge plasma and TiO₂ nanoparticles. *Desalination* 2007;212:123–8. <https://doi.org/10.1016/j.desal.2006.10.006>.
- [270] Wang H, Li J, Quan X, Wu Y, Li G, Wang F. Formation of hydrogen peroxide and degradation of phenol in synergistic system of pulsed corona discharge combined with TiO₂ photocatalysis. *J Hazard Mater* 2007;141:336–43. <https://doi.org/10.1016/j.jhazmat.2006.07.019>.
- [271] Wang H, Li J, Quan X, Wu Y. Enhanced generation of oxidative species and phenol degradation in a discharge plasma system coupled with TiO₂ photocatalysis. *Appl Catal B Environ* 2008;83:72–7. <https://doi.org/10.1016/j.apcatb.2008.02.004>.

- [272] Zhang Y, Xin Q, Cong Y, Wang Q, Jiang B. Application of TiO₂ nanotubes with pulsed plasma for phenol degradation. *Chem Eng J* 2013;215–216:261–8. <https://doi.org/10.1016/j.cej.2012.11.045>.
- [273] Li S, Wang X, Liu L, Guo Y, Mu Q, Mellouki A. Enhanced degradation of perfluorooctanoic acid using dielectric barrier discharge with La/Ce-doped TiO₂. *Environ Sci Pollut Res* 2017;24:15794–803. <https://doi.org/10.1007/s11356-017-9246-4>.
- [274] Guo H, Jiang N, Wang H, Shang K, Lu N, Li J, et al. Environmental Enhanced catalytic performance of graphene-TiO₂ nanocomposites for synergetic degradation of fluoroquinolone antibiotic in pulsed discharge plasma system. *Appl Catal B Environ* 2019;248:552–66. <https://doi.org/10.1016/j.apcatb.2019.01.052>.
- [275] Du X, Skachko I, Barker A, Andrei EY. Approaching ballistic transport in suspended graphene. *Nat Nanotechnol* 2008;3:491–5. <https://doi.org/10.1038/nnano.2008.199>.
- [276] Behineh ES, Solaimany Nazar AR, Farhadian M, Moghadam M. Photocatalytic degradation of cefixime using visible light-driven Z-scheme ZnO nanorod/Zn₂TiO₄/GO heterostructure. *J Environ Manage* 2022;316. <https://doi.org/10.1016/j.jenvman.2022.115195>.
- [277] Lei F, Li Z, Ye L, Wang Y, Lin S. One-pot synthesis of Pt/SnO₂/GNs and its electro-photo-synergistic catalysis for methanol oxidation. *Int J Hydrogen Energy* 2016;41:255–64. <https://doi.org/10.1016/j.ijhydene.2015.09.098>.
- [278] Wang H, Shen Z, Yan X, Guo H, Mao D, Yi C. Dielectric barrier discharge plasma coupled with WO₃ for bisphenol A degradation. *Chemosphere* 2021;274:129722. <https://doi.org/10.1016/j.chemosphere.2021.129722>.
- [279] Daughton CG. Green Pharmacy | Mini-Monograph Cradle-to-Cradle Stewardship of Drugs for Minimizing Their Environmental Disposition While Promoting Human Health . II . Drug Disposal , Waste Reduction , and Future Directions. *Green Pharm* 2003;111:775–85. <https://doi.org/10.1289/ehp.5948>.
- [280] Radbruch L, Glaeske G, Grond S, Münchberg F, Scherbaum N, Storz E, et al. Topical Review on the Abuse and Misuse Potential of Tramadol and Tilidine in Germany. *Subst Abus* 2013;37–41. <https://doi.org/10.1080/08897077.2012.735216>.

- [281] Eversloh CL, Schulz M, Wagner M, Ternes TA. Electrochemical oxidation of tramadol in low-salinity reverse osmosis concentrates using boron-doped diamond anodes. *Water Res* 2014;2:293–304. <https://doi.org/10.1016/j.watres.2014.12.021>.
- [282] Kostanjevecki P, Petric I, Loncar J, Smital T, Ahel M, Terzic S. Aerobic biodegradation of tramadol by pre-adapted activated sludge culture : Cometabolic transformations and bacterial community changes during enrichment. *Sci Total Environ* 2019;687:858–66. <https://doi.org/10.1016/j.scitotenv.2019.06.118>.
- [283] Bachour R, Golovko O, Kellner M, Pohl J. Behavioral effects of citalopram , tramadol , and binary mixture in zebra fi sh (*Danio rerio*) larvae. *Chemosphere* 2020;238:124587. <https://doi.org/10.1016/j.chemosphere.2019.124587>.
- [284] Ložek F, Kuklina I, Grabicová K, Kubec J, Buřič M, Grabic R, et al. Behaviour and cardiac response to stress in signal crayfish exposed to environmental concentrations of tramadol. *Aquat Toxicol* 2019;213:105217. <https://doi.org/10.1016/j.aquatox.2019.05.019>.
- [285] Soliman HAM, Sayed AEDH. Poikilocytosis and tissue damage as negative impacts of tramadol on juvenile of Tilapia (*Oreochromis niloticus*). *Environ Toxicol Pharmacol* 2020;78:103383. <https://doi.org/10.1016/j.etap.2020.103383>.
- [286] Sehonova P, Plhalova L, Blahova J, Berankova P, Doubkova V, Prokes M, et al. The effect of tramadol hydrochloride on early life stages of fish. *Environ Toxicol Pharmacol* 2016;44:151–7. <https://doi.org/10.1016/j.etap.2016.05.006>.
- [287] Banaschik R, Jablonowski H, Bednarski PJ, Kolb JF. Degradation and intermediates of diclofenac as instructive example for decomposition of recalcitrant pharmaceuticals by hydroxyl radicals generated with pulsed corona plasma in water. *J Hazard Mater* 2018;342:651–60. <https://doi.org/10.1016/j.jhazmat.2017.08.058>.
- [288] Graumans MHF, Hoeben WFLM, van Dael MFP, Anzion RBM, Russel FGM, Scheepers PTJ. Thermal plasma activation and UV/H₂O₂ oxidative degradation of pharmaceutical residues. *Environ Res* 2021;195:110884. <https://doi.org/10.1016/j.envres.2021.110884>.
- [289] Chandana L, Subrahmanyam C. Degradation and mineralization of aqueous phenol by an atmospheric pressure catalytic plasma reactor. *J Environ Chem Eng* 2018;6:3780–6.

- <https://doi.org/10.1016/j.jece.2016.11.014>.
- [290] Ghalwa AN, Abu-shawish HM, Zaggout FR, Saadeh SM, Al-dalou AR, Abou AA. Electrochemical degradation of tramadol hydrochloride : Novel use of potentiometric carbon paste electrodes as a tracer. *Arab J Chem* 2014;7:708–14. <https://doi.org/10.1016/j.arabjc.2010.12.007>.
- [291] Zimmermann SG, Schmukat A, Schulz M, Benner J, Gunten U Von, Ternes TA. Kinetic and Mechanistic Investigations of the Oxidation of Tramadol by Ferrate and Ozone. *Environ Sci Technol* 2012;46:876–84. <https://doi.org/https://doi-org.uplib.idm.oclc.org/10.1021/es203348q>.
- [292] Antonopoulou M, Konstantinou I. Photocatalytic degradation and mineralization of tramadol pharmaceutical in aqueous TiO₂ suspensions: Evaluation of kinetics, mechanisms and ecotoxicity. *Appl Catal A Gen* 2016;515:136–43. <https://doi.org/10.1016/j.apcata.2016.02.005>.
- [293] Monteil H, Oturan N, Péchaud Y, Oturan MA. Electro-Fenton treatment of the analgesic tramadol: Kinetics, mechanism and energetic evaluation. *Chemosphere* 2020;247. <https://doi.org/10.1016/j.chemosphere.2020.125939>.
- [294] Cui Y, Cheng J, Chen Q, Yin Z. The Types of Plasma Reactors in Wastewater Treatment. *IOP Conf Ser Earth Environ Sci* 2018;208. <https://doi.org/10.1088/1755-1315/208/1/012002>.
- [295] Foster JE. Plasma-based water purification: Challenges and prospects for the future. *Phys Plasmas* 2017;24:0–16. <https://doi.org/10.1063/1.4977921>.
- [296] Allabakshi SM, Srikar PSNSR, Gangwar RK, Maliyekkal SM. Feasibility of surface dielectric barrier discharge in wastewater treatment: Spectroscopic modeling, diagnostic, and dye mineralization. *Sep Purif Technol* 2022;296:121344. <https://doi.org/10.1016/j.seppur.2022.121344>.
- [297] Sato M, Ohgiyama T, Clements JS. Formation of chemical species and their effects on microorganisms using a pulsed high-voltage discharge in water. *IEEE Trans Ind Appl* 1996;32:106–12. <https://doi.org/10.1109/28.485820>.
- [298] Machala Z, Janda M, Hensel K, Jedlovský I, Leštinská L, Foltin V, et al. Emission

- spectroscopy of atmospheric pressure plasmas for bio-medical and environmental applications. *J Mol Spectrosc* 2007;243:194–201. <https://doi.org/10.1016/j.jms.2007.03.001>.
- [299] Bansode AS, More SE, Siddiqui EA, Satpute S, Ahmad A, Bhoraskar S V., et al. Effective degradation of organic water pollutants by atmospheric non-thermal plasma torch and analysis of degradation process. *Chemosphere* 2017;167:396–405. <https://doi.org/10.1016/j.chemosphere.2016.09.089>.
- [300] Nikitin D, Kaur B, Preis S, Dulova N. Persulfate contribution to photolytic and pulsed corona discharge oxidation of metformin and tramadol in water. *Process Saf Environ Prot* 2022;165:22–30. <https://doi.org/10.1016/j.psep.2022.07.002>.
- [301] Ghazouani S, Boujelbane F, Jellouli D, Bruggen B Van Der. Removal of tramadol hydrochloride, an emerging pollutant, from aqueous solution using gamma irradiation combined by nanofiltration. *Process Saf Environ Prot* 2022;159:442–51. <https://doi.org/10.1016/j.psep.2022.01.005>.
- [302] Muthukumar M, Selvakumar N. Studies on the effect of inorganic salts on decolouration of acid dye effluents by ozonation. *Dye Pigment* 2004;62:221–8. <https://doi.org/10.1016/j.dyepig.2003.11.002>.
- [303] Merouani DR, Abdelmalek F, Taleb F, Martel M, Semmoud A, Addou A. Plasma treatment by gliding arc discharge of dyes / dye mixtures in the presence of inorganic salts. *Arab J Chem* 2015;8:155–63. <https://doi.org/10.1016/j.arabjc.2011.01.034>.
- [304] Marotta E, Ceriani E, Schiorlin M, Ceretta C, Paradisi C. Comparison of the rates of phenol advanced oxidation in deionized and tap water within a dielectric barrier discharge reactor. *Water Res* 2012;46:6239–46. <https://doi.org/10.1016/j.watres.2012.08.022>.
- [305] Wojnárovits L, Tóth T, Takács E. Rate constants of carbonate radical anion reactions with molecules of environmental interest in aqueous solution: A review. *Sci Total Environ* 2020;717:1–24. <https://doi.org/10.1016/j.scitotenv.2020.137219>.
- [306] Canonica S, Kohn T, Mac M, Real FJ, Wirz J, von Gunten U. Photosensitizer Method to Determine Rate Constants for the Reaction of Carbonate Radical with Organic Compounds. *Environ Sci Technol* 2005;39:9182–8.

<https://doi.org/https://doi.org/10.1021/es051236b>.

- [307] Hoigne J, Bader H. The role of hydroxyl radical reactions in oxidation processes in aqueous solutions. *Water Res* 1976;10:377–86. [https://doi.org/https://doi.org/10.1016/0043-1354\(76\)90055-5](https://doi.org/https://doi.org/10.1016/0043-1354(76)90055-5).
- [308] Hsieh K, Wang H, Locke BR. Analysis of a gas-liquid film plasma reactor for organic compound oxidation. *J Hazard Mater* 2016;317:188–97. <https://doi.org/10.1016/j.jhazmat.2016.05.053>.
- [309] Sun Y, Pignatello JJ. Photochemical Reactions Involved in the Total Mineralization of 2,4-D by Fe³⁺/H₂O₂/UV. *Environ Sci Technol* 1993;27:304–10. <https://doi.org/https://doi.org/10.1021/es00039a010>.
- [310] Molewa BE. National Water Act 36 of 1998. vol. 1998. Pretoria: 2013.
- [311] Wang L, Wang C, Liu Q, Meng Q, Huo X, Sun P, et al. PEPT1- and OAT1/3-mediated drug-drug interactions between bestatin and cefixime in vivo and in vitro in rats, and in vitro in human. *Eur J Pharm Sci* 2014;63:77–86. <https://doi.org/10.1016/j.ejps.2014.06.019>.
- [312] Hasanzadeh V, Rahmanian O, Heidari M. Cefixime adsorption onto activated carbon prepared by dry thermochemical activation of date fruit residues. *Microchem J* 2020;152:104261. <https://doi.org/10.1016/j.microc.2019.104261>.
- [313] Kafeei R, Papari F, Seyedabadi M, Sahebi S, Tahmasebi R. Occurrence , distribution , and potential sources of antibiotics pollution in the water-sediment of the northern coastline of the Persian Gulf , Iran. *Sci Total Environ* 2018;627:703–12. <https://doi.org/10.1016/j.scitotenv.2018.01.305>.
- [314] Yang Y, Cho YI, Fridman A. Plasma Discharge in Liquid: Water Treatment and Applications. Taylor & Francis Group; 2012.
- [315] Saleem M, Biondo O, Sretenović G, Tomei G, Magarotto M, Pavarin D, et al. Comparative performance assessment of plasma reactors for the treatment of PFOA; reactor design, kinetics, mineralization and energy yield. *Chem Eng J* 2020;382:123031. <https://doi.org/10.1016/j.cej.2019.123031>.
- [316] Aziz KHH, Miessner H, Mahyar A, Mueller S, Moeller D, Mustafa F, et al. Degradation

- of perfluorosurfactant in aqueous solution using non-thermal plasma generated by nano-second pulse corona discharge reactor. *Arab J Chem* 2021;14:103366. <https://doi.org/10.1016/j.arabjc.2021.103366>.
- [317] El-Shaer M, Mobasher M, Elsebaei A, Essam N. Gliding Arc plasma for Environmental Friendly Treatment of Waste Water. *ResearchGate* 2018. <https://doi.org/10.13140/RG.2.2.11373.84964>.
- [318] Back JO, Obholzer T, Winkler K, Jabornig S, Rupprich M. Combining ultrafiltration and non-thermal plasma for low energy degradation of pharmaceuticals from conventionally treated wastewater. *J Environ Chem Eng* 2018;6:7377–85. <https://doi.org/10.1016/j.jece.2018.07.047>.
- [319] Foster J, Sommers BS, Gucker SN, Blankson IM, Adamovsky G. Perspectives on the interaction of plasmas with liquid water for water purification. *IEEE Trans Plasma Sci* 2012;40:1311–23. <https://doi.org/10.1109/TPS.2011.2180028>.
- [320] Aggelopoulos CA, Tsakiroglou CD. A new perspective towards in-situ cold plasma remediation of polluted sites: Direct generation of micro-discharges within contaminated medium. *Chemosphere* 2021;266:128969. <https://doi.org/10.1016/j.chemosphere.2020.128969>.
- [321] Gao L, Shi X, Wu X. Applications and challenges of low temperature plasma in pharmaceutical field. *J Pharm Anal* 2021;11:28–36. <https://doi.org/10.1016/j.jpha.2020.05.001>.
- [322] Subrahmanyam C, Magureanu M, Renken A, Kiwi-Minsker L. Catalytic abatement of volatile organic compounds assisted by non-thermal plasma. Part 1. A novel dielectric barrier discharge reactor containing catalytic electrode. *Appl Catal B Environ* 2006;65:150–6. <https://doi.org/10.1016/j.apcatb.2006.01.006>.
- [323] Wang J, Sun Y, Feng J, Xin L, Ma J. Degradation of triclocarban in water by dielectric barrier discharge plasma combined with TiO₂/activated carbon fibers: Effect of operating parameters and byproducts identification. *Chem Eng J* 2016;300:36–46. <https://doi.org/10.1016/j.cej.2016.04.041>.
- [324] Russo M, Iervolino G, Vaiano V, Palma V. Non-thermal plasma coupled with catalyst for the degradation of water pollutants: A review. *Catalysts* 2020;10:1–29.

<https://doi.org/10.3390/catal10121438>.

- [325] Manoj Kumar Reddy P, Mahammadunnisa S, Subrahmanyam C. Catalytic non-thermal plasma reactor for mineralization of endosulfan in aqueous medium: A green approach for the treatment of pesticide contaminated water. *Chem Eng J* 2014;238:157–63. <https://doi.org/10.1016/j.cej.2013.08.087>.
- [326] Chandana L, Sangeetha CJ, Shashidhar T, Subrahmanyam C. Non-thermal atmospheric pressure plasma jet for the bacterial inactivation in an aqueous medium. *Sci Total Environ* 2018;640–641:493–500. <https://doi.org/10.1016/j.scitotenv.2018.05.342>.
- [327] Hama Aziz KH, Miessner H, Mueller S, Kalass D, Moeller D, Khorshid I, et al. Degradation of pharmaceutical diclofenac and ibuprofen in aqueous solution, a direct comparison of ozonation, photocatalysis, and non-thermal plasma. *Chem Eng J* 2017;313:1033–41. <https://doi.org/10.1016/j.cej.2016.10.137>.
- [328] Luiz DB, Genena AK, Virmond E, José HJ, Moreira RFP, Gebhardt W, et al. Identification of Degradation Products of Erythromycin A Arising from Ozone and Advanced Oxidation Process Treatment. *Water Environ Res* 2010;82:797–805. <https://doi.org/10.2175/106143010x12609736966928>.
- [329] Murugesan P, Evanjalin Monica V, Moses JA, Anandharamakrishnan C. Water decontamination using non-thermal plasma: Concepts, applications, and prospects. *J Environ Chem Eng* 2020;8. <https://doi.org/10.1016/j.jece.2020.104377>.
- [330] Erim B, Ciğeroğlu Z, Şahin S, Vasseghian Y. Photocatalytic degradation of cefixime in aqueous solutions using functionalized SWCNT/ZnO/Fe₃O₄ under UV-A irradiation. *Chemosphere* 2022;291. <https://doi.org/10.1016/j.chemosphere.2021.132929>.
- [331] Swedha M, Okla MK, Abdel-Maksoud MA, Kokilavani S, Kamwilaisak K, Sillanpää M, et al. Photo-Fenton system Fe₃O₄/NiCu₂S₄ QDs towards bromoxynil and cefixime degradation: A realistic approach. *Surfaces and Interfaces* 2023;38. <https://doi.org/10.1016/j.surfin.2023.102764>.
- [332] Pourtaheri A, Nezamzadeh-Ejhi A. Photocatalytic properties of incorporated NiO onto clinoptilolite nano-particles in the photodegradation process of aqueous solution of cefixime pharmaceutical capsule. *Chem Eng Res Des* 2015;104:835–43. <https://doi.org/10.1016/j.cherd.2015.10.031>.

- [333] Rasouli K, Alamdari A, Sabbaghi S. Ultrasonic-assisted synthesis of α -Fe₂O₃@TiO₂ photocatalyst: Optimization of effective factors in the fabrication of photocatalyst and removal of non-biodegradable cefixime via response surface methodology-central composite design. *Sep Purif Technol* 2023;307. <https://doi.org/10.1016/j.seppur.2022.122799>.
- [334] Sanli N, Sanli S, Sızır U, Gumustas M, Ozkan SA. Determination of pK a values of cefdinir and cefixime by LC and spectrophotometric methods and their analysis in pharmaceutical dosage forms. *Chromatographia* 2011;73:1171–6. <https://doi.org/10.1007/s10337-011-2013-7>.
- [335] Hoigné J, Bader H. Rate constants of reactions of ozone with organic and inorganic compounds in water-I. Non-dissociating organic compounds. *Water Res* 1983;17:173–83. [https://doi.org/10.1016/0043-1354\(83\)90098-2](https://doi.org/10.1016/0043-1354(83)90098-2).
- [336] Boczkaj G, Fernandes A. Wastewater treatment by means of advanced oxidation processes based on cavitation – A review. *Chem Eng J* 2017;320:608–33. <https://doi.org/http://dx.doi.org/10.1016/j.cej.2017.03.084049>.
- [337] Lee S, Lee J, Nam W, Yun G. Enhanced production of hydroxyl radicals in plasma-treated water via a negative DC bias coupling. *J Phys D Appl Phys* 2022;55:455201. <https://doi.org/10.1088/1361-6463/ac9000>.
- [338] Rong S, Sun Y. Degradation of TAIC by water falling film dielectric barrier discharge - Influence of radical scavengers. *J Hazard Mater* 2015;287:317–24. <https://doi.org/10.1016/j.jhazmat.2015.02.003>.
- [339] Ternes T, Joss A, Oehlmann J. Occurrence, fate, removal and assessment of emerging contaminants in water in the water cycle (from wastewater to drinking water). *Water Res* 2015;72:1–2. <https://doi.org/10.1016/j.watres.2015.02.055>.
- [340] Zhao W, Yu G, Blaney L, Wang B. Development of emission factors to estimate discharge of typical pharmaceuticals and personal care products from wastewater treatment plants. *Sci Total Environ* 2021;769. <https://doi.org/10.1016/j.scitotenv.2020.144556>.
- [341] Gurke R, Rößler M, Marx C, Diamond S, Schubert S, Oertel R, et al. Occurrence and removal of frequently prescribed pharmaceuticals and corresponding metabolites in

- wastewater of a sewage treatment plant. *Sci Total Environ* 2015;532:762–70. <https://doi.org/10.1016/j.scitotenv.2015.06.067>.
- [342] Mutiyar PK, Gupta SK, Mittal AK. Fate of pharmaceutical active compounds (PhACs) from River Yamuna, India: An ecotoxicological risk assessment approach. *Ecotoxicol Environ Saf* 2018;150:297–304. <https://doi.org/10.1016/j.ecoenv.2017.12.041>.
- [343] Tran NH, Gin KYH. Occurrence and removal of pharmaceuticals, hormones, personal care products, and endocrine disrupters in a full-scale water reclamation plant. *Sci Total Environ* 2017;599–600:1503–16. <https://doi.org/10.1016/j.scitotenv.2017.05.097>.
- [344] Kondor AC, Jakab G, Vancsik A, Filep T, Szeberényi J, Szabó L, et al. Occurrence of pharmaceuticals in the danube and drinking water wells: Efficiency of riverbank filtration. *Environ Pollut* 2020;265. <https://doi.org/10.1016/j.envpol.2020.114893>.
- [345] Couto CF, Lange LC, Amaral MCS. Occurrence, fate and removal of pharmaceutically active compounds (PhACs) in water and wastewater treatment plants—A review. *J Water Process Eng* 2019;32:100927. <https://doi.org/10.1016/j.jwpe.2019.100927>.
- [346] Hansen É, Monteiro de Aquim P, Gutterres M. Current technologies for post-tanning wastewater treatment: A review. *J Environ Manage* 2021;294. <https://doi.org/10.1016/j.jenvman.2021.113003>.
- [347] Barillas L. Design of a Prototype of Water Purification by Plasma Technology as the Foundation for an Industrial Wastewater Plant. *J Phys Conf Ser* 2015;591. <https://doi.org/10.1088/1742-6596/591/1/012057>.
- [348] Ali F, Khan JA, Shah NS, Sayed M, Khan HM. Carbamazepine degradation by UV and UV-assisted AOPs: Kinetics, mechanism and toxicity investigations. *Process Saf Environ Prot* 2018;117:307–14. <https://doi.org/10.1016/j.psep.2018.05.004>.
- [349] Zou X, Li X, Chen C, Zhu X, Huang X, Wu Y, et al. Degradation performance of carbamazepine by ferrous-activated sodium hypochlorite: Mechanism and impacts on the soil system. *Chem Eng J* 2020;389:123451. <https://doi.org/10.1016/j.cej.2019.123451>.
- [350] Wang S, Zhou N. Removal of carbamazepine from aqueous solution using sono-activated persulfate process. *Ultrason Sonochem* 2016;29:156–62.

- <https://doi.org/10.1016/j.ultsonch.2015.09.008>.
- [351] Guo H, Zhou X, Zhang Y, Yao Q, Qian Y, Chu H, et al. Carbamazepine degradation by heterogeneous activation of peroxymonosulfate with lanthanum cobaltite perovskite: Performance, mechanism and toxicity. *J Environ Sci (China)* 2020;91:10–21. <https://doi.org/10.1016/j.jes.2020.01.003>.
- [352] Roy K, Moholkar VS. Mechanistic analysis of carbamazepine degradation in hybrid advanced oxidation process of hydrodynamic cavitation/UV/persulfate in the presence of ZnO/ZnFe₂O₄. *Sep Purif Technol* 2021;270:118764. <https://doi.org/10.1016/j.seppur.2021.118764>.
- [353] Ding Y, Zhang G, Wang X, Zhu L, Tang H. Chemical and photocatalytic oxidative degradation of carbamazepine by using metastable Bi³⁺ self-doped NaBiO₃ nanosheets as a bifunctional material. *Appl Catal B Environ* 2017;202:528–38. <https://doi.org/10.1016/j.apcatb.2016.09.054>.
- [354] Bo L, He K, Tan N, Gao B, Feng Q, Liu J, et al. Photocatalytic oxidation of trace carbamazepine in aqueous solution by visible-light-driven ZnIn₂S₄: Performance and mechanism. *J Environ Manage* 2017;190:259–65. <https://doi.org/10.1016/j.jenvman.2016.12.050>.
- [355] Asghar A, Hammad M, Kerpen K, Niemann F, Al-Kamal AK, Segets D, et al. Ozonation of carbamazepine in the presence of sulfur-doped graphene: Effect of process parameters and formation of main transformation products. *Sci Total Environ* 2023;864. <https://doi.org/10.1016/j.scitotenv.2022.161079>.
- [356] Yang B, Deng J, Yu G, Deng S, Li J, Zhu C, et al. Effective degradation of carbamazepine using a novel electro-peroxone process involving simultaneous electrochemical generation of ozone and hydrogen peroxide. *Electrochem Commun* 2018;86:26–9. <https://doi.org/10.1016/j.elecom.2017.11.003>.
- [357] Zeng J, Yang B, Wang X, Li Z, Zhang X, Lei L. Degradation of pharmaceutical contaminant ibuprofen in aqueous solution by cylindrical wetted-wall corona discharge. *Chem Eng J* 2015;267:282–8. <https://doi.org/10.1016/j.cej.2015.01.030>.
- [358] Ceriani E, Marotta E, Shapoval V, Favaro G, Paradisi C. Complete mineralization of organic pollutants in water by treatment with air non-thermal plasma. *Chem Eng J*

- 2018;337:567–75. <https://doi.org/10.1016/j.cej.2017.12.107>.
- [359] Krause H, Schweiger B, Schuhmacher J, Scholl S, Steinfeld U. Degradation of the endocrine disrupting chemicals (EDCs) carbamazepine, clofibrac acid, and iopromide by corona discharge over water. *Chemosphere* 2009;75:163–8. <https://doi.org/10.1016/j.chemosphere.2008.12.020>.
- [360] Yu J, Yan W, Zhu B, Xu Z, Hu S, Xi W, et al. Degradation of carbamazepine by high-voltage direct current gas–liquid plasma with the addition of H₂O₂ and Fe²⁺. *Environ Sci Pollut Res* 2022;29:77771–87. <https://doi.org/10.1007/s11356-022-21250-6>.
- [361] Babalola SO, Daramola MO, Iwarere SA. An investigation on the removal of tramadol analgesic in deionized water and final wastewater effluent using a novel continuous flow dielectric barrier discharge reactor. *J Water Process Eng* 2023;56:104294. <https://doi.org/10.1016/j.jwpe.2023.104294>.
- [362] Zwane S, Dlamini DS, Mamba BB, Kuvarega AT. Evaluation of the photodegradation of pharmaceuticals and dyes in water using a highly visible light-active graphitic carbon nitride modified with tungsten oxide. *Inorg Chem Commun* 2023;151:110637. <https://doi.org/10.1016/j.inoche.2023.110637>.
- [363] Lukes P, Locke BR, Brisset J-L. Aqueous-phase chemistry of electrical discharge plasma in water and in gas-liquid environments. *Plasma Chem. Catal. Gases Liq.*, Wiley-VCH Verlag GmbH & Co. KGaA; 2012, p. 243–308. <https://doi.org/https://doi.org/10.1002/9783527649525.ch7>.
- [364] Locke BR, Shih K-Y. Review of the methods to form hydrogen peroxide in electrical discharge plasma with liquid water. *Plasma Sources Sci Technol* 2011;20:034006. <https://doi.org/10.1088/0963-0252/20/3/034006>.
- [365] Kirkpatrick MJ, Locke BR. Hydrogen , Oxygen , and Hydrogen Peroxide Formation in Aqueous Phase Pulsed Corona Electrical Discharge. *Ind Eng Chem Res* 2005:4243–8.
- [366] Reddy PMK, Ramaraju B, Subrahmanyam C. Degradation of malachite green by dielectric barrier discharge plasma. *Water Sci Technol* 2013;67:1097–104. <https://doi.org/10.2166/wst.2013.663>.
- [367] Hong D, Rabat H, Bauchire JM, Chang MB. Measurement of ozone production in non-

- thermal plasma actuator using surface dielectric barrier discharge. *Plasma Chem Plasma Process* 2014;34:887–97. <https://doi.org/10.1007/s11090-014-9527-3>.
- [368] Rogli GM, Obradovi BM, Kuraica MM, Dojč BP, Než J, Manojlovi DD. Decolorization of reactive textile dyes using water falling film dielectric barrier discharge. *J Hazard Mater* 2011;192:763–71. <https://doi.org/10.1016/j.jhazmat.2011.05.086>.
- [369] Aboubakr HA, Gangal U, Youssef MM, Goyal SM, Bruggeman PJ. Inactivation of virus in solution by cold atmospheric pressure plasma : identification of chemical inactivation pathways. *J Phys D Appl Phys* 2016;49:1–17. <https://doi.org/10.1088/0022-3727/49/20/204001>.
- [370] Li Y, Yang Y, Lei J, Liu W, Tong M, Liang J. The degradation pathways of carbamazepine in advanced oxidation process: A mini review coupled with DFT calculation. *Sci Total Environ* 2021;779:146498. <https://doi.org/10.1016/j.scitotenv.2021.146498>.
- [371] Mousel D, Bastian D, Firk J, Palmowski L, Pinnekamp J. Removal of pharmaceuticals from wastewater of health care facilities. *Sci Total Environ* 2021;751:141310. <https://doi.org/10.1016/j.scitotenv.2020.141310>.
- [372] Xu M, Deng J, Cai A, Ye C, Ma X, Li Q, et al. Synergistic effects of UVC and oxidants (PS vs. Chlorine) on carbamazepine attenuation: Mechanism, pathways, DBPs yield and toxicity assessment. *Chem Eng J* 2021;413:127533. <https://doi.org/10.1016/j.cej.2020.127533>.
- [373] Deng J, Shao Y, Gao N, Xia S, Tan C, Zhou S, et al. Degradation of the antiepileptic drug carbamazepine upon different UV-based advanced oxidation processes in water. *Chem Eng J* 2013;222:150–8. <https://doi.org/10.1016/j.cej.2013.02.045>.
- [374] Kim I, Tanaka H. Photodegradation characteristics of PPCPs in water with UV treatment. *Environ Int* 2009;35:793–802. <https://doi.org/10.1016/j.envint.2009.01.003>.
- [375] Bolton JR, Bircher KG, Tumas W, Tolman CA. Figures-of-merit for the technical development and application of advanced oxidation technologies for both electric- and solar-driven systems. *Pure Appl Chem* 2001;73:627–37. <https://doi.org/10.1351/pac200173040627>.

- [376] Vanraes P, Willems G, Nikiforov A, Surmont P, Lynen F, Vandamme J, et al. Removal of atrazine in water by combination of activated carbon and dielectric barrier discharge. *J Hazard Mater* 2015;299:647–55. <https://doi.org/10.1016/j.jhazmat.2015.07.075>.
- [377] Bu L, Zhou S, Zhu S, Wu Y, Duan X, Shi Z, et al. Insight into carbamazepine degradation by UV/monochloramine: Reaction mechanism, oxidation products, and DBPs formation. *Water Res* 2018;146:288–97. <https://doi.org/10.1016/j.watres.2018.09.036>.
- [378] City of Tshwane. UpDATE. Pretoria, South Africa: 2023.

Appendices

Appendix A:

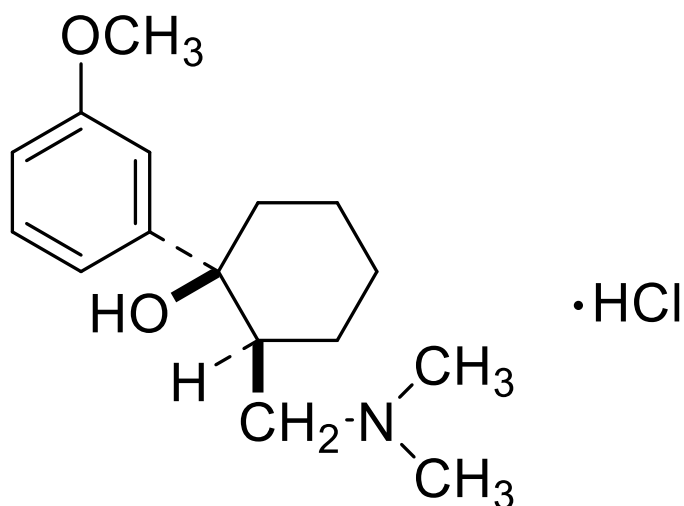


Figure A1: Molecular structure for tramadol hydrochloride.

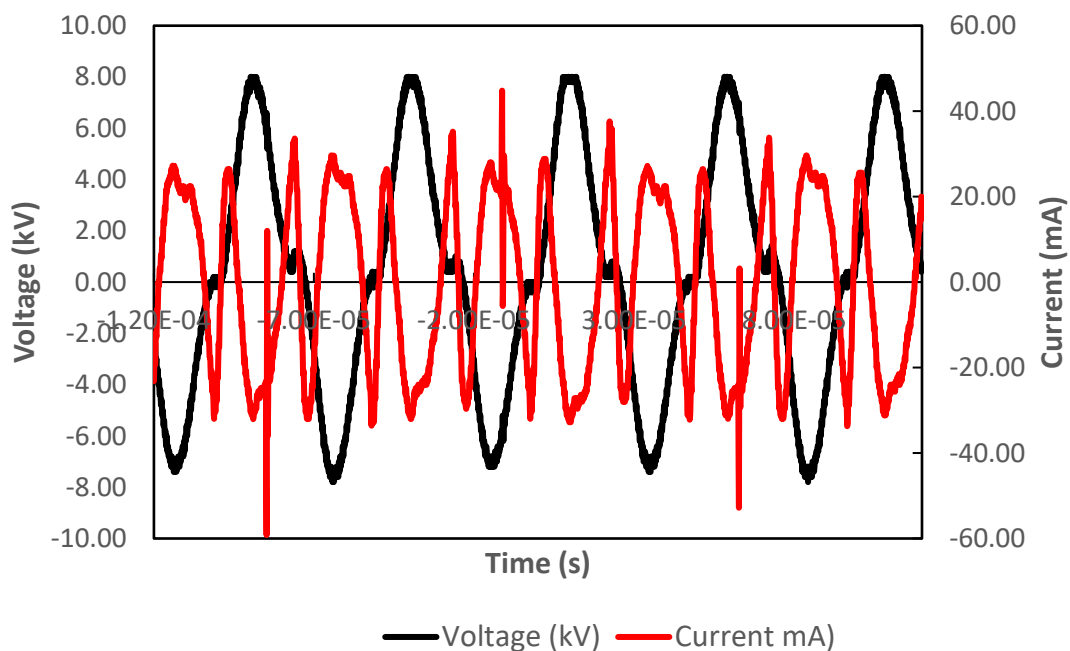
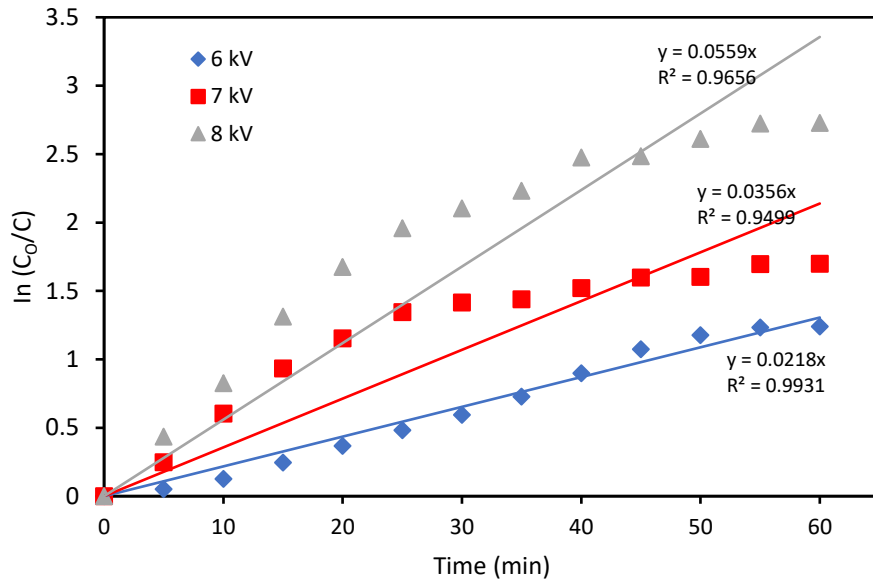
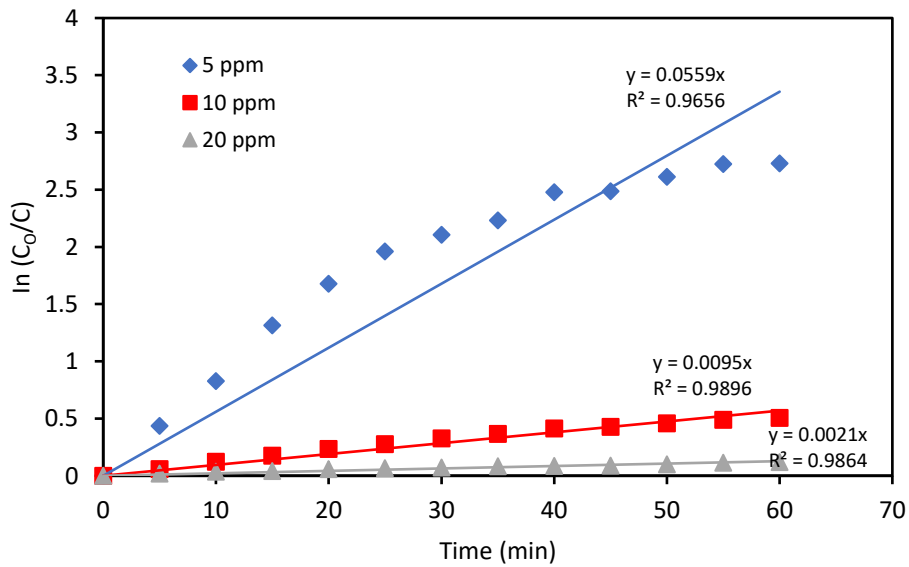


Figure A2: A typical voltage-current waveform at peak voltage 8 kV.



(a)



(b)

Figure A3: First-order plots of cefixime degradation as a function of treatment time (a) at different input voltage (b) at different initial concentration.

Table A1: Comparison of the pH, rate constant, and half-life values for tramadol degradation in different reaction solutions during an hour of plasma treatment.

| Reaction solution | pH | | k (min ⁻¹) | t _{1/2} (min) | R ² |
|--------------------------------------|---------|-------|------------------------|------------------------|----------------|
| | Initial | Final | | | |
| Deionised water | 5.62 | 3.24 | 0.0560 | 12 | 0.970 |
| FWWE | 7.26 | 8.13 | 0.0056 | 124 | 0.996 |
| FeSO ₄ ·7H ₂ O | 5.60 | 3.20 | 0.0610 | 11 | 0.927 |
| NaCl | 5.86 | 3.93 | 0.0101 | 69 | 0.965 |
| NaHCO ₃ | 8.40 | 8.77 | 0.0053 | 131 | 0.990 |
| KCl | 5.53 | 3.82 | 0.0036 | 192 | 0.900 |

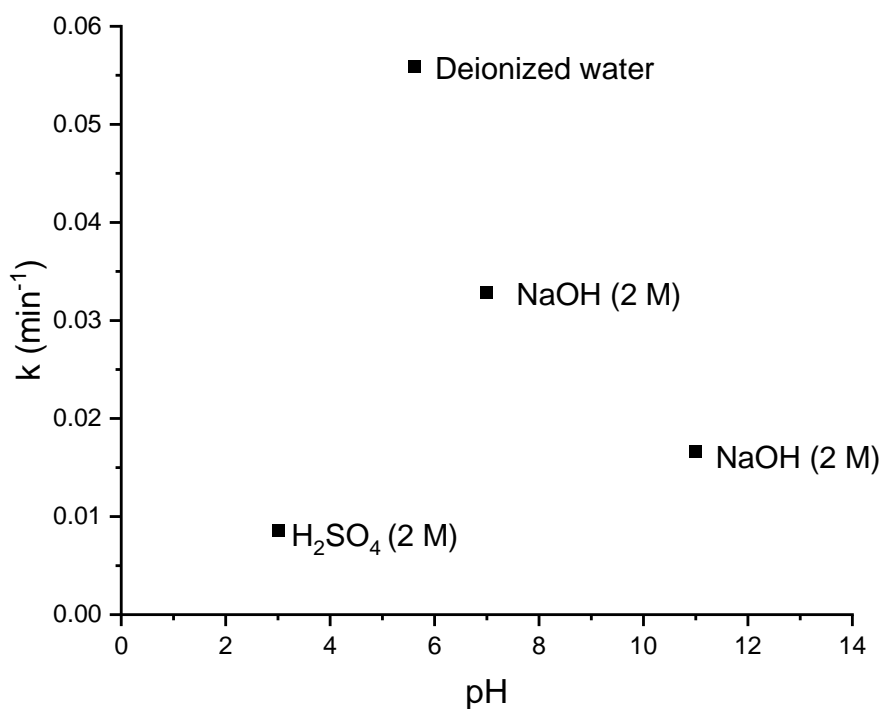


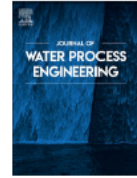
Figure A4: Relationship between pH and rate constants for tramadol degradation.



Contents lists available at [ScienceDirect](https://www.sciencedirect.com)

Journal of Water Process Engineering

journal homepage: www.elsevier.com/locate/jwpe



An investigation on the removal of tramadol analgesic in deionized water and final wastewater effluent using a novel continuous flow dielectric barrier discharge reactor

Samuel O. Babalola, Michael O. Daramola, Samuel A. Iwarere*

Department of Chemical Engineering, Faculty of Engineering, Built Environment and Information Technology, University of Pretoria, Hatfield 0028, Pretoria, South Africa

ARTICLE INFO

Keywords:

Tramadol
Wastewater effluent
Dielectric barrier discharge
Reactive species
Degradation efficiency

ABSTRACT

In this study, the degradation of tramadol (TRA) was studied for the first time in deionized water (D-I) and final wastewater effluent (FWWE) using a dielectric barrier discharge reactor operated in a continuous flow mode. Initially, the reactor was optimized for voltage and initial concentration conditions. After 60 min treatment, the degradation efficiency of TRA was 93 % in D-I and only 27 % in FWWE. Also, the pseudo-first-order rate constant in D-I (0.056 min^{-1}) was an order of magnitude higher than the FWWE (0.0056 min^{-1}). To understand the reasons for this disparity, experiments were conducted to investigate the impact of conductivity, pH, and certain natural radical scavengers present in the wastewater. The results revealed that the rate of degradation and kinetics of TRA in the presence of HCO_3^- was comparable to those observed in FWWE due to the scavenging of the $\bullet\text{OH}$ radicals. Meanwhile, Fenton reaction with TRA was confirmed with the synthetic solution based on the increased production of H_2O_2 . Toxicity tests showed that the treated TRA solution did not inhibit the growth of *Escherichia coli* as opposed to the untreated solution.

Figure A5: Title page of published chapter 2 in the Journal of Water Process Engineering.

Appendix B:

Table B1: Physicochemical properties of Cefixime.

| Parameters | Values |
|-------------------|---|
| Molecular formula | C ₁₆ H ₁₅ N ₅ O ₇ S ₂ |
| Molecular weight | 453.5 g/mol |
| Melting point | 218 – 225 °C |
| Solubility | Slightly soluble in water, soluble in methanol, sparingly in ethanol but insoluble in ethyl acetate |
| Colour | White or pale yellow |
| Density | 1.85±0.1 g/cm ³ |
| Solubility | 55.11 mg/L |
| pKa | 3.53 |
| Stability | Hygroscopic |

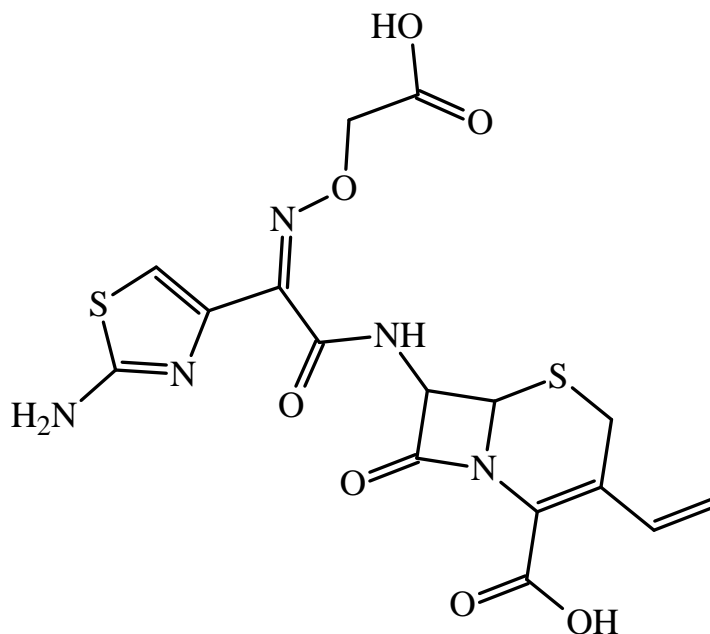


Figure B1: Molecular structure of Cefixime.

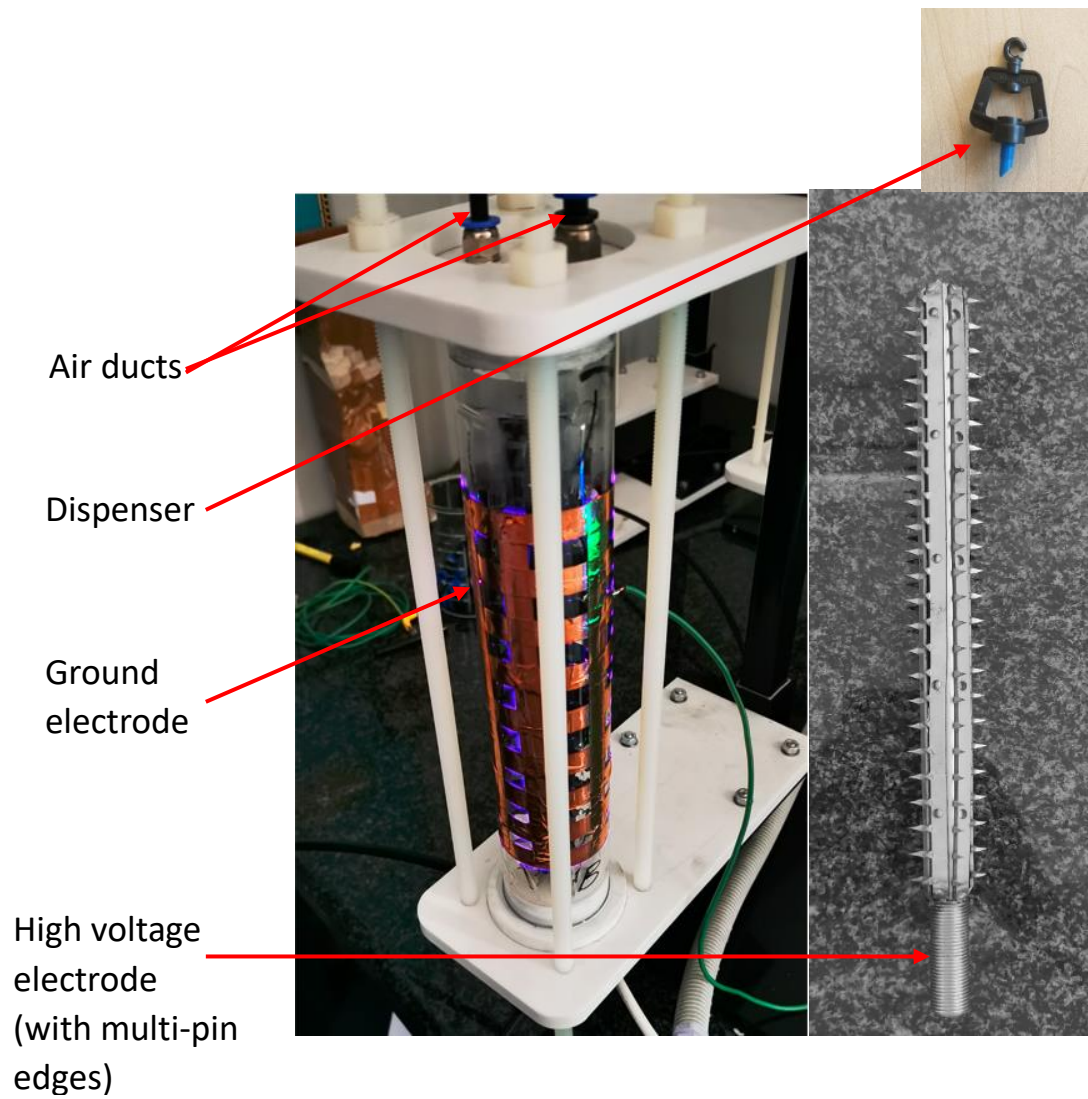
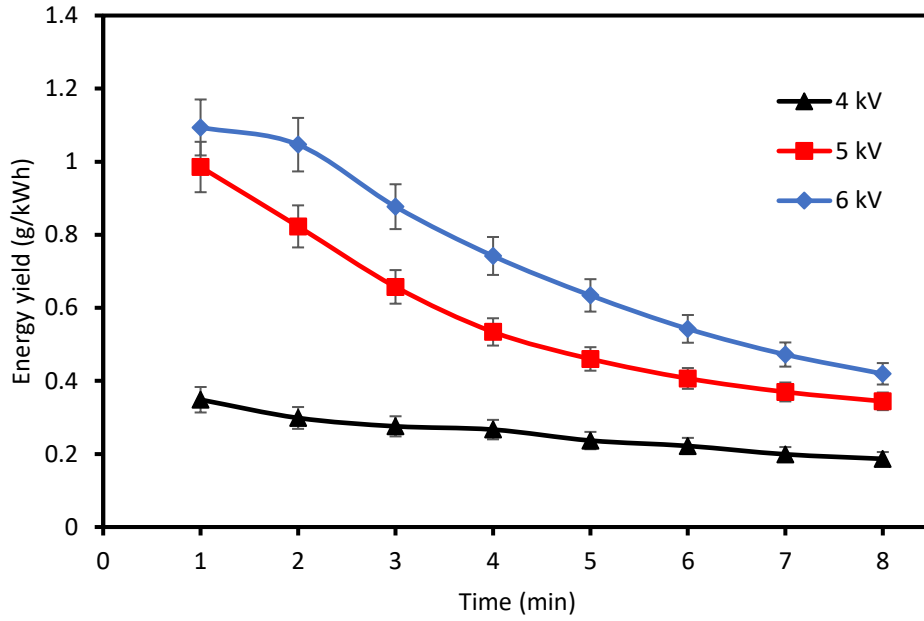
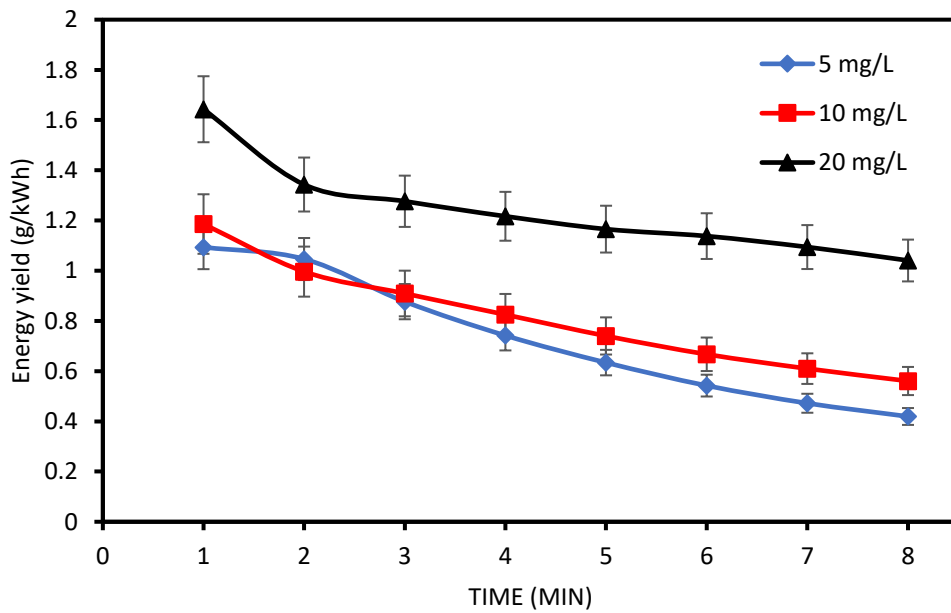


Figure B2. A picture of the DBD plasma reactor.

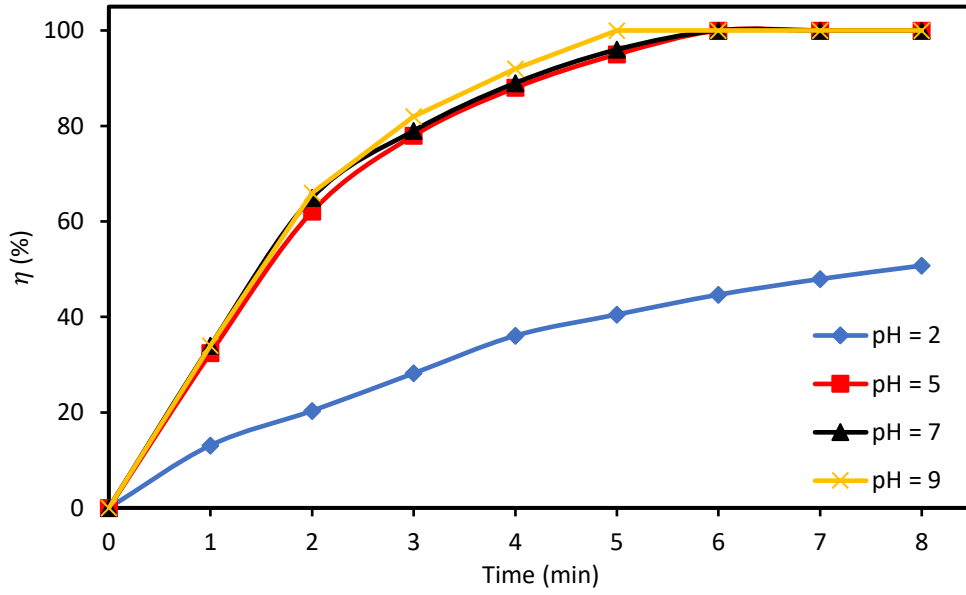


(a)

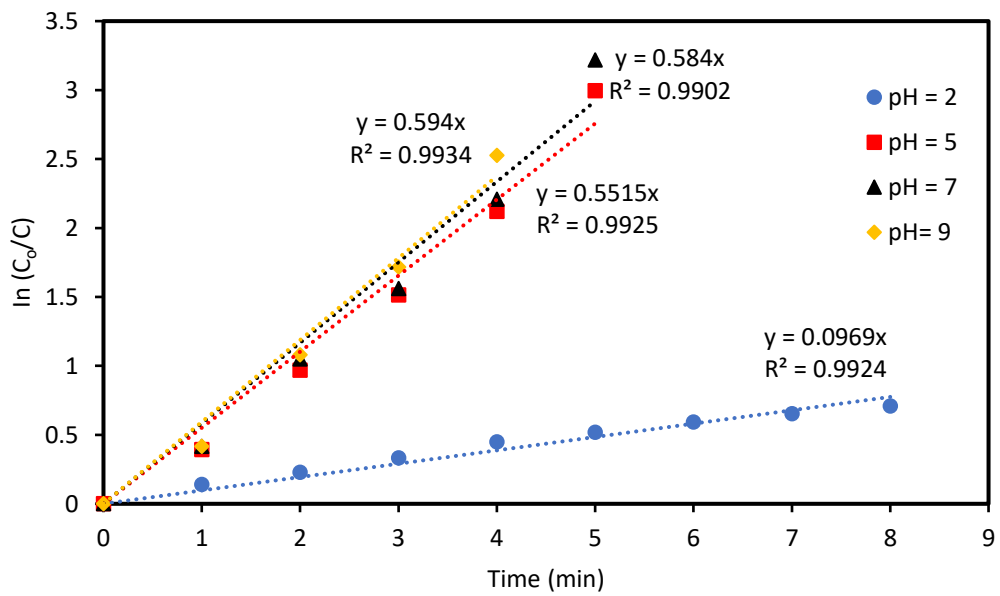


(b)

Figure B3. Energy yield comparison (a) Voltage (b) Initial concentration.

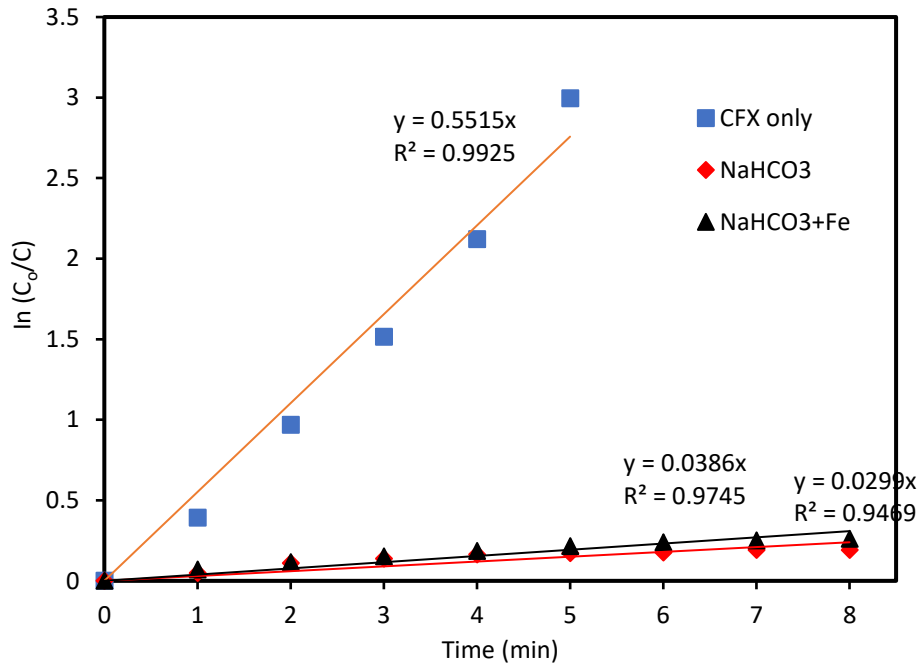


(a)

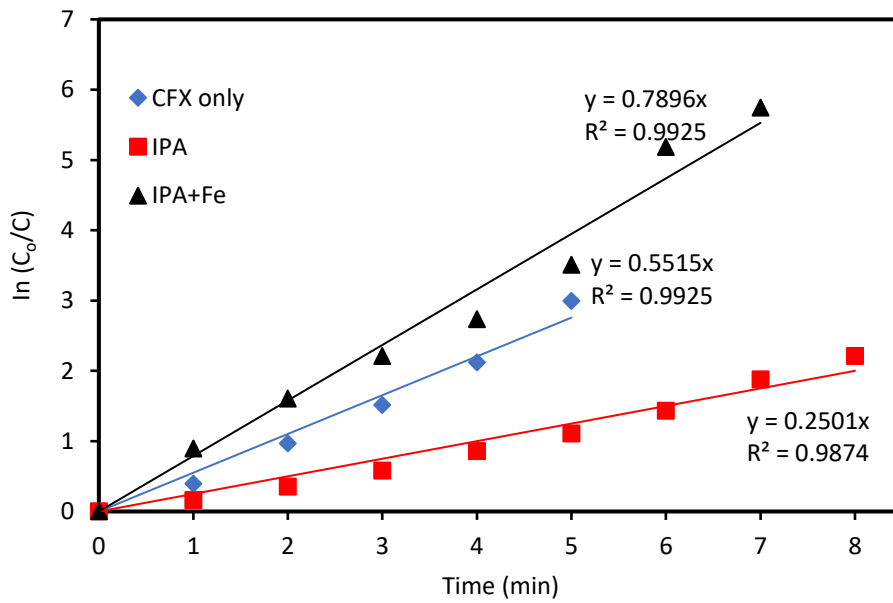


(b)

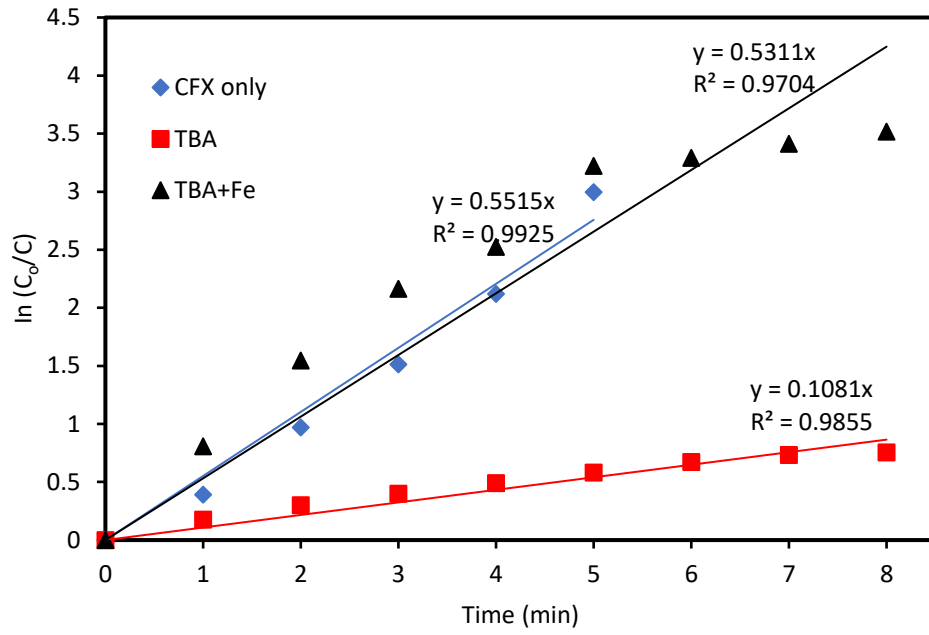
Figure B4. Effect of pH variation (a) degradation efficiency (b) rate of reaction.



(a)



(b)



(c)

Figure B5: Rate of reaction observed at the different additives (a) TBA (b) IPA (c) NaHCO_3

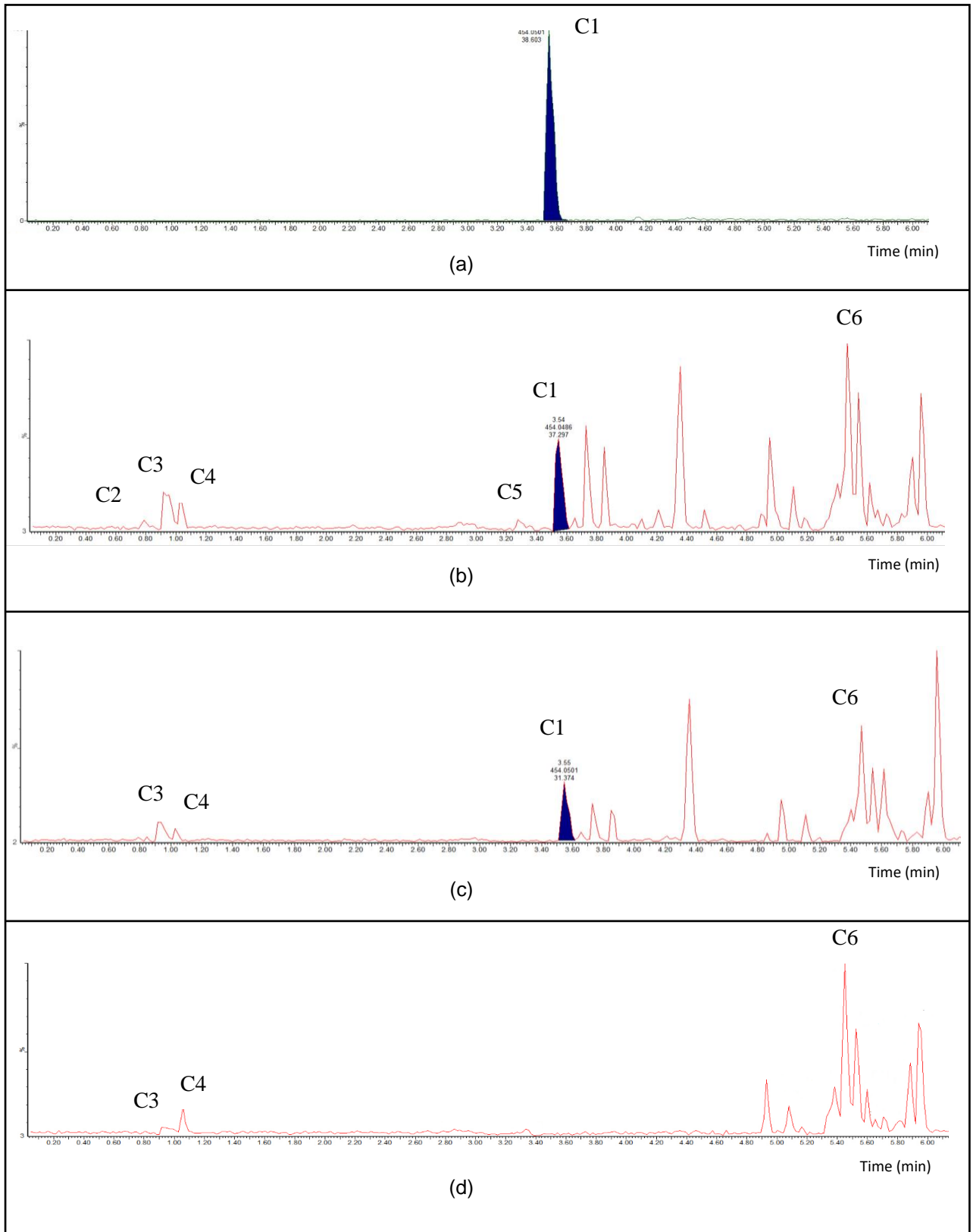


Figure B6: Chromatograms for the degraded CFX with the DBD plasma reactor at different time intervals (a) pure CFX (b) 1 min (c) 2 min (d) 8 min

SEPPUR-D-23-10232 - Confirming your submission to Separation and Purification Technology

1 message

em@editorialmanager.com <em@editorialmanager.com>
Reply-To: support@elsevier.com
To: Samuel Ayodele Iwarere <samuel.iwarere@up.ac.za>

29 November 2023 at 00:42

This is an automated message.

Mechanistic study of cefixime degradation with an atmospheric air dielectric barrier discharge – influence of radical scavengers and metal ion catalyst

Dear Dr Iwarere,

We have received the above referenced manuscript you submitted to Separation and Purification Technology. It has been assigned the following manuscript number: SEPPUR-D-23-10232.

To track the status of your manuscript, please log in as an author at <https://www.editorialmanager.com/seppur/>, and navigate to the "Submissions Being Processed" folder.

Thank you for submitting your work to this journal.

Kind regards,
Separation and Purification Technology

More information and support

You will find information relevant for you as an author on Elsevier's Author Hub: <https://www.elsevier.com/authors>

FAQ: How can I reset a forgotten password?

https://service.elsevier.com/app/answers/detail/a_id/28452/supporthub/publishing/

For further assistance, please visit our customer service site: <https://service.elsevier.com/app/home/supporthub/publishing/>

Here you can search for solutions on a range of topics, find answers to frequently asked questions, and learn more about Editorial Manager via interactive tutorials. You can also talk 24/7 to our customer support team by phone and 24/7 by live chat and email

This journal uses the Elsevier Article Transfer Service. This means that if an editor feels your manuscript is more suitable for an alternative journal, then you might be asked to consider transferring the manuscript to such a journal. The recommendation might be provided by a Journal Editor, a dedicated Scientific Managing Editor, a tool assisted recommendation, or a combination. For more details see the journal guide for authors.

At Elsevier, we want to help all our authors to stay safe when publishing. Please be aware of fraudulent messages requesting money in return for the publication of your paper. If you are publishing open access with Elsevier, bear in mind that we will never request payment before the paper has been accepted. We have prepared some guidelines (<https://www.elsevier.com/connect/authors-update/seven-top-tips-on-stopping-apc-scams>) that you may find helpful, including a short video on Identifying fake acceptance letters (<https://www.youtube.com/watch?v=o5l8thD9XtE>). Please remember that you can contact Elsevier's Researcher Support team (<https://service.elsevier.com/app/home/supporthub/publishing/>) at any time if you have questions about your manuscript, and you can log into Editorial Manager to check the status of your manuscript (https://service.elsevier.com/app/answers/detail/a_id/29155/c/10530/supporthub/publishing/kw/status/).#AU_SEPPUR#

Figure B7: Confirmation of chapter 4 submission to the Separation and Purification Journal.

Appendix C:

Confirming submission to Journal of Environmental Sciences

1 message

Journal of Environmental Sciences <em@editorialmanager.com>

1 December 2023 at 00:08

Reply-To: Journal of Environmental Sciences <jes@rcees.ac.cn>

To: Samuel Ayodele Iwarere <samuel.iwarere@up.ac.za>

This is an automated message.

Insights into the degradation of carbamazepine using a continuous-flow non-thermal plasma: mechanism, and comparison with UV-based systems

Dear Dr Iwarere,

We have received the above referenced manuscript you submitted to Journal of Environmental Sciences.

To track the status of your manuscript, please log in as an author at <https://www.editorialmanager.com/jesc/>, and navigate to the "Submissions Being Processed" folder.

Thank you for submitting your work to this journal.

Kind regards,
Journal of Environmental Sciences

More information and support

You will find information relevant for you as an author on Elsevier's Author Hub: <https://www.elsevier.com/authors>

FAQ: How can I reset a forgotten password?

https://service.elsevier.com/app/answers/detail/a_id/28452/supporthub/publishing/

For further assistance, please visit our customer service site: <https://service.elsevier.com/app/home/supporthub/publishing/>

Here you can search for solutions on a range of topics, find answers to frequently asked questions, and learn more about Editorial Manager via interactive tutorials. You can also talk 24/7 to our customer support team by phone and 24/7 by live chat and email

At Elsevier, we want to help all our authors to stay safe when publishing. Please be aware of fraudulent messages requesting money in return for the publication of your paper. If you are publishing open access with Elsevier, bear in mind that we will never request payment before the paper has been accepted. We have prepared some guidelines (<https://www.elsevier.com/connect/authors-update/seven-top-tips-on-stopping-apc-scams>) that you may find helpful, including a short video on Identifying fake acceptance letters (<https://www.youtube.com/watch?v=o5i8thD9XtE>).

Please remember that you can contact Elsevier's Researcher Support team (<https://service.elsevier.com/app/home/supporthub/publishing/>) at any time if you have questions about your manuscript, and you can log into Editorial Manager to check the status of your manuscript (https://service.elsevier.com/app/answers/detail/a_id/29155/c/10530/supporthub/publishing/kw/status/).

In compliance with data protection regulations, you may request that we remove your personal registration details at any time. (Use the following URL: <https://www.editorialmanager.com/jesc/login.asp?a=r>). Please contact the publication office if you have any questions.

Figure C1: Confirmation of chapter 5 submission to the Journal of Environmental Sciences.